



Terms and Conditions of Use of Digitised Theses from Trinity College Library Dublin

Copyright statement

All material supplied by Trinity College Library is protected by copyright (under the Copyright and Related Rights Act, 2000 as amended) and other relevant Intellectual Property Rights. By accessing and using a Digitised Thesis from Trinity College Library you acknowledge that all Intellectual Property Rights in any Works supplied are the sole and exclusive property of the copyright and/or other IPR holder. Specific copyright holders may not be explicitly identified. Use of materials from other sources within a thesis should not be construed as a claim over them.

A non-exclusive, non-transferable licence is hereby granted to those using or reproducing, in whole or in part, the material for valid purposes, providing the copyright owners are acknowledged using the normal conventions. Where specific permission to use material is required, this is identified and such permission must be sought from the copyright holder or agency cited.

Liability statement

By using a Digitised Thesis, I accept that Trinity College Dublin bears no legal responsibility for the accuracy, legality or comprehensiveness of materials contained within the thesis, and that Trinity College Dublin accepts no liability for indirect, consequential, or incidental, damages or losses arising from use of the thesis for whatever reason. Information located in a thesis may be subject to specific use constraints, details of which may not be explicitly described. It is the responsibility of potential and actual users to be aware of such constraints and to abide by them. By making use of material from a digitised thesis, you accept these copyright and disclaimer provisions. Where it is brought to the attention of Trinity College Library that there may be a breach of copyright or other restraint, it is the policy to withdraw or take down access to a thesis while the issue is being resolved.

Access Agreement

By using a Digitised Thesis from Trinity College Library you are bound by the following Terms & Conditions. Please read them carefully.

I have read and I understand the following statement: All material supplied via a Digitised Thesis from Trinity College Library is protected by copyright and other intellectual property rights, and duplication or sale of all or part of any of a thesis is not permitted, except that material may be duplicated by you for your research use or for educational purposes in electronic or print form providing the copyright owners are acknowledged using the normal conventions. You must obtain permission for any other use. Electronic or print copies may not be offered, whether for sale or otherwise to anyone. This copy has been supplied on the understanding that it is copyright material and that no quotation from the thesis may be published without proper acknowledgement.

Sequence Analysis of Alphavirus Pathogenesis

A thesis submitted to the University of Dublin, Trinity College
For the Degree of Doctor of Philosophy

by

Christopher H. Logue

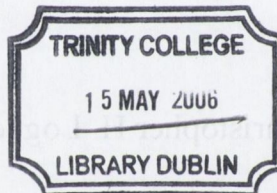
Department of Microbiology,
Moyne Institute of Preventive Medicine,
Trinity College, Dublin

September 2005 .

Sequence Analysis of Alphavirus Pathogenesis

A thesis submitted to the University of Dublin, Trinity College,
For the Degree of Doctor of Philosophy

by



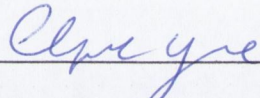
THESIS
7888

Department of Microbiology,
Moyne Institute of Preventive Medicine,
Trinity College, Dublin

September 2005

Declaration

This thesis is submitted by the undersigned to the University of Dublin, Trinity College for the examination of Doctorate of Philosophy. The work herein is entirely my own work and has not been submitted as an exercise for a degree to any other university. The librarian of Trinity College Dublin has my permission to lend or copy this thesis upon request.



Christopher H. Logue

Summary

This investigation involved the sequencing and characterisation of Chikungunya virus (CHIKV), a positive-stranded RNA virus with a genome spanning 11.8 kb. The prototype strain of CHIKV, termed Ross was used. This is the first complete genome of CHIKV to be sequenced and submitted to Genbank (Accession No. AF490259). CHIKV was analysed in relation to six other geographically distinct CHIKV strains and Semliki Forest virus which is well characterised in our laboratory. This is the first report of CHIKV being characterised both *in vitro* and *in vivo*. The rate of RNA production, rate of infection and cell tropism were investigated *in vitro*, while the multiplication of virus in the brains of infected Balb/c mice, mortality rates, and the neuropathology caused were studied *in vivo*. To fully ascertain the functions of various CHIKV genes and their possible roles in causing disease, the construction of a CHIKV full-length cDNA clone was subsequently carried out.

The existence of several different virulent and avirulent strains of SFV has allowed comparative analysis between them at the molecular level, which, combined with the development of SFV infectious cDNA clone technology, provides a useful model for analysis of the molecular basis of alphavirus neuropathogenesis.

In order to investigate whether the 5' UTR plays a role in determining the degree of virulence in infected adult mice, possibly through its involvement in RNA replication, SFV-5'UTR chimeras were constructed. This involved sequence analysis of the 5' UTRs and the construction of reciprocal chimeras that incorporated the 5' UTR nucleotide differences between virulent and avirulent strains of SFV. The survival rates of and the neuropathology caused in infected adult mice intranasally infected with each chimera and the infectious virus from three SFV infectious clones were determined.

The results showed that no marked difference between rates of RNA synthesis in BHK cells was detected. A significant increase in the survival of infected mice paralleled with a sharp reduction in neuropathology in the brains of infected mice however, was observed. Combined with sequence data this suggests that the SFV 5' UTR acts together with other genes within the SFV genome as a pathogenicity determinant.

Abbreviations

a.a.	amino acid(s)
AAP	Abridged Anchor Primer
Ab	antibody
BHK	baby hamster kidney
bp	base pair
°C	degrees Celsius
C	capsid
cDNA	complimentary DNA
CHIK V	Chikungunya virus
cm	centimetre(s)
CNP	2',3' – cyclic nucleotide 3' -phosphodiesterase
CNS	central nervous system
c.p.e.	cytopathogenic effect
c.p.m.	counts per minute
CSE	conserved sequence element
DAPI	4, -6, diamidino-2-phenylindole
DNA	deoxyribonucleic acid
dNTP	deoxynucleoside triphosphate
d.p.i.	days post infection
dsDNA	double stranded deoxyribonucleic acid
dsRNA	double stranded ribonucleic acid
<i>E. coli</i>	<i>Escherichia coli</i>
EEEV	Eastern equine encephalitis virus
ER	endoplasmic reticulum
g	gram
g	gravitational force
GSPs	genome specific primers
Gt	goat
h	hour(s)
h.p.i.	hours post infection
ic	infectious clones
i.c.	intracerebral(ly)

i.m.	intramuscular(ly)
i.n.	intranasal(ly)
i.p.	intraperitoneal(ly)
IPTG	Isopropyl- β -D-galactopyranoside
kb	kilobases
kDa	kilo Dalton
L28	Litmus 28
L38i	Litmus 38i
LF	L28i fragment
M	molar
mA	milliamps
MCS	multiple cloning site
mg	milligram(s)
MGC	mixed glial cell
MID	Middelburg virus
min	minute(s)
ml	millilitre(s)
mM	millimolar
M.O.I.	multiplicity of infection
mRNA	messenger ribonucleic acid
Ms	mouse
ng	nanogram(s)
NLS	nuclear localisation sequence
nm	nanometre(s)
nsP	non-structural protein
nt	nucleotide
ONNV	O’Nyong nyong virus
ORF	open reading frame
P	protein
pB	pBluescript SK II(+)
PBS	phosphate buffered saline
PCR	polymerase chain reaction
p.f.u.	plaque forming units
rATP	Adenosine 5’-Triphosphate

rCTP	Cytidine 5'-Triphosphate
rGTP	Guanosine 5'-Triphosphate
rUTP	Uridine 5'-Triphosphate
Rb	rabbit
RNA	Ribonucleic acid
rpm	revolutions per minute
RRV	Ross River virus
R.T.	room temperature
RT	reverse transcription
SDS	Sodium dodecyl sulphate
sec	second(s)
SFV	Semliki Forest virus
SINV	Sindbis virus
TCA	trichloroacetic acid
TD	Trinidad Donkey
ts	temperature sensitive
U	units
UAP	Universal Amplification Primer
UTR	Untranslated regions
VEEV	Venezuelen equine encephalitis virus
Vero	African green monkey kidney cells
vol	volume
WEEV	Western equine encephalitis virus
wt	weight
X-Gal	5-bromo-4-chloro-3-indolyl- β -galactopyranoside
μ Ci	micro Curie
μ g	microgram(s)
μ l	microlitre(s)
μ m	micrometer(s)
μ M	micromolar

Index of figures

Chapter one

- Figure 1.1 Phylogenetic tree of all Alphavirus species
- Figure 1.2 Structure of SFV virion
- Figure 1.3 Genome organisation of SFV and the pSP6-SFV4 infectious clone
- Figure 1.4 Schematic of the Alphavirus life cycle
- Figure 1.5 Replication and transcription of SFV RNA
- Figure 1.6 Processing pathways of SFV nonstructural proteins
- Figure 1.7 Processing of SFV structural Proteins
- Figure 1.8 Geographic distribution of CHIKV
- Figure 1.9 Phylogenetic analysis of CHIKV and ONNV
- Figure 1.10 Electron micrograph of purified CHIKV virions

Chapter two

- Figure 2.1 Schematic of 5' RACE PCR procedure
- Figure 2.2 Double-labelled immunofluorescence of CHIKV-infected rat oligodendrocytes
- Figure 2.3 CHIKV nonstructural and structural PCR amplicons
- Figure 2.4 Complete sequence of the Ross strain of Chikungunya virus
- Figure 2.5 Circularised annotated representation of Chikungunya Ross genome
- Figure 2.6 Stem-loops of CHIKV, CHIKV 37997, SFV-A7, and the Igbo Ora, Gulu and SG650 strains of ONNV
- Figure 2.7 Phylograms of CHIKV Ross vs other SF group Alphaviruses
- Figure 2.8 Immunofluorescence of uninfected oligodendrocytes
- Figure 2.9 Immunofluorescence of CHIKV infected oligodendrocytes
- Figure 2.10 Immunofluorescence of SFV-A7 infected oligodendrocytes
- Figure 2.11 Growth curves of CHIKV and SFV-A7 in BHK-21 cells

- Figure 2.12 Trypan blue exclusion assay of a primary mixed glial cell culture infected with CHIKV and SFV-A7
- Figure 2.13 Viral RNA synthesis in BHK-21 cells
- Figure 2.14 Growth curve of CHIKV and SFV-A7 in infected mouse brain following intranasal inoculation
- Figure 2.15 Survival curves for CHIKV and SFV-A7 with SFV4 and PBS controls
- Figure 2.16 Titres of virus in brains of Balb/c mice infected intranasally with seven geographically distinct strains of Chikungunya virus
- Figure 2.17 Plaque analysis of seven geographically distinct strains of Chikungunya virus, ONNV, SFV4 and SFV-A7.

Chapter three

- Figure 3.1 Linearised map of Chikungunya Ross genome showing the locations of 5 fragments of the CHIKV genome
- Figure 3.2 L28i with CHIKV fragment 1 (LF1)
- Figure 3.3 L28i with CHIKV fragment 2 (LF2)
- Figure 3.4 L28i with CHIKV fragment 3 (LF3)
- Figure 3.5 L28i with CHIKV fragment 4 (LF4)
- Figure 3.6 L28i with CHIKV fragment 5 (LF5)
- Figure 3.7 Construction of LF1-2 intermediate
- Figure 3.8 Construction of LF1-2 Δ *Nde I* intermediate
- Figure 3.9 L28i with CHIKV Fragments 1 and 2 Δ *Nde I* fragment plus Fragment 3 (LF1-2-3 Δ *Nde I*)
- Figure 3.10 L28i with complete CHIKV Fragments 1, 2, and 3 (LF1-2-3)
- Figure 3.11 LF5 with CHIKV Fragment 4 (LF5-4)
- Figure 3.12 pBluescript SK II [+] vector used for final stages of CHIKV full-length clone construction
- Figure 3.13 Oligonucleotide flanked with a *Kpn I* and *Bam HI* site at the 5' and 3' ends respectively
- Figure 3.14 Ligation of CHIKV 5' UTR into pBluescript SK II [+] vector (pB-5')

- Figure 3.15 pB5' with Fragment 123 (pB5'123)
- Figure 3.16 Construction of pB-5'123*45 Intermediate
- Figure 3.17 RT-PCR CHIKV fragment 3 / 4
- Figure 3.18 CHIKV full-length clone pB-5'12345 (pBCHIKV)
- Figure 3.19 CHIKV genome amplified over 5 fragments
- Figure 3.20 Four random LF1 colonies digested with *Nde I* and *Sac I*
- Figure 3.21 Five random LF2 colonies digested with *Stu I*
- Figure 3.22 Two random LF3 colonies digested with *Eco RV*
- Figure 3.23 Six random LF4 colonies digested with *Eco RV*
- Figure 3.24 Five random LF5 colonies digested with *Spe I* and *Stu I*
- Figure 3.25 Seven random LF1-2 colonies digested with *Nde I*
- Figure 3.26 LF1-2-3 Δ *Nde I* undigested, digested with *Nde I*, dephosphorylated and the excised *Nde I* fragment from LF1-2
- Figure 3.27 LF1-2-3 colony digested with *Xmn I*
- Figure 3.28 Three LF5-4 colonies digested with *Cla I* and *Eco RV*
- Figure 3.29 Seven pB-5'123 colonies digested with *Eco RV*
- Figure 3.30 Five pB-5'123*45 colonies digested with *Eco RV*
- Figure 3.31 Pooled Fragment 3 / 4 PCR amplicons
- Figure 3.32 pB-5'12345 CHIKV cDNA digested with *Eco RV*

Chapter four

- Figure 4.1 Schematic (1 of 2) of strategy used to site-mutagenise SFV infectious clone 5' UTRs to SFV-A7 5' UTR
- Figure 4.2 Schematic (2 of 2) of strategy used to site-mutagenise SFV infectious clone 5' UTRs to SFV-A7 5' UTR
- Figure 4.3 Schematic of strategy used to create reciprocal pSP6-SFV4 / rA7[74] 5' UTR chimeras
- Figure 4.4 Schematic of strategy used to create reciprocal pSP6-CA7 / rA7[74] 5' UTR chimeras
- Figure 4.5 Site-mutagenised clones 1-5 digested with *Sph I* and *Eco RV*
- Figure 4.6 SFV 5' UTRs

- Figure 4.7 In vitro RNA Transcription
- Figure 4.8 Sequence alignment of SFV 5' untranslated regions
- Figure 4.9 Secondary structure of SFV 5' untranslated regions
- Figure 4.10 Survival of Balb/c mice intranasally infected with SFV
- Figure 4.11 SFV titres in brains of intranasally infected Balb/c mice
- Figure 4.12 Sequence alignment of SFV 5' UTR chimeras
- Figure 4.13 Survival of Balb/c mice intranasally infected with SFV-5' UTR chimeric viruses
- Figure 4.14 RNA synthesis of SFV and SFV 5' UTR chimeric virus in BHK-21 cells

Chapter five

- Figure 5.1 Illustrative representation of the cells of the CNS
- Figure 5.2 Diagrammatic representation of a neuron
- Figure 5.3 Virus infection via the olfactory route
- Figure 5.4 Pathology photos

Index of tables

Chapter one

Table 1.1 Chronological order of CHIKV outbreaks

Chapter two

Table 2.1 Virus strains used in the characterization of Chikungunya virus

Table 2.2 Primers designed from O'nyong nyong virus Gulu to amplify the CHIKV non- structural polyprotein

Table 2.3 Primers designed from CHIKV vaccine virus to amplify the CHIKV structural polyprotein

Table 2.4 Thermocycling conditions used for PCR

Table 2.5 Percentage identity of individual CHIKV genes and other SFV subgroup alphaviruses

Chapter three

Table 3.1 Restriction enzymes used in the construction of the CHIKV full-length clone with their respective 10X Buffers

Table 3.2 Primers designed to amplify the CHIKV genome in five fragments and a 106 nt CHIKV 5' UTR oligonucleotide and its complement.

Chapter four

Table 4.1 Amino acid analysis of SFV non-structural polyprotein

Table 4.2 Amino acid analysis of SFV structural polyprotein

Table 4.3 Amino acid analysis of SFV 3' untranslated region

Table of Contents

Summary.....	i
Abbreviations.....	ii
Index of Figures.....	v
Index of Tables.....	ix

Chapter One – General Introduction

1.	Introduction	1
1.1	Alphaviruses	1
1.2	Semliki Forest Virus	3
1.2.1	Origins and Strains of SFV	4
1.2.2	SFV Virion	5
1.2.3	SFV Genome	7
1.2.4	SFV Replication cycle	10
1.2.4.1	Viral Entry	10
1.2.4.2	Viral Replication	11
1.2.4.3	Processing of non-structural proteins and their functions	15
1.2.4.3.1	nsP1	17
1.2.4.3.2	nsP2	17
1.2.4.3.3	nsP3	18
1.2.4.3.4	nsP4	18
1.2.4.4	Processing of structural proteins and virus assembly and maturation	19
1.2.4.5	Pathogenesis of SFV in mice	20
1.2.4.6	Functions of the conserved sequence elements of the SFV genome	23
1.2.4.6.1	5' Untranslated region	23
1.2.4.6.2	51nucleotide CSE in nsP1	25
1.2.4.6.3	Junction region	26
1.2.4.6.4	3' Untranslated region	27
1.2.4.7	SFV as a viral vector	29
1.3	Chikungunya Virus	30
1.3.1	Origins and Strains	32
1.3.2	Structure of CHIKV	36

1.3.3	Pathogenicity of CHIKV infection	37
1.4	Project Aims	38

Chapter Two – Sequencing and Characterisation of the Ross strain of Chikungunya Virus

2.1	Introduction	40
2.2	Sequencing strategy of CHIKV genome	41
2.3	5' RACE PCR	41
2.4	Phylogenetic Analysis	43
2.5	Virus growth <i>in vitro</i>	43
2.6	Virus growth <i>in vivo</i>	43
2.7	Virus RNA synthesis <i>in vitro</i>	44
2.8	Cell Tropism of CHIKV	44
2.9	Plaque analysis	45
2.10	Materials and Methods	46
2.10.1	Cells	46
2.10.1.1	Baby Hamster Kidney Cells	46
2.10.1.2	Neonate rat mixed glial primary cells	46
2.10.2	Viruses	47
2.10.2.1	Virus strains	47
2.10.2.2	Growth and harvest of virus	48
2.10.2.3	Plaque assays	48
2.10.3	Preparation of virus DNA	49
2.10.3.1	Virus RNA isolation	49
2.10.3.2	cDNA amplification	49
2.10.3.3	Primer design	50
2.10.3.3.1	CHIKV non-structural protein primers	50
2.10.3.3.2	CHIKV structural primers	50
2.10.3.3.3	CHIKV 5' untranslated region primers	53
2.10.3.3.4	Polymerase Chain Reaction (PCR) thermocycling conditions	53
2.10.3.3.5	PCR	55

2.10.4	Manipulation of virus DNA	55
2.10.4.1	DNA purification I	55
2.10.4.2	Restriction digestion	56
2.10.4.3	DNA purification II	56
2.10.4.4	Preparation of Litmus 28 cloning vector	56
2.10.5.4	Ligation into L28	57
2.10.4.6	Preparation of competent <i>E. coli</i> DH5 α cells	57
2.10.4.7	Transformation	57
2.10.4.8	Colony selection and linearization	58
2.10.4.9	Sequencing and sequence alignment	58
2.10.5	<i>In vitro</i> analyses	59
2.10.5.1	CHIKV growth curves in BHK-21 cells	59
2.10.5.2	Mixed glial cell viability assay	59
2.10.5.3	Virus RNA synthesis of CHIKV, SFV-A7 and six geographically distinct strains	60
2.10.5.4	Plaque analysis	61
2.10.5.5	Immunofluorescence of virus infected oligodendrocytes	61
2.10.5.5.1	Production of antibody	61
2.10.5.5.2	Preparation of cells for immunofluorescent labelling	61
2.10.5.5.3	Immunofluorescent labelling of virus antigen	62
2.10.5.5.4	Immunofluorescent labelling of oligodendrocytes	62
2.10.6	<i>In vivo</i> analyses	63
2.10.6.1	Infection of Balb/c mice with CHIKV and SFV-A7	63
2.10.6.2	Virus titres in brains of Balb/c mice infected with CHIKV and SFV-A7	63
2.10.6.3	Virus titres in Balb/c brains infected with CHIKV and six geographically distinct Chikungunya virus strains	63
2.10.6.4	Survival of Balb/c infected with CHIKV and six geographically distinct Chikungunya virus strains	64
2.11	Results	65
2.11.1	Sequence of Chikungunya Ross (CHIKV)	65
2.11.1.1	Non-translated regions of the genome	70
2.11.1.2	Non-structural genes of CHIKV	72
2.11.1.3	Structural genes of CHIKV	72

2.11.1.4	Percentage identity in nucleotide and deduced amino acid sequences between CHIKV and other alphaviruses	73
2.11.1.5	Phylogenetic analysis of CHIKV and other alphaviruses	73
2.11.1.6	Immunofluorescent labelling of virus-infected oligodendrocytes	73
2.11.1.7	Immunofluorescence of CHIKV-infected oligodendrocytes	74
2.11.1.8	Immunofluorescence of SFV-A7-infected oligodendrocytes	74
2.11.1.9	Growth curves of CHIKV and SFV-A7 in BHK-21 cells	74
2.11.1.10	Trypan-blue exclusion assay of a mixed glial cell culture infected with CHIKV and SFV-A7	74
2.11.1.11	Viral RNA synthesis in BHK-21 cells	75
2.11.1.12	Growth curves of CHIKV and SFV-A7 in infected mouse brain following intranasal inoculation	75
2.11.1.13	Survival curves of CHIKV and SFV-A7	75
2.11.1.14	Survival curves of CHIKV and six geographically distinct strains of CHIKV	75
2.11.1.15	Growth curves of CHIKV and six geographically distinct strains of CHIKV in infected mouse brain following intranasal inoculation	76
2.11.1.16	Plaque Analysis	76
2.12	Discussion	87

Chapter 3 – Construction of a Full-length Chikungunya cDNA clone

3.1	Introduction	89
3.1.1	Alphavirus infectious clones	89
3.1.2	Chikungunya vaccine	89
3.1.3	Construction of a Chikungunya full-length clone	90
3.1.4	TripleMaster PCR system	90
3.2	Materials and Methods	91
3.2.1	Molecular biology techniques used in the construction of a CHIKV full-length clone.	91
3.2.1.1	Cloning vectors	91
3.2.1.2	Restriction enzymes	91

3.2.1.3	Dephosphorylation of linearised L28i and pB cloning vectors	92
3.2.1.4	Ligation of fragments into cloning vectors	92
3.2.1.5	Transformation, colony selection and confirmation analysis	93
3.2.1.6	Primer design	93
3.2.1.7	Polymerase Chain Reaction (PCR)	94
3.2.1.8	DNA purification	94
3.2.2	Preparation and ligation of CHIKV fragments 1-5 into L28i	96
3.2.2.1	Preparation of L28i	96
3.2.2.2	Restriction Digestion	96
3.2.2.3	Ligation of CHIKV fragments 1-5 into L28i	96
3.2.2.4	Confirmation analysis of L28i – CHIKV fragment colonies	97
3.2.2.5	Confirmation analysis of L28i – Fragment 1	97
3.2.2.6	Confirmation analysis of L28i – Fragment 2	98
3.2.2.7	Confirmation analysis of L28i – Fragment 3	99
3.2.2.8	Confirmation analysis of L28i – Fragment 4	100
3.2.2.9	Confirmation analysis of L28i – Fragment 5	101
3.2.3	Construction of L28i / CHIKV Fragment (LF) intermediates	102
3.2.3.1	Construction of LF1-2 intermediate	102
3.2.3.2	Construction of LF1-2 Δ <i>Nde I</i> intermediate	103
3.2.3.3	Construction of LF1-2-3 Δ <i>Nde I</i> intermediate	104
3.2.3.4	Reinsertion of <i>Nde I</i> fragment into LF1-2-3 Δ <i>Nde I</i> intermediate	105
3.2.3.5	Construction of LF5-4 intermediate	106
3.2.4	Construction of pBluescript SK II [+] / CHIKV Fragment intermediate	107
3.2.4.1	Preparation of pBluescript SK II [+] (pB)	108
3.2.4.2	Production of CHIKV 5' UTR oligonucleotide	108
3.2.4.3	Ligation of CHIKV 5' UTR into pB cloning vector	109
3.2.4.4	Construction of pB-5' plus Fragment 1-2-3 intermediate (pB-5'123)	110
3.2.4.5	Construction of pB-5' 123 plus Fragment 5-4 intermediate (pB-5'123*45)	111
3.2.4.6	Insertion of RT-PCR 3 / 4 <i>Cla I</i> Fragment	112
3.2.4.7	Insertion of a Poly (A) tail	114
3.2.5	Production of RNA from pB-5'12345 CHIKV cDNA infectious clone (pBCHIKV)	114
3.2.6	Electroporation in BHK-21 cells	114

3.3	Results	116
3.3.1	CHIKV genome in 5 Fragments	116
3.3.2	CHIKV Fragments ligated into L28i	116
3.3.2.1	LF1	116
3.3.2.2	LF2	117
3.3.2.3	LF3	117
3.3.2.4	LF4	118
3.3.2.5	LF5	118
3.3.2.6	LF1-2 Intermediate	119
3.3.2.7	Religation of <i>Nde I</i> fragment into LF1-2-3 Δ <i>Nde I</i> Intermediate	119
3.3.2.8	LF1-2-3	120
3.3.2.9	LF5-4	121
3.3.2.10	pB-5'123	122
3.3.2.11	pB-5'123*45	123
3.3.2.12	RT-Fragment 3 / 4 (prior to <i>Cla I</i> digestion)	124
3.3.2.13	pB-5'12345	125
3.4	Discussion	126

Chapter Four – Analysis of the Semliki Forest Virus 5' Untranslated region as a pathogenicity determinant

4.1	Introduction	130
4.1.1	SFV-induced neuropathogenesis of the murine CNS	130
4.1.2	Virus produced from SFV infectious clones	130
4.1.3	Analysis of SFV genomes	131
4.1.4	Virulence determinants of SFV	131
4.1.5	Construction of SFV 5' UTR chimeras	132
4.2	Materials and Methods	133
4.2.1	Sequence analysis of SFV genomes	133
4.2.2	SFV 5' UTR Sequences	133
4.2.3	Virus strains and infectious clones	133

4.2.4	Preparation of virus DNA	134
4.2.4.1	<i>Spe I</i> linearisation of SFV infectious clones	134
4.2.4.2	<i>In vitro</i> SP6 RNA transcription	134
4.2.4.3	Electroporation	135
4.2.4.4	Harvesting SFV infectious virus	135
4.2.5	Amplification of SFV 5' UTRs	135
4.2.5.1	Primer Design	136
4.2.5.2	DNA Purification	136
4.2.5.3	Sequence Alignment	137
4.2.5.4	Prediction of Secondary structures	137
4.2.6	Survival of Balb/c mice infected with SFV-A7, SFV-L10 and infectious virus produced from pSP6-SFV4, SP6-CA7 and rA7[74]	137
4.2.7	Virus titres in BALB/c brains infected with SFV-A7, SFV-L10 and infectious virus produced from pSP6-SFV4, SP6-CA7 and rA7[74]	137
4.2.8	Construction of SFV 5' UTR chimeras	138
4.2.8.1	Preparation of chimeras I – Restriction Digestion	141
4.2.8.1.1	Preparation of SFV infectious clones with restriction enzyme <i>Nde I</i>	141
4.2.8.1.2	Preparation of SP6-SFV Δ <i>Nde I</i> infectious clones with <i>Sph I</i> and <i>Eco RV</i>	141
4.2.8.1.3	Preparation of pSP6-SFV4 / rA7[74] 5' UTR reciprocal chimeras	142
4.2.8.1.4	Preparation of SP6-CA7 / rA7[74] 5' UTR chimera	142
4.2.8.2	Preparation of SP6-SFV / SFV-A7 5' UTR chimeras	145
4.2.8.2.1	Restriction digestion of L38i with <i>Sph I</i> and <i>Eco RV</i>	145
4.2.8.2.2	Site-directed mutagenesis	145
4.2.8.2.3	PCR	147
4.2.8.2.4	Excision of site-mutated SFV-A7 5' UTR and ligation into SP6-SFV Δ <i>Nde I</i> (Δ <i>Sph I</i> / <i>Eco RV</i>) infectious clones	147
4.2.8.2.5	Religation of respective <i>Nde I</i> fragments	147
4.2.8.2.6	PCR confirmation	148
4.2.8.2.7	Production of infectious chimeric virus	148
4.2.8.2.8	Infectious virus RNA isolation and 5' RACE PCR confirmation of 5' UTRs	148
4.2.8.2.9	Plaque assay	148
4.2.8.2.10	Intranasal infection of Balb/c mice	150
4.2.8.2.11	RNA synthesis of SFV 5' UTR chimeric virus	150

4.3	Results	153
4.3.1	Analysis of SFV strains	153
4.3.1.1	Amino acid sequence analysis of prototype virulent and avirulent SFV strains	153
4.3.1.2	Sequence of SFV 5' UTR	156
4.3.1.3	Prediction of SFV 5' UTR secondary structure	157
4.3.1.4	Survival of Balb/c mice intranasally infected with SFV	158
4.3.1.5	Virus titres in Balb/c mice intranasally infected with SFV	158
4.3.2	Construction and analysis of SFV 5' UTR chimeric virus	162
4.3.2.1	Sequence of SFV chimera 5' UTRs	162
4.3.2.2	Survival of Balb/c mice intranasally infected with SFV 5' UTR chimeric virus	162
4.3.2.3	RNA synthesis of SFV strains and SFV 5' UTR chimeric viruses	162
4.4	Discussion	167

Chapter Five – Pathology

5.1	Introduction	172
5.2	Cells of the Central Nervous System	172
5.2.1	Neurons	174
5.2.2	Astrocytes	176
5.2.3	Oligodendrocytes	176
5.2.4	Epenymal Cells	177
5.2.5	Microglia	177
5.3	Pathology and its terminology	178
5.3.1	Necrosis	178
5.3.2	Demyelination	179
5.3.3	Gliosis	179
5.3.4	Inflammatory lesions	179
5.3.5	Spongiform degeneration	179
5.4	Routes of infection into the CNS	180
5.4.1	The Blood-brain barrier (BBB)	180

5.4.2	Haematogenous route	180
5.4.3	The Neural route	180
5.4.4	The olfactory system	181
5.5	Materials and Methods	183
5.5.1	Intranasal infection of Balb/c mice	183
5.5.2	Brain Perfusion and Fixation	183
5.5.3	Paraffin embedding and sectioning	183
5.5.4	Histological staining	184
5.5.5	Pathology Grading System	184
5.6	Results	185
5.6.1	Chikungunya virus – Seven geographically distinct strains	185
5.6.1.1	CHIKV – Ross	185
5.6.1.2	CHIKV – DaKAR	185
5.6.1.3	CHIKV – 37997	185
5.6.1.4	CHIKV – PO731460	186
5.6.1.5	CHIKV – 181/25	186
5.6.1.6	CHIKV PhH15483	186
5.6.1.7	CHIKV – SV450	186
5.6.2	Semliki Forest Virus strains	186
5.6.2.1	SFV-A7 and SFV-A7[74]	186
5.6.2.2	SFV4	186
5.6.2.3	CA7	186
5.6.2.4	rA7[74]	186
5.6.3	SFV 5' UTR Chimeric viruses	187
5.6.3.1	CA7 + SFV-A7 5' UTR	187
5.6.3.2	CA7 + rA7[74] 5' UTR	187
5.6.3.3	rA7[74] + SFV-A7 5' UTR	187
5.6.3.4	rA7[74] + SFV4 5' UTR	187
5.7	Discussion	189
	Chapter Six – General Discussion	190
	Chapter Seven – References	198

Chapter One

General Introduction

1. INTRODUCTION

1.1 Alphaviruses

The *Alphavirus* genus of the *Togaviridae* family is comprised of 26 globally distributed members, inclusion in the genus was originally based on serological cross-reaction; however more recently comparison of partial E1 envelope glycoprotein gene sequences has been used to construct phylogenetic trees of the alphaviruses (Powers *et al.*, 2001, figure 1.1). In nature, alphaviruses are transmitted by arthropods to vertebrates such as birds, small rodents and occasionally humans. Alphavirus infection in man causes a range of symptoms from subclinical or mild febrile illness to high fever, headache, myalgia, arthritis and occasionally encephalitis. On the basis of nucleotide and amino acid comparisons between alphaviruses, specifically between regions in the non-structural proteins (Strauss and Strauss, 1994) , the genus can be divided into two subgroups: The Old World viruses including Semliki Forest Virus (SFV), Sindbis Virus (SINV), Chikungunya virus (CHIKV), O'Nyong nyong virus (ONNV), Ross River virus (RRV), Middelburg (MID), and the New World alphaviruses including Venezuelan equine encephalitis virus (VEEV), Western equine encephalitis virus (WEEV), and Eastern equine encephalitis virus (EEEV). The Old World alphaviruses are mainly distributed throughout Africa and South-East Asia although they have occasionally also been found in Northern Europe, and RRV has been isolated in Australia (Calisher *et al.*, 1985). The New World alphaviruses are predominantly found in the Americas and regularly cause lethal encephalitis in humans although these are in low numbers (Whitley, 1990). Although alphaviruses are generally divided into the New World and Old World viruses, recombinants between viruses from both worlds are also present. CHIKV and ONNV have been responsible for numerous well documented outbreaks in Africa, causing a painful but not life-threatening illness in over two million individuals (Johnston and Peters, 1996). Alphavirus epidemics are common with the most recent outbreak of CHIKV occurring in Ile de la Reunion between 28th March and 20th June 2005, infecting 1922 people, (ProMED, 2005) Alphaviruses infect laboratory animals such as mice, hamsters, guinea pigs and rats, making these viruses ideal to use as models to evaluate their pathogenesis in vertebrates.

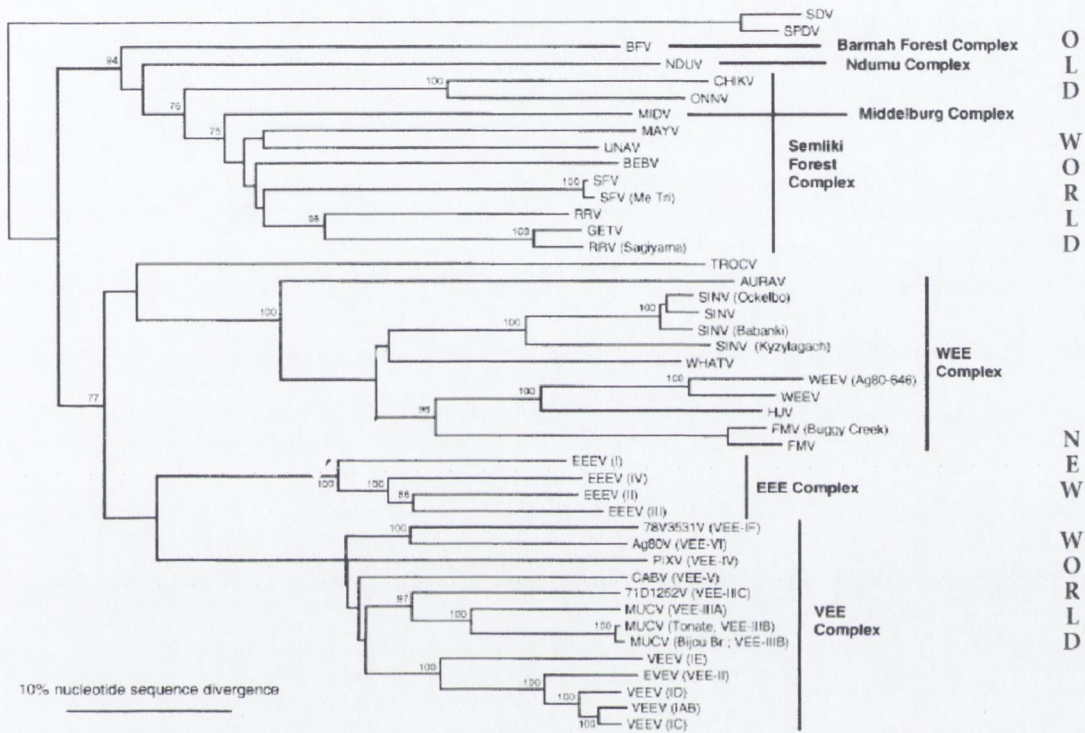


Figure 1.1 Phylogenetic tree of Alphavirus species

Phylogenetic tree is divided into 7 individual complexes, WEE, EEE, and VEE complexes make up the New World alphaviruses, whereas Barmah Forest, Ndumu, Middelburg and Semliki Forest virus make up the Old World alphaviruses. Semliki Forest, Chikungunya and O’nyong nyong viruses are members of the SFV complex. This phylogenetic tree was adapted from Powers *et al.* (2001) who generated it from partial E1 envelope glycoprotein gene sequences by using the neighbour-joining program with the F84 distance formula. It does not however, include recombinant species between Old and New World viruses. It has been used with kind permission of Dr. Ann Powers, CDC, Fort Collins, USA.

Alphaviruses are widely used as tools in molecular biology to study the relationship between the virus and host immune system in disease outcome, to elucidate what viral and host genetic factors may be responsible for the onset of disease and what cellular tropisms may be involved in virus infection. An important development in the studies of alphaviruses has been the construction of full length cDNA clones, containing the entire viral genome positioned downstream of a promoter that is used to drive RNA synthesis (Rice *et al.*, 1987; Davies *et al.*, 1989; Liljeström *et al.*, 1991; Kuhn *et al.*, 1991; Tarbatt *et al.*, 1997; Tuittila *et al.*, 2000). The resulting *in vitro* transcribed RNA can then be transfected or electroporated into cells. Transfection of full length viral RNA results in the replication and production of infectious virus. Infectious clones have been instrumental in the study of the synthesis and intracellular transport of membrane proteins (reviewed by Lundstrom, 1997), the analysis of factors influencing viral pathogenesis and cell tropism in animal models, and the identification of domains known to be essential for the replication of RNA. (Lopez *et al.*, 1994; Smyth *et al.*, 1997; Yao *et al.*, 1998)

1.2 Semliki Forest Virus

Semliki Forest Virus (SFV) is an arthropod-borne neurotropic virus that infects vertebrates. SFV is generally thought to be non-pathogenic in man with most human infections of SFV being subclinical. However, in 1979 a laboratory worker in Germany working on the Osterrieth strain of SFV died from a fatal encephalitis. SFV antibody was not detected until the time of death and the individual had a history of chronic pulmonary infection suggesting that her immune system was suppressed (Willems *et al.*, 1979). An outbreak of SFV that occurred in the Central African Republic in 1987 was reported by Mathiot *et al* in 1999. SFV was isolated from serum samples from individuals with mild clinical symptoms including fever, persistent headache, myalgias and arthralgias. SFV infects both adult and neonate mice and has an age and strain-dependent pathology including fatal encephalitis, teratogenesis, and virus-induced demyelination, thus providing a useful model for the study of viral neuropathogenesis (Atkins *et al.*, 1985). The existence of several different virulent and avirulent strains of SFV which differ in their neuropathogenicity has allowed comparative analysis between them at the molecular

level which, combined with the availability of SFV infectious cDNA clones (Liljeström *et al.*, 1991), provides a useful model for analysis of the molecular basis of alphavirus neuropathogenesis (Atkins *et al.*, 1985).

1.2.1 Origins and Strains of SFV

The original SFV strain was isolated from a pool of 130 female *Aedes abnormalis* Theobald mosquitoes by Smithburn and Haddow in Uganda in 1944. Although serologically indistinguishable from one another, the differing strains of SFV are distinguished on their degree of virulence following intraperitoneal (i.p.) inoculation of mice, guinea-pigs and rabbits. (Bradish *et al.*, 1971). The strain with the highest virulence; L10, a derivative of the original 1944 isolate is lethal to mice of any age causing encephalitis, irrespective of route. (Smithburn and Haddow, 1944). The least virulent strain of SFV, AR2066, designated A7 after seven passages in neonatal mouse brain, was isolated from a pool of 97 *Aedes argenteopunctatus* mosquitoes in Mozambique in 1959 (McIntosh *et al.*, 1961). A7 is not lethal in adult mice with mice appearing normal at all times, although inflammatory demyelinating lesions are present in the brain; A7 is however lethal in suckling mice (Atkins *et al.*, 1982). Infection of mice with A7 provides immune protection against challenge with a lethal dose of the virulent L10 strain. Strains of SFV currently used in laboratories were derived from these two virus strains. These include a temperature sensitive mutant of A7 designated *ts 22* which is teratogenic to the foetus (Hearne *et al.*, 1987) and a chemical mutant of L10 designated M9 (Barrett *et al.*, 1980). M9 produces similar brain lesions to those seen with A7, however unlike L10 it does not produce the characteristic fatal encephalitis in mice (Atkins and Sheahan., 1982). An infectious clone was constructed by Liljeström *et al* in 1991, designated pSP6-SFV4. The prototype strain from which pSP6-SFV4 was constructed (L10) resulted in a loss of some virulence due to an undetermined number of passages in cell culture between 1961 and 1991 (Glasgow *et al.*, 1991). Following *in vitro* transcription and electroporation of RNA derived from pSP6-SFV4, infectious SFV4 virus is produced. SFV4, like L10 produces lethal encephalitis in adult mice irrespective of route, however, SFV4 shows reduced virulence in mice following i.p. inoculation killing only 50-60% of mice within 5-6 days post infection. Both viruses

cause 100% mortality in intranasally (i.n.) infected mice with a mean day of death 4-5 days post infection (Atkins *et al.*, 1990). An avirulent strain designated SFV-A7[74] was derived by further selection for avirulence from the SFV-A7 strain (Bradish *et al.*, 1971), the nomenclature based on the 74th plaque being selected. The pathogenicity of these SFV strains is discussed in more detail in section 1.2.4.5.

1.2.2 SFV Virion

The virion of SFV consists of a nucleocapsid enclosed in an envelope of host-derived membrane from which 80 virus spike glycoproteins protrude (Vogel *et al.*, 1986). The nucleocapsid is made up of 240 copies of a single repeating capsid (C) protein that is complexed with the single-stranded positive-sense RNA genome. (Schlesinger and Schlesinger, 1996). The spike proteins of the envelope are composed of three virus-specific glycoproteins: E1 (MW 49 kDa), E2 (MW, 52 kDa) and E3 (MW 10 kDa), with three heterotrimers forming each spike (Simons *et al.*, 1973, Garoff *et al.*, 1974). The nucleocapsid and viral envelope are organised into T = 4 icosahedral lattices (Choi *et al.*, 1991, Paredes *et al.*, 1992, 1993, von Bonsdorff and Harrison, 1975). This structure renders the encapsidated RNA sensitive to RNase, and shrinking at low pH with subsequent loss of viral RNA has been observed (Soderland *et al.*, 1979)

The C protein is made up of 267 amino acids (aa) and has a molecular weight of 30 kDa. It contains a conserved C-terminal chymotrypsin-like serine protease region (Choi *et al.*, 1991) that enables cleavage from the nascent structural polypeptide (Hahn and Strauss, 1990, Melancon and Garoff, 1987). An RNA-binding domain resides in the N-terminus of the C protein, and is recognised by the signal recognition particle targeting the nascent chain-ribosome complex to the endoplasmic reticulum (ER) membrane (Owen and Kuhn, 1996, Bonatti *et al.*, 1984, Garoff *et al.*, 1978). It is subsequently cleaved into the three structural membrane proteins p62 (precursor of E2 and E3), 6K and E1 (Liljeström and Garoff, 1991, Garoff *et al.*, 1990, Melancon and Garoff, 1987) E2 and E1, are transmembrane glycoproteins with short internal domains; they are intertwined in a heterodimer formation to which E3, a peripheral protein, is associated non-covalently (Garoff and Simons, 1974; Garoff and Soderlund, 1978).

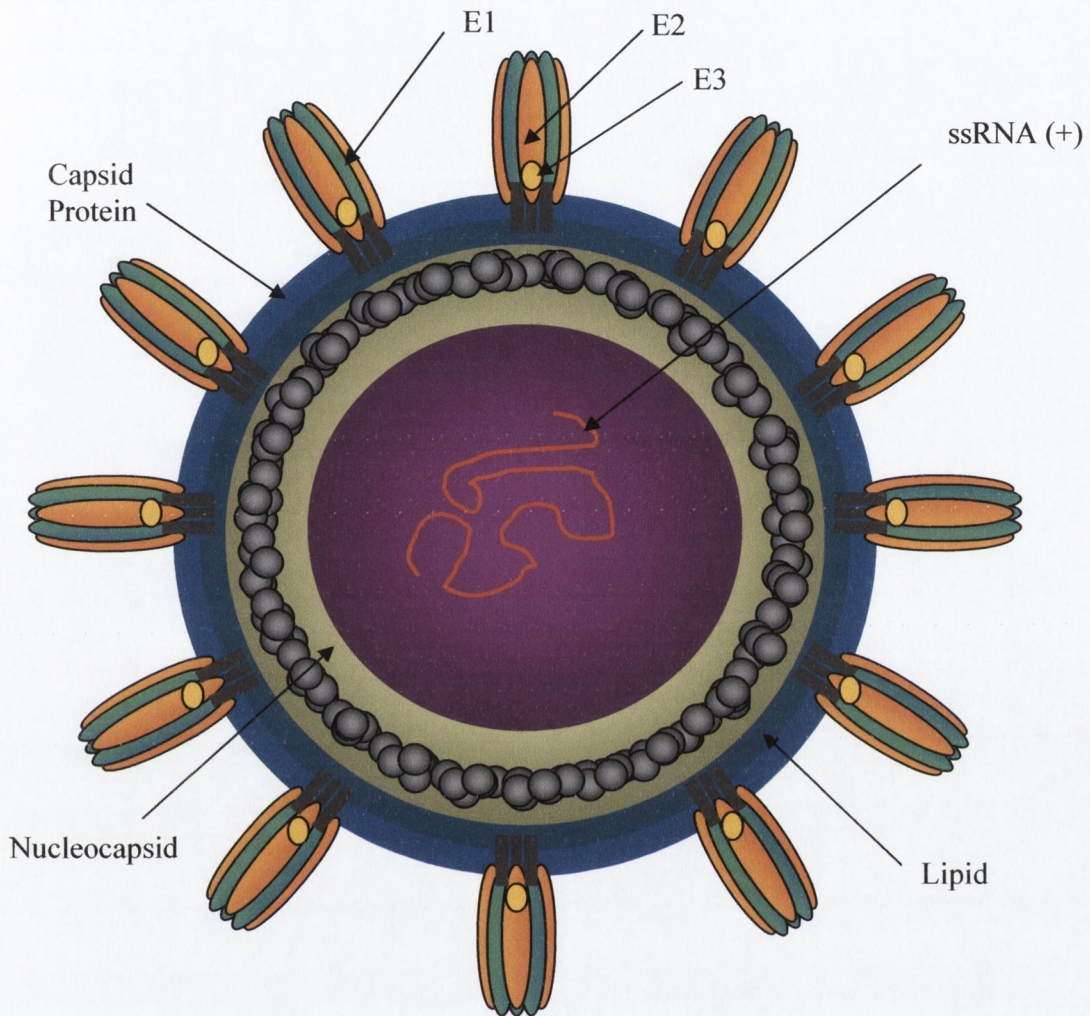


Figure 1.2 Structure of SFV Virion

The SFV virion is 60-65 nm in diameter and consists of a nucleocapsid containing 240 copies of the Capsid protein and a single stranded RNA genome of positive polarity. The host-derived lipid membrane contains 80 spikes, each consisting of 3 copies of the E1, E2 and E3 glycoproteins.

In contrast to SFV, the E3 protein of both CHIKV and SINV is released in the culture medium and only E1 and E2 glycoproteins are found on the viral envelope (Simizu *et al.*, 1984, Mayne *et al.*, 1984). 6K remains in the cytoplasm of infected cells, this is discussed in more detail in section 1.2.4.4

The E1 glycoprotein is made up of 438 aa with a molecular weight of 49 kDa and contains a hydrophobic transmembrane region separating the glycosylated ectodomain at the N-terminus from two arginine residues at its C-terminal (Wahlberg *et al.*, 1992) making it responsible for maintaining spike stability, enabling viral entry and fusion.

The E2 glycoprotein has a molecular weight of 52 kDa and consists of 422 aa, that contain a large N-terminal ectodomain that serves as a receptor binding subunit (Simmons and Garoff, 1980). Also within the E2 glycoprotein of the viral membrane, a hydrophobic transmembrane region and a 31 aa C-terminal region have been shown to interact with the nucleocapsid (Metsikko and Garoff, 1990, Skoging *et al.*, 1996). As previously mentioned, E2 is formed from the precursor p62 which is cleaved during virus maturation, which also contains a smaller 66 aa protein (E3) with a molecular weight of 10 kDa. The function of E3 has yet to be completely determined however; the N-terminus functions as a signal peptide for p62 during viral replication (Sariola *et al.*, 1995) and it remains non-covalently associated with the SFV virion, although is shed into the culture fluid upon maturation in the cases of SINV and CHIKV (Garoff *et al.*, 1974, Simizu *et al.*, 1984, de Curtis and Simons, 1988). Another small 60 aa viral membrane protein with a molecular weight of 6 kDa termed 6K is present in submolar quantities and is thought to be involved in viral budding (Loewy *et al.*, 1995; Strauss and Strauss, 1994; McInerney *et al.*, 2004).

1.2.3 SFV Genome

Within the SFV nucleocapsid is the viral RNA which is single stranded and of positive polarity, which functions directly as mRNA (Kaarianen *et al.*, 1987). The genome has a sedimentation coefficient of 42S with the 5' end capped with a 7-methylguanosine residue ($m^7GpppN_1pN_2pN_3$) and has a polyadenylated 3' end (Clegg and Kennedy, 1974; Schlesinger *et al.*, 1990). The SFV genome size is approximately 11.4 kb (Garoff *et al.*, 1980; Takkinen, 1986) and contains untranslated regions (UTRs)

at both the 5' and 3' ends and a short UTR between the two open reading frames of the genome termed the junction region (Strauss *et al.*, 1984).

The 5' two-thirds of the SFV genome code for the non-structural polyprotein precursor which is processed to yield four non-structural proteins termed nsP1 to nsP4 which are required for RNA replication and transcription (Strauss and Strauss, 1983; Takkinen, 1986). The remaining one third of the genome serves as mRNA for the synthesis of the structural proteins, although these are translated from a smaller co-linear subgenomic 26S RNA rather than from the 42S RNA. The 26S RNA species which is capped and polyadenylated codes for the capsid, p62 (a precursor of the glycoproteins E2 and E3), 6K and E1 structural proteins. (Garoff *et al.*, 1980). A graphic representation of the linearised SFV genome can be seen in figure 1.3.

Four conserved regions or sequence elements (CSEs) have been identified through sequence analysis of different alphaviruses and are thought to play important roles in RNA replication (Ou *et al.*, 1993). Of the four CSEs found in the SFV genome, three are located in untranslated regions. The first CSE is a conserved stem-loop structure formed by a sequence of 40 nt in the 5' UTR (Ou *et al.*, 1983; Levinson *et al.*, 1990). The second CSE is a region of 51 nt found at the 5' end of the nsP1 protein coding sequence which can form two stable hairpin structures (Ou *et al.*, 1983). Further downstream a 21 nt CSE spanning the untranslated junction region between the non-structural and structural genes including the initiation of translation sequence can be found. The final CSE is found in the 3' UTR and comprises 19 nt immediately preceding the poly (A) tail (Levinson *et al.*, 1990). These four sequence elements are discussed in more detail in section 1.2.4.6.

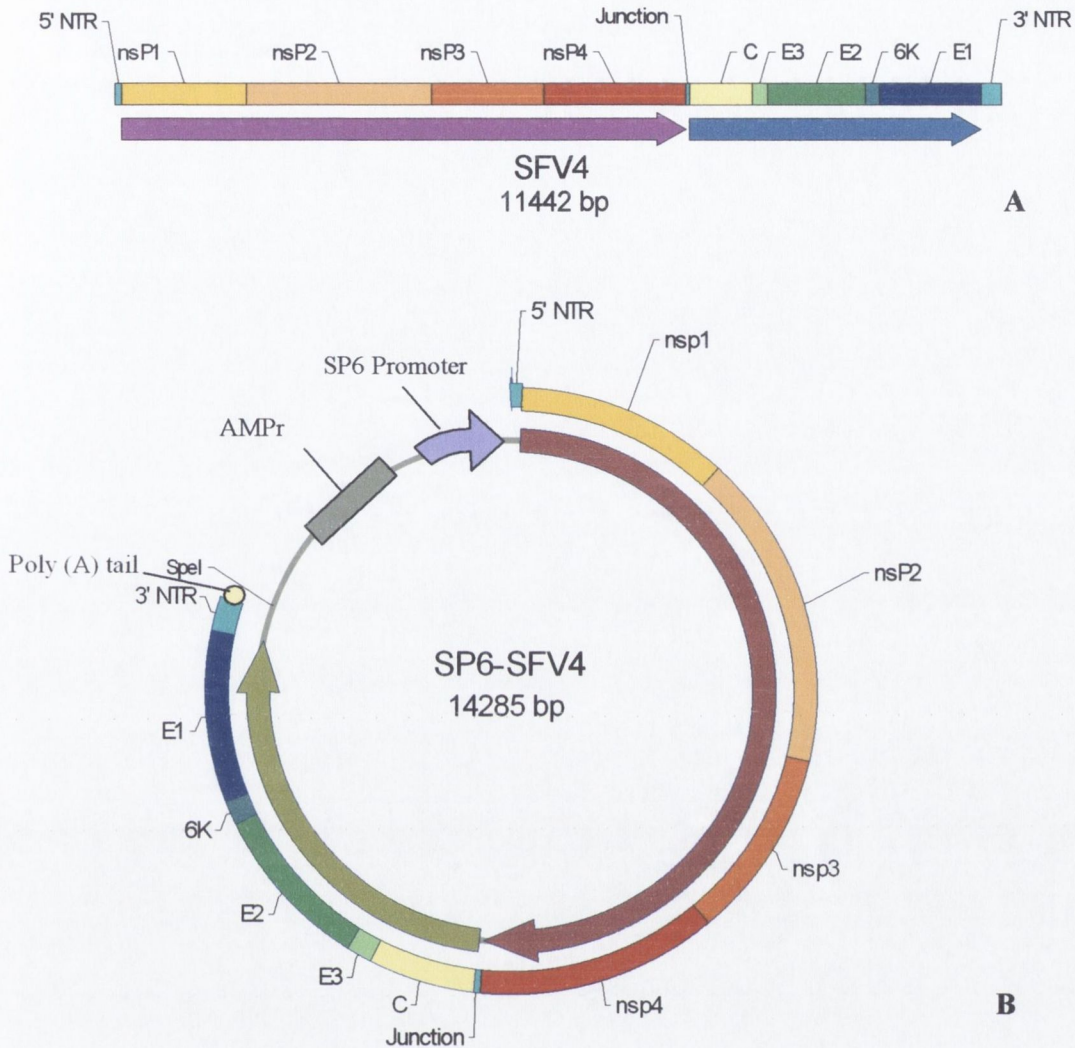


Figure 1.3 Genome organisation of Semliki Forest Virus (A) and the pSP6-SFV4 infectious clone (B).

SFV genome is 11442 nt in length including the 5' and 3' Untranslated regions (UTRs) (A). It consists of 2 open reading frames: the first consists of the non-structural genes and the second, the structural genes. The subgenomic promoter begins within the junction region. The SFV infectious clone constructed by Liljeström *et al* (1991) contains the complete SFV genome downstream of an SP6 promoter; an Ampicillin resistance gene is upstream of the promoter (B). The infectious clone is linearised for *in vitro* transcription using a unique *Spe I* restriction site at the end of the virus poly(A) tail at the 3' end of the genome

1.2.4 The SFV Replication cycle

The replication cycle of alphaviruses involves a series of stages illustrated in figure 1.4. Initially the virus attaches itself to the surface of a host cell, fuses with the endosomal membrane and enters the cytoplasm. Subsequent steps involve the release of the viral RNA into the cytoplasm, with translation, replication and transcription of the RNA genome resulting in the production of non-structural and structural proteins, virus assembly, budding and maturation.

1.2.4.1 Viral Entry

The virus binds to a receptor on the cell surface. Virus adsorption and entry into the host cell are dependent on virus-host protein interactions. The virus glycoprotein responsible for these interactions with cell receptors has been identified as E2 (Dubuisson and Rice, 1993). As alphaviruses have a broad host range and replicate in a variety of different cell types and species it is possible that the viruses use a variety of different molecules or a ubiquitous surface molecule for attachment (Strauss *et al.*, 1994). In the case of Sindbis virus (SINV), the laminin receptor has been identified as a major mammalian cellular receptor (Wang *et al.*, 1992) although other molecules may facilitate SINV entry.

After binding to a receptor on the cell surface, the virus undergoes receptor-mediated endocytosis. There are 4 main stages of endocytosis, beginning with binding of the virus at coated pits on the cell surface and then internalisation via clathrin-coated vesicles which transfer the virus into intracellular endosomes (DeTulleo and Kirchhausen, 1998). Low pH induces a number of conformational changes in the SFV spike resulting in the dissociation of the E1/E2 heterodimer (Lescar *et al.*, 2001; Lobigs *et al.*, 1990b; Wahlberg and Garoff, 1992) which enables the E1 subunit to mediate fusion of the viral envelope with the endosomal membrane (Wahlberg *et al.*, 1992). The dissociation of the E2 subunit stimulates E1 to extend a portion of the spike, initiating the formation of a stable E1 trimer (Fuller *et al.*, 1995). This subsequently leads to formation of a pore in the virion membrane by the E1 trimer interacting hydrophobically with the lipid bilayer of the cell membrane. It has been shown that this fusion cannot occur in the absence of cholesterol and sphingolipids (Phalen and Kielian, 1991; Smit *et al.*, 1999; Moesby *et al.*,

1995). Once virus and cell membrane association occurs a pH and temperature lag follow culminating in the mixing of the virus and cell membranes. This results in the release of the nucleocapsid into the cytoplasm where it is uncoated by ribosomes, liberating the viral RNA genome for initiation of replication (Dick *et al.*, 1996; Singh and Helenius, 1992).

1.2.4.2 Viral replication

Replication of virus RNA takes place in the cytoplasm of infected cells in association with cytoplasmic membranes. As the RNA of SFV is single-stranded with positive polarity it functions directly as mRNA. The first stage in RNA replication is the translation of the 5' two-thirds of the genome coding for the non-structural precursor polyprotein termed P1234 (Garoff *et al.*, 1974; Takkinen *et al.*, 1986, 1991). Following translation of P1234 the non-structural proteins are cleaved (Hardy and Strauss, 1988, 1989) into four individual non-structural proteins nsP1, nsP2, nsP3 and nsP4. The non-structural proteins form replicase complexes for transcription of minus-strand replicative intermediate RNA and positive strand RNAs (Hardy *et al.*, 1990; Strauss and Strauss, 1994).

The structural proteins are translated from the subgenomic 26S RNA (Garoff *et al.*, 1980) with transcription initiated by the 26S promoter on the 42S minus-strand replicative intermediate (Sawicki *et al.*, 1978, Levis *et al.*, 1990). The structural proteins are translated as a polyprotein NH₂-C-p62 (E3/E2)-6K-E1-COOH (Garoff *et al.*, 1980a, b). A more detailed description of alphavirus replication can be seen in figure 1.5.

Figure 1.4 Schematic of the *Alphavirus* Life Cycle

An overview of the 13 principle steps of virus replication: on binding to the cellular receptor the virus is internalised in the cell cytoplasm by receptor-mediated endocytosis (1). Through conformational changes induced by a change in pH positive-sense virus RNA is released into the cytoplasm (2). The RNA is initially translated to give a non-structural polyprotein, which is then cleaved into the non-structural proteins (nsP1-4) (3). nsP2 and nsP3 proteins are then involved in the synthesis of the 26S subgenomic RNA (4) which is then translated (5) to give a structural polyprotein which is cleaved to generate capsid, p62 and E1 proteins (6). The p62 and E1 proteins are translocated to the endoplasmic reticulum (ER, 7) where p62 and E1 dimerise before moving to the Golgi apparatus (GA, 8). The dimerised p62 protein is cleaved to give E2 and E3 within the trans-Golgi network and the spike (E1E2E3 heterotrimer) proteins are transported to the cell membrane (9). Virus RNA (10) and the capsid proteins (11) migrate to the cell membrane and form the nucleocapsid. At the plasma membrane the trimers interact with the nucleocapsid and the capsid proteins bind to the E2 domain of the spike protein causing the plasma membrane to wrap around the nucleocapsid thereby budding off (12) and releasing progeny virus (13).

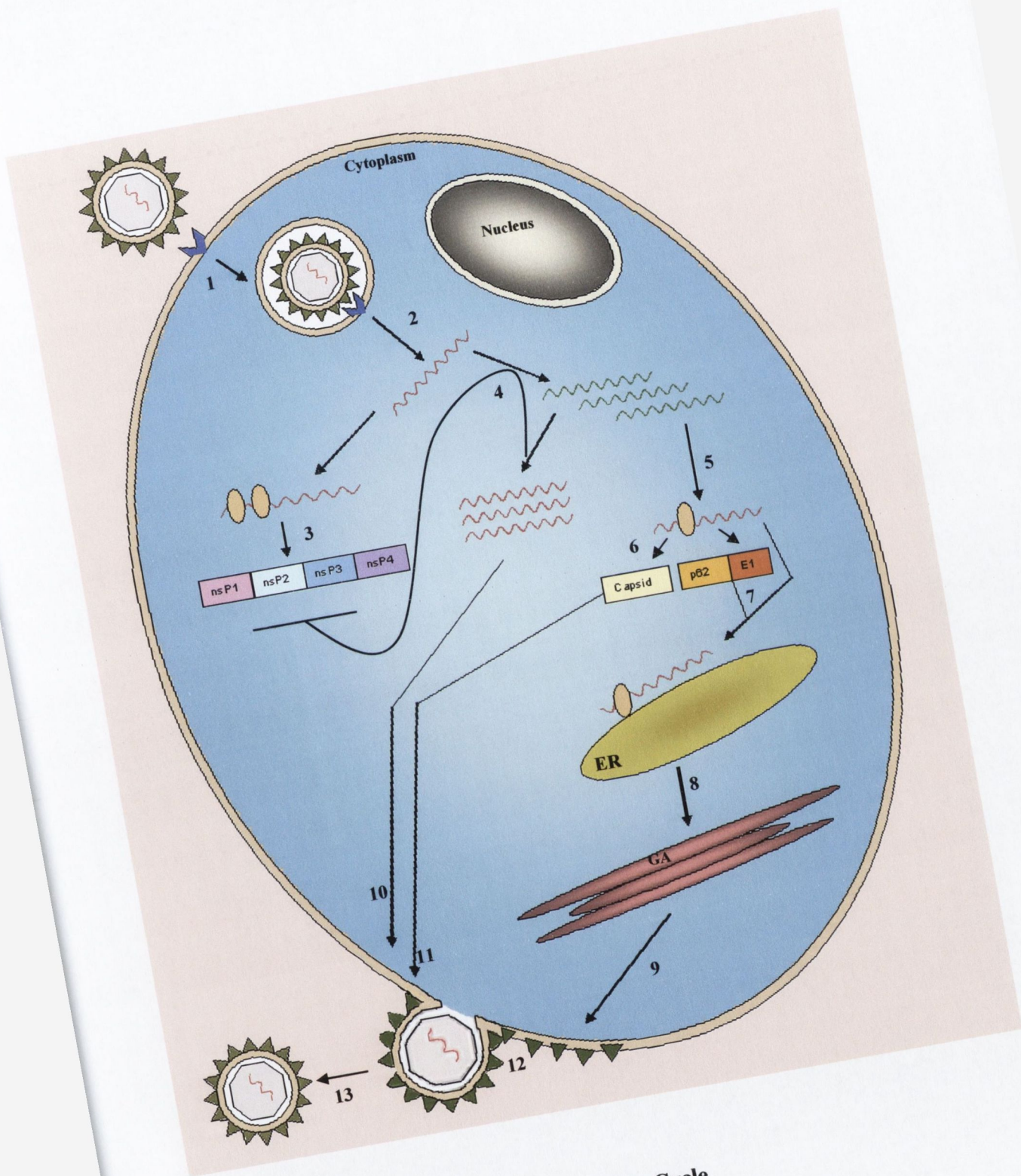


Figure 1.4 Schematic of the *Alphavirus* Life Cycle

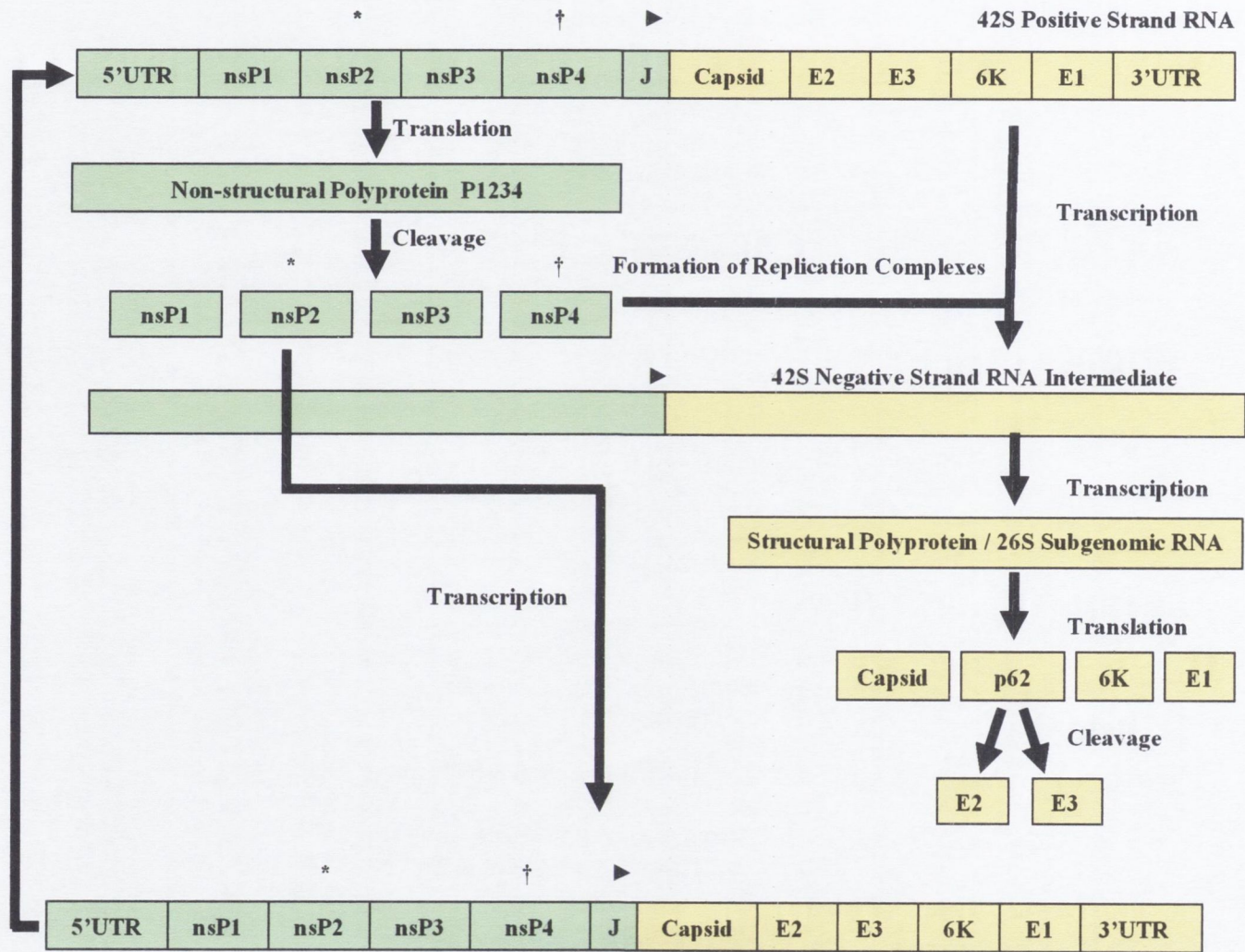


Figure 1.5 Replication and Transcription of Semliki Forest Virus (SFV) RNA. (*, †, ► represent helicases, replicases and the subgenomic promoter respectively).

1.2.4.3 Processing of non-structural proteins and their functions

SFV, unlike SINV and most other alphaviruses has no opal codon (UGA) in the non-structural open reading frame between nsP3 and nsP4 proteins due to it being replaced by an arginine codon (CGA). In infected mammalian cells the production of P1234 is due to read-through of the opal codon, in SINV this occurs approximately 10 to 20% of the time with P123 being produced the remainder of the time (Li and Rice, 1993; Shirako and Strauss, 1994). There are two pathways by which the polyprotein precursor P1234 can be processed.

Both SFV and SINV produce P123 and nsP4 proteins early in infection and P12 and P34 later in infection. However, SFV produces greater amounts of nsP4 protein and nsP4-containing polyproteins than SINV (deGroot *et al.*, 1990, Takkinen *et al.*, 1991). It has been shown that the P123 + nsP4 protein pathway in SFV is the principal route and that nsP4 protein possesses autoprotease activity responsible for the cleavage of the nascent P1234 polyprotein (Hardy and Strauss, 1988; Takkinen *et al.*, 1990, 1991, Figure 1.6). nsP2 protein has a role in processing P1234 by initially cleaving the nsP1/nsP2 protein bond and is not dependent on cleavage of the nsP2/nsP3 protein (deGroot *et al.*, 1990, Shirako and Strauss, 1994). LaStarza *et al.* (1994) showed that uncleaved P123 in association with nsP4 protein is responsible for minus-strand synthesis. The initial cleavage of nsP1/nsP2 protein causes a conformational change of P123 and a build up of enough nsP2 protein protease activity to shut-off negative-strand synthesis (Shirako and Strauss, 1994). Cleavage defects in nsP1/nsP2 protein and nsP2/nsP3 protein in SINV results in decreased levels of subgenomic RNA synthesis (Lemm and Rice, 1993a). It has also been shown that for RNA replication to occur the expression of P123 and P34 is essential (Lemm and Rice, 1993b). Previously, Hahn *et al.* (1989) showed by using nsP4 protein *ts* mutants at non permissive temperatures that viral RNA was not produced. As nsP4 protein is unstable and short-lived in infected cells (Keranen and Ruohonen, 1983) it degenerates rapidly allowing a build up of P123 (figure 1.6, pathway II) and P34 from the first processing pathway (figure 1.6, pathway I). The accumulation of these proteins brings about the shut-off of minus-strand synthesis and initiation of plus-strand synthesis. P34 then acts as the functional polymerase for plus-strand RNA synthesis (Kim *et al.*, 2004; Vasiljeva *et al.*, 2003).

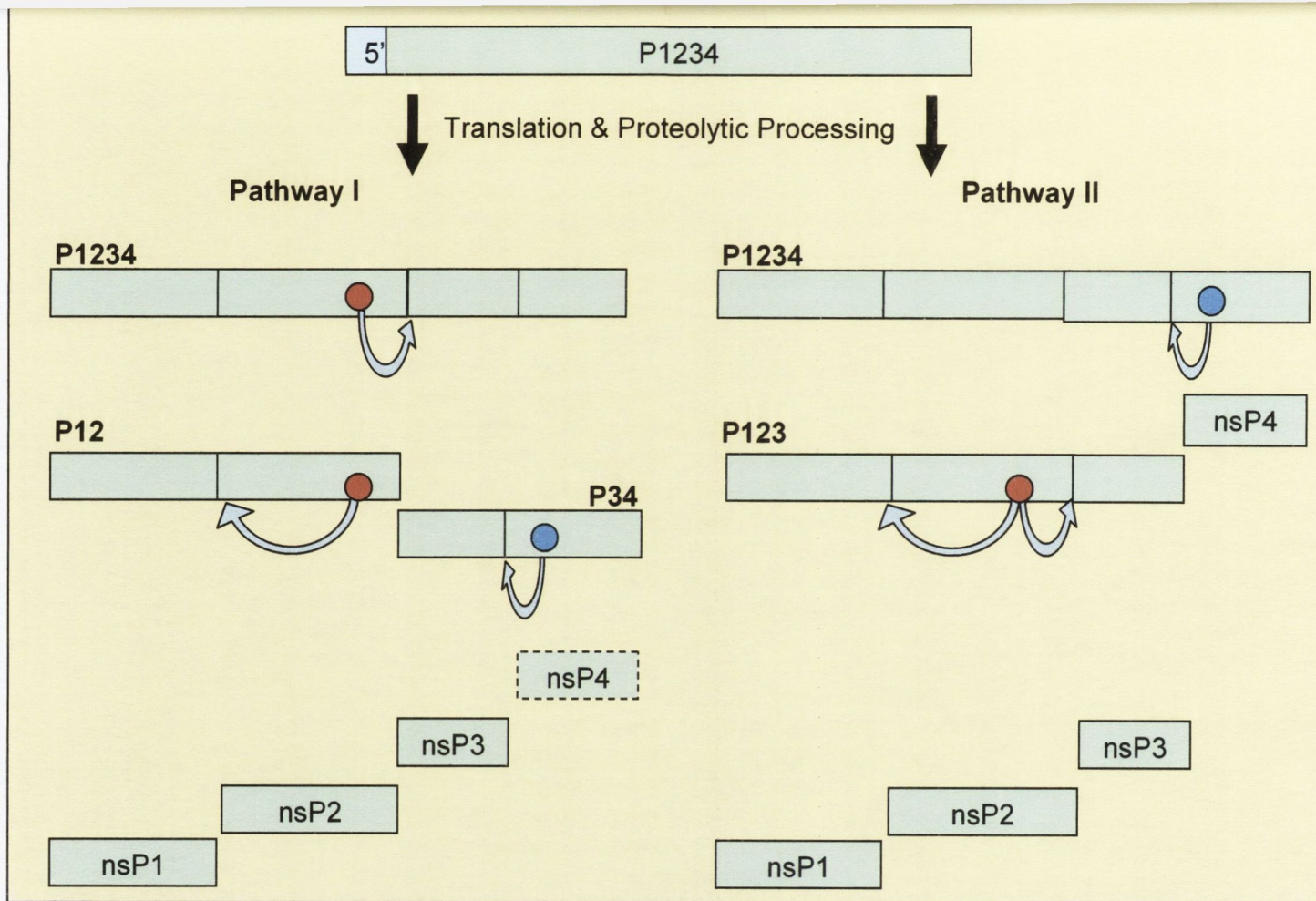


Figure 1.6 Processing pathways of SFV Non-structural Proteins: Schematic representation of the two alternative processing pathways of the polyprotein P1234 yielding either (I) P12 and P34 or (II) P123 and nsP4. The amino-terminal domain of nsP4 protein is represented with a blue circle while the carboxy-terminal of the nsP2 protein serine protease domain is shown as a red circle. The broken box in pathway I represents the breakdown product of P34 which is thought to be unstable.

1.2.4.3.1 nsP1 protein

nsP1 protein of SFV is 1610 nt in length and is thought to have three main functions. Hahn *et al.*, (1989) suggested that nsP1 protein is required for the initiation of or continuation of synthesis of minus-strand RNA. On moving a temperature sensitive mutant (*ts11*) to non-permissive temperature it ceases to produce minus-strand RNA although plus-strand synthesis continues (Wang *et al.*, 1991; Sawicki *et al.*, 1986).

Another function of nsP1 protein lies in it binding tightly to intracellular membrane structures when expressed alone in HeLa cells (Peranen *et al.*, 1995), suggesting a role in anchoring the replication complexes to intracellular membrane structures (Laakkonen *et al.*, 1996) and acting in association with nsP3 protein to target the polyprotein to intracellular vesicles (Lampino *et al.*, 2000; Salonen *et al.*, 2003). nsP1 protein has also been shown to be responsible for capping the genomic and subgenomic RNAs during transcription as it has guanine-7-methyl- and guanyltransferase activities (Cross, 1981, 1983; Scheidel *et al.*, 1987; Mi and Stollar, 1991; Ahola *et al.*, 1997, 2000). More recently Shirako *et al.* (2000) and Fata *et al.* (2002 a, b) have also shown for SINV, direct interactions between nsP1 protein and nsP4 protein in minus-strand RNA synthesis.

1.2.4.3.2 nsP2 protein

In studies using temperature sensitive mutants nsP2 protein has been shown to be involved in the synthesis of the 26S subgenomic RNA (Sawicki and Sawicki, 1985). As previously mentioned (section 1.2.4.3) nsP2 protein has autoprotease activity in its C-terminus (figure 1.6, pathway I). However, in SFV nsP4 is responsible for the proteolytic processing of the intermediate P34 (Takkinen *et al.*, 1991) whereas this is the role of nsP2 protein in SINV. The N-terminal domain of nsP2 protein is a helicase involved in duplex unwinding during RNA replication and transcription (Gomez de Cedron *et al.*, 1999), an NTPase (Rikkonen *et al.*, 1994) which is essential for virus infectivity and an RNA triphosphate (Vasiljeva *et al.*, 2000) characterised by two motifs (in SINV) one starting at residue 189 (GSGKS) and the second starting at residue 252 (DEAF) (Gorbalyena *et al.*, 1988, 1990; Hodgman, 1988). In SFV-infected cells approximately half of nsP2 protein is found in the nucleus, mainly in the nucleolus (Peranen *et al.*, 1990) and a nucleus targeting

signal (NLS) starting at residue 648 (PRRRV) is also found in the C-terminus (Rikkinen *et al.*, 1992).

1.2.4.3.3 nsP3 protein

The function of nsP3 protein is not fully understood, however it has been suggested that it is involved in the synthesis of subgenomic and minus-strand RNA as mutations in the N-terminus of nsP3 protein (in SINV) render the virus unable to synthesise RNA at nonpermissive temperatures (Hahn *et al.*, 1989; LaStarza *et al.*, 1994, Wang *et al.*, 1994). nsP3 protein is phosphorylated, the phosphorylation sites have recently been mapped to serine and threonine residues in the C-terminus (Vihinen and Saarinen, 2000). nsP3 protein is thought to participate with nsP1 protein in anchoring the replication complex to cytoplasmic membrane structures (Peranen and Kaariainen, 1991; Peranen *et al.*, 1988). Current work in our lab (Galbraith *et al.*, in press) has indicated that deletions in the C-terminus of nsP3 protein decrease virus yield and total viral RNA synthesis of SFV. These viruses are avirulent i.p. and intramuscularly (i.m) and less virulent when administered to mice i.n. This could be due to the reduction of the ability to anchor the replication complex to cytoplasmic membrane structures.

1.2.4.3.4 nsP4

nsP4 protein has been shown to possess autoprotease activity responsible for the cleavage of the nascent P1234 polyprotein (section 1.2.4.3). Although nsP4 protein is unstable and short-lived in infected cells (Keränen and Ruohonen, 1983), it has been suggested (Strauss and Strauss., 1994) that nsP4 protein associated with the RNA replicase complex may be protected from degradation, whereas free nsP4 protein is degraded more rapidly (deGroot *et al.*, 1991). The presence of a GDD sequence motif, typical of RNA-dependent RNA polymerases shows that nsP4 protein is the RNA polymerase of the virus (Argos, 1988).

1.2.4.4 Processing of Structural proteins and virus assembly and maturation

Structural proteins are translated from the 26S subgenomic RNA as a polyprotein NH₂-C-p62 (E3/E2)-6K-E1-COOH within 3 hours of infection (Garoff *et al.*, 1982). The C protein is cleaved from the nascent polyprotein precursor by its own C-terminal serine (Ser 268) protease activity (Melancon and Garoff, 1987). The C protein associates with the large ribosomal subunit and assembles as nucleocapsids within the cytoplasm of the infected cell (Ulmanen *et al.*, 1976; Strauss *et al.*, 1995). Specific encapsidation signals have been located that are required for efficient assembly of nucleocapsids within the infected cell (Weiss *et al.*, 1989; Strauss *et al.*, 1995). The capsid binds to the RNA at this encapsidation signal located at the N-terminal of the capsid protein (Geigenmuller-Gnirke *et al.*, 1993; Forsell *et al.*, 1995; Frolov *et al.*, 1997) initiating binding of additional capsid protein molecules to form the final structure of the nucleocapsid in the cytoplasm (Strauss *et al.*, 1995, figure 1.7)

The cleavage of the C protein at Ser 268 reveals the N-terminus of the p62 protein which is the signal sequence for initiating chain translocation across the endoplasmic reticulum (ER) membrane (Melancon and Garoff, 1987; Garoff *et al.*, 1990). The p62 signal sequence is not removed by signal peptidase as one may expect but instead is translocated as part of p62 to be glycosylated soon after release into the lumen of the ER (Garoff *et al.*, 1990). The p62 signal sequence is necessary only for initiation as the completion of the chain translocation is determined by signal sequences located at the C-terminus of p62 and 6K to promote 6K and E1 translocations respectively (Liljeström and Garoff, 1991; Melancon and Garoff, 1986). p62, 6K and E1 proteins are therefore translocated co-translationally (Barth *et al.*, 1995). Shortly after synthesis, PE2 and E1 form a heterodimer in the ER (Garoff *et al.*, 1982; Yao *et al.*, 1996) which is exported through the secretory pathway and the PE2 protein is cleaved to produce E2 and E3 within the trans-Golgi network by a furin-like proteinase. (Carleton *et al.*, 1997). The spike protein, nucleocapsid and the 6K protein are transported to the cell membrane where 6K disassociates and is excluded from virus progeny (Lusa *et al.*, 1991). Loewy *et al.* (1995) showed that the 6K protein was also involved in virus budding, as deletion mutants resulted in a significant reduction of virus release. Yao *et al.* (1996) also demonstrated the requirement of a sequence-specific interaction between the 6K protein and the E1 and E2

glycoproteins for virus assembly to occur. They suggested that the 6K protein promotes the correct folding of the E1 protein in its heterodimeric form (E1E2) in order for the E2 subunit to be positioned correctly in the plasma membrane for budding. In SFV the E3 protein remains non-covalently associated with the E1E2 heterodimer contributing to the stabilisation of the heterodimeric complex (Garoff and Simons, 1974, Lobigs *et al.*, 1990). At the plasma membrane, the E1E2 heterodimers form trimers that interact with the nucleocapsid (Schlesinger *et al.*, 1993). The C-terminus of the capsid proteins bind to the E2 domain of the spike protein (Choi *et al.*, 1991), causing the plasma membrane to wrap around the nucleocapsid thereby budding off and releasing progeny virus (Garoff *et al.*, 1982).

1.2.4.5 Pathogenesis of SFV infection in mice

Infection of the murine central nervous system (CNS) with SFV has been employed as a model for viral neuropathogenesis. Strains of SFV elicit different degrees of virulence in mice depending on the route of administration, the age of the host and the strain used. All strains of SFV are lethal when administered to neonatal mice. The prototype strain of SFV termed L10, was derived from the isolate originally isolated by Smithburn and Haddow in 1944 by eight intracerebral passages through adult and two through baby mouse brains. Lethal encephalitis by CNS infection is caused in mice of all ages, regardless of the route of infection, (reviewed by Atkins *et al.*, 1999). The original cDNA infectious clone of SFV is derived from L10, and termed pSP6-SFV4 (Liljeström *et al.*, 1991). Transcription from this cDNA produces infectious virus termed SFV4 that has a slight reduction in virulence, most likely due to an undetermined number of passages of the prototype strain in cell culture (Glasgow *et al.*, 1991). SFV4 causes lethal encephalitis 4 to 5 days post infection in mice infected intranasally (i.n.), when virus is administered by the intraperitoneal route (i.p.) only 60-70% of adult mice die. A slightly higher mortality rate is observed when mice are infected intramuscularly (i.m.) although less than i.n. infected mice (Glasgow *et al.*, 1991; Atkins *et al.*, 1999). In 1961, McIntosh *et al.*, described another strain of SFV designated A7 after seven passages in neonatal mouse brain of the original AR2066 isolate, extracted from mosquitoes in Mozambique.

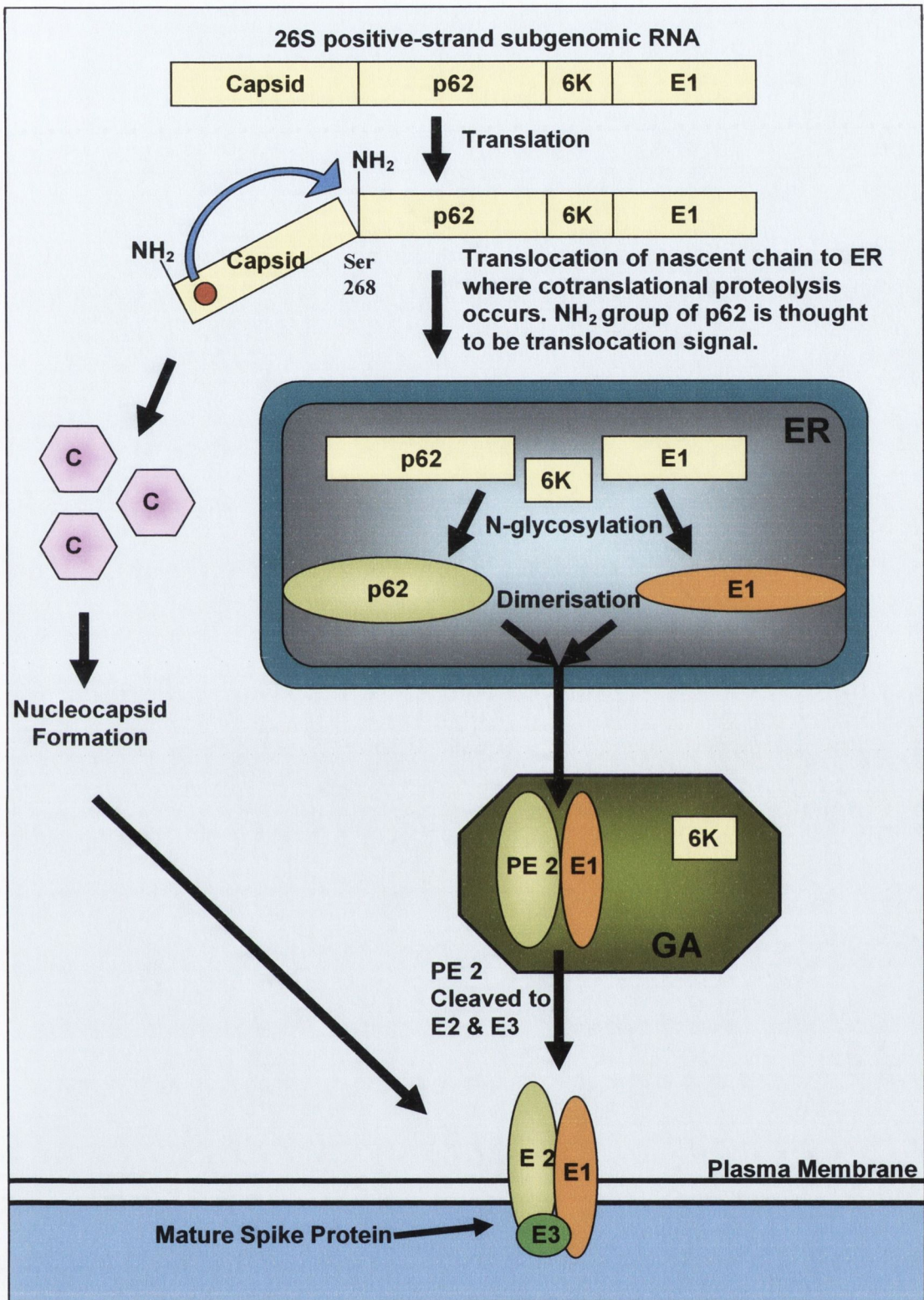


Figure 1.7 Processing of SFV Structural proteins: The capsid protein is released from the nascent polyprotein by autoproteolysis. The protease domain is represented as a red circle present in the N-terminus of the capsid protein. Free capsids interact rapidly with newly synthesised 42S RNAs to form nucleocapsids. The nucleocapsid binds to the internal E2 section of the transmembrane spike protein to initiate budding.

A7 was avirulent in adult mice, fatal in neonatal mice and caused foetal death in pregnant females. The adult survivors of A7 infection show demyelination in the CNS, most likely triggered by the infection of oligodendrocytes (Atkins *et al.*, 1985; 1994) and partially immune-mediated (Gates *et al.*, 1984; Fazakerley and Webb., 1987; Subak-Sharpe *et al.*, 1993).

Although A7 is avirulent in adult mice, it replicates at least as efficiently as the virulent L10 and SFV4 in cultured cells such as BHK-21 cells (Atkins *et al.*, 1983; Glasgow *et al.*, 1997; Atkins *et al.*, 1999).

Another SFV strain was derived from A7 by further colony selection for avirulence on chick embryo fibroblasts by Bradish *et al* in 1971, termed A7[74]. Infection with A7[74] is lethal only for mice younger than 2 weeks; in adult mice spread is partially restricted in CNS neurons and infection remains asymptomatic, as is the case for A7 (Fazakerley *et al.*, 1993; Oliver *et al.*, 1997; Atkins *et al.*, 1985). Infectious cDNA clones for A7 and A7[74] have been constructed (Tarbatt *et al.*, 1997; Tuittila *et al.*, 2000), termed pSP6-CA7 and rA774 respectively. pSP6-CA7 was constructed by removing fragments of the SFV4 genome from pSP6-SFV4 and replacing them with those of A7; Tarbatt *et al* compared the virulence between SFV4 and infectious virus produced from the pSP6-CA7 termed CA7 by creating a series of reciprocal chimeras spanning the genome. CA7 contains the complete translated region from A7 with only the 5' untranslated region (UTR) from SFV4 and kills over 30% of mice when administered i.n. (Tarbatt, C.J. unpublished data). In addition, lesions induced in the CNS of mice inoculated i.n. are more severe at 14 days post infection (d.p.i.) than those infected by the same route with A7. These results indicate that CA7 unlike A7 is not totally avirulent, clearly having retained a degree of virulence, possibly due to the 3 nucleotide changes in the 5'UTR, although only two changes were noted by Tarbatt *et al* (1997). Mutations in the 5' UTR of VEE in combination with a mutation in the E2 gene (Kinney *et al.*, 1993) have been shown to influence virulence. This is discussed in more detail in section 1.2.4.6.1.

It has been shown that virulent strains of SFV induce more extensive damage to neurons in the CNS than avirulent strains (Atkins *et al.*, 1985). It is the partial restriction of the ability of avirulent strains to multiply in neurons that is responsible for the slower

multiplication in the CNS (Gates *et al.*, 1985; Balluz *et al.*, 1993; Fazakerley *et al.*, 1993). Therefore the fundamental difference between virulent and avirulent strains of SFV is the rapidity of spread of neuronal damage in the CNS (Balluz *et al.*, 1993) resulting in a lethal threshold in the case of L10 and SFV4 before the immune system can intervene. The virus properties controlling these functions remain to be fully elucidated.

1.2.4.6 Functions of the Conserved Sequence Elements of the SFV genome

On sequence comparison of several alphavirus genomes (Ou *et al.*, 1981, 1982 a, b, 1983), four conserved sequence elements (CSE) were identified that include a conserved hairpin structure at the extreme 5' end of the genome, a 51-nt sequence found in the coding sequence of nsP1 protein also capable of forming hairpin structures, a 21-nt sequence of which 19-nts are found in the untranslated junction region preceding the first 2-nts of the 26S RNA, and a 19nt conserved sequence adjacent to the poly(A) tract at the 3' end of the genome. Evidence from several viral systems indicates that the untranslated regions of viral genomes may be important as virulence determinants and in virus pathogenicity, presumably through their effects on and involvement in genome replication, translation, or transcription. Each of the four CSEs are individually examined in more detail below.

1.2.4.6.1 5' Untranslated Region

The 5' UTR has a low overall nucleotide identity in alphaviruses but shares a conserved predicted secondary structure (Ou *et al.*, 1983). Studies have been carried out on the 5' UTRs of several different viruses including poliovirus where the importance of the 5' UTR demonstrated by comparison of nucleotide sequences between virulent and attenuated variants and their revertants, and from mapping the virulence determinants (Kawamura *et al.*, 1989). In the case of the Sabin type 3 poliovaccine genome a single nucleotide change in the 5' UTR significantly increased neurovirulence (Evans *et al.*, 1985). The effects of substitutions and deletions in the 5' UTRs have been investigated for several alphaviruses, namely SINV virus (Gorchakov *et al.*, 2004; Fayzulin and Frolov, 2004; Frolov *et al.*, 2001; McKnight *et al.*, 1996; Kuhn *et al.*, 1992; Neisters *et al.*, 1990) and Venezuelan equine encephalomyelitis (VEE) virus (Kinney *et al.*, 1993).

Frolov *et al* (2001) carried out a series of trans-competition experiments using SINV / SFV chimeras that showed that replacement of the SINV 5' UTR by heterologous UTRs derived from SFV abolished RNA replication *in vivo* and negative-strand RNA synthesis *in vitro*. They suggested that sequences at the 5' end of the RNA genome (including the 51nt CSE in nsP1, discussed later) and the complementary sequences at the 3' end of minus-strand RNAs play crucial roles in translation and replication of alphaviruses. In SINV if a first stem-loop structure is replaced with the SFV 5'-terminal stem-loop structure, all RNAs produced were incapable of replication, making the first terminal stem loop the most important (Ilya Frolov, personal communication). The SFV 5' end is incapable of binding host and/or SINV-specific protein factors required for initiation of the negative-strand synthesis (Frolov *et al.*, 2001). In earlier studies Neisters and Strauss (1990 a, b) using SINV 5'UTR deletion mutants, suggested that a characteristic feature of the 5' terminal sequences of alphavirus genomes is that they are predicted to fold into compact structures that bring the 5'UTR and the 51nt CSE into close proximity. Kobiler *et al* (1999) showed that much like poliovirus the 5' UTR was important in neurovirulence; in their study on rats they noted that a single nucleotide substitution in the 5'UTR of SINV (SINVN) transformed a neurovirulent but non-lethal virus in 3-week-old rats into a lethal virus. Similarly site directed mutations in another strain of SINV (S.A. AR86) significantly reduced mortality and increased survival in mice inoculated intracerebrally (i.c. Johnston *et al.*, 1996). Kinney *et al* (1993) carried out mouse challenge experiments with VEE viruses of the virulent Trinidad donkey (TD) strain and its attenuated vaccine derivative (TC-83) that indicated that attenuation is partially determined by mutations within the 5'UTR, with mutations in the E2 envelope glycoprotein also playing a role.

This polygenic influence in virulence was investigated further in SINV by Kobiler *et al* (1999), where they showed that substitution of 2 amino acids in E2 of the nonlethal neurovirulent strain SINVN with Met-190 and Lys-260 of the lethal SINVNI strain resulted in the induction of paralysis in 2 and 5-week-old rats. Only substitution of both the 5' UTR and E2 SINVNI determinants produced virus with virulence properties indistinguishable from those of SINVNI parent virus. As E2 is involved in receptor binding and penetration (described previously in section 1.2.4.4) it is possible that age-dependent resistance is influenced by changes in viral receptors during neuronal maturation. In SFV there are 8

amino acid changes in the E2 envelope glycoprotein between the avirulent A7 strain and the virulent SFV4 strain, although in a paper published by Tarbatt *et al* (1997) the author did not report an M/K amino acid difference at position 215 of E2, thus reporting only 7 amino acid changes. The investigation carried out by Tarbatt *et al* involved constructing an avirulent A7 infectious clone and involved several intermediate SFV4-A7 chimeras, one of which termed C8930/11033 involved the substitution of a 2104 nt fragment that encompassed 5 of the 8 amino acid changes in E2 as well as 6 in E1. When mice were administered C8930/11033 virus i.p. only 20% of mice died in comparison to 60% of those infected with parental SFV4; none died when infected with SFV-A7. This result suggests that E2 may play an important part in neurovirulence. Tarbatt *et al* did not substitute the 5'UTR of the SP6- SFV4 infectious clone with that of A7 (unpublished results) which may be relevant regarding the CA7 infectious clone retaining a significant degree of virulence for infected mice. To date no group has investigated the 5'UTR of SFV strains and a possible role as a neurovirulence determinant either functioning alone or polygenically with E2 or another virus gene.

1.2.4.6.2 51 nucleotide CSE in nsP1

The high degree of conservation of the 51-nt sequence element suggests that this short sequence is important in the replication of alphaviruses. Ou *et al* (1983) hypothesised that cyclisation of the 49S RNA could be important in RNA replication as it could result in the recognition elements of the 5' end of the genome being in close proximity to the 3' end recognition element (described later in section 1.2.4.6.4). This would allow the replicase to interact with both sequences simultaneously, allowing only intact 49S positive RNA strands to be replicated to produce negative strands and the exclusion of the 26S RNA from replication as shown by Martin *et al* in 1979. The involvement of the 51-nt CSE in replication was further investigated by Niesters *et al* (1990b) who through a series of mutational analyses examined 25 substitution mutants. Of the 21 silent changes (not involving an amino acid change), 19 were deleterious for replication resulting in a decrease in virus growth of 2 to 4 orders of magnitude. The 51-nt sequence is capable of forming two hairpin structures that serve as a replication enhancer in mammalian cells with multiple mutations in this region destabilising the secondary structure but not abolishing the

replication of the SINV genome RNA although they did down-regulate RNA synthesis as much as 10-fold (Frolov *et al.*, 2001). However, changes that did not disrupt the structures were deleterious, indicating that the linear sequence is also important. In a recent study by Fayzulín and Frolov (2004) SINV viruses containing mutations in this sequence demonstrated that this CSE is dispensible for SINV replication in cells of vertebrate origin, however the same mutations had a deleterious effect on virus replication in mosquito cells. This demonstrates an excellent potential of alphaviruses for adaptation, with SINV adapting to replication in cells of a vertebrate or invertebrate origin within one passage. It therefore seems that the 51-nt CSE increases RNA replication and in SINV its integrity is more important in mosquito cells than in mammalian cells (Neisters *et al.*, 1990b).

1.2.4.6.3 Junction region

The junction region was originally postulated to be 21 nts in length and to act as a promoter of the subgenomic RNA (Ou *et al.*, 1982). However in a later study by Levis *et al* (2000) it was shown that the junction region CSE is precisely 24 nts in length (AUCUCUACGGUGGUCCUAAAUAGU), including 19 nt 5' of the start site and 5 nts downstream of the start site and is necessary and sufficient to promote transcription of the 26S subgenomic RNA. This promoter sequence is highly conserved in alphaviruses although some differences are present and have been shown to influence the efficiency of translation (Raju *et al.*, 1991).

A double subgenomic system in SINV RNA genomes that transcribe two different subgenomic RNAs by using two independent promoters was constructed by Raju *et al* (1991) allowing direct comparison of the relative efficiencies of different promoters. By carrying out site-specific mutagenesis to change the 24 nt promoter of SINV to that of other alphaviruses this system indicated that almost all alphavirus promoters tested were recognised by the SINV RNA polymerase with varying degrees of efficiency. In the case of SFV, which differs from SINV by two nucleotide differences in this region; a relative promoter strength of 75% that of SINV was observed. This suggests that promoter strength is regulated by the virus because of a need to balance the production of genomic RNA and subgenomic RNA following infection with an overly strong promoter being selected against. This study confirmed earlier work by Grakoui *et al* (1989) who inserted 3 nts into

the subgenomic promoter of wild-type SINV and found that transcription of subgenomic RNA was dramatically reduced to a level that made the resulting virus barely viable. A later investigation by Durbin *et al* (1991) suggested the involvement of host proteins in the recognition of the subgenomic promoter and that the optimal promoter sequence may depend on the normal host cell of the virus. This was elegantly shown using a mutant of SINV with a silent nucleotide substitution in the subgenomic promoter that led to decreased synthesis of 26S RNA in mosquito cells but not in chicken cells. Host cell selective recognition of promoter sequences is not unique to the junction CSE and is more apparent in the 3' UTR of alphaviruses.

1.2.4.6.4 3'Non translated region

The 3'-untranslated region (UTR) of alphavirus genomes ranges from 77nt in Pixuna virus, a subtype of VEEV to 547 nts in Ndumu virus. In SFV, SINV, ONNV and CHIKV the 3' UTR is 264, 323, 425 and 503 nts in length respectively (Pfeffer *et al.*, 1998). Although there is considerable variation in length of the 3' UTR between alphaviruses the sequence is not particularly conserved; there is a 19-nucleotide sequence (AUUUUGUUUUUAAUAUUUC-A_N) immediately preceding the 3'-poly(A) tail that is highly conserved in all alphaviruses. Initial investigations of the 3' conserved sequence element (3' CSE) involved substitutions and deletions of the 19nt sequence of SINV (Kuhn *et al.*, 1990) and showed a decrease in the ability of virus to replicate by 2 or more orders of magnitude. However deletions of large areas upstream of the 19nt were deleterious although not lethal in mosquito cells indicating that the entire 3'UTR was important for virus replication. The 3' CSE and poly(A) tail were therefore assumed to constitute the core promoter for minus-strand RNA synthesis during genome replication.

It was also noted by the authors that these mutants affected differently the ability of the virus to grow well in chicken, mosquito and mouse cells. This suggested that host cell factors, presumably proteins, bind to these CSEs, and as the CSEs are all quite different, it is likely that different cellular proteins interact with the different CSEs to promote RNA replication. Recently, Hardy and Rice (2005) examined the role of the CSEs in the initiation of minus-strand RNA synthesis. They found that for efficient minus-strand RNA synthesis the wild-type 3' CSE and the poly(A) tail are required. They showed that the poly

(A) tail must be a minimum of 11 to 12 residues in length and immediately follow the 3' CSE and deletion or substitution of the 3' 13 nucleotides of the 3' CSE severely inhibits minus-strand RNA synthesis. The authors were also able to show that templates possessing non-wild-type 3' sequences previously demonstrated to support virus replication do not program efficient RNA synthesis.

In a follow-up study to their initial findings, Kuhn *et al* (1992) tested for rates of RNA synthesis, virus production in chicken, mosquito and mouse cells, and examined virulence and virus production in different tissues in mice. By constructing 4 mutants with changes in the 5'UTR and 4 with changes in the 3'UTR sequence elements they were able to show that all mutants had defects in RNA synthesis and that virus production was host cell dependent with mouse, chicken and mosquito cells responding differently to each change from the wild-type sequence elements. Therefore it seems that wild-type sequence elements have been adapted to interact with all of the natural hosts but are not necessarily optimal for a particular host.

Interestingly one of the mutants in this investigation that had nucleotides 18-25 of the 3' UTR deleted demonstrated tissue specific differences, growing less well than the parent virus in mouse cells but growing to a titre of almost 10 times that of the parent virus in the mouse brain. These results suggest that host proteins interacting with these CSEs in both a species specific and tissue specific manner may serve to modulate tissue tropism of alphaviruses. Studies using minus-sense riboprobes of 60-120nt corresponding to the first 250nt of the 3' end of the minus strand of SINV genomic RNA mixed with extracts from infected and uninfected chicken and mosquito cells (Pardigon and Strauss, 1992a, b) showed that binding of host proteins was sequence specific. More interestingly however, it was found that the same mosquito protein bound to riboprobes from other alphaviruses (SFV, Ross River (RR)), demonstrating that binding of this protein is a general phenomenon of alphavirus infection.

1.2.4.7 SFV as a viral vector

SFV has several traits that make it a good viral vector candidate. It has an RNA genome of positive polarity thus functioning as mRNA. Infectious RNA can be obtained by transcription of the full-length cDNA copy of the genome. As well as having a very efficient replication that occurs in the cytoplasm of infected cells, SFV has a broad host range and has been shown to infect a range of different cells in culture, including mammalian, avian, amphibian and insect (Clark *et al.*, 1973, Griffin, 1986, Stollar, 1980). In man SFV has a low pathogenicity with most people outside of Africa having no pre-existing immunity against the virus.

In 1991, Liljeström and Garoff manipulated the SFV genome to produce a novel DNA protein expression system. The structural proteins of the SFV genome were removed from the infectious clone to allow insertion of the foreign gene/s of interest. The foreign DNA sequence was then transcribed to produce recombinant RNA which can be subsequently electroporated into BHK-21 cells. The SFV replicase system replicates the recombinant RNA within the cells and expression results in considerable production of foreign proteins (Berglund *et al.*, 1993). The SFV expression system may also be used to facilitate packing of the RNA into infectious virus “suicide particles”. Utilising a helper RNA molecule deficient in its own packaging signals, the recombinant RNAs are packaged utilising the helper structural proteins (Liljeström and Garoff, 1991; Berglund *et al.*, 1993).

The development of the SFV as a vector system has opened a broad range of opportunities for vaccine development. The inclusion of mutations specifying maturation defects of the helper ensuring that only one round of replication is possible has further increased the vectors biosafety. SFV vectors have been shown to successfully induce humoral and cell-mediated immunity against several diseases (Berglund *et al.*, 1999, 1997; Fleeton *et al.*, 1999, 2000; Morris-Downes *et al.*, 2001).

Recently the SFV vector system has been tested as a means of delivery into the CNS, and this shows great potential for the treatment of CNS diseases. Current research has indicated that high levels of protein expression were detected in the CNS following intranasal inoculation of recombinant SFV particles expressing a reporter gene, with no vector RNA detected in areas of the CNS and no damage detected in the brains of infected mice (Jerusalmi *et al.*, 2003).

Although *Aedes albopictus* is considered to be the primary vector of CHIKV in Asia and a secondary vector in Africa (Jupp and McIntosh, 1981), laboratory studies have indicated that *Aedes albopictus* appears to be a more competent vector than *Aedes aegypti* (Turell *et al.*, 1992, Diallo *et al.*, 1999, Thaikruea *et al.*, 1997).

With a little over 500 published papers on CHIKV one would assume that it was very well characterised, however an overwhelming majority of the work carried out on CHIKV are reports of outbreaks of the virus (Table 1.1), or novel methods of virus detection and diagnosis, and descriptions of the types of mosquito vector involved in transmission.. The most recent study not involving the above criteria was carried out by Khan *et al* (2002) who detected the presence of an internal polyadenylation site within the 3' UTR of the S27 strain of CHIKV. This however has not been observed in any other fully or partially sequenced CHIKV genome, including the Ross strain, 37997 strain and the vaccine strain, and may have arisen due to a history of multiple passage as the S27 strain used in this investigation had been passaged over 50 times using the *Aedes albopictus* clone C6/36 cell line (Khan *et al.*, 2002). Other investigations not related to the reporting of outbreaks of CHIKV include Powers *et al* (2000), who investigated the phylogenetic relationship of several CHIKV strains in relation to other alphaviruses, Blackburn *et al* (1995) who investigated the antigenic relationship between CHIKV and the closely related O'nyong nyong virus (ONNV) and Ranadive and Banerjee (1990) who examined the expression of CHIKV structural proteins in *E. coli*.

Levitt *et al* (1986) produced an attenuated CHIKV vaccine, used by the US military with controversial consequences, while Simizu *et al* (1984) deduced that unlike in SFV the E3 glycoprotein of CHIKV was not associated with mature virions but released into culture fluids. Much of the earlier work although carried out on CHIKV was common to most alphaviruses with Chanas *et al* (1979a, b) carrying out early biological comparisons between CHIKV and ONNV in the mouse, Precious and Webb (1974) isolated CHIKV from mouse neuronal cell cultures, Davis *et al* (1971) grew CHIKV to high titres in BHK-21 cells, Igarashi *et al* (1970) carried out analyses on protein synthesis and virus formation of CHIKV in infected BHK-21 cells and finally Ross in 1956 who initially isolated and

described the virus. To date, a conclusive characterisation of CHIKV has not been carried out, investigating not only the genome structure and phylogenetic relationship of the CHIKV genome with other alphaviruses, but studying also the *in vitro* effects of infection using different animal cell lines, the *in vivo* effect on an animal model, the detection of virus in cells of the CNS and its relevance to neuropathologies caused by other alphaviruses. In order to get a more complete picture of CHIKV it is also important to determine the efficiency of a range of molecular functions of CHIKV such as its ability to synthesise RNA, and to carry out comparisons between geographically distinct CHIKV strains.

1.3.1 Origins and Strains

Since the first recognised epidemic of CHIKV in Tanzania in 1953, it has been shown that Chik fever is widely distributed in tropical areas in Africa and Asia, producing a febrile and sometimes haemorrhagic fever in humans.

In Africa, it is thought that non-human primates such as monkeys and baboons are responsible for amplifying and maintaining virus circulation. In 1969, Ibadan city in Nigeria experienced the first outbreak of CHIKV fever in the region (Moor *et al.*, 1974). A subsequent serological survey of four ecological zones of Nigeria to detect the presence of antibodies to CHIKV in humans and domestic animals showed the highest percentage of human sera positive for CHIKV in Ibadan city. Possibly due to the climatic conditions in the rainforest zone which seem suitable for the survival of the virus and the maintenance of a high population of the vector (Adesina and Odelola, 1991). The presence of CHIKV antibody in animal sera points to the important role that domestic animals can play in the transmission and maintenance of the virus in Nigeria. Serological investigations have also confirmed the prevalence of CHIKV antibodies in 9 prefectures in the Republic of Guinea (Ivanov *et al.*, 1992); no information was available on the presence of CHIKV in this region before this investigation. An outbreak of febrile illness in the northern province of Sudan occurred in 1989, and antibody investigations indicated the presence of several arboviruses including CHIKV (Watts *et al.*, 1994). The most recent African outbreak occurred in the Democratic Republic of Congo in 1999 to 2000 (Porter *et al.*, 2004) after an absence of 30 years also thought to have been related to a combination of climatic conditions.

In Asia, the pattern of the virus transmission is very different from that seen in Africa and it has been suggested that *Aedes aegypti* is responsible for transmission of virus from human to human. It seems that Asian monkeys have never been implicated in any way in the maintenance and transmission of the virus in this continent, although they develop high titres of viraemia following CHIKV inoculation (Fields *et al.*, 2001). Several epidemics have been reported in different areas in Asia (table 1.1) following the first isolation of CHIKV in Tanzania in 1952-1953. CHIKV was also isolated from humans in Thailand and the Philippines in association with haemorrhagic fever in 1958 (Halstead *et al.*, 1960). Several outbreaks have also been recognised in India (Chaudhuri *et al.*, 1964). Antibody surveys show that CHIKV was also circulating in Yangon, Myanmar in Burma during 1984, and results indicated the association of the virus with haemorrhagic fever (Thein *et al.*, 1992). CHIKV fever has been also reported in the Republic of South Vietnam. Clinical features of the disease were described in American soldiers serving in Vietnam in 1966 (Deller *et al.*, 1967). A comprehensive list of outbreaks since CHIKV was isolated by Ross in 1952 is described in table 1.1. Recently several outbreaks of CHIKV in Indonesia have been reported via the International Society for Infectious Disease's Program for Monitoring Emerging Diseases ProMED-mail (<http://www.promedmail.org>) infecting several thousands of people. A small outbreak was also recently recorded in the Comoros Islands off the South East coast of Africa, with sufferers having previously spent several days in Indonesia.

To date approximately 20 different geographically distinct strains of CHIKV have been isolated. In 2000, Powers *et al.* extensively investigated the phylogenetic relation of these strains and were able to divide them into 3 distinct genotypes in relation to their locations: Asian genotype, Central/Eastern African genotype and West African genotype based on the comparison of a 1050bp partial sequence in the E1 envelope glycoprotein. This analysis also proved that the closely related alphavirus ONNV was not a subtype of CHIKV as was previously thought, and it is likely that these two viruses diverged thousands of years ago. The phylogenetic relationship of these CHIKV strains and ONNV are illustrated in figure 1.9.

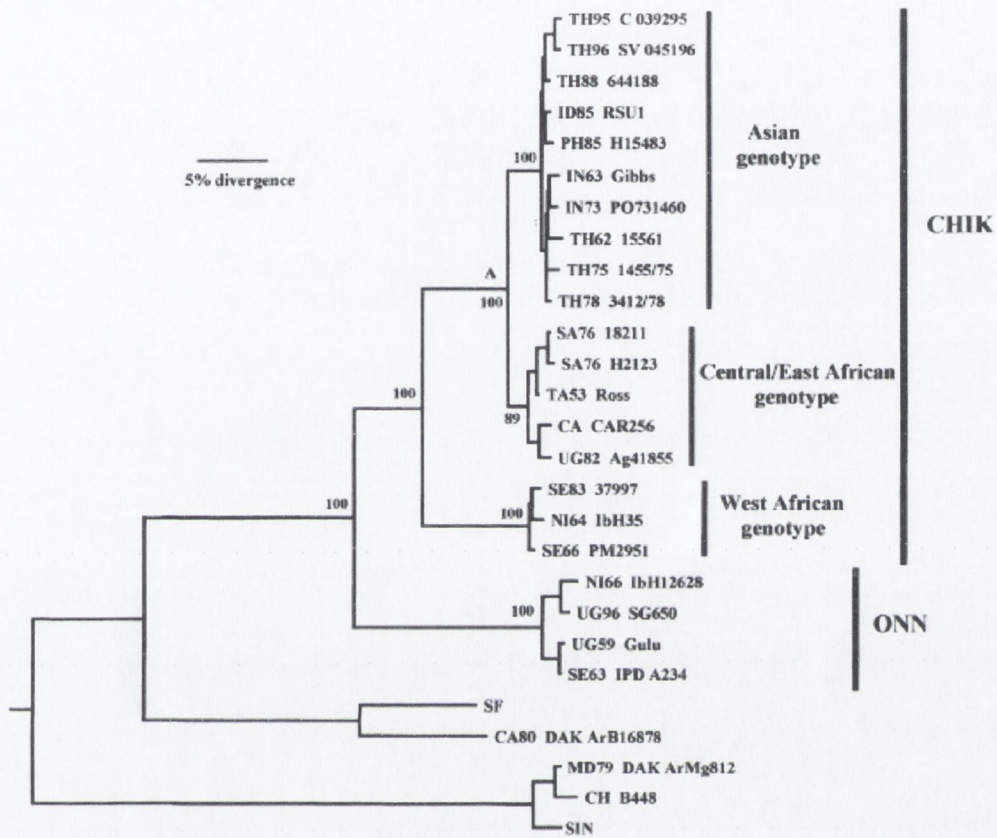


Figure 1.9 Phylogenetic analysis of CHIKV and ONNV .

Generated by performing a PAUP analysis on the 1050bp partial E1 gene sequence. (This figure has been used with the kind permission of Dr Ann Powers, CDC, Fort Collins, USA)

Year of Outbreak	Location	Author(s) and Year
1952-53	Tanzania	Ross, 1956; Mason and Haddow., 1957
1958	Entebbe Peninsula, Uganda	Weinbren, MP., 1958
1960	Upper Uele, Congo	Osterrieth, PE., 1961
1960	Thailand	Thaikruea <i>et al.</i> , 1997
1961	Northern Rhodesia	Rodger, LM., 1961
1962-64	Thailand	Halstead <i>et al.</i> , 1969
1963	Cambodia	Chastel, C., 1961
1963	Southern Rhodesia	McIntosh <i>et al.</i> , 1963
1964-65	Calcutta, Indis	Chaudhuri <i>et al.</i> , 1964
1964	Vellore, South India	Myers <i>et al.</i> , 1965; Reuben, R., 1967; Carey <i>et al.</i> , 1969
1965	South Vietnam	Halstead <i>et al.</i> , 1965
1965	Ceylon, India	Munasinghe <i>et al.</i> , 1966; Mendis, NM., 1967
1965-69	Malaysia	Marchette and Rudnick., 1980
1966	Senegal	Roche and Robin., 1967
1967	Taiwan	Clarke <i>et al.</i> , 1967
1967	Vietnam	Deller <i>et al.</i> , 1967
1970	Southern Africa	McIntosh, BM., 1970
1970	Kenya	Surtees <i>et al.</i> , 1970
1971	Australia	Lancet 1(7694) 331-2
1971	Entebbe Region, Uganda	McCrae <i>et al.</i> , 1971
1973	Burma	Matthew and Thiruvengadam., 1973
1973	Barsi, India	Padbidri and Gnaneswar., 1979
1974	Ibadan, Nigeria	Moore <i>et al.</i> , 1974; Tomori <i>et al.</i> , 1975
1975	Igbo Ora, Nigeria	Fagbami, A., 1977
1980	Kainji Lake Basin, Nigeria	Adekolo-John and Fagbami., 1983
1980-82	Burundi	Rodhain <i>et al.</i> , 1987
1982	Indonesia	Pastorino <i>et al.</i> , 2004
1982	West Senegal	Saluzzo <i>et al.</i> , 1983
1983	Pakistan	Darwish <i>et al.</i> , 1983
1985	Uganda	Kalunda <i>et al.</i> , 1985
1987-89	Malawi	van den Bosch and Lloyd., 2000
1990	Australia	Harnett and Bucens., 1990
1991	Thailand	Thaikruea <i>et al.</i> , 1997
1992	Republic of Guinea,	Ivanov <i>et al.</i> , 1992
1995	Thailand	Thaikruea <i>et al.</i> , 1997
1996	Kaffrine, Senegal	Diallo <i>et al.</i> , 1999
1998-99	Malaysia	Lam <i>et al.</i> , 2001
1999	Yogyakarta, Indonesia	Porter <i>et al.</i> , 2004
1999-00	Democratic Republic of the Congo	Muyembe-Tamfum <i>et al.</i> , 2003; Pastorino <i>et al.</i> , 2004
2001-03	Indonesia	Laras <i>et al.</i> , 2005
2003	West Timor	Rukman and Fointuna; Banks, 2003*
2004	West Jakarta, Indonesia	Santoso, D., 2004*
2005 April	West Lombok, Indonesia	Banks, A., 2005*
2005 April	Comoros Island, E. African Coast	Bannatyne, S., 2005*
2005 June	Mauritius and Ile de la Reunion	Pierre; Issack, M., 2005*
2005 July	Tangerang Subdistrict, Indonesia	Price, D., 2005*

Table 1.1 Chronological order of CHIKV outbreaks

* Corresponding submitters to International Society for Infectious Disease's Program for Monitoring Emerging Diseases ProMED-mail, The global electronic reporting system for outbreaks of emerging infectious diseases & toxins (<http://www.promedmail.org>)

1.3.2 Structure of CHIKV

CHIKV belongs to the Alphavirus genus of the *Togaviridae* family, and has been grouped serologically with the SFV subgroup (Calisher *et al.*, 1980). Electron microscopy studies of CHIKV in green monkey kidney (Vero) cells have revealed a structure characteristic of members of the Alphavirus genus (figure 1.10). In thin sections, the virus shows a roughly spherical shape with a diameter of 42 nm, and composed of a 25 to 30 nm core (Higasshi *et al.*, 1967).

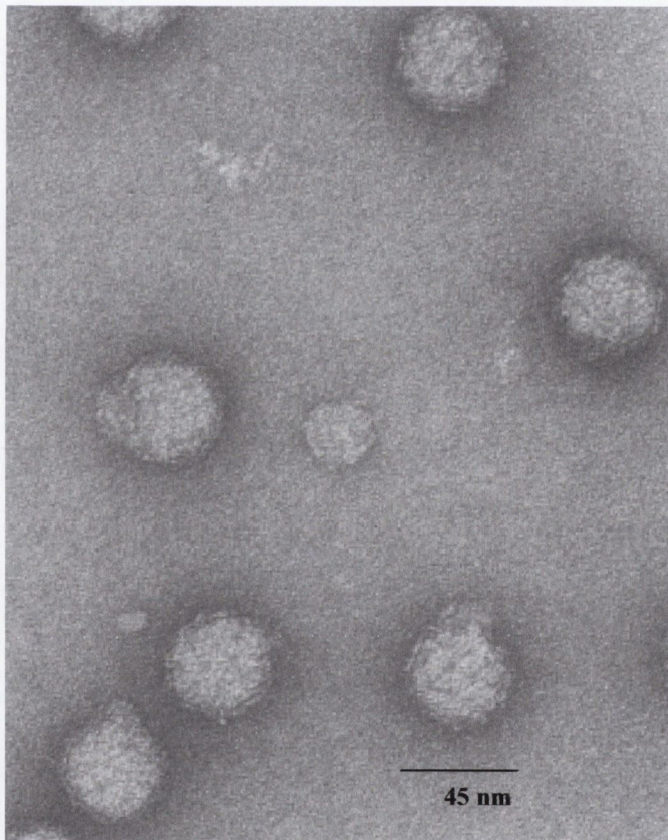


Figure 1.10 Electron micrograph of purified CHIKV virions

CHIKV virions exhibit typical Alphavirus structure and have a diameter of between 40-60 nm (adapted from Simizu *et al.*, 1984)

The envelope glycoproteins of CHIKV have been analysed using polyacrylamide gel electrophoresis and the results show that the envelope of CHIKV contains two glycoproteins, E1 and E2, which migrate very closely to one another (Igarashi *et al.*, 1970; Simizu *et al.*, 1984). The E1-E2 association of CHIKV is similar to that of SFV glycoproteins, and E1 has haemagglutination activity in both viruses. However, E3 of CHIKV is not associated with virions but released into culture fluids, in contrast to E3 of SFV (Simizu *et al.*, 1984).

1.3.3 Pathogenicity of CHIKV infection

CHIKV is a mosquito-borne virus, and the transmission cycle of the viral infection by mosquitoes begins with the infection of cells of the mid-gut and passes into the hemocoel, eventually reaching the salivary glands (Zytoon *et al.*, 1993) ready to be transmitted when a host is bitten.

In spite of several clinical and epidemiological studies that have been done on CHIKV disease, very little is known of the pathology of CHIKV infection in humans. CHIKV has been described as an acute viral infection, and clinically the infection is associated with high fever of sudden onset, followed by symptoms which include; rigor headache, diarrhoea, vomiting, rash, and severe joint pains, largely confined to the knees which may persist for many months after the fever has subsided (Morrison, 1979; Fields *et al.*, 2001; Adesina and Odelola, 1991) Due to the symptoms being very similar to those caused by Dengue virus (DENV), it is thought that CHIKV fever may have been misdiagnosed as Dengue fever and thus under-reported. During the outbreak of CHIKV fever in Calcutta in India, cases occurred where haemorrhagic manifestations of various grades of severity (Sarkar *et al.*, 1965), which upon histopathological investigation showed a perivascular lymphocytic infiltrate in the upper half of the dermis, and red blood cell extravasation was seen in the superficial capillaries (Morrison, 1979).

As mentioned previously, a live, attenuated vaccine was developed for CHIKV (Levitt *et al.*, 1986), which was shown to be safe for humans. Turell and Malinoski (1992) have demonstrated that it is unlikely that mosquitoes can become infected by feeding on a person inoculated with the live, attenuated CHIKV vaccine due to low viremia produced in

inoculated humans. However, there is a possibility that a live virus vaccine has the potential to revert to a more virulent form. Investigation of the neuropathology caused in mouse-models and further characterisation of CHIKV warrant further analysis; the construction of an infectious clone could also be exploited in the production of novel vaccines. There is no specific treatment for CHIKV fever but symptomatic medications for fever and headache are usually needed, and supportive care with rest is indicated during acute joint symptoms. CHIKV is a large public health problem in Central Africa and South-East Asia and is a medically important virus due to the transitory debilitating symptoms from which infected individuals recover.

1.4 Project Aims

Knowledge of the molecular biology of alphaviruses is based predominantly on studies with three members of the group, Venezuelan equine encephalitis virus (VEE), Semliki Forest virus (SFV), and Sindbis virus (SINV). SINV is the classic prototype strain for studying the molecular basis of alphavirus neurovirulence with most work having been carried out by researchers in the USA. The majority of research on SFV, which shows a greater range and diversity of virulence in the animal model system, has been carried out in Europe.

SFV infects both the adult mouse and the neonate and has a diverse age and strain-dependent pathology including fatal encephalitis, teratogenesis, and virus-induced demyelination, thus providing a useful model for the study of viral neuropathogenesis (Atkins *et al.*, 1985). The existence of several different virulent and avirulent strains of SFV has allowed comparative analysis between them at the molecular level, which, combined with the development of SFV infectious cDNA clone technology, provides a useful model for analysis of the molecular basis of alphavirus neuropathogenesis. Reciprocal chimeras between SFV infectious clones producing virulent and avirulent chimeric infectious virus have proved indispensable in elucidating the gene functions in the SFV genome. Several coding regions of the SFV genome have been assigned functions as a result of these reciprocal exchanges, although the precise influence of the non-coding regions of SFV is not quite clear. The role of the 5' untranslated region (UTR) of SFV is

particularly not well understood . In SINV this region has proved to be important in RNA replication.

This project's original aims included fully sequencing CHIKV in order to construct an infectious clone of CHIKV. Reciprocal chimeras were then going to be constructed in order to ascertain what proteins may be involved in virus-mediated demyelination. However, the infectious virus produced from the SFV-A7 infectious clone (CA7) was shown to kill up to 40% of intranasally infected mice although no deaths were expected. An analysis of the SFV-A7 genome was undertaken to ascertain the reasons behind the observed mortality. Previous unpublished work carried out in our lab suggested that CHIKV did not cause demyelination, however upon detailed analysis in this investigation it was shown that CHIKV did induce demyelination in the brains of infected mice, albeit slightly less than that caused by SFV-A7. Thus constructing reciprocal chimeras between CHIKV and SFV-A7 to determine the proteins potentially involved in virus-mediated demyelination would be unproductive. The aims of the project were therefore adapted to include:

- Use of the avirulent SFV-A7 infectious clone and the virulent SFV4 infectious clone to investigate the function of the SFV 5' UTR in relation to neuropathogenicity.
- Construction of 5' UTR chimeric viruses between SFV-A7 and CA7, pA774 and SFV4 and comparing their rates of replication, the efficiency of RNA synthesis, the survival of infected mice and the subsequent neuropathology caused in the brains of infected mice.
- Fully sequence and characterise the Ross strain of CHIKV in order to further investigate differences in virulence and viral neuropathogenesis with SFV.
- Construct a full length CHIKV cDNA clone for future functional comparative studies with the SFV cDNA clones, and the possible design of a more efficient and safer CHIKV vaccine.
- Collaboration with Dr. Ann Powers (CDC, USA) to investigate the neuropathology between the characterised Ross strain of CHIKV and 6 geographically distinct strains of CHIKV.

Chapter Two

Sequencing and Characterisation of Chikungunya virus, Ross strain.

2. Sequencing and Characterisation of Chikungunya virus, Ross strain.

2.1 Introduction

Several alphaviruses have been sequenced and characterised to date, however until this project was initiated Chikungunya virus (CHIKV) had only been partially sequenced and submitted to Genbank (Accession no. L37661) by Parker, M.D. (1994). As CHIKV is a medically important virus infecting thousands of individuals in Africa and South-East Asia each year with debilitating symptoms, it was felt that a more detailed characterisation of the virus merited further investigation. The original strain of CHIKV, referred to as the Ross strain (Powers *et al.*, 2000) was isolated in 1953 from the serum of a febrile human following the Newala epidemic in Tanzania (Ross *et al.*, 1956). In order to characterise this virus it was first sequenced and submitted to Genbank (Accession No. AF490259). A series of analyses to investigate properties CHIKV may share with other SFV subgroup alphavirus members was then pursued. A complete sequence analysis and comparison of these findings with other sequenced SFV group members and several *in vitro* studies were carried out.

Throughout these investigations SFV-A7 was used as a positive control as it is well characterised within our laboratory (Tarbatt *et al.*, 1997, Atkins *et al.*, 1985, 1995). The rate of replication of CHIKV in BHK-21 cells was studied as was the rate of infection in a rat mixed glial cell (MGC) primary culture. As MGCs are composed of several cell types, including astrocytes, neurons and oligodendrocytes, the ability of CHIKV to infect some of these cell types was investigated by immunofluorescence.

The multiplication of virus in the brains of infected BALB/c mice and the survival of these mice when infected by the intranasal and intraperitoneal routes were studied. The neuropathology induced in the brains of infected mice which is discussed in detail in “Chapter 5 – Pathology” was also examined. In collaborating with Dr. Ann Powers (CDC, Fort Collins, USA) comparative studies on the survival of infected mice and the neuropathology caused by infection with seven geographically distinct strains of CHIKV were carried out. Hereafter, the Ross strain of Chikungunya will be referred to as CHIKV with all other strains of Chikungunya described with their strain name.

2.2 Sequencing strategy of CHIKV genome

In an initial experiment, the 3873bp sequence spanning most of the structural polyprotein (26S) of the vaccine strain of Chikungunya virus: 181/25 (Accession No. L37661) was aligned to the published sequences of several alphaviruses. Of these the Gulu strain of O'nyong nyong virus (ONNV, Accession No. M20303) had the closest nucleotide identity with the CHIKV vaccine 26S sequence. Therefore both the CHIKV vaccine 26S sequence and the ONNV Gulu sequence were used as templates to design primers for amplification of CHIKV. Each primer pair was designed to produce a 500-600bp product for ease of sequencing with each overlapping the last such that the primer sites utilised would be incorporated in the overlapping regions.

The strategy involved incorporating an *Eco RI* restriction enzyme (New England Biolabs; NEB, USA) cleavage site at the 5' end of the primer pairs. The amplicon was purified using a Qiagen PCR cleanup Kit (Qiagen, UK) and digested with *Eco RI*. Similarly the cloning vector Litmus 28 (L28; NEB, USA) was linearised using *Eco RI*, and in order to prevent recircularisation its 5' overhang was dephosphorylated using Antarctic phosphatase (NEB, USA). The Amplicons were ligated into L28, transformed in *E. coli* cells, and colonies selected using Blue/White *LacZ* selection marker. The extracted DNA was then sent for sequencing. The resulting sequence was aligned to the template sequence using multiple sequence alignment software Multalin (Laboratoire de Genetique Cellulaire, France), with each overlapping amplicon sequenced, the sequence of the CHIKV genome was deduced.

2.3 5' RACE PCR

RACE PCR is a method by which the PCR technique can be used to amplify the 3' and 5' ends of a cDNA using a small stretch of known sequence within the gene in combination with a primer that is homologous to a "tail" sequence that is attached to either the 5' or 3' ends of the genome. This procedure is made more powerful by the use of nested primers, which reduce non-specific amplification and ensure the production of relatively pure specific product. An overview of this technique is illustrated in figure 2.1.

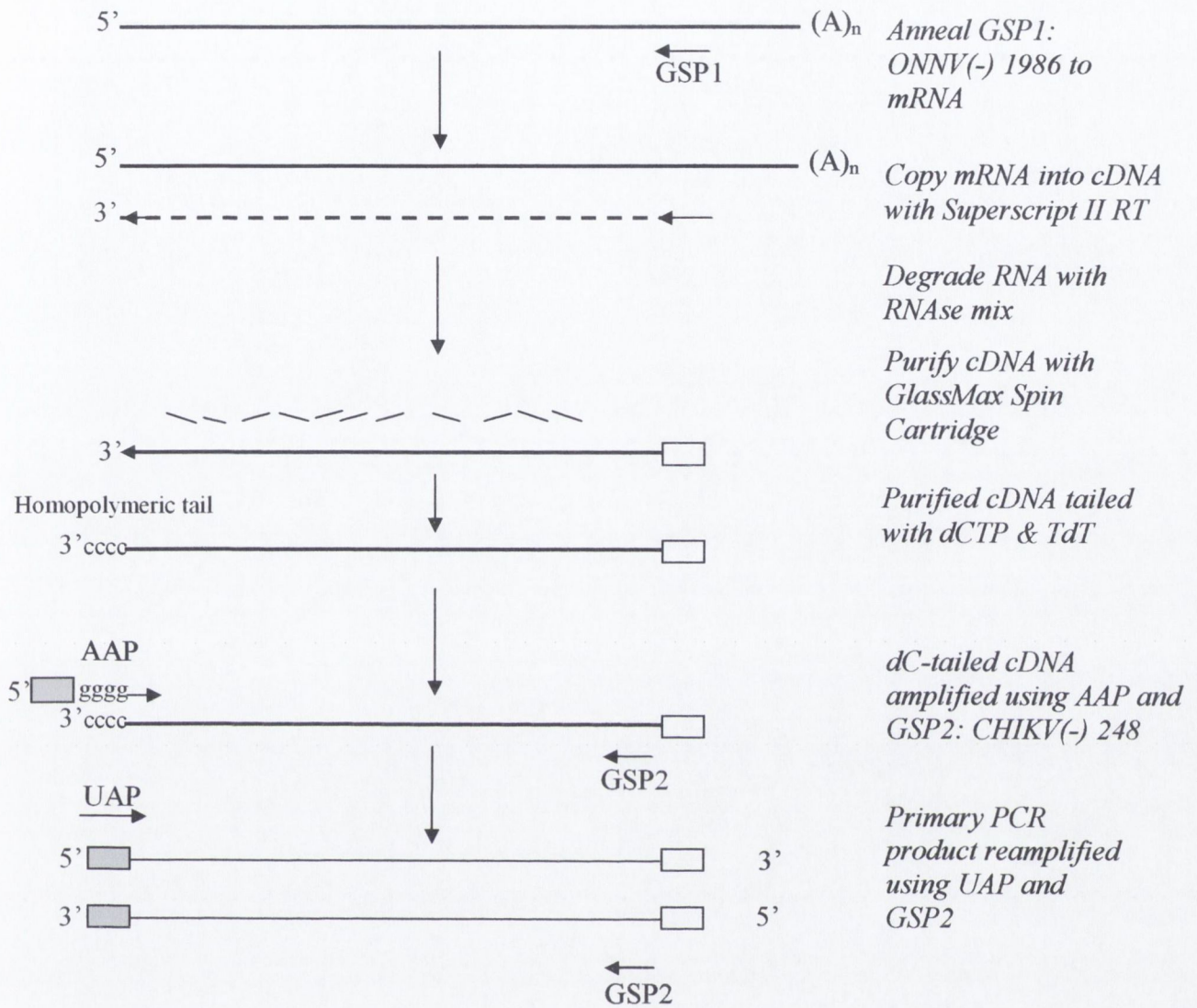


Figure 2.1 Schematic of 5' RACE PCR procedure.

Primer GSP1 was designed from ONNV and produced an amplicon size of 1986 base-pairs (bp). The nested primer GSP2, designed from CHIKV gave an amplicon size of 248 bp when used in combination with the forward Abridged Anchor Primer (AAP, Gibco BRL, USA) which was then purified and further amplified with GSP2 and the forward Universal Amplification Primer (UAP, Gibco BRL, USA). This was then purified and sequenced to generate the 5' UTR sequence of CHIKV.

2.4 Phylogenetic Analysis

Comparative analysis of virus gene sequences has enabled us to deduce the evolutionary relationships between viruses. Since originally sequencing the CHIKV genome (AF490259) a Senegalese strain of Chikungunya isolated in 1983 has been sequenced, termed 37997 (AY726732). Other Chikungunya strains have since been partially sequenced namely the structural polyprotein of the Nagpur strain (India, AY424803). The vaccine strain 181/25 (Thailand, L37661) structural polyprotein was originally sequenced in 1994 by Parker, M.D. Recently another Chikungunya strain termed S27 has been sequenced (NC004162) , however this sequence was not available at the time of these analyses and is therefore excluded from this investigation. Comparing these sequences with those of other SFV subgroup alphaviruses, in particular the Gulu strain of O'nyong nyong virus (M20303) and the recently updated avirulent A7 strain of SFV (Z48163), allows these viruses to be grouped together in terms of genome sequence identity and allows any differences between each virus on an individual gene level to be recorded.

2.5 Virus growth *in vitro*

A virus's ability to grow in host cells is a paramount consideration when investigating the pathology caused to the host. The rate of virus growth *in vitro* can act as an indication of the severity of the symptoms in infected animals. In this investigation we compare the rate of growth of CHIKV and SFV-A7 in BHK-21 cells and then in a cell line more typical of those infected *in vivo*; a primary mixed glial cell line produced from neonate rat brains.

2.6 Virus growth *in vivo*

The ability of SFV4 and SFV-L10 to grow rapidly in neurons results in infected animals dying within 4-5 days post infection (Atkins *et al.*, 1985). However, the avirulent strains of SFV, namely A7 and A774 grow much slower in neurons affording the immune system enough time to be activated resulting in survival of infected animals. Having recorded the level of *in vitro* virus growth in a primary cell line the next step was to investigate the rate of virus growth *in vivo*. In order to ascertain the titres of virus produced in the brains of infected BALB/c mice, they were infected intranasally with CHIKV and SFV-A7. Over a course of time points the

animals were sacrificed, their brains removed, homogenised in medium and the virus titres determined by plaque assay.

2.7 Virus RNA synthesis *in vitro*

In order to investigate virus RNA synthesis, actinomycin D, a chemical that inhibits cellular DNA synthesis so that the RNA synthesis of the virus could be studied, was introduced to infected BHK-21 cells. A radioactive labelled probe [³H]-*methyl* uridine is added that is incorporated into new strands of virus RNA produced. The amount of virus RNA produced over a series of set time points was measured using a scintillation counter. This analysis was carried out for CHIKV, with SFV-A7 used as a control.

2.8 Cell Tropism of CHIKV

In order to show whether CHIKV infects cells of the central nervous system (CNS), oligodendrocytes in particular (Figure 2.2), an immunofluorescent double-labelling approach was used. Initially anti-SFV4 antibody raised in New Zealand white rabbits was used to label the CHIKV infected cells. Antibodies to SFV4 have been shown to cross-react with other members of the SFV group of alphaviruses (Powers *et al.*, 2000). A biotinylated goat anti-rabbit secondary antibody and a rhodamine-avidin immunofluorescent probe were used to detect the SFV-A7 and CHIKV antibody. In order to see which of the infected cells, were oligodendrocytes, a mouse anti CNPase (2', 3' -cyclic nucleotide 3' -phosphohydrolase) antibody was also used. CNPase is strongly associated with myelinated tissues and is localised in the cytoplasmic membrane of oligodendrocytes and Schwann cells (Reynolds *et al.*, 1989). A fluorescein-conjugated streptavidin probe was then attached to a biotinylated goat anti mouse secondary antibody. This process is illustrated in figure 2.2.

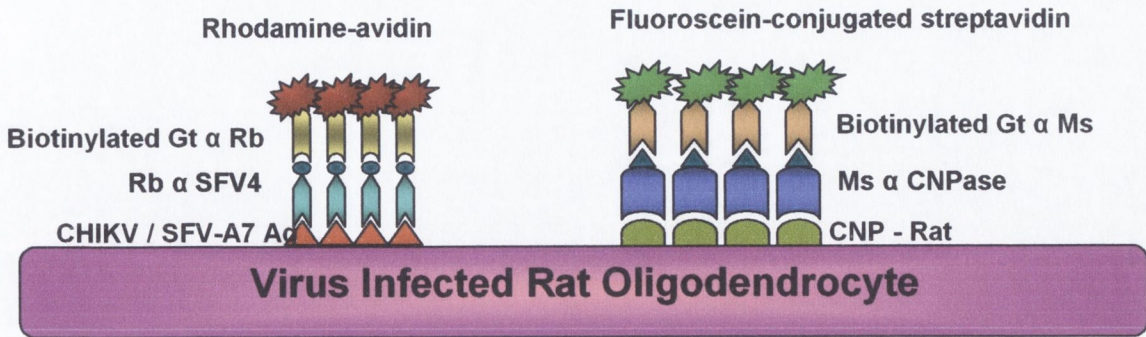


Figure 2.2. Double labelled immunofluorescence of CHIKV infected rat oligodendrocytes. On infection with CHIKV and SFV-A7, a rabbit α SFV4 antibody was used to detect virus antigen, similarly a mouse α CNPase antigen was used to detect CNP in the rat oligodendrocyte. Biotinylated antibodies were then attached to the primary antibodies enabling the addition of rhodamine-avidin (red immunofluorescent label) and fluorescein-conjugated streptavidin (green immunofluorescent label). Oligodendrocytes and virus antigen were then visualised at their respective wavelengths using fluorescence microscopy (Nikon).

2.9 Plaque analysis

When cells are infected with serial dilutions of a virus and overlaid with an agar and growth medium mixture, the results are a series of circular plaques forming on the monolayers where foci of infected cells have died. This technique is generally used to determine virus titre, however, viruses of the same subgroup tend to produce similarly sized plaques and viruses from different geographical origin may differ in their plaque appearance. This is a simple qualitative tool in combination with sequence analysis and phylogeny. The viruses used in this study included SFV4, SFV-A7, ONNV Gulu, CHIKV and 6 geographically distinct strains of CHIKV, one of which had not been definitively classified.

2.10 Materials and methods

2.10.1 Cells

2.10.1.1 Baby Hamster Kidney Cells

The Baby Hamster Kidney 21 (BHK-21; ATCC, USA) cell line was used for virus growth and RNA isolation. Cells were seeded at $1 \times 10^6 \text{ ml}^{-1}$ in 75 cm^2 plastic tissue culture flasks (Iwaki, Japan) and incubated in 15 ml of BHK-21 medium (Glasgow MEM; Invitrogen, UK), supplemented with 5% (v/v) newborn calf serum (NCS), 5% (v/v) tryptose phosphate broth (Invitrogen, UK), 100 U/ml penicillin, 100 $\mu\text{g/ml}$ streptomycin and 2 mM L-glutamine (Sigma, USA). Cells were maintained at 37°C in a humidified atmosphere of 5% CO_2 until confluent for use, storage or passage. Cells were passaged as follows: cell monolayers were washed twice with Dulbecco's phosphate buffered saline without calcium and magnesium (D-PBS; Invitrogen, UK) and incubated with 0.5% trypsin 5.3 mM EDTA (Invitrogen, UK) at 37°C until cell detachment was evident, typically within 2-3 minutes (min). The flask was tapped to complete detachment and supplemented BHK-21 medium was added to terminate trypsinisation. The resulting cell suspension was aspirated several times to break up cell clumps and split at a 1:3 ratio into new 75 cm^2 flasks containing 15 ml BHK-21 medium.

2.10.1.2 Neonate Rat Mixed Glial Primary Cells

Preparation of glial cell cultures was based on the method of Chapman and Rumsby, (1982) later modified by Gates *et al.* (1985). Day old neonate rats were sacrificed by decapitation and the forebrains aseptically removed. Individual cerebra were divided along the longitudinal fissure into separate hemispheres and the meninges removed by blotting on sterile filter paper. The tissue was placed in a Petri dish, chopped finely with a scalpel and 2 ml of Dulbecco's modified Eagle's medium (DMEM; Invitrogen, UK), supplemented with 10% (v/v) foetal calf serum (FCS), 1% (v/v) sodium pyruvate MEM (100 mM) (Invitrogen, UK), 100 U/ml penicillin and 100 $\mu\text{g/ml}$ streptomycin (Sigma, USA) was added. The mixture was lightly pulped using a spatula and a further 6 ml of supplemented DMEM was added and the tissue expelled 5 times through a 19-gauge hypodermic needle and 10 times through 21- and 23-gauge hypodermic needles respectively. Cells were counted using a

haemocytometer and seeded at a density of 1×10^5 cells per 4 cm^2 well of a two-well chamber slide (Falcon, USA). Cells were maintained at 37°C in a humidified atmosphere of 5% CO_2 , the growth medium was replaced at 3 days post seeding, and every 2 days thereafter until confluency was achieved, typically between 9 and 10 days post seeding.

2.10.2 Viruses

2.10.2.1 Virus Strains

The Ross strain of CHIKV and ONNV strain Gulu were obtained from Dr. V. Deubel, Pasteur Institute, Paris. Seven geographically distinct strains of CHIKV: 37997, 181/25, DAK ArB16878, PO 731460, PH H15483 and SV-0451/96 were obtained from Dr. Ann Powers, CDC, Fort Collins, Colorado, USA. The A7 strain of SFV was obtained from Dr. C. Bradish, Microbiology Research Establishment (MRE), Porton Down, Wiltshire, UK.

Strain	Location	Date	Host	Passage History*	Virus
Ross	Tanzania	1953	Human	SM-175, V-1	CHIKV
37997	Senegal	1983	<i>Ae. furcifer</i>	AP61-1, V-2	CHIKV
181/25	Thailand	1962	Human	MRC5-18, V-1	CHIKV
PO 731460	India	1973	Human	V-2, M-1	CHIKV
PH H15483	Philippines	1985	Human	V-5	CHIKV
SV-0451/96	Thailand	1996	Human	RMK-1, V1	CHIKV
DAKAr B16878	C.A.R**	1980	<i>An. funestus</i>	SM-5, BHK-1	SFV, CHIKV ?
SFV-A7	Mozambique	1959	<i>Ae. argentopinctatus</i>	SM, BHK-21	SFV
Gulu	Uganda	1959	Human	SM-1, V-3, BHK-1	ONNV

Table 2.1 Virus strains used in the characterization of CHIKV virus

Adapted from Powers *et al.*, 2000, 2001. * Cell type followed by number of passages in that cell. BHK, baby hamster kidney cells; V, Vero cells; SM, suckling mouse; AP61, *Ae. Pseudoscutellaris* mosquito cells; M, mosquito; MRC5, human lung cells; RMK, rhesus monkey kidney (LLC-MK2) cells. ** C.A.R. Central African Republic

2.10.2.2 Growth and Harvest of virus

Working stocks of the viruses in table 2.1 were obtained by allowing 1 ml of plaque-purified stocks to adsorb onto subconfluent BHK-21 cell monolayers in 75 cm² plastic tissue culture flasks (Iwaki, Japan) for 1 hour (h) at 37°C in a humidified atmosphere of 5% CO₂. A homogenous infection was achieved with rocking movements every 15 min. Virus inoculum was removed after 1 h and 15 ml of supplemented BHK-21 medium was added before a 24 h incubation at 37°C in a humidified atmosphere of 5% CO₂. Between 24 h and 36 h the cell monolayer exhibited cytopathogenic effect (c.p.e) and the supernatant was removed, and virus was harvested. To harvest virus, the supernatant was removed, centrifuged at 3,000 x g for 10 min to remove cellular debris, and filtered through a 0.2 µm filter (Pall Life Sciences, USA). The resulting working stock virus, was stored at -70°C in 1 ml aliquots. Virus titre was established by plaque assay, and diluted before administration *in vivo*.

2.10.2.3 Plaque assays

Viral titres were measured by plaque assay in BHK-21 cells. Cells were seeded at 1×10^5 ml⁻¹ in a total volume of 3 ml per 60 mm² cell culture dish (Iwaki, Japan), incubated at 37°C in a humidified atmosphere of 5% CO₂, and allowed to reach subconfluence. The cells were inoculated in duplicate with 0.5 ml of each serial dilution of working stock virus in D-PBS (Invitrogen, UK) from 10⁻² to 10⁻¹⁰. The infected cells were then incubated for 1 h at 37°C in a humidified atmosphere of 5% CO₂ and rocked every 15 min to ensure homogenous infection. Two dishes were inoculated with 0.5 ml D-PBS alone as negative controls. On removal of the inoculum, equal volumes of 1.8% noble agar (Difco, USA) at 45°C and overlay medium (10X Minimal Essential Medium (MEM) supplemented with 10% NCS, 10% tryptose phosphate broth, 200 U/ml penicillin, 200 µg/ml streptomycin, 4mM L-glutamine and distilled water) at 37°C were mixed and added to the dishes to a final volume of 3 ml per dish. When the agar had solidified, typically within 5 min at room temperature (RT), the plates were incubated for 48 h at 37°C in a humidified atmosphere of 5% CO₂. At 48 hours post-infection (h.p.i) 3 ml of neutral buffered formalin (NBF; BDH, UK) was added to each dish and allowed to fix for 15 min, the NBF and agar were then removed under running tap water. Cells were then stained with 2 ml of crystal violet (Clin-Tech, UK) for 3 min then rinsed under running tap

water. The dishes were left to dry at room temperature and plaques counted against a light background and viral titre expressed as plaque forming units (p.f.u) / ml.

2.10.3 Preparation of Virus DNA

2.10.3.1 Virus RNA isolation

The supernatant of infected BHK-21 cell monolayers in 75 cm² plastic tissue culture flasks (Iwaki, Japan) exhibiting c.p.e was removed, typically 24 h.p.i. To extract virus RNA 1 ml of Trizol reagent (Invitrogen, UK) was added to the infected monolayer and left at R.T. for 2 min. Cells were then detached from the flask using a cell scraper (Nalge Nunc, USA) and incubated in a 1.7 ml microtube (Axygen, USA) for a further 5 min at R.T. 200 µl of chloroform (BDH, UK) were added and the mixture gently shaken for 15 seconds (sec) until emulsified and incubated at RT for a further 15 min. Cells were then centrifuged at 18,400 x g for 15 min at 4°C and the aqueous phase transferred to a fresh 1.7 ml microtube. The RNA was precipitated by the addition of 500 µl of isopropanol (BDH, UK), incubated at R.T. for 5 min and then centrifuged as described above for 10 min, at which point a pellet was visible. The supernatant was removed and the RNA pellet washed by the addition of 1 ml of 70% ethanol (BDH, UK). The microtube was gently shaken and centrifuged as previously described for 10 min, the ethanol was removed using an RNase- / DNase-free pipette (Axygen, USA) and the pellet allowed to partially air-dry at R.T. 100 µl of nuclease-free dH₂O (Promega, USA) was added and the mixture incubated at 50°C on a BT-1 block thermostat (Grant, UK) for 5 min. The RNA was then dissolved by gentle pipetting and 4 µl aliquots were stored at -70°C in 700 µl PCR tubes (Axygen, USA).

2.10.3.2 cDNA amplification

First strand cDNA was synthesised as follows: 1µl of Oligo (dT)₁₈ primer (0.5 µg/µl; Promega, USA) was added to 4 µl of virus RNA (0.25 µg/µl), then heated at 70°C for 5 min, and placed on ice for 5 min. 15µl of a reaction mix containing 4µl of ImProm-II 5x reaction buffer, 1µl dNTP mix (10mM), 20 U RNasin, 2.4 µl MgCl₂ (25mM), 6.1 µl of nuclease free water, and 1 µl of ImProm-II reverse transcriptase, was then added to the 5 µl RNA / Oligo (dT)₁₈ mixture. The total cDNA reaction mixture (20 µl) was then gently vortexed and briefly spun down before being

incubated at 25°C for 5 min, at 42°C for 60 min and at 70°C for 15 min (table 2.4). The cDNA (20µl) was then stored at -20°C until needed for the polymerase chain reaction (PCR). Negative control samples contained 4µl RNase-free water instead of virus RNA.

2.10.3.3 Primer design

Oligonucleotide primer pairs were designed to be 20-40 basepairs (bp) in length and had approximately 50% G/C content. The sequences of the primers were designed to avoid internal secondary structure and complementary areas of sequence which result in the formation of “primer dimers”. The sequences of the designed primers were specific to the area of DNA template to which they hybridise and produce specific amplicons during PCR. For cloning purposes, an enzyme restriction site was incorporated at the 5' end of each primer, along with three random bases 5' of the enzyme restriction site. The random bases facilitate digestion with the appropriate restriction enzyme. The melting temperatures of the designed primers were typically 2-3 °C above the annealing temperatures chosen for cycling conditions as this reduces non-specific primer binding.

2.10.3.3.1 CHIKV Nonstructural protein primers

The sequence of ONNV Gulu strain shares a 78% nucleotide identity over the structural region of the CHIKV vaccine strain and was used as template to design primers to amplify the CHIKV non-structural coding region. The sequences of the primers designed along with their positions on the ONNV Gulu genome are shown in table 2.2. Amplification of the coding region was carried out by designing 28 pairs of overlapping primers to amplify between 500 and 600bp fragments across the entire length of the genome

2.10.3.3.2 CHIKV Structural protein primers

Structural primers were designed as described in section 2.10.3.3.1 although the CHIKV structural polyprotein sequence submitted by Parker, M.D. (1994) was used rather than ONNV Gulu virus sequence. The sequences of the primers designed along with their positions are shown in table 2.3

Primer name	Primer Sequence	Primer position
NSP Fwd 1 NSP Rev 1	ctcgaattcattggctgcgtgagacacacg cacgaattcgtacagcatagacgtcttgg	(1-21) (526-546)
NSP Fwd 2 NSP Rev 2	cggaattcacagatgatcatgt ctggaattcatgatgagtaccgcatac	(485-500) (982-1000)
NSP Fwd 3 NSP Rev 3	cggaattcaaggctacgtcgta cgagaattcgattctagtcctcaacggg	(924-938) (1462-1480)
NSP Fwd 4 NSP Rev 4	cacgaattcgacagcttgggtaccgag gaggaattccgtgtacaccatcg	(1418-1438) (1950-1964)
NSP Fwd 5 NSP Rev 5	gtgggatcctagtgccctcaggctacgcaa gtgggatcctacaacacgtcgactggtc	(1890-1910) (2412-2430)
NSP Fwd 6 NSP Rev 6	ctcgaattctagagatatctgcacgtacgg gaggaattcatgacctcgtgtccacgatagtc	(2361-2381) (2788-2810)
NSP Fwd 7 NSP Rev 7	ctcgaattcgtagtgacactacaggct gaggaattcccctccggtaatatgcc	(2701-2719) (3225-3241)
NSP Fwd 8 NSP Rev 8	gtcgaattcacgactagacagtggttcc tctgaattcgcagtgcaaggctacat	(3175-3193) (3621-3637)
NSP Fwd 9 NSP Rev 9	gtagaattcctcattagtgccgaac cggaattcaaggctgcattcagt	(3529-3544) (4051-4065)
NSP Fwd 10 NSP Rev 10	gtcgaattccagcaacactgagatgtt gtggaattccagtagatgaccacgtctgcat	(3969-3987) (4501-4521)
NSP Fwd 11 NSP Rev 11	tctgaattccacaggtgtatactcaggag gcggaattccacacaattatgcttga	(4421-4442) (4944-4962)
NSP Fwd 12 NSP Rev 12	gtcgaattcgtatgcagatgcatcatc gtagaattcctcggacgtagccat	(4851-4867) (5370-5385)
NSP Fwd 13 NSP Rev 13	gcagaattcctgactgtgacatgc ctcgaattctgagcacgtggaccag	(5328-5342) (5752-5770)
NSP Fwd 14 NSP Rev 14	gtagaattcggagactcctacccgg gtagaattcatctggtacgacgccactg	(5711-5727) (6213-6231)
NSP Fwd 15 NSP Rev 15	tgtgaattcatcgacgctgcaac gcagaattccaagtctcagtcgta	(6173-6187) (6567-6583)

Table 2.2 Primers designed from O'nyong nyong virus Gulu to amplify the CHIKV non-structural polyprotein. gaattc: *Eco RI* restriction enzyme recognition sequence, ggtacc: *Bam HI* restriction enzyme recognition sequence (NSP5 Fwd/Rev primers).

Primer name	Primer Sequence	Primer position
SP Fwd 1 SP Rev 1	cgcgaattctagagaactgcctactgg ctcgaattcagtgagcgc caatgagtcgtc	(6464-6482) (6958-6978)
SP Fwd 2 SP Rev 2	gtcgaattcgcgccgtattggaaccgatat gaggaattcctctgcagccagtgca	(6915-6935) (7461-7477)
SP Fwd 3 SP Rev 3	gtagaattcctgtcagctgggcaaaccgct gcggaattccttgactcgaagatgcaatc	(7405-7425) (8053-8073)
SP Fwd 4 SP Rev 4	gtggaattctgcgcggtacctcaaca gtggaattctgtccacgtcaccacggaga	(7877-7895) (8438-8458)
SP Fwd 5 SP Rev 5	tgtgaattcacagcggcagaccgatctt cac gaattc atcgtgcacgggtgctga	(8354-8372) (8956-8972)
SP Fwd 6 SP Rev 6	ctcgaattcgattggaccaagctgcg gaggaattcttaggcaccctgcatgca	(8881-8897) (9485-9503)
SP Fwd 7 SP Rev 7	ctcgaattcgcaaggtgatcaatgccatg cgcgaattctcatagtagggtacagctc	(9353-9373) (9774-9793)
SP Fwd 8 SP Rev 8	ctggaattcgcgagccgtacaagtattggc gaggaattcagctgtctgtacgcgctcaca	(9692-9711) (10136-10156)
SP Fwd 9 SP Rev 9	cacgaattcgtaatgagcgtcgggtccc gacgaattcgtcaattgcgta	(10113-10131) (10445-10457)
SP Fwd 10 SP Rev 10	cgcgaattctacagctgtaagtc ctcgaattcactgaagccagatggt	(10371-10385) (10853-10869)
SP Fwd 11 SP Rev 11	tctgaattccaggacaattggcgac tctgaattccccaagtctgaggagt	(10735-10751) (11068-11084)
SP Fwd 12 SP Rev 12	cgcgaattctaaccggacatgctgt cgcgaattcgggcacatatacctggta	(11032-11046) (11515-11532)
SP Fwd 13 SP Rev 13	cacgaattcaatcgtggtgctatgc ggggaattctaacatctcctag	(11429-11444) (12001-12013)

Table 2.3 Primers designed from CHIKV Vaccine virus to amplify the CHIKV structural polyprotein. gaattc: *Eco RI* restriction enzyme recognition sequence.

2.10.3.3.3 CHIKV 5' Nontranslated region (UTR) Primers

The 5' RACE Abridged anchor primer (AAP) and the Universal Amplification primer (UAP) were supplied in the 5'/3' RACE PCR Kit (Roche, Switzerland). The Genome Specific Primers (GSPs) were reverse nested primers designed from the CHIKV (GSP2) and ONNV Gulu (GSP1) genome templates respectively.

AAP: 5'-GGCCACGCGTCGACTAGTACGGGGGGGGGG-3'
UAP: 5'-CUACUACUAGGCCACGCGTCGACTAGTAC-3'
GSP1: ONNV(-)1986 5'-CGGTTCACAAACTCTCGCTC-3'
GSP2: Chik(-) 248 5'-GTCGGGATCAATTCCTGCTC-3'

cDNA was prepared using a nested primer designed from ONNV (GSP1, figure 2.1). Newly synthesised cDNA strand then had a homopolymeric tail added to its 3' end using terminal transferase. The 5' RACE Abridged Anchor Primer was then used to generate second-strand cDNA. This dsDNA then served as the template for a secondary PCR reaction using a nested gene-specific primer (UAP) and inner primer designed from CHIKV (GSP2). The 5' RACE PCR was carried out at the CDC (Fort Collins, USA) in accordance to manufacturer's recommendations, using the same PCR conditions as shown in table 2.4, an overview of this technique was illustrated in figure 2.1.

2.10.3.3.4 Polymerase Chain Reaction (PCR) thermocycling conditions

PCR was carried out on a Hybaid PCR Express Thermal cycler, the PCR conditions used are described in table 2.4. 1µl of each amplicon produced was run on a 0.8% (wt/vol) agarose gel (figure 2.3).

RT-Step cycle (1 cycle)	annealing temperature	42° C	60 min
	denaturing temperature	72° C	5 min
	holding temperature	72° C	5 min
Initial cycle	denaturing temperature	95° C	2 min
Step cycle (30 cycles)	denaturing temperature	95° C	30 sec
	annealing temperature	49° C	30 sec
	extension temperature	72° C	4 min
Final cycle	denaturing temperature	72° C	1 min

Table 2.4 Thermocycling conditions used for PCR. Reverse transcription (RT) step was carried out to generate cDNA using oligo dT₍₁₈₎ (Promega, USA) and polyadenylated mRNA template (section 2.10.3.2). The resulting cDNA was then used for subsequent PCR steps described in section 2.10.3.3.5.

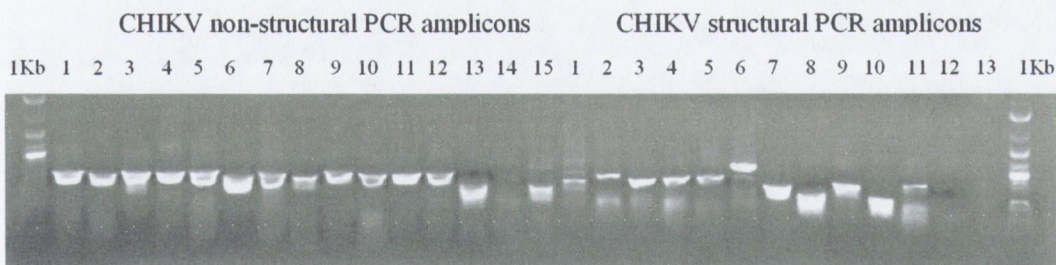


Figure 2.3 CHIKV non-structural and structural PCR amplicons were run on a 0.8% agarose gel. 1kb markers are present in lanes annotated 1kb. Bands of expected size (400-600bp) were excised, gel purified, digested with *Eco RI*, ligated into the Litmus 28 expression vector (NEB, USA) and sent to LARK technologies (U.K) for sequencing.

Lane 13 of the structural amplicons gave no amplification. This was due to the low sequence identity between the 3' untranslated region (UTR) of ONNV and that of CHIKV, this region was subsequently sequenced using SP Fwd 13 primer and an Oligo dT₁₈ reverse primer (results not shown).

2.10.3.3.5 PCR

The first-strand cDNA synthesised as described in section 2.10.3.2 was used to amplify double-stranded cDNA by PCR using the custom made primers and cycle conditions outlined in section 2.10.3.3. PCR primers were designed to incorporate an *Eco RI* restriction enzyme (*Bam HI* in the case of NSP5 fwd / rev primers) at the 5' end to facilitate cloning and each primer pair was designed to produce a 500-600 bp product for ease of sequencing. Similarly, each primer pair was designed to overlap such that the primer sites utilised would be incorporated in the overlapping regions.

The first-strand cDNA (20 µl, approximately 10^5 target molecules of template DNA) was set up in 100 µl volumes in 700 µl sterile microcentrifuge tubes (Axygen, USA) with the following final concentrations: 200 µM cDNA reaction dNTPs, 2 mM MgCl₂, 10x Pfu Polymerase buffer (Mg²⁺ free), 0.1 µM forward and reverse CHIKV or ONNV primers and 2.5 U of Pfu DNA Polymerase (Promega, USA). Negative control samples contained 20 µl of the cDNA amplification negative control described in section 2.10.3.2.

2.10.4 Manipulation of Virus DNA

2.10.4.1 DNA purification I

To purify amplified DNA fragments, 25 µl of loading buffer (33% (vol/vol) glycerol, 0.05% (wt/vol) bromophenol blue, 0.05% (wt/vol) xylene cyanole FF; Promega, USA) was added to each 100 µl PCR reaction and run on a 0.8% (wt/vol) agarose gel (0.8% agarose, 3.0 µl 10 mg/ml ethidium bromide in 40 ml TBE) in 1x TBE (89 mM Tris base, 89 mM boric acid, 2 mM EDTA (pH 8.0)) at 86 milli-amps (mA) for purification using the Promega Wizard Kit (Promega, USA). Fragments were excised from the agarose using a sterile surgical blade, placed in a 1.7 ml microtube (Axygen, USA) and weighed.

A binding buffer (4.5M guanidine isothiocyanate, 0.5M potassium acetate (pH 5.0)) was added at a rate of 3 volumes of buffer to 1 volume of gel (300 µl of buffer to 100 µg of gel) and the mixture incubated for 10 min at 60°C, with vortexing every 3 min. The buffer solubilises the agarose gel slice, and provides appropriate conditions for binding of DNA to a silica membrane in a Wizard Column. The mixture was added to a Wizard column and centrifuged (10,000g, 30 sec). The flow-through was discarded

and 700 µl of wash buffer (10mM potassium acetate (pH 5.0), 80% ethanol, 16.7 µM EDTA (pH 8.0)) added and centrifuged (10,000g, 30 sec), A further 500 µl of wash buffer was added to remove all traces of agarose and centrifuged (10,000g, 5min). Purified DNA was eluted in 50 µl of pre-heated (60°C) nuclease-free water.

2.10.4.2 Restriction Digestion

DNA was digested with *EcoRI* (*Bam HI* for NSP5 Fwd/Rev amplicon) to create the 5' overhang needed to ligate into the *EcoRI*-linearised Litmus 28 cloning vector (New England Biolabs (NEB), USA) for sequencing. The following reaction mixtures were digested for 2 h at 37°C: 15 µl Purified PCR product, 2 µl nuclease-free water, 2 µl 10X *EcoRI* NEBuffer (150 mM NaCl, 10 mM Tris-HCl, 10mM MgCl₂, 1mM dithiothreitol pH 7.9) and 20U *EcoRI* enzyme (NEB, USA).

2.10.4.3 DNA purification II

Digested reactions were purified using the QIAGEN Nucleotide Removal Kit (Qiagen, USA). 200 µl of Buffer PN which promotes the absorption of DNA fragments greater than 17 bases and less than 10 kilobases (kb) to the silica membrane in the Qiagen elute-column, was added to the 20 µl digested DNA. The mixture was added to the Qiagen elute-column and centrifuged (10,000g, 1 min). The DNA was then washed by adding 750 µl of PE Buffer and centrifuged (10,000g, 1 min). The centrifuge step was repeated without the addition of PE Buffer in order to get rid of any excess buffers. Purified, *EcoRI*-digested DNA was eluted in 20 µl of preheated (60°C) nuclease-free water. Final product was analysed and quantified by electrophoresis of a 1µl aliquot on a 0.8% (wt/vol) agarose gel. A concentration was deduced by comparison of band intensity to a molecular weight 1KB marker (NEB, USA).

2.10.4.4 Preparation of Litmus 28 cloning vector

Litmus 28 (L28) plasmid was linearised (1µg) with *EcoRI* for 2 h at 37°C and the DNA purified as previously described in section 2.10.4.3. The purified DNA was then treated with Antarctic phosphatase (NEB, USA), this catalyzes the removal of 5' phosphate groups from DNA. Without the 5' phosphoryl termini required by ligases these treated plasmids cannot self ligate, thus decreasing the vector background in cloning. 5 units (1µl) of Antarctic phosphatase (in 10mM Tris-HCl (pH7.4), 1mM

MgCl₂, 1mM DTT, 50% glycerol) were added to 1 µl 10X Antarctic Phosphatase reaction buffer (50mM Bis Tris-Propane, 1 mM MgCl₂, 0.1 mM ZnCl₂, pH 6.0. NEB, USA) and 1 µg of cut DNA, the reaction was then mixed and incubated at 37°C for 15 min. The reaction was heat inactivated for 5 minutes at 65°C before further DNA purification and ligation.

2.10.4.5 Ligation into L28

Dephosphorylated, *Eco RI*- linearised L28 was added in a 1:16 ratio to a 700 µl microfuge tube containing 16 µl of each purified *Eco RI* digested CHIKV amplicon as described in section 2.10.4.3. 2 µl of T4 10X ligase buffer and T4 ligase (Promega, USA) were then added, the reaction was gently vortexed and incubated overnight at room temperature.

2.10.4.6 Preparation of competent *E. coli* DH5α cells

Escherichia coli (*E. coli*) strain DH5α cells (NEB, USA) were used for transformation of recombinant Litmus constructs. A 2 ml overnight culture was prepared in L-broth which was used to inoculate an additional 500 ml of fresh L-broth in a 2 litre baffled flask. The culture was incubated at 37°C with shaking (200 revolutions per minute (rpm)) until the cells reached an optical density of 0.45-0.55 at a 600 nanometre (nm) wavelength. The culture was then incubated on ice for 2 h after which the cells were centrifuged at 3,000 x g for 20 min at 4°C. The supernatant was discarded and the bacterial pellet resuspended in 500 ml of titration buffer (100 mM CaCl₂ (Merck, Germany), 70 mM MgCl₂ (BDH, UK), 40 mM NaOAc and placed on ice for 45 min. Cells were pelleted as described above and gently resuspended in 2 x 20 ml ice cold 100 mM MgCl₂. 80% glycerol (BDH, UK) was added drop-wise with gentle swirling to a final concentration of 15% (vol/vol). The cell-glycerol suspension was then aliquoted on ice and snap-frozen in liquid nitrogen and stored at -70°C.

2.10.4.7 Transformation

Competent *E. coli* DH5α cells were transformed with each L28-CHIKV PCR reaction by incubating 180 µl of competent cells with 20 µl of each plasmid DNA ligation reaction for 1h on ice, followed by heat shocking of cells for 1 min 30 sec at 42°C. Cells were then cooled on ice for 10 min before being transferred to 800 µl of L broth without drug selection. Cells were allowed to recover for 1 h shaking at 37°C

before the addition of 100 µg ampicillin. Cells were then allowed to grow for a further 1 h. Transformed colonies were then plated onto L-agar plates containing 100 µg/ml ampicillin and 100µl of a 1:1 X-Gal / IPTG mixture and incubated overnight at 37°C.

2.10.4.8 Colony Selection and Linearisation

Isolated colonies of recombinant plasmids (white colonies) were inoculated in 30 ml of L broth containing 100 µg/ml ampicillin. Cells were grown overnight with shaking at 37°C. From each culture a 20 ml aliquot was removed and mixed with 15% (wt/vol) 80% glycerol. These were then stored at -70°C in 1 ml aliquots. The remaining culture was used to purify the plasmid DNA, using the QIAGEN Miniprep Plasmid Purification Kit (Qiagen, UK). This kit is based on a modified alkaline lysis protocol. Cells were harvested by centrifugation (10,000g, 10 min, 4°C). Each pellet was resuspended in 250µl of buffer P1 (10mM EDTA, 100µg/ml Rnase A, 50 mM Tris-HCL, pH 8.0), and transferred to a microfuge tube. Cells were lysed by the addition of 250µl of buffer P2 (200 mM NaOH, 1% (wt/vol) SDS). 350 µl of buffer N3 was added, and mixed gently prior to centrifugation (10,000g, 10 min). The supernatant was applied to a QIAprep column and further centrifuged (10,000g, 1 min). The column was then washed with 500 µl of buffer PB, to remove all trace of nuclease activity. The column was again washed with 750 µl of buffer PE, and centrifuged twice (10,000g, 1 min). Clean DNA was eluted in 30µl of water by centrifugation (10,000g, 1 min). Each DNA was digested for 1 h at 37°C with *Eco RI* enzyme to confirm correct plasmid. Products were confirmed by mixing a 1µl aliquot with 1µl loading buffer and running this on a 0.8% (wt/vol) agarose gel in TBE at 75 mA.

2.10.4.9 Sequencing and sequencing alignment

PCR products were cleaned using the QIAquick PCR Purification Kit (Qiagen, UK) and eluted in 30µl nuclease-free water. The purified PCR products and 20µl of each primer (0.02µg µl⁻¹) used to amplify the products were sent to LARK Technologies (Essex, UK) for sequencing. Sequence was sent via e-mail 3-4 working days upon receipt of products and primers. Sequences were initially submitted in an online BLAST search (<http://www.ncbi.nlm.nih.gov/blast>) and subsequently analysed using Redasoft Visual Cloning 2000 software (Redasoft, Canada). Once accurate sequences were determined and added to the CHIKV genome, sequence alignments

were pursued, these were carried out using an online multi-alignment software package termed Multalin (Laboratoire de Genetique Cellulaire, France).

2.10.5 *In vitro* Analyses

2.10.5.1 CHIKV growth curves in BHK-21 cells

BHK-21 cells were seeded at $1 \times 10^4 \text{ ml}^{-1}$ in 6-well plates. Cells were infected at a multiplicity of infection (M.O.I.) of 10 p.f.u / cell in a total volume of 500 μl infection medium for 1 hour, with rocking movements every 15 min to achieve a homogenous infection. Cell culture fluid was harvested at 2, 4, 6, 8, 10, 14, 18, 22 h.p.i and production of virus was quantified by plaque assay as described in section 2.10.2.3. Infection medium alone was used as a mock-infection negative control, each sample was performed and analysed in triplicate

2.10.5.2 Mixed Glial Cell Viability Assay

To measure growth in cultured cells following SFV-A7 and CHIKV infection, mixed glial cells were seeded at $1 \times 10^4 \text{ ml}^{-1}$ in 6-well plates. Cells were infected at M.O.I. of 10^{-2} in a total volume of 500 μl infection medium for 1 hour, with rocking movements every 15 min to achieve a homogenous infection. Infection medium alone was used as a mock-infection negative control. Fresh Dulbecco's MEM medium was added and the cells were incubated at 37°C in a humidified atmosphere of 5% CO_2 .

The viability of CHIKV, SFV-A7 and mock-infected MG cells was determined by trypan blue exclusion. The dye trypan blue (Sigma, USA) is excluded from viable cells, and under bright field microscopy membrane-damaged cells stain blue-violet, whereas healthy, viable cells appear translucent. At 12 h intervals, the medium from SFV-A7, CHIKV and mock-infected control cells was removed and cell monolayers washed twice in Dulbecco's PBS. Cells were then trypsinised with 500 μl 0.25% (w/v) trypsin / EDTA (Gibco BRL, UK) solution for 5 min at 37°C , the plates tapped to complete trypsinisation and 500 μl Dulbecco's MEM added to terminate trypsinisation a give a total volume of 1 ml. A 100 μl aliquot of each sample was removed and added to 100 μl 0.45% (w/v) trypan blue solution. A 100 μl aliquot of this mixture was applied to a haemocytometer and viable cells were counted. Cells

were harvested and analysed each 12 hours over a period of 72 hours, each sample was performed and analysed in triplicate.

2.10.5.3 Virus RNA synthesis of CHIKV, SFV-A7 and six geographically distinct CHIKV strains

The rate of RNA synthesis of virus was measured by infecting subconfluent BHK-21 cell monolayers with viruses at a high M.O.I. (10 p.f.u./cell). Virus was allowed to adsorb for 1 h at 37°C in a humidified atmosphere of 5% CO₂, at which point the inoculum was replaced with BHK medium containing 5 µg/ml actinomycin D and reincubated for 2 h at 37°C in a humidified atmosphere of 5% CO₂. The inoculum was then removed and fresh BHK medium containing 5 µg/ml actinomycin D and 1 µCi/ml [³H]-*methyl* uridine (Amersham Pharmacia Biotech, Sweden) was added. The cell monolayers were returned to 37°C for a further 2 h. Cell monolayers were then washed twice with PBS and dissolved in 2 ml of 1% (w/v) sodium dodecyl sulphate (SDS) to lyse the cells. On adding 2ml of ice-cold 10% (w/v) trichloroacetic acid (TCA) the mixture was allowed to stand on ice for 15 min. The resulting precipitate was collected on glass fibre discs (Whatmann, USA) using a vacuum manifold (Millipore, USA) and washed twice with 4 ml of ice-cold 5% (w/v) TCA and once with 100% ethanol and air-dried. Filters were then placed in plastic scintillation vials into which 4 ml scintillation fluid (ICN, USA) was added prior to counting using a Tricarb 1500 scintillation counter (3 min count/sample). This procedure was carried out in triplicate for each virus at 2, 4, 6, and 8 hours post infection (h.p.i).

2.10.5.4 Plaque Analysis

Plaque assays were performed as described in section 2.3.4 on the 37997, 181/25, DAK ArB16878, PO 731460, PH H15483, SV-0451/96 and Ross strains of CHIKV and the Gulu strain ONNV. The titres were recorded and the size and shape of plaques produced by each virus observed.

2.10.5.5 Immunofluorescence of virus infected oligodendrocytes

Immunofluorescence was used in order to determine the cell tropism for Chikungunya and SFV-A7 in a mixed glial cell population. Of particular interest were oligodendrocytes, a mouse anti-CNP antibody (Sigma, USA) was therefore used to target these cells. CNP (2',3'-cyclic nucleotide 3'-phosphohydrolase) is strongly associated with myelinated tissues and is localized in the cytoplasmic membrane of oligodendrocytes and Schwann cells. A rabbit anti-SFV antibody was used to target any virus present within these cells.

2.10.5.5.1 Production of antibody

SFV-A7 virus antibody was produced by infecting 2 New Zealand white rabbits inter-peritoneally (IP) with 500 μ l virus at a titre of 1.0×10^6 p.f.u./ml. The rabbits were given a second SFV-A7 virus boost inoculation 14 days after the initial infection and were sacrificed 14 days later. Blood was removed, centrifuged at 700 \times *g* for 10 minutes, the serum supernatant was then removed, aliquoted in 10 μ l quantities and stored at -70°C .

2.10.5.5.2 Preparation of cells for immunofluorescent labeling.

Neonate mixed glial cells were grown as described in section 2.10.5.2 and seeded in 2-well chamber slides (Falcon, USA) rather than 6 well plates. At 24 hpi, chambers were removed from the chamber slides as described in manufacturer's instructions. Slides were fixed in 25 ml of acetone for ten minutes, then washed twice for ten minutes in Phosphate Buffer Saline (PBS; Oxoid, UK). Swine Normal Serum (DAKO, Denmark) was diluted 1 in 20 in PBS and 100 μ l added to each slide. Strips of parafilm (American National Can, USA) of similar size to each slide were cut, placed on each slide, and placed in a humidified chamber at 37°C for 1hr. The cells were then ready for the addition of the primary antibody.

2.10.5.5.3 Immunofluorescent labeling of virus antigen

100 μ l primary anti-SFV antibody (Rb α SFV4 diluted 1:1000 in D-PBS) (Invitrogen, UK) was added to each slide, which were then covered with parafilm strips and incubated in a humidified chamber at 37°C for 1hr. Slides were washed twice for ten minutes in PBS-Tween containing 0.05% Tween 80 (Merck), then rinsed twice for 5

minutes in PBS. 15 μ l of biotinylated Gt α Rb antibody (DAKO, Denmark) was added to 985 μ l of PBS and 100 μ l was added to each slide, then covered with parafilm strips and incubated for 30mins at room temperature. Slides were washed twice in PBS-Tween and PBS as previously described. A 10mM HEPES (GibCo BRL, UK), 0.5M NaCl solution was made up and 5 μ l of rhodamine-avidin DCS (Vector Laboratories, USA) was added to 995 μ l of it. 100 μ l of this was then added to each slide. Slides were then covered with parafilm strips and incubated at room temperature in the dark for 30 mins. Slides were then placed in the HEPES/NaCl solution described above, for ten minutes before being washed in PBS Tween and PBS as previously described. At this stage the avidin was blocked using an avidin/biotin blocking Kit (Vector Laboratories, USA) for 15 minutes, then washed in PBS for 5 minutes, biotin was blocked using the same kit and washed in PBS. The mixed glial cells on the slides were then ready for oligodendrocyte labelling.

2.10.5.5.4 Immunofluorescent labeling of Oligodendrocytes

Slides were blocked and incubated in 1:20 normal goat serum as described previously for swine normal serum in section 2.10.5.5.3. A 1 in 10 dilution of Ms α CNP (Sigma, USA) in PBS was made and 100 μ l was added to each slide, which were then covered with parafilm strips and incubated in a humidified chamber at 37°C for 2 h. Slides were then washed in PBS Tween and PBS as described previously. Biotinylated Gt α Ms secondary antibody was then added as described previously and the slides incubated at room temperature for 30 min. Slides were washed and Fluorescein-Conjugated Streptavidin was diluted 1:100 in HEPES/NaCl solution described previously, 100 μ l was then added to each slide, which were incubated at room temperature for a further 30 min. Following a 10 min wash in HEPES/NaCl solution and PBS Tween / PBS washes the slides were placed in distilled water for 5 minutes. 25 μ l of DAPI (a fluorescent nuclear label) was added to 975 μ l of Mowiol, the slides were individually mounted in 60 μ l mowiol and cover slips were placed on each slide.

2.10.6 *In vivo* Analyses

2.10.6.1 Infection of Balb/c mice with CHIKV and SFV-A7

Two groups of 10 female BALB/c mice aged 60-80 days were intranasally infected with 20 µl per nostril of SFV-A7 and CHIKV virus with concentrations of 1×10^8 p.f.u / ml. A third group of 10 mice were mock-infected with PBS. The health, clinical signs and time of death were recorded over a 14 day period at which point the mice were reinfected with SFV-L10 to ensure that initial doses of SFV-A7 and CHIKV had been adequate to induce partial immunity. Mice were monitored for a further 6 days and then sacrificed.

2.10.6.2 Virus titres in brains of Balb/c mice infected with CHIKV and SFV-A7

Two groups of 30 female BALB/c mice aged 60-80 days were intranasally infected with SFV-A7 and CHIKV as described in section 2.10.6.1. Brains were aseptically removed from 3 mice from each group at 24 h time points. The brains were placed in a bijoux and weighed. An equal weight/volume (w/v) of Dulbecco's PBS was added, the mixture manually homogenised in a 10 ml homogeniser (Falcon, USA) and placed in a centrifuge tube and spun at 700 x g for 10 min to sediment the debris. The supernatant was removed and placed in a bijou at -70°C until a plaque assay (described in section 2.10.2.3) was performed.

2.10.6.3 Virus titres in Balb/c brains infected with CHIKV and six geographically distinct Chikungunya virus strains.

Seven groups of 30 female BALB/c mice aged 60-80 days were intranasally infected with 37997, 181/25, DAK ArB16878, PO 731460, PH H15483, SV-0451/96 and CHIKV as described in section 2.10.6.1. Brains were aseptically removed from 3 mice from each group at 24 h time points. The brains were placed in a bijoux and weighed. An equal weight/volume (w/v) of Dulbecco's PBS was added, the mixture manually homogenised in a 10ml homogeniser (Falcon) and placed in a centrifuge tube and spun at 700 x g for 10 min to sediment the debris. The supernatant was removed and placed in a bijou at -70C until plaque assay as described in section 2.10.2.3 could be performed.

2.10.6.4 Survival of Balb/c mice infected with CHIKV and six geographically distinct Chikungunya virus strains.

Seven groups of 10 female BALB/c mice aged 60-80 days were intranasally infected with 20µl per nostril of 37997, 181/25, DAK ArB16878, PO731460, PHH15483, SV-0451/96 and CHIKV with concentrations of 1×10^8 p.f.u/ml. An eighth group of 10 mice were mock-infected with PBS. The health, clinical signs and time of death were recorded over a 14 day period at which point the mice were reinfected with SFV-L10 to ensure that initial doses of SFV-A7 and CHIKV had been adequate to induce partial immunity. Mice were monitored for a further 6 days and then sacrificed.

2.11 Results

2.11.1 Sequence of Chikungunya Ross (CHIKV)

The complete genomic RNA sequence of CHIKV was found to be 11,813 nucleotides in length, including the 5' untranslated region (UTR), the untranslated junction region and the 3' UTR and had a typical alphavirus genome organisation. The base composition was calculated using DNAsis MAX analysis software (Hitachi, Japan), and gave the following percentages: 29.63% A, 24.97% C, 25.18% G and 20.27% T. The genome is organised into two open reading frames (ORFs), one containing a non-structural polyprotein (42S RNA) and the other a structural polyprotein (26S RNA). The genetic location of the nonstructural and structural polyproteins was deduced by comparing the amino acid and nucleotide sequences of other alphaviruses with known cleavage sites. The 5' UTR of CHIKV is 76 nucleotides in length and has 2 stem-loop structures at nucleotide positions 3-25 and 33-70. The region between the two identified ORFs coding for the nonstructural polyprotein and the structural polyprotein is not translated and is referred to as the junction region. In CHIKV it is 65 nucleotides in length spanning from nucleotide position 7502 to 7566. The 3' UTR is 499 nucleotides in length, it is located at position 11314 and extends until the end of the RNA genome at position 11813. The non-structural ORF is 7425 nucleotides in length, and is initiated by a start codon triplet (ATG) at position 77-79 terminating at a stop codon triplet (TAG) at position 7499-7501. The ORF coding the non-structural polyprotein is 2474 amino acids in length, individual non-structural proteins (NSP1-4) are subsequently formed by proteolytic cleavage. The ORF coding for the structural polyprotein is 3744 nucleotides in length and is initiated by a start codon at position 7567-7569 terminating at a stop codon triplet (TAA) at position 11311-11313. This ORF coding for the structural proteins: Capsid, E3, E2, 6K and E1 is 1248 amino acids in length. In accordance to the genomic organisation of other sequenced alphaviruses, the genome of CHIKV can therefore be considered to be: 5' cap-nsP1-nsP2-nsP3-nsP4-Junction region-Capsid-E3-E2-6K-E1-poly(A) 3'. The genome sequence of CHIKV is illustrated in figure 2.4 and the individual genes are annotated in figure 2.5.

1 ATGGCTGCGT GAGACACACG TAGCCTACCA GTTCTTACT GCTCTACTCT GCAAAGCAAG
 61 AGATTAAGAA CCCATCATGG ATCCTGTGTA CGTGGACATA GACGCTGACA GCGCCTTTTT
 121 GAAGGCCCTG CAACGTGCGT ACCCCATGTT TGAGGTGGAA CCTAGGCAGG TCACACCGAA
 181 TGACCATGCT AATGCTAGAG CGTCTCGCA TCTAGTATA AAACCTAATAG AGCAGGAAAT
 241 TGATCCCAGC TCAACCATCC TGGATATTGG TAGTGCGCCA GCAAGGAGGA TGATGTCCGA
 301 CAGGAAGTAC CACTGCGTTT GCCCGATGCG CAGTGCAGAA GATCCCAGGA GACTCGCCAA
 361 TTATGCGAGA AAGCTAGCAT CTGCCGACAG AAAAGTCTTG GACAGAAAACA TCTCTGGAAA
 421 GATCGGGGAC TTACAAGCAG TAATGGCCGT GCCAGACACG GAGACGCCAA CATCTGCTT
 481 ACACACAGAT GTATCATGTA GACAGAGAGC AGACGTCGCG ATATACCAAG ACGTCTATGC
 541 TGTACACGCA CCCACGTGCG TATACCACCA GCGGATTAAA GGGGTCCGAT TGGCGTACTG
 601 GGTAGGGTPT GACACAACCC CGTTCATGTA CAATGCCATG GCGGGTGCCT ACCCCTCATA
 661 CTCGACAAT GTGGCAGACT AGCAGGTACT GAAGGCTAAG AACATAGGAT ATCTTCAAC
 721 AGACCTGACG GAAGGTAGAC GAGGCAAATT GTCTATTATG AGAGGAAAAA AGCTAGAACC
 781 GTGCGACCGT GTGCTGTTCT CAGTAGGGTC AACGCTCTAC CCGGAAAGCC GTAAGCTACT
 841 TAAGAGCTGG CACCTACCAT CGGTGTTCCA TTTAAAGGGC AAGCTCAGCT TCACATGCCG
 901 CTGTGATAAC GTGGTTTCGT GCGAAGGCTA CGTCGTTAAG AGAATAACGA TACGCCCAGG
 961 CCTTTACGGA AAAACCACAG GGTATGCGGT AACCCACCAC GCAGACGGAT TCCTGATGTG
 1021 CAAGACCACC GACACGGTTG ACGGCGAAAG AGTGTCAATC TCGGTGTGCA CGTACGTGCC
 1081 GCGGACCATT TGTGATCAAA TGACCCGCAT CCTTGCTACA GAAGTCACGC CCGAGGATGC
 1141 ACAGAACCTG TTGGTGGGCG TGAACCAGAG AATAGTGGTT AACGCGAGAA CGCAACGGAA
 1201 TACGAACACC GTGAAAAAT ATATGATTCC CGTGGTCCGC CAAGCCTTCA GTAAGTGGGC
 1261 AAAGGAGTGC CGGAAAGACA TGAAGATGA AAAACTCCTG GGGGTGAGAG AAAGAACACT
 1321 GACCTGCTGC TGTCTATGGG CATTAAAGAA GCAGAAAACA CACACGGTCT ACAAGAGGCC
 1381 TGATACCAGT TCAATTGAGA AGGTTGAGC CGAGTTGAC AGCTTTGCTG TACCGAGCCT
 1441 GTGGTCCGTC GGGTTGTCAA TCCCGTTGAG GACTAGAATC AAAATGGTTGT TAAGCAAGGT
 1501 GCCAAAAACC GACCTGACCC CATAACGCGG GGACGCCCAA GAAGCCCGGG ACGCAGAAAA
 1561 AGAAGCAGAG GAAGAAGCAG AAGCAGAACT GACTCTTGAA GCCCTACCAC CCCTTCAGGC
 1621 AGCAAGGAA GATGTTCCAG TCGAAATCGA CGTGGAACAG CTTGAGGACA GAGCGGGTGC
 1681 AGGAATAATA GAGACTCCGA GAGGAGCTAT CAAAGTTACT GCCCAACCAA CAGACCACGT
 1741 CGTGGGAGAG TACTTGTTTC TTTCCCGCA GACCGTACTA CGTAGCCAAA AGCTTAGCCT
 1801 GATTACACGT TTGGCGGAGC AAGTGAAGAC GTGCACGCAC AGCGGACGAG CAGGGAGGTA
 1861 TGGGTCGAA GGTACGACG GCAGAGTCTT AGTGCCCTCA GGCTACGCAA TCTCGCTGA
 1921 AGACTTCCAG AGCCTAAGCG AAAGCGCAAC GATGGTGTAC AACGAAAGAG AGTTTCGTAA
 1981 CAGAAAGCTA CACCATATTG CGATGCATGG ACCAGCCCTG AACACCGAGG AAGAGTCGTA
 2041 TGAGTGGTG AGGGCAGAGA GGACAGAACTA CGAGTACGTC TACGACGTGG ACCAGAGAG
 2101 ATGCTGTAAG AAGTAAGAAG CTGCAAGACT GGTACTGGTG GCGGACTTGA CTAATCCGCC
 2161 CTACCACGAA TTCGCATATG AAGGGCTAAA AATCCGCCCT GCCTGCCCAT ACAAATTGCG
 2221 AGTCATAGGA GTCTCCGAG TACCAGGATC TGGCAAGTCA GCTATTATCA AGAACCTAGT
 2281 TACCAGGCAA GACCTGGTGA CTAGCGGAAA GAAAGAAAAC TGCCAAGAAA TCACCACCGA
 2341 CGTGATGAGA CAGAGAGGTC TAGAGATATC TGCACGTACG TTGACTCGC TGTCTTGAA
 2401 TGGATGTAAC AGACCAGTCG ACGTGTGTA CGTAGACGAG GCGTTTGCCT GCCACTCTGG
 2461 AACGTTACTT GCATTGATCG CCTTGGTGAG ACCAAGACAG AAAGTTGTAC TTTGTGGTGA
 2521 CCCGAAGCAG TGCGGCTTCT TCAATATGAT GCAGATGAAA GTCAACTATA ATCACAACAT
 2581 CTGCACCCAA GGGTTAACCA AAGTATCTC CAGGCGGTGT ACACTGCCTG CTAATCCGAT
 2641 TGTGTCATCG TTGCATTACG AAGGCAAAAT GCGCACTACG AATGAGTACA ACAAGCCGAT
 2701 TGTAGTGGAC ACTACAGGCT CAACAAAACC TGACCCTGGA GATCTCGTGT TAACGTGCTT
 2761 CAGAGGATGG GTTAAACAAC TGCAAATTGA CTATCGTGA CACGAGGTCA TGACAGCAGC
 2821 CGCATCCCAA GGGTTAACCA GAAAAGGAGT TTACGCAATT AGGCCAAAAG TTAACGAAAA
 2881 CCCGCTTTAT GCATCAACGT CAGAGCACGT CAACGTAICT CTAACGCGTA CCGAAGGTAA
 2941 ACTGGTATGG AAGACACTCT CCGGTGACCC GTGGATAAAG ACGTGCAGA ACCCACCAGAA
 3001 AGGAAACTTC AAAGCAACTA TTAAGGAGTG GGAGGTGGAG CATGCATCAA TAATGGCGGG
 3061 CATCTGCACT CACCAAAATG CTTTGTATAC ATTCCAAAAC AAAGCCAACG TTTGTGGCG
 3121 TAAGAGTTTG GTCCCTATCC TCGAAACAGC GGGGATAAAA CTAACGACA GGCAGTGGTC
 3181 CCAGATAATT CAAGCCTTCA AAGAAGACAA AGCATATTCA CCCGAAGTAG CCCTGAATGA
 3241 AATATGCACG CGCATGTATG GGGTGGATCT AGACAGCGGG CTATTTTCTA AACCGTTGGT
 3301 GTCTGTGTAT AACGCGGATA ACCACTGGGA TAATAGGCCT GGAGGGAAGA TGTTCGGATT
 3361 CAACCCGAG GCAGCATCCA TTCTAGAAAG AAAGTATCCA TTTACAAAAG GGAAGTGGAA
 3421 CATCAACAAG CAGATCTGCG TGACTACCAG GAGGATAGAA GACTTCAACC CTACCACCAA
 3481 CATTATACCG GCCAACAGGA GACTACCACA CTCATTAGTG GCCGAACACC CCCCAGTAAA
 3541 AGGGGAAAGA ATGGAATGGC TGGTTAACAA GATAAACGGC CACCACGTGC TCCTGGTAC
 3601 TGGCTGTAGC CTTGCACTGC CTAATAAGAG AGTCACTTGG GTAGCGCCAC TAGGTGTCCG
 3661 CGGAGCGGAC TATACATACA ACCTAGAGTT GGGTCTGCCA GCAACGCTTG GTAGGTATGA
 3721 CCTAGTGGTC ATAAACATCC ACACACCTTT TCGCATACAC CATTATCAAC AGTGCGTAGA
 3781 CACGCAATG AACCTGCAAA TGCTCGGGGG TGACTCATTG AGACTGCTCA AACCGGGTGG
 3841 CTCTCTATTG ATCAGAGCAT ATGGTTACGC AGATAGAACC AGTGAACGAG TCATCTGCGT
 3901 ATTTGGGACG AAGTTTATAG CATCTAGAGC GTTGAACCAA CCATGTGTCA CCAGCAACAT
 3961 TGAGATGTTT TTTCTATTCA GCAACTTTGA CAATGGCAGA AGGAATTTCA CAACTCATGT
 4021 CATGAACATA TACTTAATG CAGCCTTTGT AGGACAGGCC ACCCGAGGCC AAGTGCACC
 4081 GTCGTACCGG GTAAAAACGCA TGGATATCGC GAAGAACGAT GAAGAGTGCG TAGTCAACGC
 4141 CGCCAACCTT CCGGGTTTAC CAGGTGACGG TGTTCGCAAG GCAGTATACA AAAATGGCC
 4201 GGAGTCCCTT AAGAACAGTG CAACACCACT GGGAACCGCA AAAACAGTCA TGTGCGGTAC
 4261 GTATCCGTTA ATCCAGCCG TTTGACCAAA CTCTCTAAT TATTGCGAGT CTGAAGGGGA
 4321 CCGAGAAATT GCGGCTGCCT ATCCGAGAAGT CGCAAAGGAG GTAACCTAGAC TGGGATGAAA

5' UTR
NSP1

NSP2

NSP3

4381	TAGTGTAGCT	ATACCTCTCC	TCTCCACAGG	TGTATACTCA	GGAGGGAAG	ACAGGCTGAC
4441	CCAGTCACTG	AACCACTCT	TTACAGCCAT	GGACTCGACG	GATGCAGACG	TGGTCACTTA
4501	CTGCCGCGAC	AAAAGATGGT	AGAAGAAAAA	ATCTGAGGCG	ATACAGATGC	GGACCCAAGT
4561	GGAGCTGCTG	GATGAGCACA	TCTCCATAGA	CTGCGATGTT	GTTCGCGTGC	ACCCTGACAG
4621	CAGCTTGCA	GGCAGAAAAA	GATACAGCAC	CACGGAAGGC	GCACTGTACT	CATATCTAGA
4681	AGGGACCCGT	TTTACCAAAA	CGGCAGTGG	TATGGCAGAG	ATATATACTA	TGTGGCCAAA
4741	GCAAAACAG	GCCAACGAGC	AAGTTTGCCT	ATATGCCCTG	GGGAAAAGTA	TTGAATCGAT
4801	CAGGCAGAAA	TGCCCGGTGG	ATGATGCAGA	TGCATCATCT	CCCCGAAAA	CTGTCCCCTG
4861	CCTCTGCCGT	TACGCCATGA	CACCAGAACG	CGTTACCCGA	CTTCGCATGA	ACCATGTAC
4921	AAGCATAATT	GTGTGTCTTT	CGTTTCCCCT	TCCAAAGTAC	AAAAAGAAAG	GAGTGCAAAA
4981	AGTCAAATGC	TCCAAGGTAA	TGCTATTTGA	CCACAACGTG	CCATCGCGCG	TAAGTCCAAG
5041	GGAATACAGA	CCTTCCCAGG	AGTCTGTACA	GGAAGCGAGT	ACGACCACGT	CACTGACGCA
5101	TAGCCAATTC	GATCTAAGCG	TTGACGGCAA	GATACTGCC	GTCCCGTCAG	ACCTGGATGC
5161	TGACGCCCCA	CCCCTAGAAC	CAGCCCTTGA	CGACGGGGCG	ATACACACGT	TGCCATCTGC
5221	AACCCGAAAC	GTTGCGGCGG	TGTCTGACTG	GGAATGAGC	ACCTTACCTG	TGCGCCGCGC
5281	CAGAAGAAGG	CGAGGGAGAA	ACCTGACTGT	GACATGCGAC	GAGAGAGAAG	GGAATATAAC
5341	ACCCATGGCT	AGCGTCCGAT	TCTTTAGGGC	AGAGCTGTGT	CCAGTTCGTAC	AAGAAACAGC
5401	GGAGACGCGT	GACACAGCTA	TGTCTCTTCA	GGCACCGCGG	AGTACCGCCA	CGGAACTGAG
5461	TCACCCGCGG	CTTCCCTTCG	GTGCACCAAG	CGAGACGTTG	CCCATCACAT	TTGGGGACTT
5521	CAACGAAGGA	GAAATCGAAA	GCTTGTCTTC	TGAGCTACTA	ACTTTCGGAG	ACTTCTTACC
5581	CGGAGAATG	GATGATTTGA	CAGATAGCGA	CTGGTCCACG	TGCTCAGACA	CGGACGACGA
5641	GTTACGACTA	GACAGGGCAG	GTGGGTATAT	ATTCTCGTCG	GACACTGGTC	CAGGTCATTT
5701	ACAAAGAAAG	CTCAGTCCGC	AGTCAGTGC	GCCGGTGAAC	ACCTTGGAGG	AGGTCACGA
5761	GGAGAAGTGT	TACCCACCTA	AGCTGGATGA	AGCAAAGGAG	CACTACTACT	TTAAGAAACT
5821	CCAGGAGAGT	GCATCCATGG	CCAACAGAAG	CAGGTATCAG	TCGCGCAAAG	TAGAAAACAT
5881	GAAAGCAACA	ATCATCCAGA	GACTAAAGAG	AGGCTGTAGA	TTATACTTAA	TGTCAGAGAC
5941	CCCAAAACAG	CACGCTTACC	GGACACATA	TCCGGCGCCT	GTGTACTCGC	CTCCGATFAA
6001	CGTCCGACTG	TCCAACCCCG	AGTCCGCACT	GGCAGCATGC	AATGAGTTCT	TGGCTAGAAA
6061	CTATCCAAC	GTTCATCAT	ACCAAATCAC	CGACGAGTAT	GATGCATATC	TAGACATGTT
6121	GGACGGGTCG	GAGAGTTGTC	TGGACCGGGC	GACGTTCAAT	CCGTCAAAA	TTAGGAGCTA
6181	CCCAAAACAG	CACGCTTACC	ACGCGCCCTC	CATCAGAAGC	GCTGTACCGT	CCCCATCCA
6241	GAACACACTA	CAGAATGTAC	TGGCAGCAGC	CACGAAAAGA	AACTGCAACG	TCACACAGAT
6301	GAGGGAATTA	CCCACTTTGG	ACTCAGCAGT	ATTCAACGTG	GAGTGTTC	AAAAATTCGC
6361	ATGCAACCAA	GAATACTGGG	AAGAATTTGC	TGCCAGCCCT	ATCAGGATAA	CAACTGAGAA
6421	TTTAAACAAC	TATGTTACTA	AACTAAAGGG	GCCAAAAGCA	GCAGCGCTAT	TTGCAAAAC
6481	CCATAATCTG	CTGCCACTGC	AGGAAGTGCC	AATGGATAGG	TTCACAGTAG	ACATGAAAAG
6541	GGATGTGAAG	GTGACTCCTG	GTACAAAGCA	CACAGAGGAA	AGACCTAAGG	TACAGGTTAT
6601	ACAGGCGGCT	GAACCCCTGG	CAACAGCATA	CCTATGTGGG	ATTCACAGAG	AGCTGGTTAG
6661	GACGCTGAAC	CGCCTTACC	TACCCAATGT	ACATACACTA	TTTGACATGT	CTGCCGAGGA
6721	TTTCGATGCC	ATCATAGCCG	CACACTTTAA	GCCAGGAGAC	ACTGTTTTAG	AAACGGACAT
6781	AGCCTCCTTT	GATAAGAGCC	AAGATGATTC	ACTTGCCTTT	ACTGCTTTAA	TGCTGTTAGA
6841	GGATTTAGGG	GTGGACTCACT	CCCTGTTGGA	CTTGATAGAG	GCTGCTTTTC	GAGAGATTTT
6901	CAGCTGTCA	GTACCCGAG	TACGCGCTT	CAAGTTCGGC	CCCATGATGA	AATCTGGTAT
6961	GTTCCTAACT	CTGTTCTGCA	ACACACTGCT	AAATATCACC	ATCGCCAGCC	GAGTGTGGA
7021	AGATCGTCTG	ACAAAATCCG	CGTGCCGAGC	CTTCATCGGC	GACGACAACA	TAATACATGG
7081	AGTCGTCTCC	GATGAATTTGA	TGGCAGCCAG	ATGCGCCACT	TGGATGAACA	TGGAAGTGA
7141	GATCATAGAT	GACAGTTGAT	CCCAGAAAGC	CCCTTACTTT	TGTGGAGGGT	TTAATCTCAA
7201	CGATATCGTG	ACAGGAACAG	CTTGCCAGAGT	GGCAGACCCG	CTAAAAGGC	TATTTAAACT
7261	GGGCAAAACG	CTAGCCGAG	GTGACGAACA	AGATGAGGAT	AGAAGACGAG	CGCTGGCTGA
7321	CGAAGTGGTC	AGATGGCAAC	GAACAGGGCT	AATTTGATGAG	TTGGAGAAAG	CGGTATACTC
7381	TAGGTATGAA	GTGACGGGTA	TATCAGTTGT	GGAATGTC	ATGGCCACT	TTCTCAAGTC
7441	CAGATCCAAC	TTGAGAAAGC	TCAGAGGACC	CGTCGTAACT	TTGTACGGCG	GTCTTAAATA
7501	GTACGCACT	ACAGCTACT	ATTTTGCAGA	AGCCGACAGT	AAGTACCTAA	ACACTAATCA
7561	GCTACAATGG	AGTTTATCCC	AAACCAACT	TTTTACAACA	GGAGGTACCA	GCCTCGACCT
7621	TGACTCCGCG	CGCTCATAT	CCAAGTCATC	AGGCCAGAC	CGCCGCCGCA	GAGGCAAGCT
7681	GGGCAACTTG	CCCAGCTGAT	CTCAGCAGTT	AATAAACTGA	CAATGCGCGC	GGTACCCCAA
7741	CAGAAGCCAC	GCAGGAATCG	GAAGAATAAG	AAGCAAAAGC	AAAAGCAACA	GGCGCCACAA
7801	AACAACACAA	ACCAAAGAA	GCAGCCACCT	AAAAAGAAAC	CAGTCAAAA	GAAAAAGAAAG
7861	CCGGCCGCA	GAGAGAGGAT	GTGCATGAAA	ATCGAAAATG	ACTGTATTTT	CGAAGTCAAG
7921	CACGAAGGTA	AGGTAACAGG	TTACGCGTGC	TTGGTGGGGG	ACAAAAGTAA	GAAACCAGCA
7981	CACGTAAAGG	GGACCATCGA	TAACGCGGAC	CTGGCCAAAT	TGGCCTTTAA	GCGGTCACTC
8041	AAGTACGACC	TTGAATGCGC	GCAGATAACC	GTGCATGTA	AGTCCGACGC	TTCGAAGTTC
8101	ACCCATGAGA	AACCGGAGGG	GTACTACAAC	TGGCACCCAG	GAGCAGTACA	GTACTCAGGA
8161	GGCCGGTTCA	CCATCCCTAC	AGGTGCGGGC	AAACCAGGGG	ACAGCGGTAG	ACCGATCTTC
8221	GACAACAAGG	GACGCGTGGT	GGCCATAGTC	TTAGGAGGAG	CTAATGAAGG	AGCCGGTACA
8281	GCCCTCTCAG	TGTTGACCTG	GAATAAAGAC	ATTGTCACTA	AAATCACCCC	TGAGCCGAGCC
8341	GAAGAGTGG	GTCTTGCCAT	CCCAGTTATG	TGCCTGTTGG	CAAAATACCAC	GTTCCTTGC
8401	TCCAGCCCC	CTTGCATACC	CTGCTGCTAC	GAAAAGGAAC	CGGAGGAAAC	CCTACGCATG
8461	CTTGAGGACA	ACGTCAATGAG	ACCTGGGTAC	TATCAGCTGC	TACAAGCATC	ATTAACATGT
8521	TCTCCCCACC	GCCACGACG	CAGCACCAAG	GACAACCTCA	ATGTCTATAA	AGCCACAAGA
8581	CCATACCTTAG	CTCACTTCC	CGACTGTGGA	GAAGGGCACT	CGTGCCATAG	TCCCGTAGCA
8641	CTAGAACGCA	TCAGAAATGA	AGCGACAGAC	GGGACGCTGA	AAATCCAGGT	CTCCTTGCAA
8701	ATTGGAATAG	GGACGGATGA	TAGCCATGAT	TGGACCAAGC	TGCGTTACAT	GGACAATCAC
8761	ATACCAGCAC	ACGACGGGAG	GGCCGGGCTA	TTTGTAAAGAA	CATCAGCACC	ATGCACAGT
8821	ACTGGAACAA	TGGGCACTT	CATCCTGGCC	CGATGTCGCA	AAGGAGAAAC	CTGACCGGTG
8881	GGATTCAC	ACAGTAGGAA	GATTAGTCAC	TCATGTACGC	ACCCATTTCA	CCACGACCTT
8941	CCTGTGATAG	GCCGGGAAAA	ATTCCATTCC	CGACCGCAGC	ACGGTAAAGA	GCTACCTTGC

NSP4

JUNCTION
CAPSID

E3

E2

9001	AGCACGTACG	TGCAGAGCAA	CGCCGCAACT	GCCGAGGAGA	TAGAGGTACA	CATGCCCCCA
9061	GACACCCCTG	ATCGCACATT	GCTGTCCACAA	CAGTCCGGCA	ACGTAAGAT	CACAGTCAAC
9121	GGCCGGACGG	TGCGGTATAA	GTGTAATTGC	GGTGGCTCAA	ATGAAGGACT	AATAACTACA
9181	GATAAAGTGA	TTAATAACTG	CAAGGTTGAT	CAATGTCATG	CCGCGGTAC	CAATCACAAA
9241	AAGTGGCAGT	ATAACTCCCC	TCTGGTCCCG	CGTAACGCTG	AACTCGGGGA	CCCAAAAGGA
9301	AAAATTCA	TCCCCTTTCC	GCTGGCAAAT	GTAACATGCA	TGGTGCCTAA	AGCAAGGAAC
9361	CCCACCGTGA	CGTACGGGAA	AAACCAAGTC	ATCATGCTAC	TGTATCCTGA	CCACCCAACA
9421	CTCCTGTCTT	ACCGGAGTAT	GGGAGAAGAA	CCAAACTATC	AAGAAGAGTG	GGTGACGCAC
9481	AAGAAGGAGG	TCGTGCTAAC	CGTGCCGACT	GAAGGGCTCG	AGGTTACGTG	GGGCAACAAC
9541	GAGCCGTATA	AGTATTGGCC	GCAGTTATCT	GCAAAACGGTA	CAGCCCACGG	CCACCCGCAT
9601	GAGATAATCT	TGTACTATTA	TGAGCTGTAC	CCTACTATGA	CTGTAGTAGT	TGTGTCAGTG
9661	GCCTCGTTCA	TACTCCTGTC	GATGGTGGGT	ATGGCAGTGG	GGATGTGCAT	GTGTGCACGA
9721	CGCAGATGCA	TCACACCATA	CGAACTGACA	CCAGGAGCTA	CCGTCCCTTT	CCTGCTTAGC
9781	CTAATATGCT	GCATCAGAAC	AGCTAAAGCG	GCCACATACC	AAGAGGCTGC	GGTATACCTG
9841	TGGAACGAGC	AGCAACCTTT	GTTTTGGCTA	CAAGCCCTTA	TTCCGCTGGC	AGCCCTGATT
9901	GTCCTATGCA	ACTGTCTGAG	ACTCTTACCA	TGCTGTTGTA	AAACGTTGGC	TTTTTTTAGCC
9961	GTAATGAGCA	TCGTGCCCCA	CACTGTGAGC	GCGTACGAAC	ACGTAACAGT	GATCCCGAAC
10021	ACGGTGGGAG	TACCGTATAA	GACTCTAGTC	AACAGACCGG	GCTACAGCCC	CATGGTACTG
10081	GAGATCGAAT	CATGCAAAAC	AGAATTTGCA	CCAACGCTAT	CGCTTGATTA	CGTCACGTGC
10141	GAATACAAAA	CCGTCATCCC	GTCTCCGTAC	GTGAAATGCT	GCGGTACAGC	AGAGTGCAAG
10201	GACAAAAACC	TACCTGACTA	CAGCTGTAAG	GTCTTACC	GCGTCTACCC	ATTTATGTGG
10261	GGCGGCGCCT	ACTGCTTCTG	CGACGCTGAA	AACACGCAAT	TGAGCGAAGC	ACATGTGGAG
10321	AAGTCCGAAT	TAGGGAACAT	ACCAGGACAA	TTTGGCGATA	TCCAAGTCCG	CGACCTGAG
10381	TCAGCTAAGC	TCCGCGTCCT	TTACCAAGGA	AATAACATCA	CTGTAAGTGC	CTATGCAAAC
10441	GGCGACCATG	CCGTACAGT	TAAGGACGCC	AAATTCATTG	TGGGGCCAAT	GTCTTACAGC
10501	TGGACACCTT	TCGACAACAA	AATCGTGGTG	TACAAAGGTG	ACGTTTACAA	CATGGACTAC
10561	CCGCCCTTTG	GCGCAGGAG	ACCAGGACAA	TTTGGCGATA	TCCAAGTCCG	CGACCTGAG
10621	AGCAAAGACG	TCTATGCTAA	CACACAAC	GTACTGCAGA	GACCGGCTGC	GGGTACGGTA
10681	CACGTGCCAT	ACTCTCAGGC	ACCATCTGGC	TTTAAGTATT	GGTTAAAAGA	ACGAGGGGCG
10741	TCGCTACAGC	ACACAGCAC	ATTTGGCTGC	CAAATAGCAA	CAAACCCGGT	AAGAGCGATG
10801	AAGTGGCGCG	TAGGGAACAT	GCCATCTCC	ATCGACATAC	CGGATGCGGC	CTTCACTAGG
10861	GTCGTCGACG	CGCCCTCTTT	AACGGACATG	TCATGCGAGG	TACCAGCCTG	CACCCATTCC
10921	TCAGACTTTG	GGGGCGTGC	CATTATTAAA	TATGCAGTCA	GCAAGAAAGG	CAAGTGTGCG
10981	GTGCATTGCA	TGACCAACGC	CGTCACTATC	CGGGAAGCTG	AGATAGAAGT	TGAAGGGAAT
11041	TCTCAGCTGC	AAATCTCTTT	CTCGACGGCC	TTGGCCAGCG	CCGAATCCG	CGTACAAGTC
11101	TGTTCTACAC	AAGTACACTG	TGCAGCCGAG	TGCCACCCTC	CGAAGGACCA	CATAGTCAAC
11161	TACCCGGCGT	CACATACCAC	CCTCGGGGTC	CAGGACATTT	CCGCTACGGC	GATGTCATGG
11221	GTGCAGAAGA	TCACGGGAGG	TGTGGGACTG	GTTGTGCTG	TTGCAGCACT	GATTCTAATC
11281	GTGGTGTCTAT	GCGTGTCTGTT	CAGCAGGCAC	TAACCTGACG	ACTAAGCATG	AAGGTATATG
11341	TGTCCCTTAA	GAGACACACC	GTATATAGCT	AATAATCTGT	AGATCAAAGG	GCTATATAAC
11401	CCCTGAATAG	TAACAAAATA	CAAAATCACT	AAAAATTATA	AAAAACAGAA	AAATATATAA
11461	ATAGGTATAC	GTGTCCCTTA	AGAGACACAT	TGTATGTAGG	TGATAAGTAT	AGATCAAAGG
11521	GCCGAACAAC	CCCTGAATAG	TAACAAAATA	TAAAAATTA	TAAAAATCAT	AAAAATAGAAA
11581	AACCATAAAC	AGAAGTAGTT	CAAAGGGCTA	TAAAAACCC	TGAATAGTAA	CAAAACATAA
11641	AACTAATAAA	AATCAAATGA	ATACCATAAT	TGGCAAACGG	AAGAGATGTA	GGTACTTAAG
11701	CTTCTTAAAA	GCAGCCGAAC	TCACTTTGAG	ATGTAGGCAT	AGCATAACCGA	ACTCTTCCAC
11761	GATTCTCCGA	ACCCACAGGG	ACGTAGGAGA	TGTTATTTTG	TTTTTAATAT	TTC

6K

E1

3' UTR

Figure 2.4 Complete Sequence of the Ross strain of Chikungunya virus. Sequence submitted to Genbank on 29th March 2002 (Accession Number: AF490259). Individual genes are labelled and individually annotated by normal / bold typeface fonts.

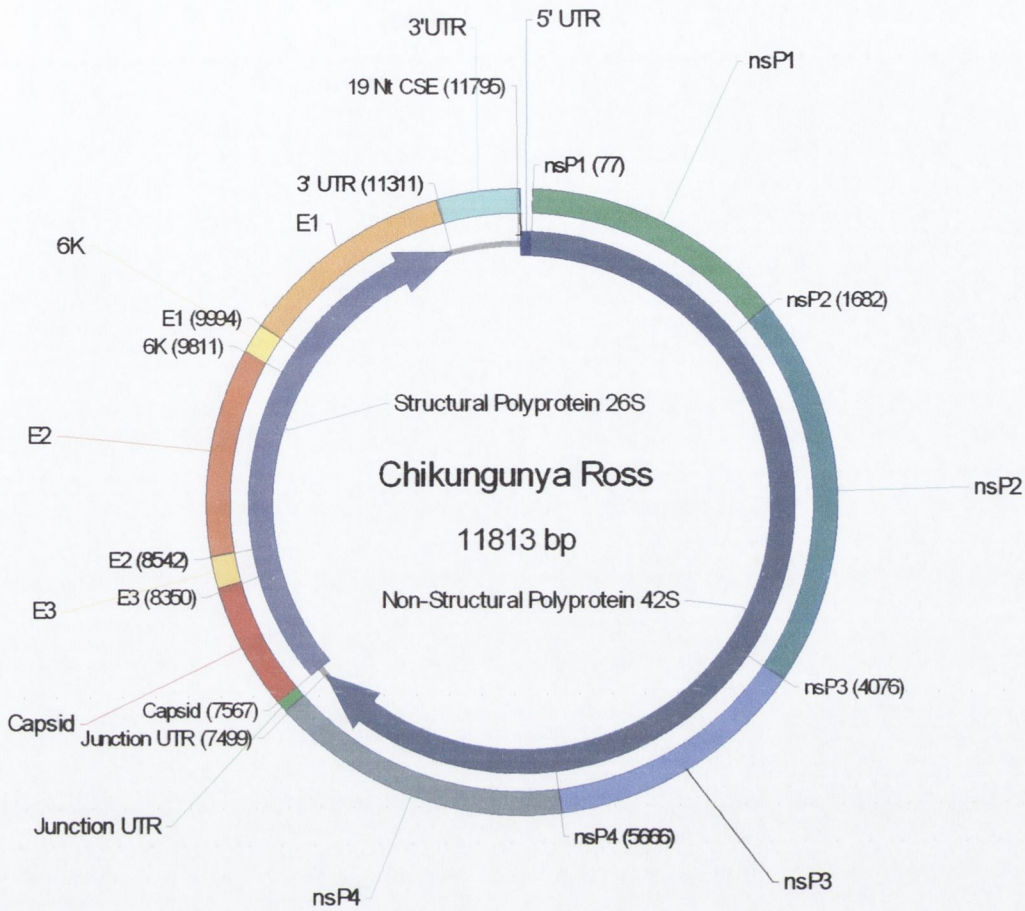


Figure 2.5 Circularised annotated representation of Chikungunya Ross genome. The first open reading frame (ORF) starting at position 77 and ending at position 7488 contains the non-structural genes. The second ORF initiating at position 7567 and terminating at 11310 contains the structural proteins. There are three untranslated regions (UTRs); the 5' UTR (1-76), the junction region (7489-7566) and the 3' UTR (11314-11813). The 3' UTR contains a highly conserved 19 nt sequence element starting at position 11795. Other sequence elements within the 5' UTR, nsP1 and the junction region are not included in this figure but are presented in more detail later in this section.

2.11.1.1 untranslated regions of the Genome

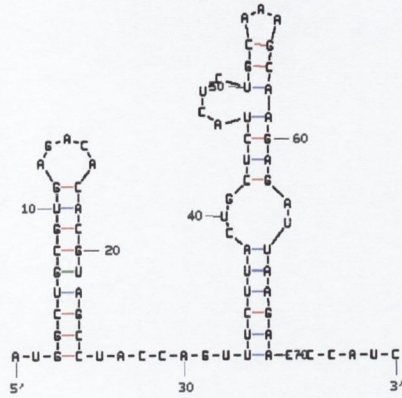
There are three untranslated regions, the 5' UTR, the junction region lying between both ORFs, and the 3' UTR. Secondary structures of the 5' UTR were predicted for CHIKV, CHIKV 37997 and ONNV Gulu and SFV-A7 using Mfold (version 3.0). CHIKV has two distinct stem loops in its 5' UTR as illustrated in figure 2.6. The nucleotide sequences at the 5' termini of alphaviruses are conserved more in potential secondary structure than in sequence, the conserved secondary structure may be important for virus RNA replication. The 5' UTR of CHIKV spans the first 76 nt of the genome.

Both CHIKV strains share identical secondary structure even though CHIKV 37997 has 3 nucleotide changes: A/G, A/U, A/U at positions 53, 54 and 67 respectively. A cysteine residue is also inserted at position 64 in CHIKV 37997. CHIKV and ONNV share almost complete secondary structure homology within the first stem loop, although differing in structure in the second stem loop, ONNV Igbo-Ora having closest secondary structure with CHIKV than either Gulu or SG650 strains. SFV-A7 shares no recognisable secondary structure with CHIKV or ONNV. The secondary structures at the 5' UTR of both CHIKV and ONNV are very similar and may play an important role in virus RNA replication

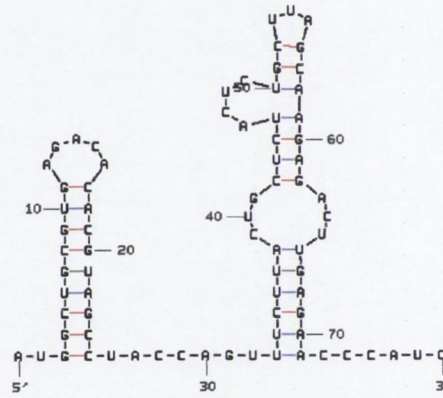
The untranslated junction region of CHIKV was 65 nt in length, nucleotides 7502 to 7566, a 24 nt conserved region was detected between nts 7479 and 7502 (CTTTGTACGGCGGTCCTAAATAGG) differing in only 5 nts to that of SFV. This region is necessary to promote transcription of 26S subgenomic RNA.

The 3' untranslated Region was 499 nt in length spanning from 11,314 to the final CHIKV genome nucleotide at position 11,813. A 19nt conserved sequence at the 3' UTR (ATTTTGTTTTTAATATTC) was observed at position 11,795-11,813 adjacent to where one would expect a poly(A) tract to begin.

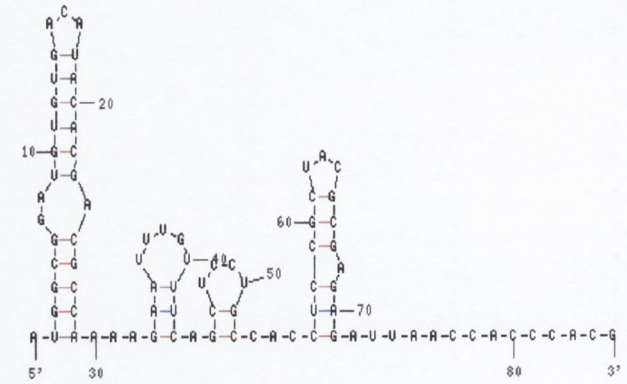
CHIKV Ross (dG=-23.4)



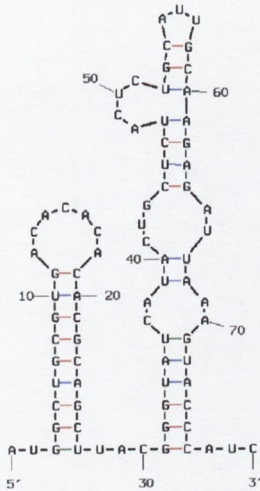
CHIKV 37997 (dG=-23.8)



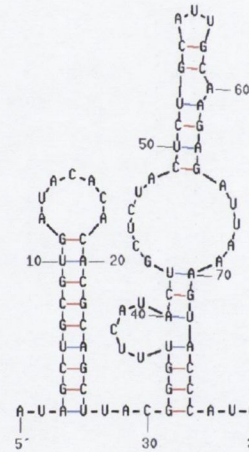
SFV A7 (dG=-19.7)



ONNV Igbo Ora (dG=-27.2)



ONNV Gulu (dG=24.8)



ONNV SG650 (dG=24.8)

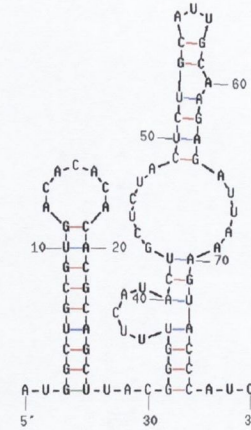


Figure 2.6 Stem-loops of CHIKV, CHIKV 37997, SFV-A7, and the Igbo Ora, Gulu and SG650 strains of ONNV

Mfold version 3.0 was used to predict secondary structure of the 5' UTR free energy values are noted in parentheses..

2.11.1.2 Non-structural Genes of CHIKV

The first of the non-structural genes to be processed is nsP1, this is initiated at an ATG motif at position (77-79). nsP1 therefore begins at position 77 ending at position 1681 making it 1605 nucleotides (nt) long and consisting of 535 amino acids (a.a.). Based on information we have for other alphaviruses, nsP1 is thought to be involved with negative strand RNA synthesis and capping of RNA. At a.a. position 31-47 a conserved (among alphaviruses) 17 aa sequence (QVTPNDHANARAFSHLA) is present. nsP2 is the largest gene spanning 2394 nt and 798 aa. Beginning at position 1682 and ending at position 4075 it contains helicase and proteinase motifs and is involved in proteolytic cleaving. A three amino acid motif (CWA) of the non-structural proteinase among alphaviruses was also identified in the nsP2 of CHIKV at aa position 478-480. A replicase motif was found (GXXXXGKS, where X represents any amino acid) at position 186-193 in nsP2.

nsP3 begins at nt position 4076, ending at position 5665 making it 1590 nt long and spanning 530aa, it may be involved in RNA synthesis although this remains to be determined. The final nonstructural gene: nsP4 contains the virus RNA polymerase with the Gly-Asp-Asp (GDD) located at position 465-467. nsP4 spans from nt position 5666 – 7498, making it 1833nt long consisting of 611amino acids. The a.a. percentage identity of each CHIKV gene with those of CHIKV 37997, ONNV Gulu and SFV-A7 is discussed in more detail later in section 2.11.1.4.

2.11.1.3 Structural genes of CHIKV

The capsid protein starts at an ATG codon at position 7567-7569 and continues until nt position 8349, it is 783nt long and consists of 261aa. E3 is a smaller envelope glycoprotein than E1 and E2 only spanning 64 aa and 192 nt, it begins at position 8350 and ends at position 8541. E2 has two possible glycolysation sites at positions 263 and 345 assigned by the sequence Asn-X-Ser / Thr (where X is any amino acid except proline), it is 423 aa in length, beginning at position 8542 and spanning 1269 nt and ending at position 9810. 6K is the smallest of the structural genes consisting of only 61 amino acids and 183 nts, it spans position 9811-9993. Conversely E1 is the largest of the structural genes containing 439 amino acids and 1317 nucleotides, excluding the final TAA opal codon it spans from position 9994 to 11310.

2.11.1.4 Percentage identity in nucleotide and deduced amino acid sequences between CHIKV and other alphaviruses

CHIKV shared the highest nucleotide (nt; 84.82%) and amino acid (aa; 95.54 %) identity over the entire coding regions of the genome with the 37997 strain. However, the amino acid sequence identity of the complete structural polyprotein of Nagpur strain of CHIKV shares highest identity with CHIKV (96.54%), this is also true for the Capsid (98.47%) and E2 (96.68%) genes. Over the E3 genes both Nagpur and 181/25 share the highest amino acid identity to CHIKV (93.65%). The 6K gene has highest aa identity between CHIKV and 37997 (95.08%) and E1 with 181/25 (97.23%). nsP3 had the lowest sequence identity of the genes (90.00%), this was also the case for ONNV Gulu (66.73%) and SFV-A7 (51.31%). nsP2 on the other hand shared the highest (97.74%), identity between viruses also the case with ONNV Gulu (91.48 %). Over the entire coding regions of the genome CHIKV had an 85.55% identity with ONNV Gulu compared to only a 67.11% identity with SFV-A7, which had most sequence identity over nsP1 (76.02%). Higher identities were observed over the 5' UTR than 3' UTR and Junction regions for all viruses.

2.11.1.5 Phylogenetic analysis of CHIKV and other alphaviruses

The phylogram calculated using bootstrap analysis (x1000) of the complete coding genome sequences (figure 2.7a) clearly separates CHIKV, ONNV and SFV strains, SIN was used as the out-parameter. CHIKV Ross and CHIKV 37997 differ within the CHIKV group. The CHIKV group and ONNV group are clearly separate with the ONNV Gulu strain showing closest similarity to CHIKV. The SFV group is markedly separate from both the CHIKV and ONNV groups. The same trend is observed over the nonstructural polyprotein (figure 2.7b). However, the structural polyproteins of Nagpur and 181/25 (vaccine strain) have also been sequenced and phylogenetic analysis of this region showed that CHIKV is closer to Nagpur and 181/25 than 37997 (figure 2.7c) other trends were similar to the previous two phylograms.

2.11.1.6 Immunofluorescent labeling of virus infected oligodendrocytes

The numbers of mock-infected oligodendrocytes were considerably higher than those infected with either CHIKV or SFV-A7, as less cell death occurred (figure 2.8a). The morphology of mock-infected oligodendrocytes was closer to the natural state of uninfected oligodendrocytes than either of the virus infected cells (figure 2.8b). As

expected, no virus antigen was detected in the mock-infected oligodendrocytes (figure 2.8c) although a small degree of non-specific background staining was observed.

2.11.1.7 Immunofluorescence of CHIKV infected oligodendrocytes.

Fewer cell nuclei could be detected in the CHIKV-infected oligodendrocytes suggesting depletion by virus-induced cell death (figure 2.9a). Infected oligodendrocytes had a more rounded morphology suggestive of apoptosis (figure 2.9b). CHIKV antigen was very apparent on the infected oligodendrocytes, indicating that oligodendrocytes are infected by CHIKV and confirming the cross-reactivity of SFV antibody with CHIKV (figure 2.9c).

2.11.1.8 Immunofluorescence of SFV-A7 infected oligodendrocytes.

Results similar to those found for CHIKV-infected oligodendrocytes were observed in SFV-A7 infected cells. Fewer numbers of cell nuclei were visible than in mock-infected cells (figure 2.10a), infected oligodendrocytes appeared rounded or blebbed indicative of apoptosis (figure 2.10b). SFV-A7 antigen was also detected on the infected oligodendrocytes (figure 2.10c)

2.11.1.9 Growth curves of CHIKV and SFV-A7 in BHK-21 cells

A single cycle of infection was induced by infecting BHK-21 cells at a multiplicity of infection (M.O.I) of 10 p.f.u / cell (figure 2.11). Both viruses replicated in BHK-21 cells reaching a peak titre at 14 h.p.i. SFV-A7 replicated more rapidly than CHIKV, this was reflected in the appearance of cytopathic effect (c.p.e) at 16 h.p.i for SFV-A7 and at 24 h.p.i. for CHIKV. Titres were only comparable from 6 h.p.i (after one cycle of virus replication) as plates were not washed on removal of inoculum and virus detected may have been initial inoculum,

2.11.1.10 Trypan blue exclusion assay of a mixed glial cell culture infected with SFV-A7 and CHIKV.

Both CHIKV and SFV-A7 caused c.p.e in the infected mixed glial cell primary culture (figure 2.12). SFV-A7 caused a higher degree of c.p.e within the first 12 h of infection than CHIKV. At 24 h.p.i. cells infected with SFV-A7 had a reduced level viability compared to CHIKV. At 72 h.p.i a negligible amount of SFV-A7 infected

mixed glial cells remained with over half of those initially infected with CHIKV remaining viable.

2.11.1.11 Viral RNA synthesis in BHK cells

Total viral RNA synthesis was measured in BHK cells for both CHIKV and SFV-A7 (figure 2.12). CHIKV had reduced viral RNA synthesis compared to SFV-A7, with both viruses reaching peak synthesis at 4 h.p.i.

2.11.1.12 Growth curve of CHIKV and SFV-A7 in infected mouse brain following intranasal inoculation.

Virus titres from extracted brains of intranasally infected Balb/c were recorded and are shown in figure 2.14. Both CHIKV and SFV-A7 multiplied efficiently in brain tissue with maximum titres obtained at 5 d.p.i. for both viruses. CHIKV virus was not detected in the brain until 3 d.p.i and cleared by 9 d.p.i. compared to SFV-A7 which was detected in the brain 24 h.p.i and cleared by 8 d.p.i.

2.11.1.13 Survival Curves of CHIKV and SFV-A7

All ten mice in both groups intranasally infected with CHIKV and SFV-A7 survived, however only those mice infected with CHIKV showed slight fur ruffling at 6 d.p.i. The positive control SFV4 showed 100% mortality in mice by day 5. All mice survived challenge with SFV-L10 (figure 2.15).

2.11.1.14 Survival Curves of CHIKV and 6 Geographically distinct strains of CHIKV

All ten mice in each group intranasally infected with CHIKV, 37997, 181/25, DAK ArB16878, PO 731460, PH H15483 and SV-0451/96 survived infection. Mice infected with CHIKV and DAK ArB16878 exhibited clinical signs at 4 d.p.i and 5 d.p.i. respectively, including ruffled fur and slight crouching. Signs of lethargy between days 4 to 6 post infection was observed in CHIKV infected mice but not in mice infected with other strains.

2.11.1.15 Growth curve of CHIKV and 6 geographically distinct strains of CHIKV in infected mouse brain following intranasal inoculation.

Virus titres from extracted brains of intranasally infected Balb/c were recorded in triplicate and are shown in figure 2.16. Both CHIKV and DAK ArB16878 multiplied efficiently in brain tissue with maximum titres obtained at 5 d.p.i.. CHIKV was not detected in the brain until 3 d.p.i and cleared by 9 d.p.i. compared to DAK ArB16878 which was detected in the brain 2 d.p.i and cleared by 8 d.p.i. Other strains of CHIKV were not detected in the brain. On intranasally infecting 5 new groups of 6 mice with 37997, 181/25, PO 731460, PH H15483 and SV-0451/96 using a virus titre 1 log higher than previously used, no virus was detected at the two time points used, 4 d.p.i and 5 d.p.i respectively, suggesting the inability of these 5 strains to grow in the adult murine brain.

2.11.1.16 Plaque Analysis

Plaque assays were performed as described in section 2.3.4 on the 37997, 181/25, DAK ArB16878, PO 731460, PH H15483, SV-0451/96 and Ross strains of CHIKV and the Gulu strain ONNV (figure 2.17). Plaques visible of SFV4 and SFV-A7 were indistinguishable, CHIKV 181/25 (vaccine strain) was unique among the strains examined causing numerous barely visible small plaques. Very little difference was observed between ONNV and 37997, PO 731460, PH H15483, SV-0451/96. CHIKV exhibited the largest plaques of the strains examined with DAK ArB16878 sharing the closest plaque size. DAK ArB16878 appears to have two distinct sizes of plaque suggesting the possible presence of 2 distinct populations.

Genome Region	CHIKV 37997	CHIKV Nagpur	CHIKV Vaccine	ONNV Gulu	SFV A7
Complete coding (nt)	84.82	-	-	75.75	64.21
Complete coding (aa)	95.54	-	-	85.55	67.11
5' UTR (nt)	94.80	-	-	82.28	58.82
nsPolyP (nt)	85.70	-	-	75.64	65.67
nsPolyP (aa)	95.68	-	-	85.61	69.49
nsP1 (nt)	87.85	-	-	79.13	62.27
nsP1 (aa)	97.19	-	-	91.10	76.02
nsP2 (nt)	86.97	-	-	79.32	66.25
nsP2 (aa)	97.74	-	-	91.48	72.97
nsP3 (nt)	82.52	-	-	64.91	57.13
nsP3 (aa)	90.00	-	-	66.73	51.31
nsP4 (nt)	84.99	-	-	77.78	69.14
nsP4 (aa)	96.56	-	-	90.84	75.00
Junction (nt)	76.81	-	-	61.77	39.71
sPolyP (nt)	84.48			78.47	64.59
sPolyP (aa)	95.27	96.54	96.29	85.42	62.40
Capsid (nt)	85.44			89.92	70.75
Capsid (aa)	96.94	98.47	98.09	88.51	73.79
E3 (nt)	83.85			75.00	63.78
E3 (aa)	92.19	93.65	93.65	82.82	66.67
E2 (nt)	81.84			74.07	59.47
E2 (aa)	92.77	96.68	94.79	81.80	57.45
6K (nt)	85.79			76.50	54.65
6K (aa)	95.08	95.00	95.00	81.97	44.26
E1 (nt)	86.56			76.69	61.33
E1 (aa)	97.08	97.03	97.23	87.93	62.64
3' UTR (nt)	75.00			58.05	45.00

Table 2.5 Percentage identity of individual CHIKV genes and other SFV subgroup alphaviruses. Nucleotide identities are in normal typeface, amino acid sequence identities in bold typeface. Only amino acid analyses were carried out between virus structural genes.

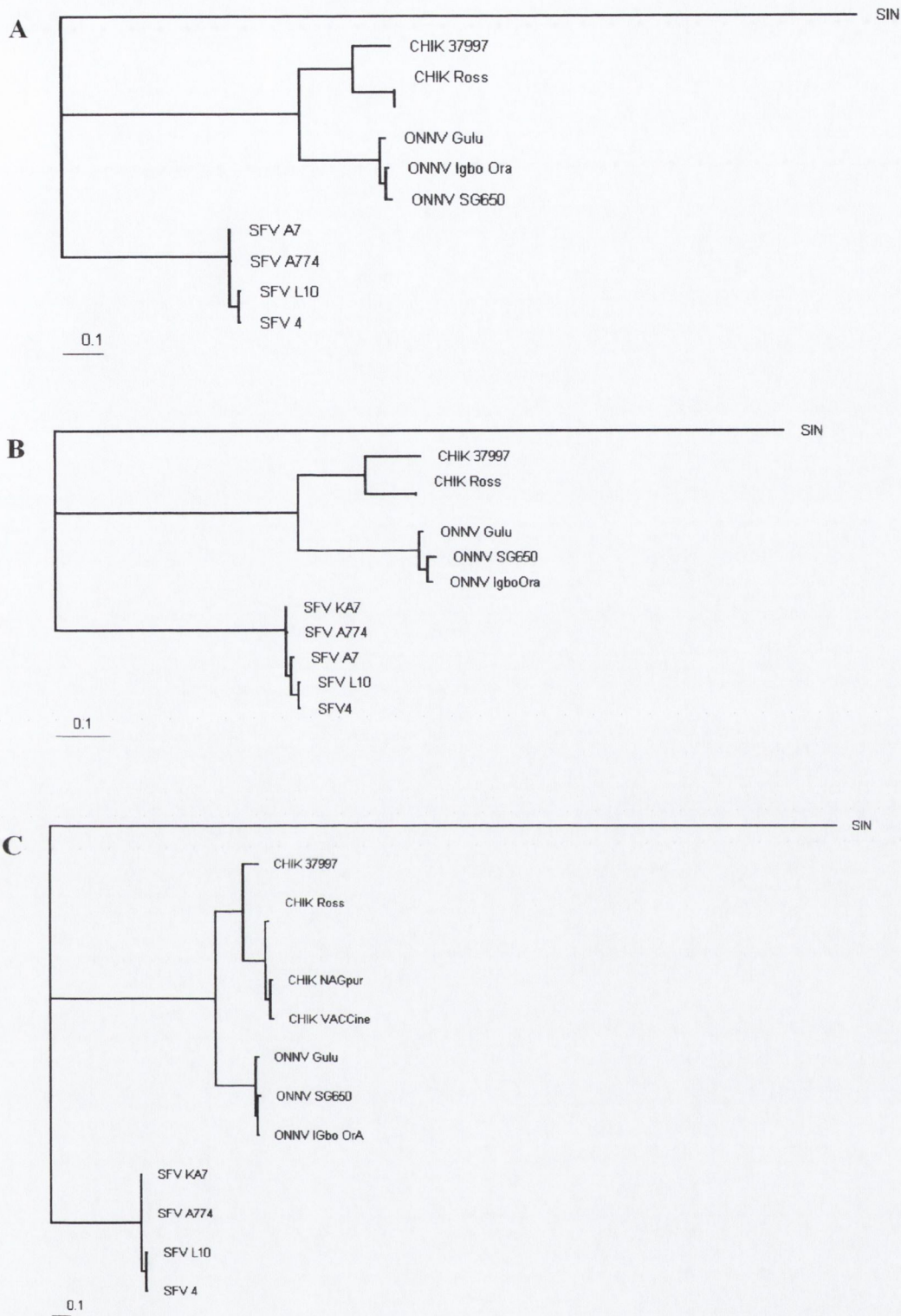


Figure 2.7 Phylograms of CHIKV Ross vs other SF group Alphaviruses

Complete genome coding sequence (A), Phylograms generated by performing PAUP analysis on the complete coding sequence (A), the nonstructural polyprotein nucleotide (nt) sequence (B) and the structural polyprotein nt sequence (C). Numbers indicate bootstrap values for groups to the right. The bar indicates horizontal distance corresponding to 1% nucleotide sequence divergence.

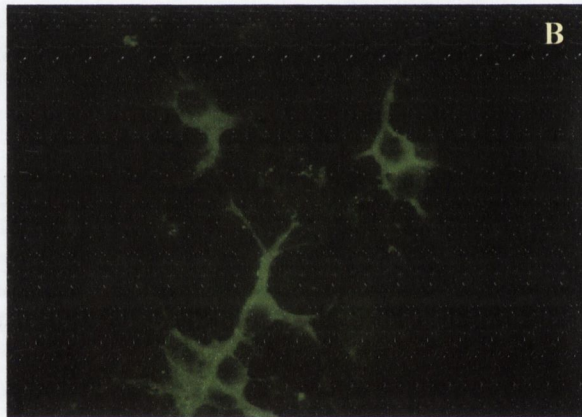
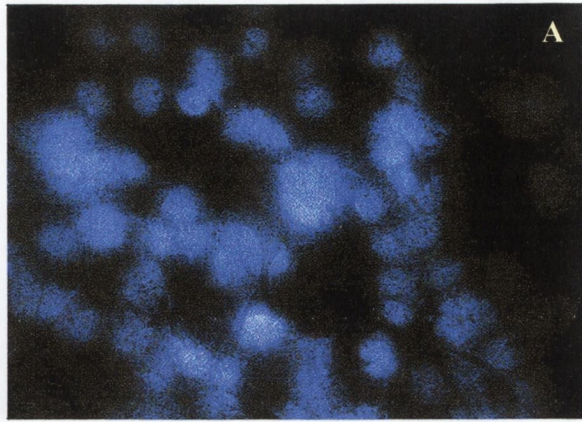


Figure 2.8 Immunofluorescence of uninfected oligodendrocytes.

Cell nuclei are counter stained with DAPI (A), while uninfected oligodendrocytes labelled with a fluorescein-conjugated secondary antibody (Ab) and an anti-CNP primary Ab are visible (B). No virus antigen was detected in the uninfected cells when labelled with a rhodamine-conjugated secondary Ab and an anti-SFV primary Ab (C).

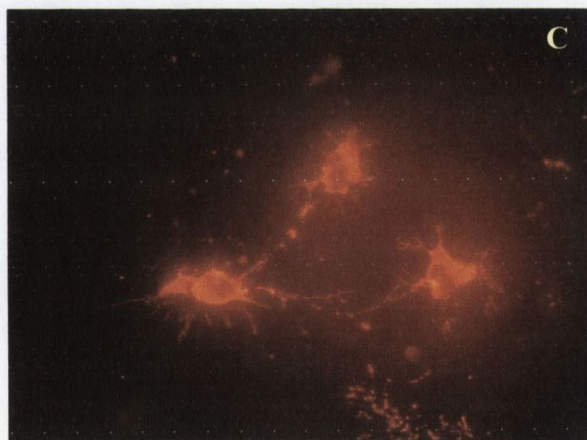
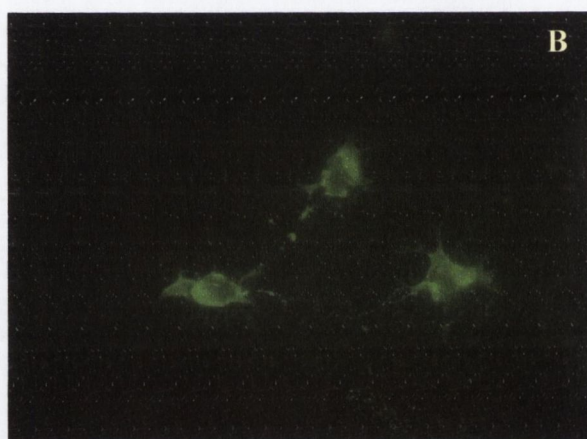
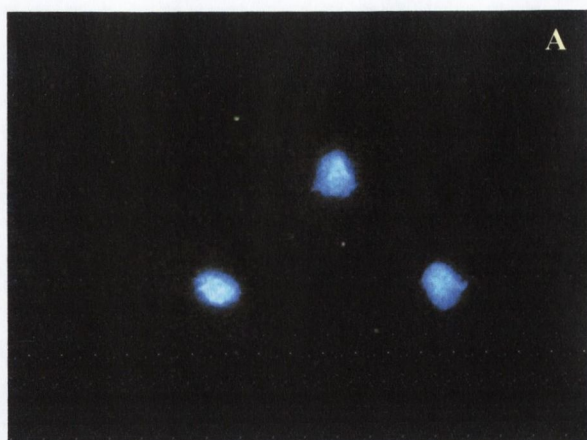


Figure 2.9 Immunofluorescence of CHIKV infected oligodendrocytes.

Cell nuclei were counterstained with DAPI (A). CHIKV infected oligodendrocytes labelled with a fluorescein-conjugated secondary antibody (Ab) and an anti-CNP primary Ab are visible (B). CHIKV antigen was detected in the oligodendrocytes when labelled with a rhodamine-conjugated secondary Ab and an anti-SFV primary Ab (C).

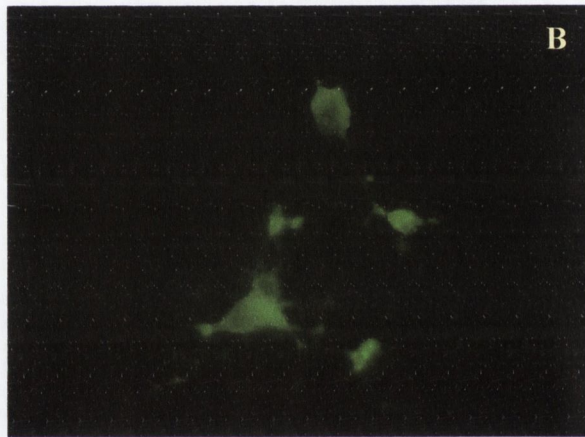
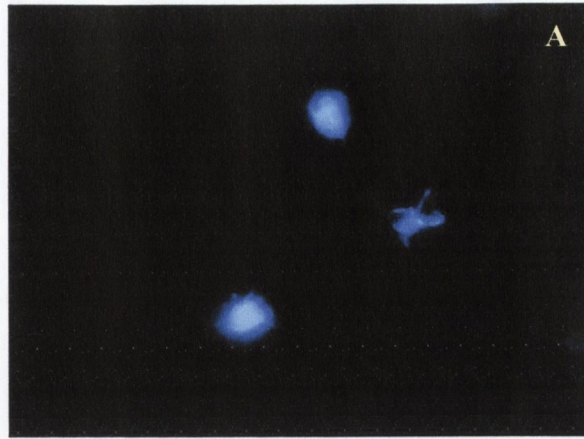


Figure 2.10 Immunofluorescence of SFV-A7 infected oligodendrocytes.

Cell nuclei were counter stained with DAPI (A). Oligodendrocytes infected with SFV-A7 and labelled with a fluorescein-conjugated secondary antibody (Ab) and an anti-CNP primary Ab (B). SFV-A7 antigen was detected in the infected oligodendrocytes when labelled with a rhodamine-conjugated secondary Ab and an anti-SFV biotinylated primary Ab (C). Virus detection is less than seen with CHIKV possibly due to cell death.

2.11.1.5 *In vitro* growth of CHIKV virus

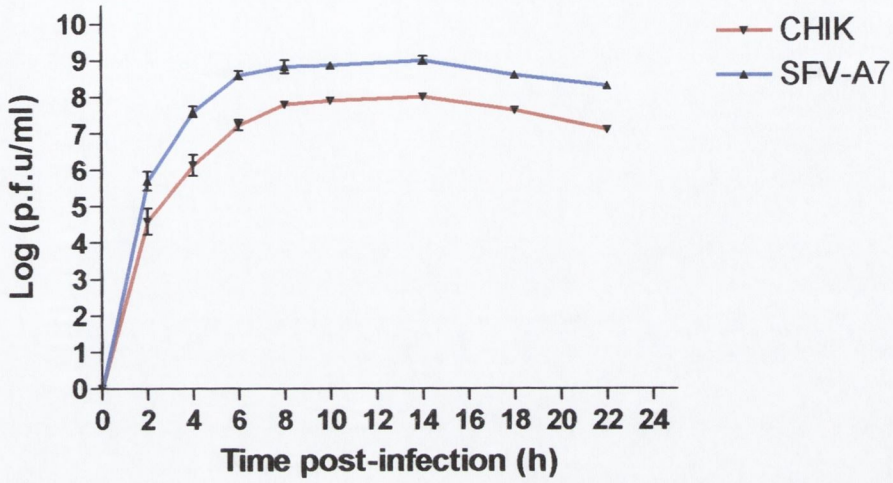


Figure 2.11 Growth curves of CHIKV and SFV-A7 in BHK-21 cells

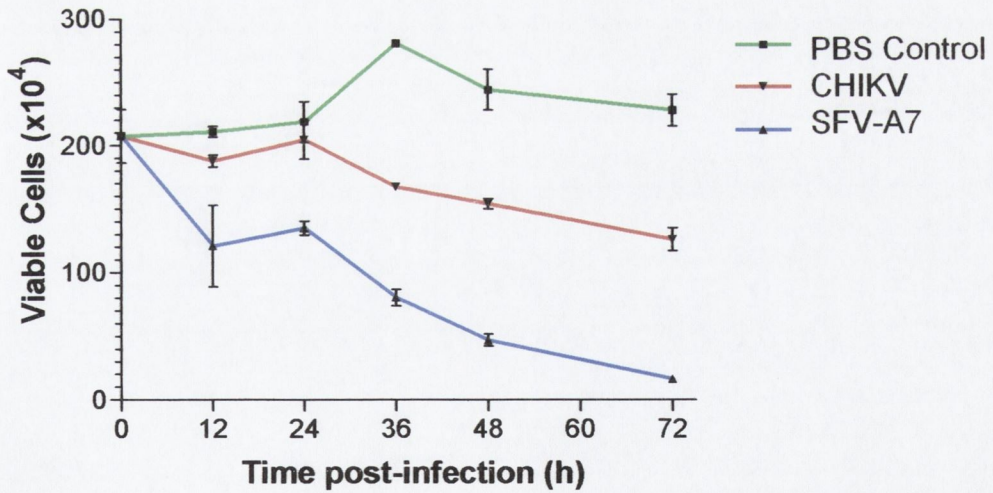


Figure 2.12 Trypan blue exclusion assay of a primary mixed glial cell culture infected with CHIKV and SFV-A7. Cells originated from 12 day-old rat brains.

2.11.1.6 *In vivo* growth of CHIKV virus

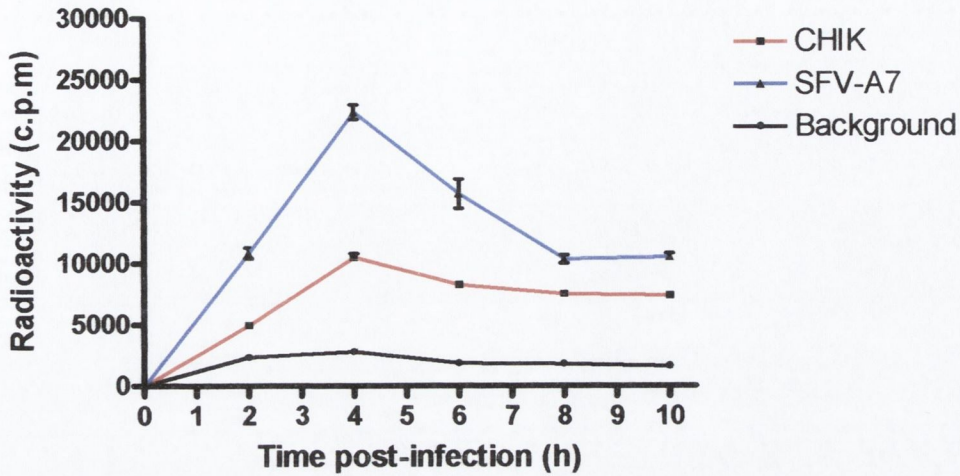


Figure 2.13 Viral RNA synthesis in BHK cells

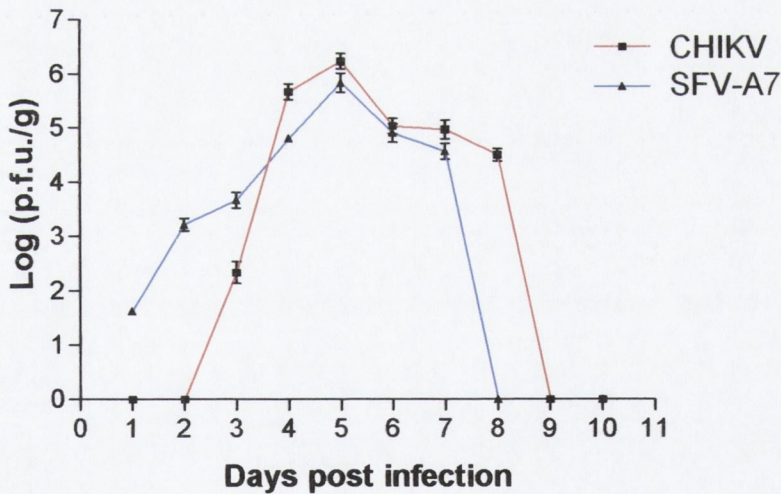


Figure 2.14 Growth curve of CHIKV and SFV-A7 in infected mouse brain following intranasal inoculation. Time points represent the infectious content of homogenates from 3 mice.

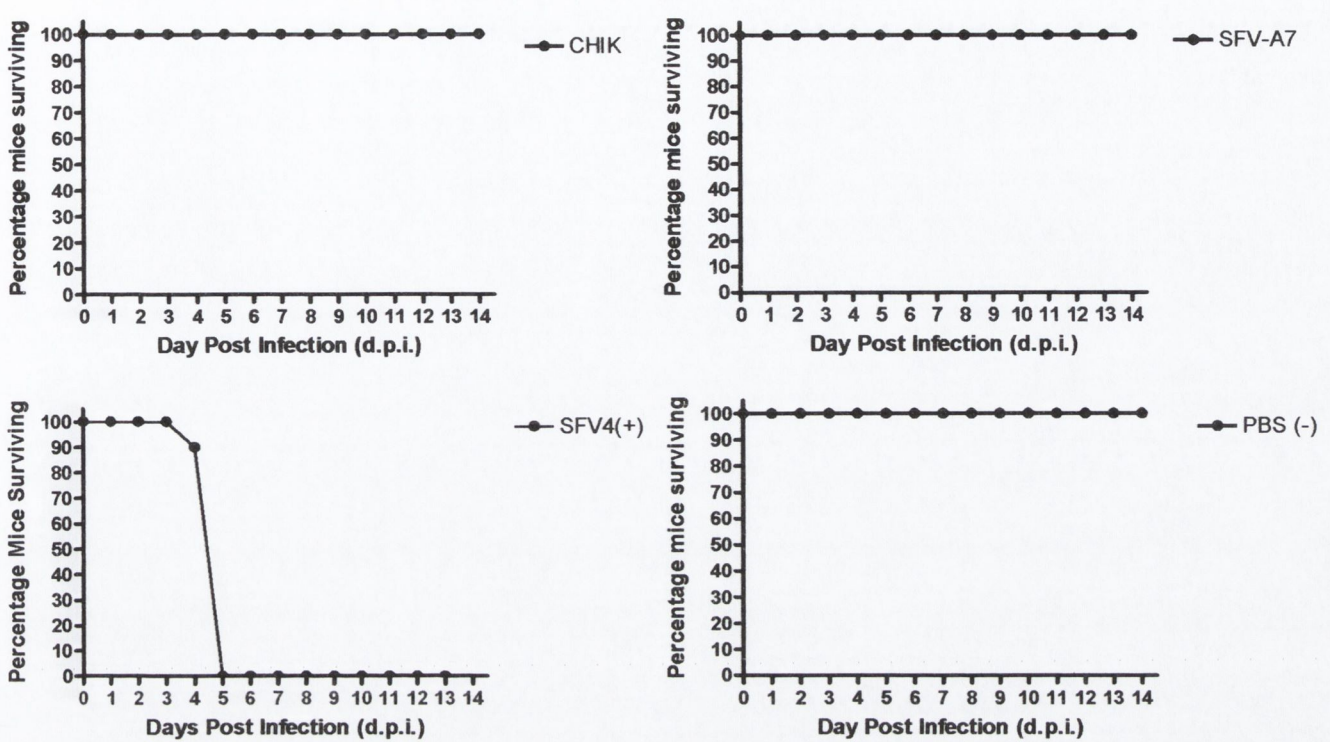


Figure 2.15 Survival curves of Balb/c mice intranasally infected with CHIKV and SFV-A7 with SFV4 and PBS positive and negative controls.

Virus Titres in Balb/c Brains intranasally infected with 7 Geographically Distinct CHIK strains

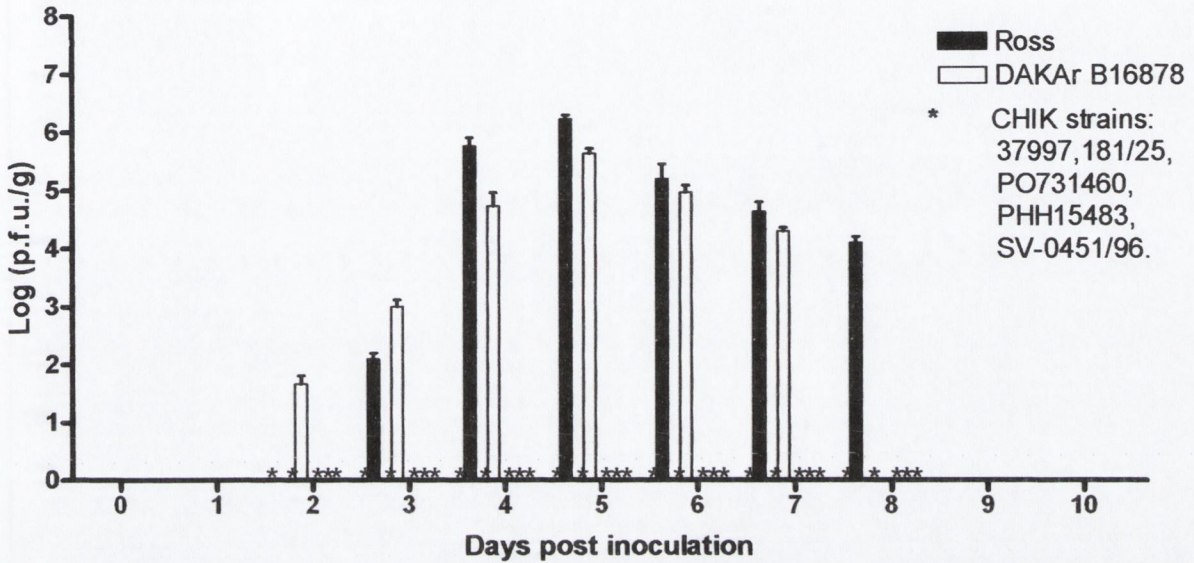


Figure 2.16 Titres of virus in brains of Balb/c mice infected intranasally with seven geographically distinct strains of Chikungunya virus.

Brains were sampled in triplicate at each time point for each virus and titred by plaque assaying serial dilutions of brain-homogenates on BHK-21 cells. No virus was seen in the brains of mice infected with five strains of Chikungunya including 37997, 181/25, PO731460, PHH15483, SV-0451/96. Infection was repeated using new mice for these five groups for timepoints day four and five using a virus with a concentration one log higher than previously used. No virus was detected in the brains of these mice. No clinical signs were apparent in any of the mice used. Previous studies showed no viremia following CHIKV infection of some vertebrate hosts (Jupp and McIntosh, 1988). Only DAKAr B16878 and CHIKV grew efficiently in the brains of intranasally infected Balb/c mice. No virus was detected in the blood of Balb/c mice in this study.

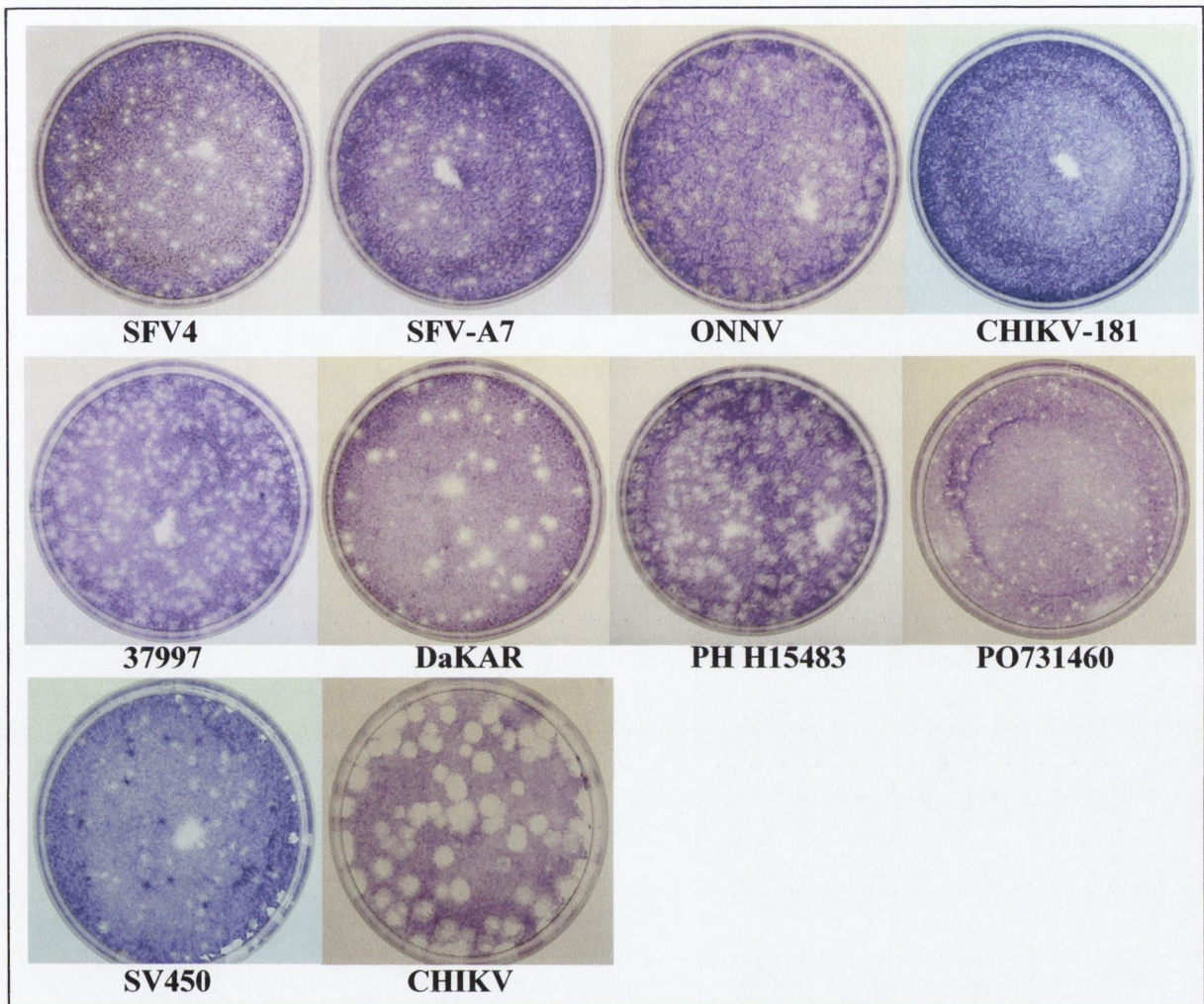


Figure 2.17 Plaque Analysis of 7 geographically distinct strains of Chikungunya virus, ONNV, SFV4 and SFV-A7. Large plaque-like feature in the centre of each dish resulted from the addition of medium-overlay and was excluded from any comparisons.

2.12 Discussion

On sequencing the entire nucleotide sequence of CHIKV and comparing the nucleotide and deduced amino acid sequence with other SFV group alphaviruses, several similarities were noted. These included the presence of two stem loops in its 5' UTR which showed greatest similarity between CHIKV and the Igbo Ora strain of ONNV than between CHIKV and other ONNV strains. Two stem loops were present for CHIKV and ONNV strains however four stem loops were present in SFV-A7. The structure of these stem loops may play a role in each virus' ability to replicate RNA. Other similarities between CHIKV and the SFV group alphaviruses include a conserved amino acid sequence (QVTPNDHANARAFSHLA) at position 31-47 of nsP1, a 24 nt conserved untranslated region within the junction region, and a 19 nt conserved sequence in the 3' UTR terminus adjacent to the poly (A) tract. Helicase, protease and replicase motifs were all also found as expected within nsP2. The CHIKV RNA polymerase motif (GDD) was found in nsP4. Hence, CHIKV appears to be a typical alphavirus from a nucleotide and amino acid sequence stance. On comparing the CHIKV amino acid sequence with that of CHIKV 37997 it was clear that the two strains shared a high degree of sequence identity at 95.54%, however, as only the structural polyproteins of two other CHIKV strains; Nagpur and the 181/25 vaccine strain had been sequenced, they could be compared only over this region. Interestingly, Nagpur had a higher sequence identity over this region than CHIKV 37997 and the vaccine strain, this was even more apparent when a bootstrap analysis (x1000) was carried out showing 37997 to be on a different branch than CHIKV, Nagpur and vaccine strains. Both these latter strains are both considered to be of Asian genotype, whereas the 37797 is West African genotype and CHIKV Central/East African genotype. A more detailed comparison could be made if these strains were to be fully sequenced and the complete genomes compared, a greater divergence in sequence within the non-structural polyprotein than structural polyprotein could explain this finding.

On initiating this investigation it was not know whether CHIKV infected the CNS. It was shown here that CHIKV infects oligodendrocytes and in a parallel study looking at the neuropathology caused in mice intranasally infected with CHIKV ,(discussed in more detail in Chapter 5 "Pathology") demyelinating lesions were observed. These may be due to the direct infection of oligodendrocytes as illustrated in

this investigation, although several other mechanisms of virus-induced demyelination may also be involved and are discussed in more detail in Chapter 6 “General Discussion”. The *in vitro* results obtained in this study have confirmed the ability of CHIKV to multiply efficiently in BHK and mixed glial cells, CHIKV also appears to synthesise RNA at a similar efficiency as SFV-A7 both *in vitro* and *in vivo*. An earlier study showed rapid growth of Chikungunya virus in other cell lines including vero cells (Davis *et al.*, 1971). Previous studies have also shown no viremia following CHIKV infection of some vertebrate hosts such as horses, cattle, goats, sheep and various species of birds (Jupp and McIntosh, 1988), it therefore seems likely that CHIKV cannot reach the brain via the blood circulation. In this investigation detection of CHIKV in the brain following intranasal infection demonstrated that CHIKV travelled via the olfactory pathway, using the neuronal route described by Kaluza *et al.* (1987) for SFV. However it is also apparent that some geographically distinct CHIKV strains seem unable to travel into the brain of intranasally infected mice, this may be due to their passage history and their inability to grow to sufficient titres outside their natural host. The exception to these viruses was DAKAr B16878 which has not been definitively classified as a Chikungunya virus strain within the SFV subgroup and appears to be phylogenetically closer to SFV than CHIKV. On qualitatively analysing the plaque assays for these strains of CHIKV and other SFV subgroup alphaviruses, DAKAr B16878 appeared to have plaques both similar to SFV but also to those of CHIKV, although the neuropathology induced appeared similar but less severe than CHIKV.

It is clear that with over 20 different strains of Chikungunya virus currently isolated, it is a virus that continues to emerge and cause numerous epidemics in Africa and South-east Asia. Although a live attenuated virus (Levitt *et al.*, 1986) exists and may stimulate good immunity, the potential to cause disease in immuno-compromised host or by reversion is present. A new vaccine based on using a Chikungunya virus infectious clone may be more advantageous in efficiently stimulating the immune system and more importantly if based on the SFV vector system would lose the ability to replicate, increasing biosafety. An eventual aim of a system like this would be to generate cheap “one-stop” safe alphavirus vaccine vector that immunised against several alphaviruses, relieving the physical and financial effects of alphavirus epidemics in Africa and Asia.

Chapter Three

The Construction of a Full-length Chikungunya virus cDNA Clone

3.1 Introduction

3.1.1 Alphavirus full-length clones

The construction of full-length cDNA alphavirus clones capable of being transcribed to generate infectious RNA has enabled us to investigate and understand the functions of various genes and their potential roles in causing disease in their hosts (Liljeström *et al.*, 1991; Santagati *et al.*, 1994, 1995; Tarbatt *et al.*, 1997). While this has proved exciting and very beneficial, other developments involving alphavirus full-length clones have proved equally so, namely the development of the SFV expression vector system. Although the pSP6-SFV4 full-length clone developed by Liljeström and Garoff (1991) has predominantly been used for molecular analysis studies, it is now regarded not only as a vector of foreign proteins but also as a potential vaccine system. The structural proteins of the SFV genome are removed from the full-length clone and replaced by foreign genes of interest. SFV particles that carry a recombinant RNA molecule undergo only one round of RNA replication in the infected cell and as the structural genes are removed, no progeny virus can be produced. The cell infected with the replicating vector is killed within a few days (Glasgow *et al.*, 1998). A study using the SFV expression system to vaccinate mice against influenza A virus reported influenza-specific humoral and cell mediated responses (Berglund *et al.*, 1999). Similarly, SFV particles encoding prME or NS1 proteins of louping ill virus protected both mice and sheep from lethal challenge (Morris-Downes *et al.*, 2001; Fleeton *et al.*, 2000).

3.1.3 Chikungunya vaccine

For a vaccine to be beneficial, it must display high efficiency and biosafety. Live attenuated pathogens, while inducing high cellular immune responses and immunological memory, can cause unwanted side effects. On the other hand subunit vaccines are considerably safer but do not always display a high degree of efficiency. An experimental live attenuated CHIKV vaccine exists (Levitt *et al.*, 1986) developed for production for human use. CHIKV strain 15561 was isolated in Thailand and subjected to 18 plaque-to-plaque passages in MRC-5 cultures before CHIKV 181/clone 25 was selected. Although this vaccine induces long-term protection by neutralizing antibody, it is not widely available in the countries most affected by CHIKV epidemics as it was primarily designed with the US military in mind when

developed at the United States Army Medical Research Institute for Infectious Diseases, Maryland, USA (USAMRIID). The development of this vaccine has been the topic of much controversy to the extent that in the developer's testimony to the U.S. Senate in 1988, he felt that it was unsafe (Neil Levitt, personal communication). It has been shown by several groups including our own, that viral vectors offer the opportunity to express a desired antigen *in vivo*, with potentially less biosafety problems and side effects than attenuated vaccines (Atkins *et al.*, 1996). Systems such as the pSP6-SFV4 full-length clone mentioned above have been developed that do not lead to productive replication in the host and is highly modified to increase biosafety (Fleeton *et al.*, 1999). In order to fully ascertain the functions of various CHIKV genes and their possible roles in causing disease, the construction of a CHIKV full-length clone is evidently the logical and valuable next step towards understanding this virus and the first step in developing an effective and safe vaccine.

3.1.2 Construction of a Chikungunya full-length clone

The construction of the CHIKV full-length clone used the complete genome sequence of the Ross strain of CHIKV as described previously in Chapter 2. A strategy was developed that incorporated the use of two different commercial cloning vectors and the insertion of the CHIKV genome in 5 separate fragments into these vectors. Subsequently the genome was exchanged in 2 large fragments from one vector into the other using a range of restriction enzyme sites within the CHIKV genome. This strategy kept the need for PCR at a minimum, thus reducing the chances of spontaneous mutations materialising within the genome. The PCR that was carried out used a novel type of polymerase that ensured the maximal proofreading fidelity.

3.1.3 TripleMaster PCR system

TripleMaster Enzyme Mix combines the efficiency of Taq DNA Polymerase with the 3' – 5' exonuclease activity of a proofreading thermostable enzyme, along with a polymerase-enhancing factor that provides an extremely high extension rate and maximal proofreading assisted fidelity. The error rate of using Taq DNA Polymerase alone in PCR is 2.2×10^{-5} errors per nt per cycle whereas the enzyme mix of the TripleMaster shows fidelity being improved 4 – 5 times compared with Taq. When amplifying CHIKV fragments ranging in size from 1.2 – 3.5 kb, reducing the possible error rate is crucial. Thus, TripleMaster was used throughout this project.

3.2 Materials and methods

3.2.1 Molecular biology techniques used in the construction of a CHIKV full-length clone.

3.2.1.1 Cloning vectors

Two cloning vectors were chosen for the construction of the CHIKV full-length clone. On sequencing the CHIKV genome in 5 fragments each was initially ligated into litmus 28i (L28i; NEB, USA) due to the location of restriction sites in its multiple cloning site (MCS). Fragments were excised and ligated between these vectors until 3 consecutive fragments were in one and 2 in another. At this point another cloning vector was introduced, namely pBluescript SK II (+) (pB; Stratagene, USA). As the 5 fragments spanning the genome did not include the CHIKV 5' untranslated region pB was selected as the location of its restriction sites allowed a strategy to be used that incorporated the insertion of the CHIKV 5' UTR and the fragments from the L28i vectors. pB has also been shown to be a very efficient cloning vector with a T7 promoter capable of high rates of transcription (Dr. Ann Powers, personal communication).

3.2.1.2 Restriction enzymes

Several enzymes were used to excise fragments throughout the construction procedures these were supplied by NEB, USA and can be seen in table 3.1 below along with reaction conditions and components of their 10x buffers. Identical amounts of each enzyme buffer (2 μ l), enzyme (20 U), water (2 μ l) and sample DNA (0.6 - 0.8 μ g) were used for each restriction digestion step. Each digestion step was carried out at 37°C in quintuplicate, pooled and DNA purified using the QIAGEN Nucleotide Removal Kit (Qiagen, USA) to manufacturer's recommendations. Other enzymes were used for confirmation analysis of successful ligation, only 5 U of enzyme and 0.2 μ g of DNA was used for such analyses. Hereafter, all restriction digestion descriptions will be limited in detail to the name of the enzyme used, as the conditions and quantities of reagents are detailed above and in table 3.1.

Enzyme	10X Buffer	Buffer components / Reaction Conditions
Bam HI	NEB Buffer 2	150 nM NaCl, 10mM Tris-HCl, 10 mM MgCl ₂ , 1mM dithiothreitol (pH 7.9)
Bst BI	NEB Buffer 4	50 mM potassium acetate, 20 mM Tris-acetate, 10 mM magnesium acetate, 1 mM di thiothreitol (pH 7.9)
Cla I	NEB Buffer 4	50 mM potassium acetate, 20 mM Tris-acetate, 10 mM magnesium acetate, 1 mM di thiothreitol (pH 7.9)
Eco RV	NEB Buffer 3	100 mM NaCl, 50 mM Tris-HCl, 10 mM MgCl ₂ , 0.025% Triton-X-100 (pH 7.5)
Kpn I	NEB Buffer 1	10 mM Bis Tris-Propane-HCl, 10 mM MgCl ₂ , 1 mM dithiothreitol (pH 7.0)
Nde I	NEB Buffer 4	50 mM potassium acetate, 20 mM Tris-acetate, 10 mM magnesium acetate, 1 mM di thiothreitol (pH 7.9)
Sac I	NEB Buffer 1	10 mM Bis Tris-Propane-HCl, 10 mM MgCl ₂ , 1 mM dithiothreitol (pH 7.0)
Spe I	NEB Buffer 2	150 nM NaCl, 10mM Tris-HCl, 10 mM MgCl ₂ , 1mM dithiothreitol (pH 7.9)
Stu I	NEB Buffer 2	150 nM NaCl, 10mM Tris-HCl, 10 mM MgCl ₂ , 1mM dithiothreitol (pH 7.9)

Table 3.1 Restriction enzymes used in the construction of the CHIKV full-length clone with their respective 10X Buffers (NEB, USA)

3.2.1.3 Dephosphorylation of linearised L28i and pB cloning vectors

Cloning vectors that were linearised by digestion by more than one enzyme did not need to be dephosphorylated as the 5' and 3' overhangs were not compatible for religation to each other. However, linearised cloning vector (1µg) digested by only one restriction enzyme, was treated with 5 units (1µl) of Antarctic phosphatase (in 10mM Tris-HCl (pH7.4), 1mM MgCl₂, 1mM DTT, 50% glycerol) and added to 1 µl 10X Antarctic Phosphatase reaction buffer (50mM Bis Tris-Propane, 1 mM MgCl₂, 0.1 mM ZnCl₂, pH 6.0. NEB, USA). The reaction was then mixed and incubated at 37°C for 15 min and heat inactivated for 5 minutes at 65°C before further DNA purification and ligation.

3.2.1.4 Ligation of fragments into cloning vectors

L28i and pB were both linearised and dephosphorylated in the case of restriction digestion by one enzyme, or simply linearised by the removal of a region by two different restriction enzymes. Linearised vector was added in a 1:16 ratio to a 700 µl microfuge containing 16 µl of each purified restriction enzyme-digested CHIKV fragment, 2 µl of T4 10X ligase buffer and 1 µl T4 ligase (Promega, USA). The reaction was gently vortexed and incubated overnight at room temperature.

Subsequent reactions involved the excision of ligated fragments from one successful fragment-vector clone being ligated into other successful fragment-vector clones. This is described in more detail for each clone in sections 3.2.3.1 to 3.2.3.5

3.2.1.5 Transformation, colony selection and confirmation analysis

All ligation reactions involving the L28i cloning vector were transformed in competent *E. coli* DH5 α cells and selected for as described previously for the sequencing of the CHIKV genome in section 2.10.4.6. Ligation reactions involving the pB cloning vector were transformed in ultra-competent *E. coli* XL-10 Gold cells (Stratagene, USA) following manufacturer's guidelines. Of the transformed recombinant vectors, typically 5-20 white colonies were selected for each ligation reaction. DNA was extracted and restriction digestion confirmation analysis performed as previously described in section 2.10.4.8 with the appropriate enzyme and 10X buffer.

3.2.1.6 Primer design

CHIKV virus RNA was isolated, cDNA amplified and oligonucleotide primer pairs designed as described previously in sections 2.10.3.1 and 2.10.3.2 respectively. However, the five amplicons produced ranged from 1220 nt to 3401 nt in size, significantly larger than the 500 – 600 nt amplicons typically produced and described in section 2.10.3.3. Five fragments were amplified using the primers 1-5 described in table 3.2. Primer "Fragment 5 Rev" included a "TTCGAA" oligonucleotide sequence at the 5' end to generate a unique *Bst* *BI* restriction site for insertion into L28i.

One primer pair termed Fragment 3 / 4 was used later in the construction of the CHIKV full-length clone and produced a 3384 nt fragment containing internal *Cla* *I* sites at each end, this fragment is discussed in more detail in section 3.2.4.5. The 5' UTR oligonucleotides incorporated a *Kpn* *I* site (*ggtacc*) and a *Bam* *HI* (*ggatcc*) at the 5' and 3' ends respectively. Both of these sites were flanked by 3 random nucleotides to maximize digestion efficiency and are discussed in more detail later in section 3.2.4.2.

Primer	Sequence (5'-3')	Genome Position
Fragment 1 Fwd	ATGGCTGCGTGAGACACA	77-95
Fragment 1 Rev	TTCATCTGCATCATATTGAAGAAGCCGCAC	2530-2559
Fragment 2 Fwd	GCGATGCATGGACCAGCCCTGAACACCGAC	2000-2029
Fragment 2 Rev	GTATACTGCCTTGCAAACACCGTCACCTGG	4160-4189
Fragment 3 Fwd	ATGCTCGGGGGTGACTCATTGAGACTGCTC	3800-3829
Fragment 3 Rev	ACCACTTCGTCAGCCAGCGCTCGTCTTCTA	7300-7329
Fragment 4 Fwd	TTGGATGAACATGGAAGTGAAGATCATAGA	7120-7149
Fragment 4 Rev	TCTGCAGTACCAGTTGTGTGTTAGCATAGA	10631-10660
Fragment 5 Fwd	GTCTTCAGCCTGGACACCTTTCGACAACAA	10491-10520
Fragment 5 Rev	TTCGAAATATTA AAAAACAAAATAACATCTCCTACG	11782-11813
Fragment 3 / 4 Fwd	GGATATGGCAGAGATATATACTATG	4708-4732
Fragment 3 / 4 Rev	AAGCGTCCGACTTCATGTGCACG	8070-8092
5'UTR Oligo Fwd	TTGGGTACCTA ATACGACTCACTATAGGGATGGCTGC GTGAGACACACGTAGCCTACCAGTTTCTTACTGCTCT ACTCTGCAAAGCAAGAGATTAAGAACCCATCATGGAT CCGCG	1-76
5'UTR Oligo Rev	CGCGGATCC CATGATGGGTTCTTAATCTCTTGCTTTGCA GAGTAGAGCGATCCGCGCTGGTAGGCTACGTGTGTCT CACGCAGCCATCCCTATAGTGAGTCGTATTAGGTACC CAA	76-1

Table 3.2 Primers designed to amplify the CHIKV genome in five fragments and a 106 nt CHIKV 5' UTR complementary oligonucleotide pair .

3.2.1.7 Polymerase Chain Reaction (PCR)

PCR was carried out following the TripleMaster Long range PCR system (Eppendorf, USA) guidelines, with the following thermocycling conditions; an initial cycle of 2 min at 95° C, followed by 35 cycles of 30 sec at 95° C, 30 sec at 55° C and 5 min extension at 72° C. A final extension time of 15 min at 72° C was added and the samples stored at -20° C until DNA purification could be carried out.

3.2.1.8 DNA purification

All five amplified fragments spanning the CHIKV genome were DNA purified using the Promega Wizard Kit (Promega, USA) as described in section 2.10.4.1. Figure 3.1 illustrates the fragment sizes upon restriction digestion, and the genes each fragment encompasses.

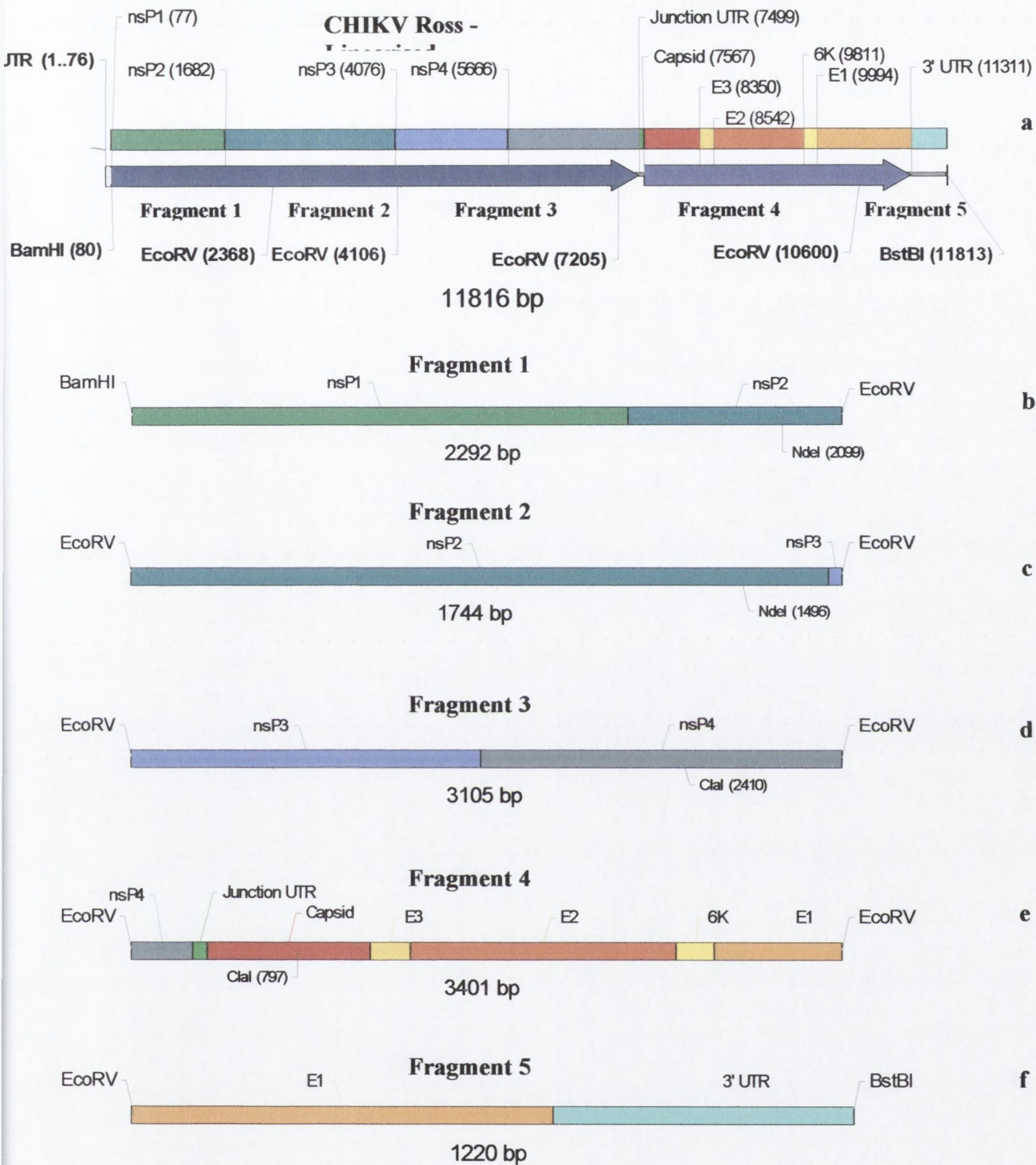


Figure 3.1 Linearised map of Chikungunya Ross genome showing the locations of 5 fragments of the CHIKV genome. (a) Figures b-f show the individual fragments 1-5 with their respective restriction enzyme sites for cloning into the Litmus 28i cloning vector at each end are also shown. Sizes of the fragments are shown below each figure and are inclusive of the entire undigested terminal restriction sites. The first 76 nucleotides of the CHIKV genome 5' UTR were intentionally not incorporated in fragment 1 (elaborated on later in section 3.2.4.2).

3.2.2 Preparation and ligation of CHIKV fragments 1-5 into L28i

3.2.2.1 Preparation of L28i

Litmus 28i plasmid was linearised (1µg) with *Eco RV* for 2 h at 37°C, the DNA purified as previously described and dephosphorylated. Unlike fragments 2, 3 and 4 which contained *EcoRV* restriction sites at both 5' and 3' ends, fragment 1 contained a *Bam HI* at its 5' end and an *Eco RV* site at its 3' end and fragment 5 contained a *Bst BI* restriction site at its 3' end with an *Eco RV* site at its 5' end. Preparation of L28i for the insertion of fragments 1 and 5 therefore each required an additional restriction digestion of L28i previously digested with *Eco RV*, with *Bam HI* and *Bst BI* respectively. Conditions of digestion were identical to those used with *Eco RV* with the exception of the restriction enzymes used and their respective buffers.

3.2.2.2 Restriction Digestion

All five DNA fragments were digested with *Eco RV* to create the 5' overhang needed to ligate into the *Eco RV*-linearised Litmus 28iii cloning vector (New England Biolabs (NEB), USA). The following reaction mixtures were digested for 2 h at 37°C: 15 µl Purified PCR product, 2 µl nuclease-free water, 2 µl 10X NEBuffer 3 (100 mM NaCl, 50 mM Tris-HCl, 10mM MgCl₂, 1mM dithiothreitol pH 7.9) and 20U *Eco RV* enzyme (NEB, USA). Fragments 1 and 5 were additionally digested with *Bam HI* and *Bst BI* restriction enzymes as described for L28i in section 3.2.4. Each digestion for all fragments was done in quintuplicate and pooled.

3.2.2.3 Ligation of CHIKV fragments 1-5 into L28i

Eco RV digested CHIKV fragments 2, 3 and 4 were ligated into dephosphorylated, *Eco RV*-linearised L28i. Double-digested fragments 1 (*Eco RV* / *Bam HI*) and 5 (*Eco RV* / *Bst BI*) were ligated into their respective double-digested L28i cloning vectors in the same manner described for the *EcoRV* single-digested fragments above. Ligation reactions were left at room temperature overnight and subsequently transformed as described in section 3.2.1.5.

3.2.2.4 Confirmation analysis of L28i-CHIKV fragment colonies

In order to confirm successful ligation of each of the five CHIKV fragments into their respective restriction-digested L28i cloning vectors, random colonies of each were picked and DNA isolated. The DNA from each L28i-Fragment colony was then digested with the appropriate restriction enzyme.

3.2.2.5 Confirmation analysis of L28i-Fragment 1

DNA was isolated from 4 random transformed L28i-Fragment 1 (LF1, 5064 nt) colonies. These were then double-digested with restriction enzymes *Nde I* (2674, absent in L28i) and *Sac I* (4823, absent in CHIKV). A positive ligation was recorded if 2 DNA bands of 2149 and 2915 nt were observed when run on a 0.8% agarose gel. Figure 3.2 shows fragment 1 inserted in L28i with the relevant restriction enzymes and their respective positions in brackets.

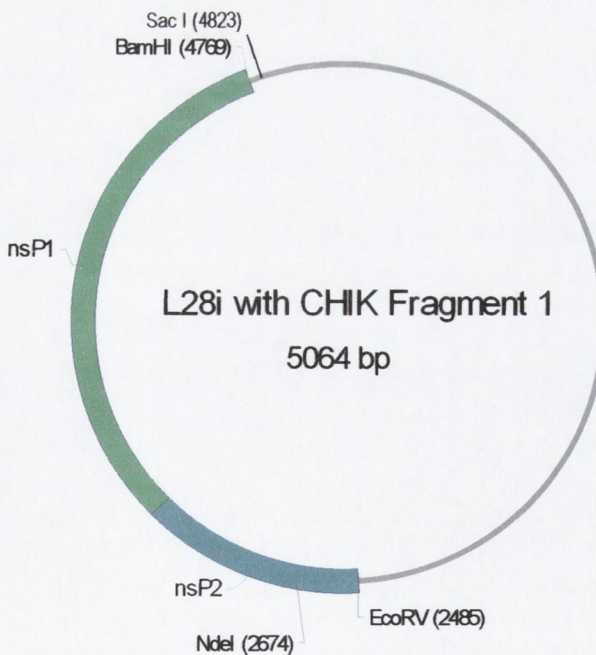


Figure 3.2 L28i with CHIKV fragment 1 (LF1)

3.2.2.6 Confirmation analysis of L28i-Fragment 2

L28i-Fragment 2 (LF2, 4561 nt) was digested with *Stu I* (3493 and 4340, present once in CHIKV Fragment and once in L28i vector). Positive conformational analysis resulted in the presence of 2 DNA bands of 3714 and 847 nt in size when run on a 0.8% agarose gel. The map of LF2 with relevant restriction enzymes and gene location can be observed in figure 3.3.

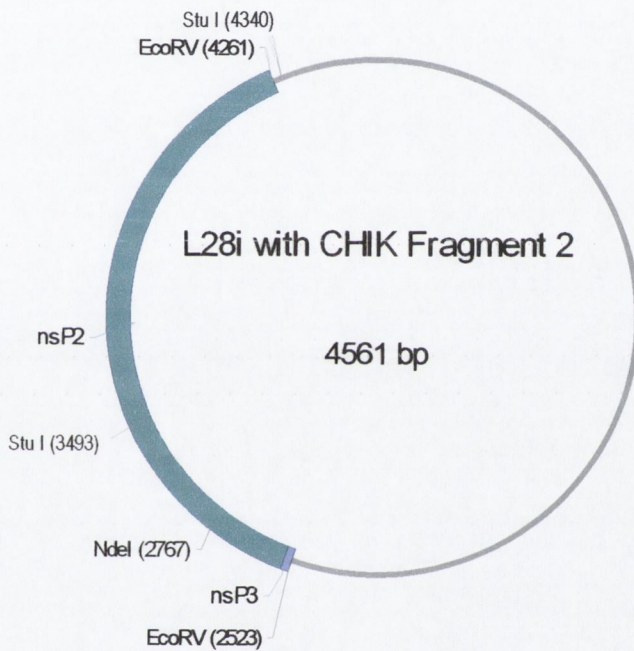


Figure 3.3 L28i with CHIKV fragment 2 (LF2)

3.2.2.7 Confirmation analysis of L28i-Fragment 3

L28i-Fragment 3 (LF3, 5922 nt) was digested with *EcoRV* (2523 and 5622, both sites in CHIKV Fragment 3). Positive conformational analysis resulted in the presence of 2 DNA bands of 2823 and 3099 nt in size when run on a 0.8% agarose gel. The map of LF3 can be observed in figure 3.4.

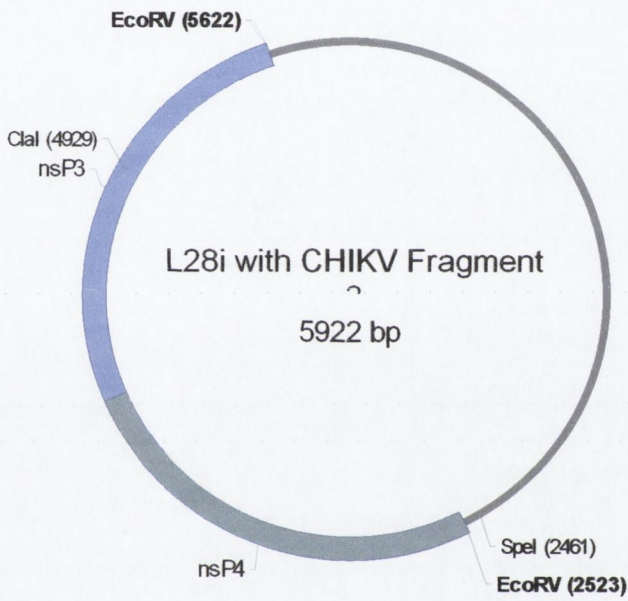


Figure 3.4 L28i with CHIKV Fragment 3 (LF3)

3.2.2.8 Confirmation analysis of L28i-Fragment 4

Like LF3, L28i-Fragment 4 (LF4, 6218 nt) was digested with *EcoRV* (2523 and 5918, both sites in CHIKV Fragment 4). Positive conformational analysis resulted in the presence of 2 DNA bands of 2823 and 3395 nt in size when run on a 0.8% agarose gel. The map of LF4 can be observed in figure 3.5.

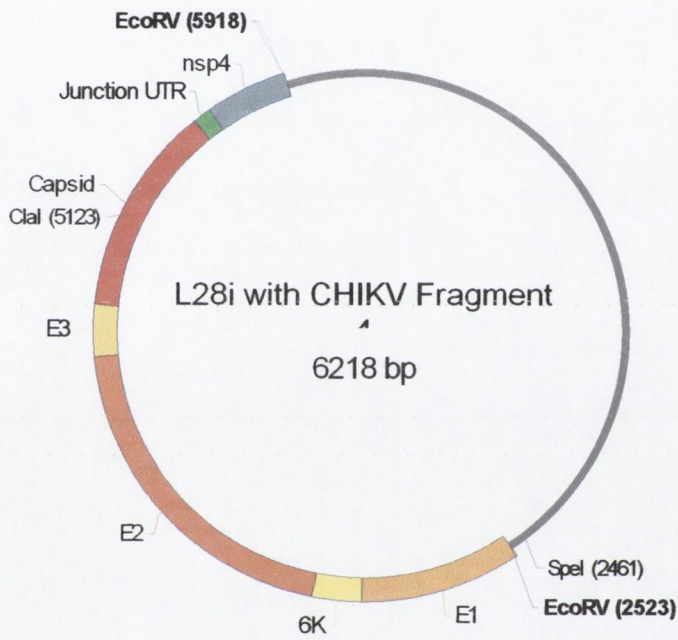


Figure 3.5 L28i with CHIKV Fragment 4 (LF4)

3.2.2.9 Confirmation analysis of L28i-Fragment 5

L28i-Fragment 5 (LF5, 3992 nt) DNA was double-digested with restriction enzymes *Spe I* (2461, absent in CHIKV) and *Stu I* (3771, absent in L28i). A positive ligation was recorded if 2 DNA bands of 1310 and 2682 nt were observed when run on a 0.8% agarose gel. Figure 3.6 shows fragment 5 inserted in L28i with the relevant restriction enzymes and their respective positions in brackets.

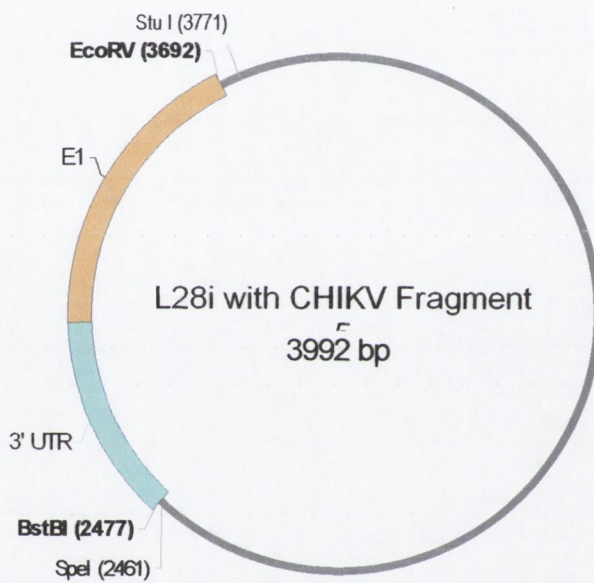


Figure 3.6 L28i with CHIKV Fragment 5 (LF5)

3.2.3 Construction of L28i / CHIKV Fragment (LF) intermediates

With the entire CHIKV genome inserted into 5 respective L28i cloning vectors (LF1-5), 1 colony of each was chosen for manipulation, subsequent steps in the construction of a CHIKV full-length clone involved excising the fragments from each clone and constructing full-length clone intermediates in L28i.

3.2.3.1 Construction of LF1-2 intermediate

Fragment 2 was excised from LF2 and LF1 linearised, both with *Nde I*. Linearised LF1 was dephosphorylated to prevent recircularisation and Fragment 2 was ligated in, with the resulting intermediate termed LF1-2. Confirmation analysis was carried out on LF1-2 using *Nde I* (2729 and 4412). If Fragment 2 was inserted in the correct orientation 2 bands of 1683 and 5119 nt when run on a 0.8% agarose gel were observed (figure 3.7). In the case of Fragment 2 being inserted in the reverse orientation 2 bands: 413 and 6389 nt in size would have been observed.

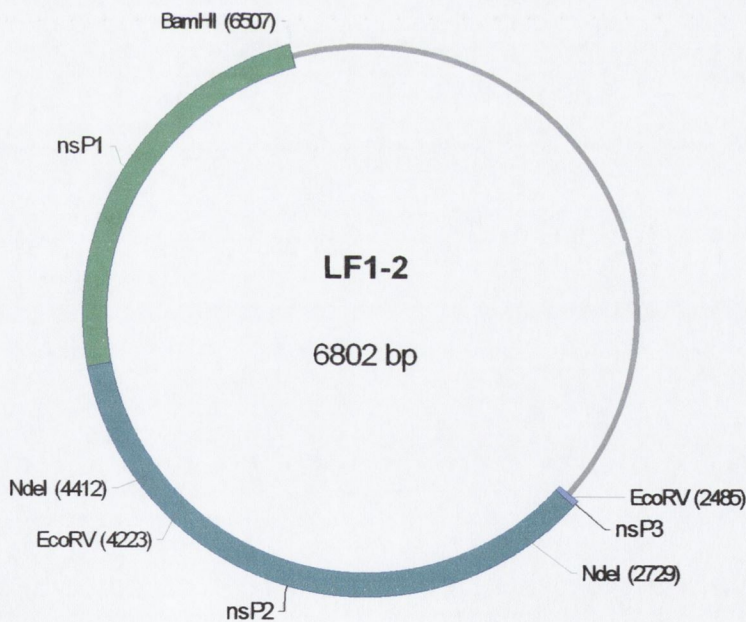


Figure 3.7 Construction of LF1-2 intermediate resulting from the ligation of Fragment 2 into *Eco RV*-linearised LF1.

3.2.3.2 Construction of LF1-2 Δ *Nde I* intermediate

By removing the *Eco RV* restriction site at position 4223, only one *Eco RV* site was present at nucleotide position 2485. Fragment 3 could be ligated into LF1-2. This was carried out using the *Nde I* restriction enzyme that cuts LF1-2 at positions 2729 and 4412. The intermediate generated was termed LF1-2 Δ *Nde I* (5119 nt) and was recircularised using T4 ligase (NEB, USA). The excised 1683 nt *Nde I* fragment was DNA purified and stored at -20°C for subsequent reinsertion. A map of LF1-2 Δ *Nde I* can be seen in figure 3.8 below.

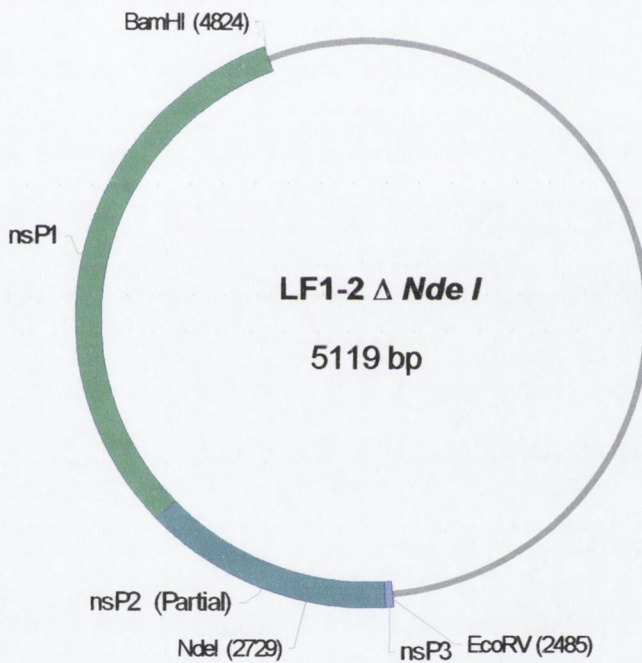


Figure 3.8 Construction of LF1-2 Δ *Nde I* intermediate

3.2.3.3 Construction of LF1-2-3 Δ *Nde I* intermediate

LF1-2 Δ *Nde I* was linearised using *Eco RV* and dephosphorylated to prevent recircularisation. Fragment 3 was then excised from LF3 using *Eco RV* and ligated into the *Eco RV*-linearised LF1-2 Δ *Nde I* clone. The resulting intermediate clone, termed LF1-2-3 Δ *Nde I* (8218 nt) underwent confirmation orientation analysis by restriction digestion with *Nde I* (5828) and *Cla I* (either position 3176 if fragment 3 ligated in positive orientation or position 4893 in negative orientation). Positive confirmation resulted in 2 bands, 2652 and 5566 nt in length when run on a 0.8% agarose gel, insertion of Fragment 3 in the reverse confirmation produced two bands of 935 and 7283 nt. Figure 3.9 shows the map of LF1-2-3 Δ *Nde I* with fragment 3 in positive orientation.

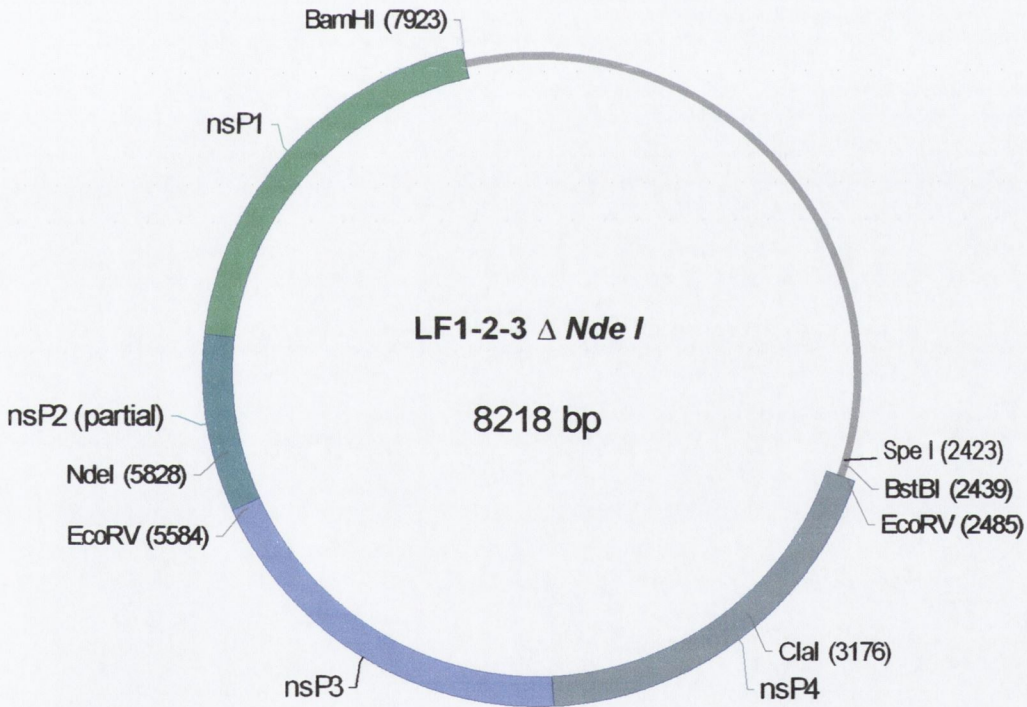


Figure 3.9 L28i with CHIKV Fragments 1 and 2 Δ *Nde I* fragment plus Fragment 3 (LF1-2-3 Δ *Nde I*)

3.2.3.4 Reinsertion of *Nde I* fragment into LF1-2-3 $\Delta Nde I$ intermediate

LF1-2-3 $\Delta Nde I$ was linearised with *Nde I* (5828) and the 1683 nt DNA purified *Nde I* fragment excised in section 3.2.3.2 was religated using T4 ligase. The resulting clone was termed LF1-2-3 (9901 nt) and the orientation of the *Nde I* insert was checked using *EcoRV* (positions 2485, 5584 and 7322 in positive orientation or 2485, 5584 and 6017 in the negative orientation). Positive orientation resulted in three DNA bands of 1738, 3099 and 5064 nt respectively when run on a 0.8% agarose gel. Negative orientation resulted in three bands of 433, 3099 and 6369 nt in length. Figure 3.10 shows LF1-2-3 in positive orientation, an open reading frame (ORF) is also depicted in order to show that the ligations of CHIKV fragments 1, 2 and 3 maintained the correct ORF sequence.

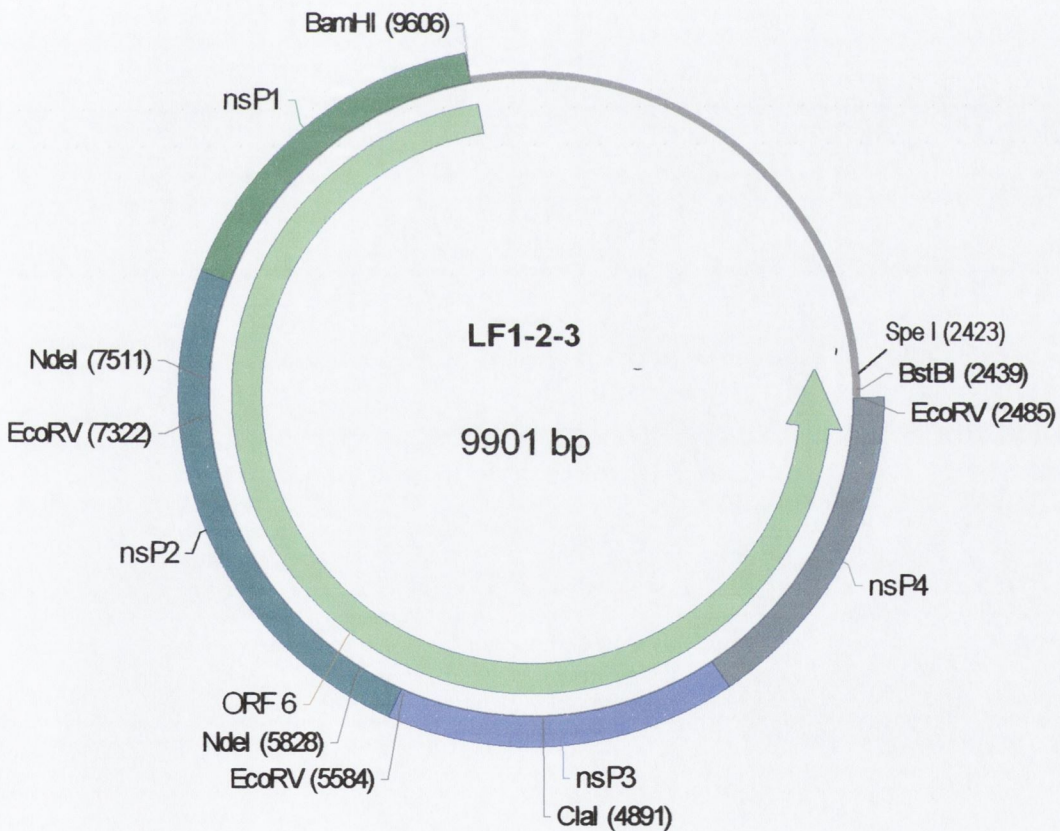


Figure 3.10 L28i with complete CHIKV Fragments 1, 2 and 3 (LF1-2-3)

3.2.3.5 Construction of LF5-4 intermediate

An intermediate clone incorporating CHIKV fragment 4 (3395 nt) into LF5 (3992 nt) was constructed by excising fragment 4 from LF4 with *Eco RV* (at positions 2623 and 5918) and ligating it into an *Eco RV* (3692)- linearised and dephosphorylated LF5 clone. The resulting clone was termed LF5-4 (7387 nt). Positive orientation was determined by double digestion with *Spe I* (2461, unique to L28i) and *Cla I* (6292 in positive orientation, 4487 in negative orientation). Upon running the digested LF5-4 DNA on an agarose gel positive orientation of the fragment 4 insert was detected with bands of 3831 and 3556 nt whereas negative orientation fragment insertion produced DNA bands of 2026 and 5361 nt in length. Figure 3.11 illustrates the positive orientation map of LF5-4.

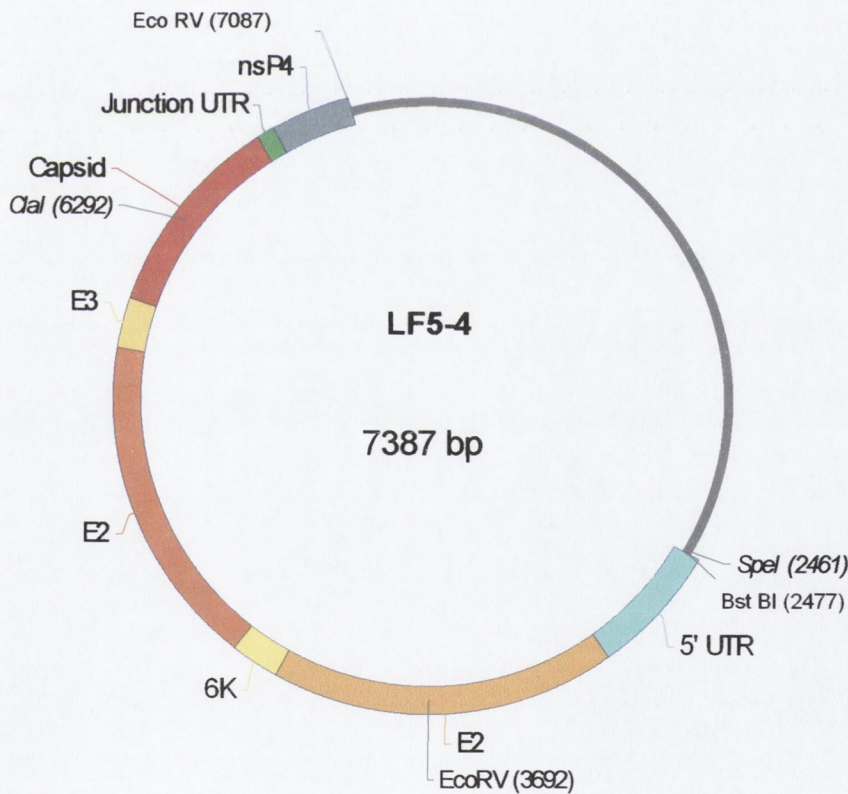


Figure 3.11 LF5 with CHIKV Fragment 4 (LF5-4)

3.2.4 Construction of pBluescript SK II [+] / CHIKV Fragment intermediates

With fragments 1, 2 and 3 in one L28i vector (LF1-2-3) and fragments 4 and 5 in another (LF5-4) with respective sizes of 9901 and 7387 nt the next step of the full-length clone construction strategy was carried out. pBluescript SK II(+) (pB, Stratagene, USA, figure 3.12) was chosen as the cloning vector for the final full-length clone because of its successful previous use as the parent backbone of an O'nyong nyong (ONNV) full-length clone and because the selection of restriction sites in its multiple cloning site allowed the introduction of the CHIKV 5' UTR (pB-5').

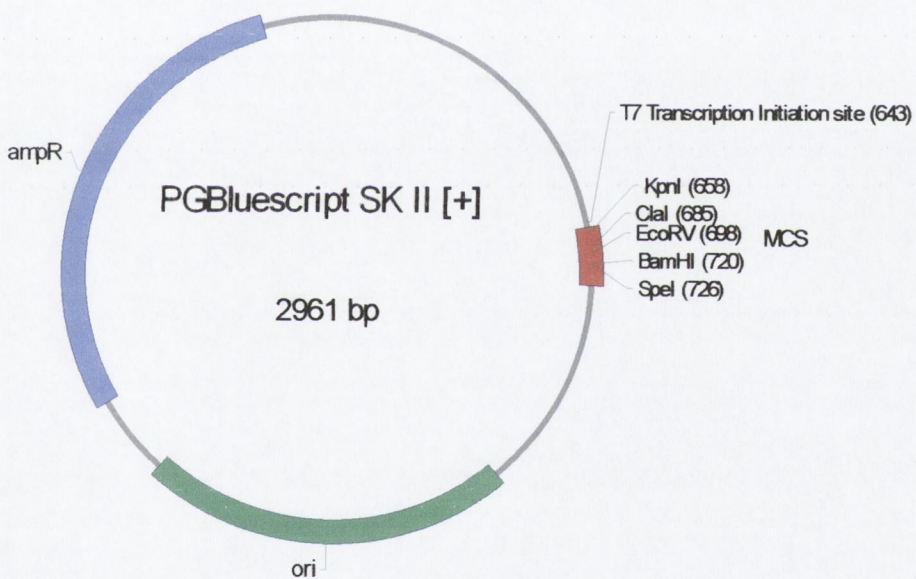


Figure 3.12 pBluescript SK II [+] vector used for final stages of CHIKV full-length clone construction.

3.2.4.1 Preparation of pBluescript SK II [+] (pB)

A 62 nt region of the pB multiple cloning site (MCS) containing unique restriction sites for *Cla I* and *Eco RV* was removed by pB digestion with *Kpn I* (658) and *Bam HI* (720), which flank either side of the *Cla I* and *Eco RV* sites. The linearised pB cloning vector was then DNA purified and was ready for the ligation of the CHIKV 5' UTR.

3.2.4.2 Production of the CHIKV 5' UTR oligonucleotide

A complementary pair of 113 nt oligonucleotides (table 3.1) were designed to incorporate a *Kpn I* site and an additional T7 promoter immediately preceding the CHIKV 5' UTR nucleotide sequence. CHIKV fragment 1 contained a *Bam HI* restriction site at its 5' end, therefore the oligonucleotide designed for insertion into pB contained this site at its 3' end. Mixed equimolar amounts of each oligonucleotide and a 2x ligation buffer were heated to 94 °C for 5 min and allowed to cool to room temperature to anneal, the reaction was run on 2% agarose gel, extracted, purified and digested with *Kpn I* and *Bam HI*. A map of the oligonucleotide is illustrated in figure 3.13 below.

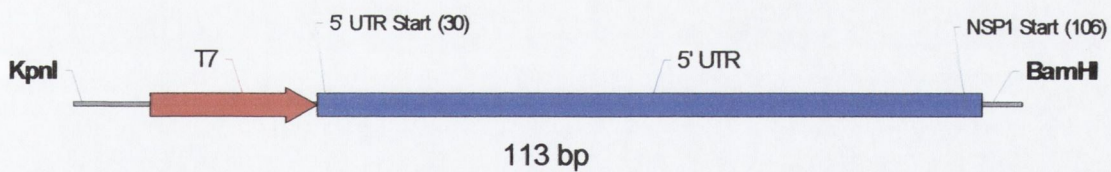


Figure 3. 13 Oligonucleotide flanked with a *Kpn I* and *Bam HI* site at the 5' and 3' ends respectively. Incorporated within these sites was a T7 promoter site and the CHIKV 5' UTR.

3.2.4.3 Ligation of CHIKV 5' UTR into pB cloning vector

The *Kpn I* / *Bam HI* – digested CHIKV 5' UTR oligonucleotide was ligated into the *Kpn I* / *Bam HI* –linearised pB cloning vector and the resulting clone termed pB-5' (figure 3.14). Confirmation analysis was carried out by restriction digestion with *Spe I* (764, present only in pB) and *Kpn I* (685) present only in the inserted oligonucleotide. For positive confirmation 2 DNA bands should be observed when run on a 0.8% agarose gel, these are 106 and 2893 nt in length respectively.

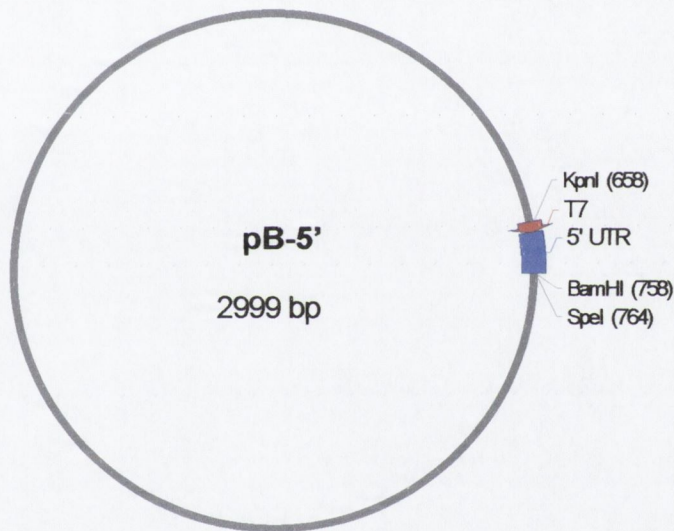


Figure 3.14 Ligation of CHIKV 5' UTR into pBluscript SK II [+] vector (pB-5')

3.2.4.4 Construction of pB-5' plus Fragment 1-2-3 intermediate (pB-5'123)

Fragment 123 was excised from LF1-2-3 using *Bam* HI (9609) and *Spe* I (2423). The resulting clone from this stage was termed pB-5'123 and can be seen in figure 3.15.

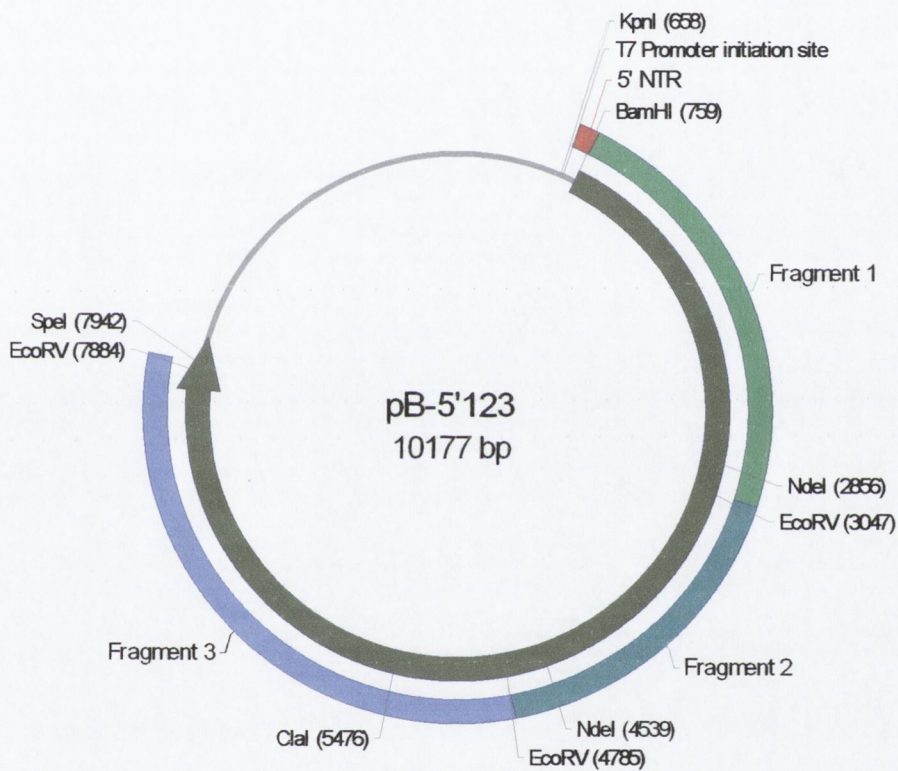


Figure 3.15 pB5' with Fragment 123 (pB5'123)

3.2.4.5 Construction of pB-5'123 plus Fragment 5-4 intermediate (pB-5'123*45)

pB-5'123 was digested with *Cla*I (4891) and *Spe*I (2423), as was LF5-4 at its respective *Cla*I (6292) and *Spe*I (4261) sites. The 2468 nt drop-out fragment from p-5'123 containing approximately three quarters of Fragment 3 was discarded (figure 3.16a), the remaining linearised clone intermediate was then termed pB-5'123*. The excised fragment from LF5-4 contained all of fragment 5 and most of fragment 4 and was termed fragment *45 (figure 3.16b). Fragment *45 was then ligated into pB-5'123* and the resulting clone termed pB-5'123*45 (figure 3.16c).

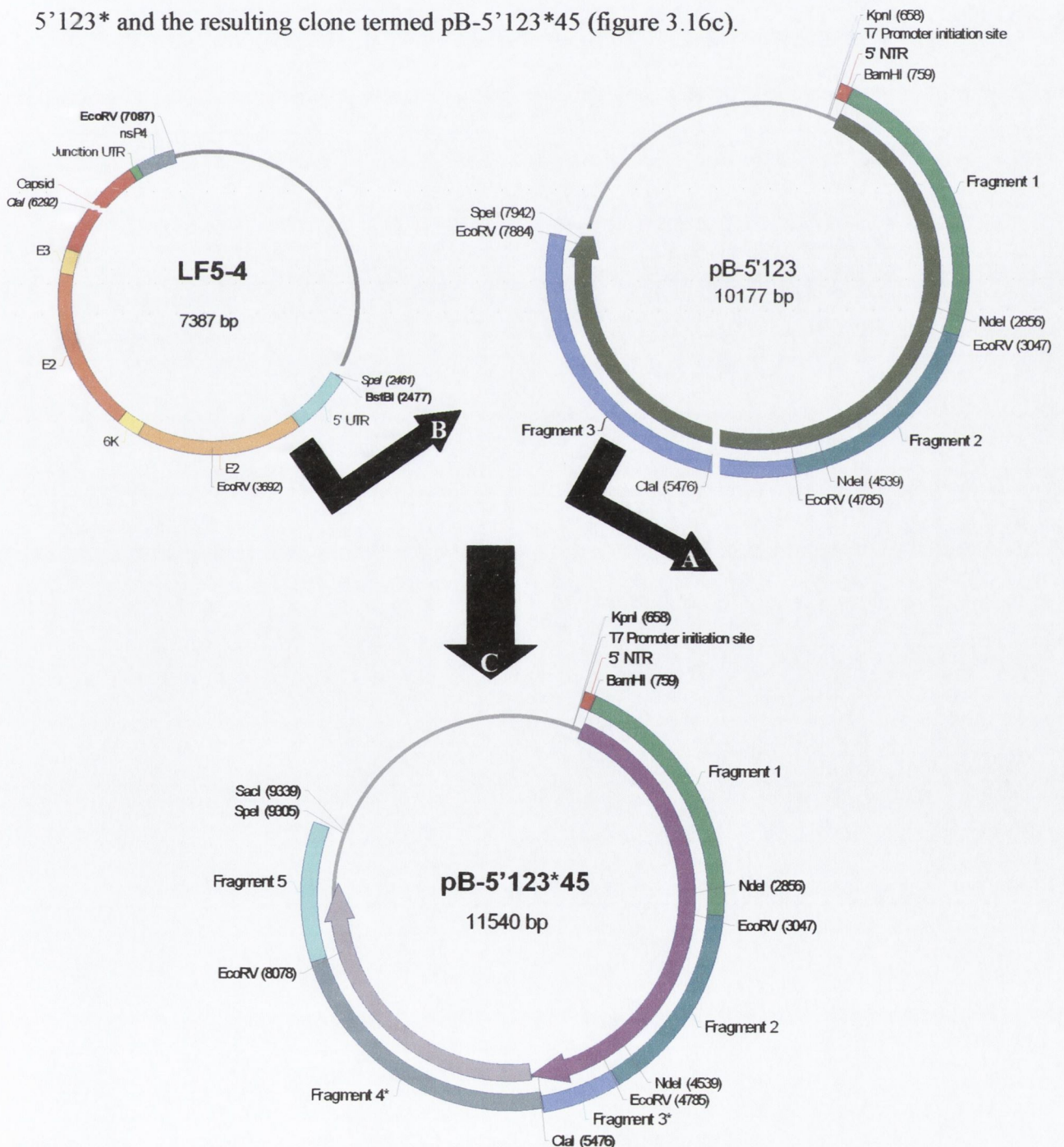


Figure 3 16 Construction of pB-5'123*45 Intermediate

3.2.4.6 Insertion of RT-PCR 3 / 4 *Cla I* Fragment

The region of the CHIKV genome lost in section 3.2.4.5, combining the latter three quarters of fragment 3 and the first 795 of fragment 4 spanned 3201 nt in length. Primers were thus designed to amplify this region (table 3.1), making sure that the forward primer lay upstream of the *Cla I* site of the CHIKV genome at position 4797 and the reverse primer downstream of the *Cla I* site at position 7998. Upon amplifying by RT-PCR a 3384 nt fragment encompassing this region, the amplicon was DNA purified and digested with *Cla I* to produce the 3201 nt fragment (figure 3.17) for insertion into pB-5'123*45 (figure 3.18a). Successful ligation produced a full-length clone containing the entire CHIKV genome, termed pB-5'12345 (figure 3.18b).

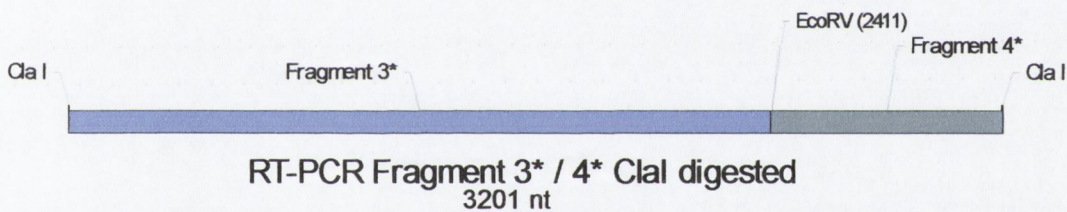


Figure 3.17 RT-PCR CHIKV fragment 3 / 4, incorporating regions of fragment 3 and 4 that were lost to allow the ligation of fragment *45 into pB-5' 123*. Fragment was digested with *Cla I* for insertion into pB-5'123*45.

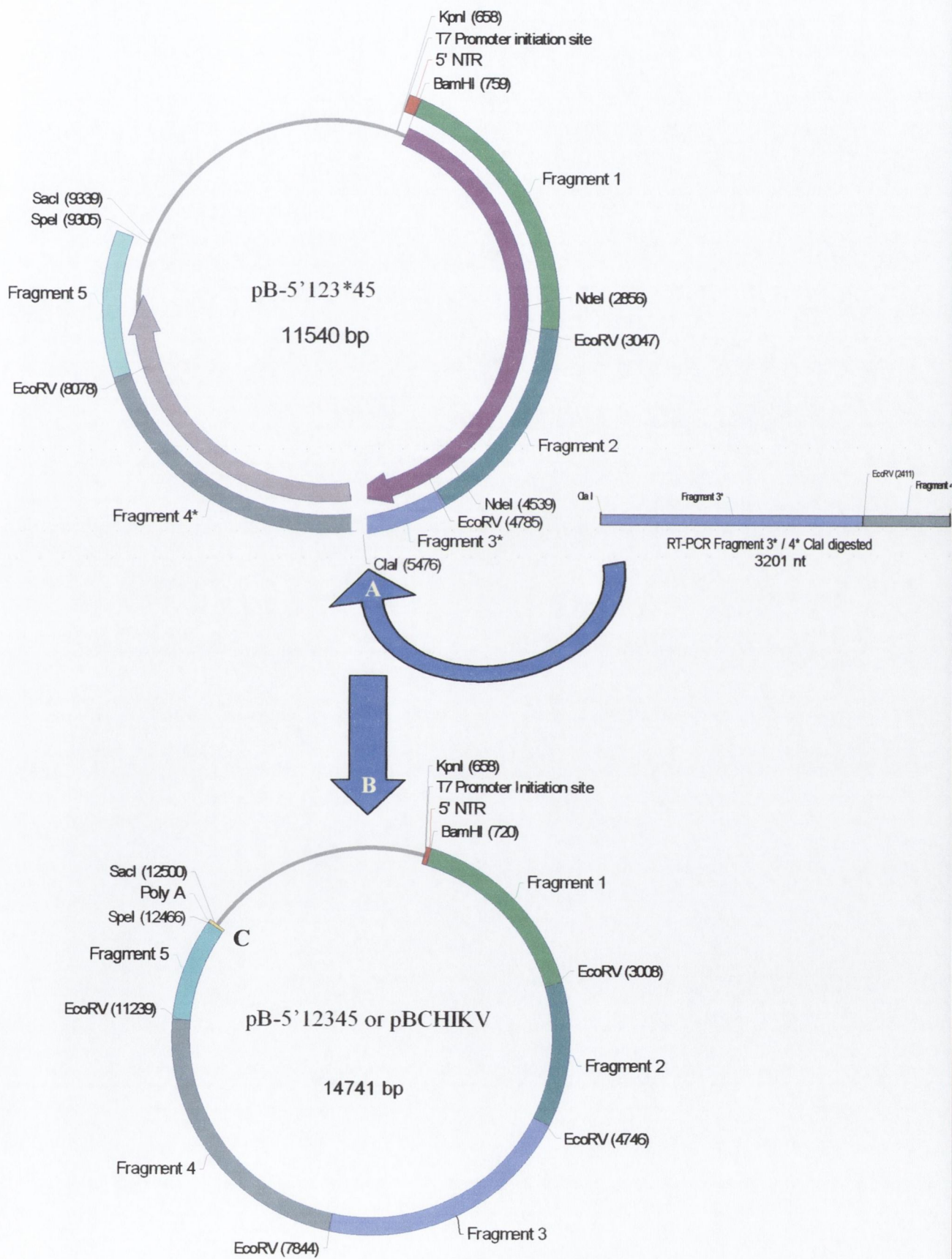


Figure 3.18 CHIKV Full-length clone pB-5'12345 (pBCHIKV)

3.2.4.7 Ligation of a Poly (A) tail

An oligonucleotide was designed to incorporate an *Spe I* restriction enzyme site at its 5' end and a *Sac I* at its 3' end. A run of 18 adenine residue lay between these two restriction sites, thus incorporating a polyA tract within the CHIKV full-length clone.

3.2.5 Production of RNA from pB-5'12345 CHIKV cDNA full-length clone (pBCHIKV)

10 µg of pBCHIKV cDNA was linearised (14741 nt) with *Sac I* at position 12500 and purified as described in section 3.2.1.2. pBCHIKV DNA concentration was assessed by mixing a 1 µl aliquot with 1 µl loading buffer and running this on a 0.8% agarose gel (wt/vol). The concentration was estimated from this gel by comparing band intensity with that of 5 and 10 µl Lambda (NEB, *Hind III* and *Eco RI*) DNA molecular weight marker.

5 µl of DNA at a concentration of 1µg / µl was added to a reaction mix containing the following: 5 µl DTT (100mM), 5 µl of rNTP capping mix (5 mM rATP, rCTP, rUTP and 0.5 mM rGTP), 5 µl Ribo m⁷G Cap Analog (5 mM), 10 µl Transcription Optimised 5x Buffer, 50 U Recombinant RNasin Ribonuclease Inhibitor, 40 U T7 RNA polymerase and nuclease free water to give a final volume of 50 µl (Promega, USA). The mixture was lightly vortexed and incubated at 37° C for 1h, at which point an additional 40 U of T7 RNA polymerase was added to the mixture and incubated for a further hour. 5 µl was removed and run on a 1% RNase-free gel to verify RNA quality.

3.2.6 Electroporation in BHK-21 cells

Three 75 cm² tissue culture flasks containing BHK-21 cells approximately 80% in confluence were used for each electroporation. The cell monolayers were washed twice with Dulbecco's phosphate buffered saline without calcium and magnesium (D-PBS; Invitrogen, UK) and incubated with 0.5% trypsin 5.3 mM EDTA (Invitrogen, UK) at 37°C until cell detachment was evident, typically within 2-3

minutes (min). The flasks were tapped to complete detachment and 10 ml supplemented BHK-21 medium was added. The resulting cell suspensions were aspirated several times to break up cell clumps and centrifuged (1500 rpm, 15 min). Pellets were resuspended in 10 ml D-PBS and centrifuged as before. Each *in vitro*-transcribed RNA reaction contained 50 µl of CHIKV, SFV4 or D-PBS (SFV4 acting as a positive control and D-PBS as the negative). Cells were resuspended in 700 µl of D-PBS and were added to 50 µl of each RNA and placed on a 0.4 µm electroporation cuvette. The cuvette was then electroporated at 0.85 kV and 25 µF capacitance using a BioRad Gene Pulser II. Following 2 pulses, cells were mixed with 20 ml of fresh BHK medium, transferred to 75 cm² tissue culture flasks and incubated for 24-36 h at 37° C in a humidified atmosphere of 5% CO₂. After this time, flasks were observed under a microscope for signs of the cell layers exhibiting cytopathogenic effect (c.p.e), at which point full-length virus was harvested and passaged a further two times in BHK-21 cells. Virus was filter-purified and titre established by plaque assay. Infectious virus RNA was isolated from infected cell monolayers as described previously in section 2.10.3.1.

3.3 Results

3.3.1 CHIKV genome in 5 Fragments

The CHIKV genome was successfully amplified over 5 Long PCR fragments as shown in figure 3. 19 below.

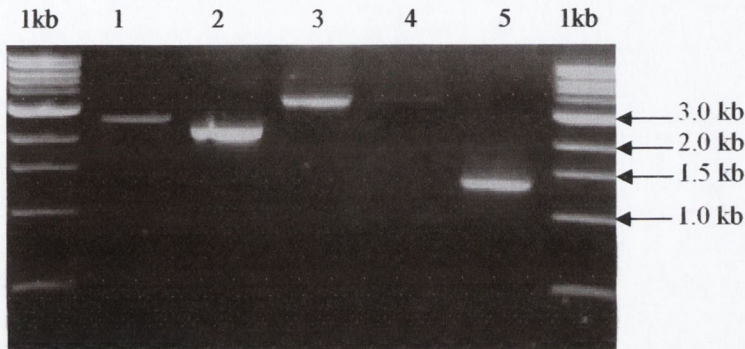


Figure 3.19 CHIKV genome amplified over 5 fragments

0.8% agarose gel stained with ethidium bromide, 1kb markers supplied by NEB. Lane 1: Fragment 1 (2482 nt). Lane 2: Fragment 2 (2189 nt). Lane 3: Fragment 3 (3529 nt). Lane 4: Fragment 4 (3540 nt). Lane 5: Fragment 5 (1322 nt).

3.3.2 CHIKV Fragments ligated into L28i

3.3.2.1 LF1

Confirmation analysis of four CHIKV Fragment 1s ligated into L28i (LF1) colonies by restriction digestion with *Nde I* and *Sac I*. Positive ligation was detected in 3 out of four colonies where 2 bands of 2949 and 2149 nt were observed, figure 3.20.

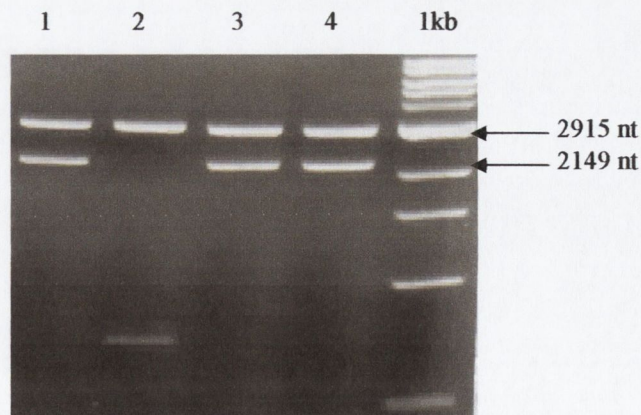


Figure 3.20 Four random LF1 colonies digested with *Nde I* and *Sac I*

0.8% agarose gel stained with ethidium bromide, 1kb markers supplied by NEB. Lanes 1-4: LF1 digested with *Nde I* and *Sac I*, positive colonies have 2 bands of 2915 and 2149 nt in length. Lanes 1, 3, 4 are positive, Lane 2 is negative.

3.3.2.2 LF2

Confirmation analysis of five CHIKV Fragment 2s ligated into L28i (LF2) colonies by restriction digestion with *Stu I*. Positive ligation was detected in 4 out of 5 colonies where 2 bands of 3714 and 847 nt were observed, figure 3.21.

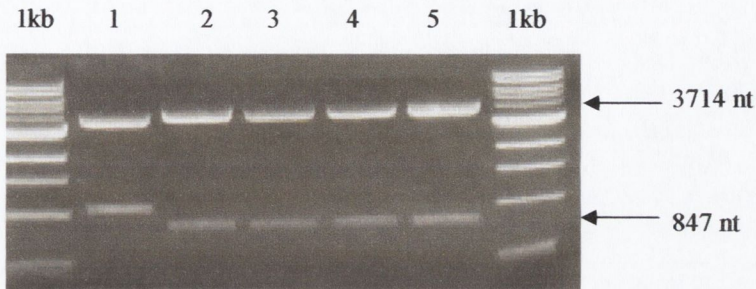


Figure 3.21 Five random LF2 colonies digested with *Stu I*

0.8% agarose gel stained with ethidium bromide, 1kb markers supplied by NEB. Lanes 1-5: LF2 digested with *Stu I*, positive colonies have 2 bands of 3714 and 847 nt in length. Lane 1 is negative Lanes 2 - 4 are positive.

3.3.2.3 LF3

Confirmation analysis of two CHIKV Fragment 3s ligated into L28i (LF3) colonies by restriction digestion with *Eco RV*. Positive ligation was detected in both colonies where 2 bands of 3099 and 2823 nt were observed, figure 3.22.

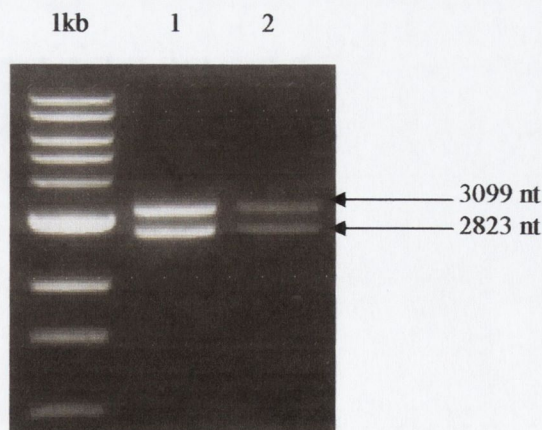


Figure 3.22 Two random LF3 colonies digested with *Eco RV*

0.8% agarose gel stained with ethidium bromide, 1kb markers supplied by NEB. Lanes 1-2: LF3 digested with *Eco RV*, positive colonies have 2 bands of 3099 and 2823 nt in length. Both lanes are positive.

3.3.2.4 LF4

Confirmation analysis of six CHIKV Fragment 4s ligated into L28i (LF4) colonies by restriction digestion with *Eco RV*. Positive ligation was detected in both colonies where 2 bands of 3395 and 2823 nt were observed, figure 3.23.

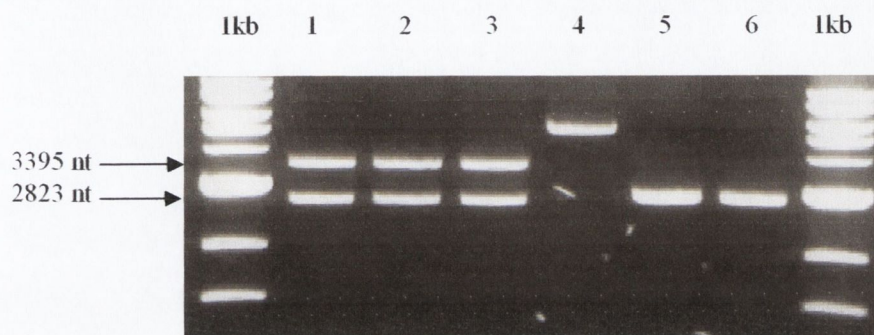


Figure 3.23 Six random LF4 colonies digested with *Eco RV*

0.8% agarose gel stained with ethidium bromide, 1kb markers supplied by NEB. Lanes 1-6: LF4 digested with *Eco RV*, positive colonies have 2 bands of 3099 and 2823 nt in length. Lanes 1-3 are positive.

3.3.2.5 LF5

Confirmation analysis of five CHIKV Fragment 5s ligated into L28i (LF5) colonies by restriction digestion 2682 and 1310 nt were observed, figure 3.24.

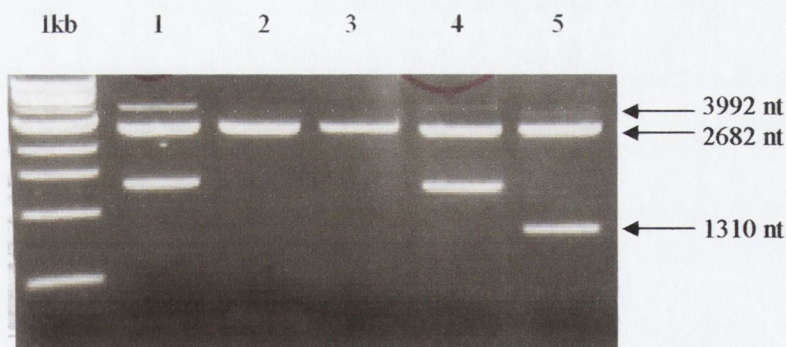


Figure 3.24 Five random LF5 colonies digested with *Spe I* and *Stu I*

0.8% agarose gel stained with ethidium bromide, 1kb markers supplied by NEB. Lanes 1-5: LF5 digested with *Spe I* and *Stu I*, positive colonies have 2 bands of 2682 and 1310 nt in length. Lane 5 is positive. Some faint undigested LF5 may also be seen in lane 5.

3.3.2.6 LF1-2 Intermediate

Confirmation analysis of seven LF1-2 intermediate colonies by restriction digestion with *Nde I*. Positive ligation was detected in both colonies where 2 bands of 5119 and 1683 nt were observed (figure 3.25). The 5119 nt LF1-2 Δ *Nde I* fragment was subsequently excised from the gel, purified and religated, the 1683 nt fragment was excised, purified and stored at -20° C until it was religated into LF1-2-3 Δ *Nde I*.

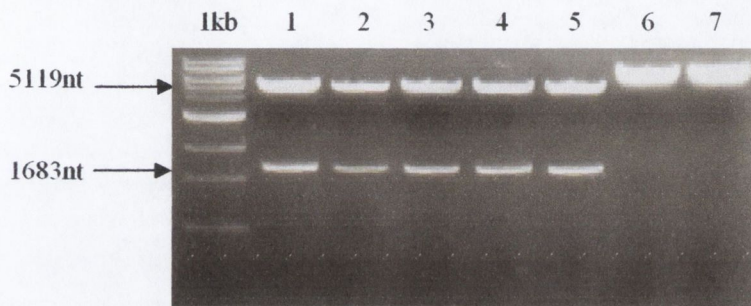


Figure 3.25 Seven random LF1-2 colonies digested with *Nde I*

0.8% agarose gel stained with ethidium bromide, 1kb markers supplied by NEB. Lanes 1-7: LF1-2 digested with *Nde I*, positive colonies have 2 bands of 5119 and 1683 nt in length. Lanes 1-5 are positive.

3.3.2.7 Religation of *Nde I* fragment into LF1-2-3 Δ *Nde I* Intermediate

One LF1-2-3 Δ *Nde I* Intermediate colony was linearised with *Nde I* and dephosphorylated. The excised *Nde I* fragment from section 3.2.2.6 was prepared for religation into LF1-2-3 Δ *Nde I*. (figure 3.26)

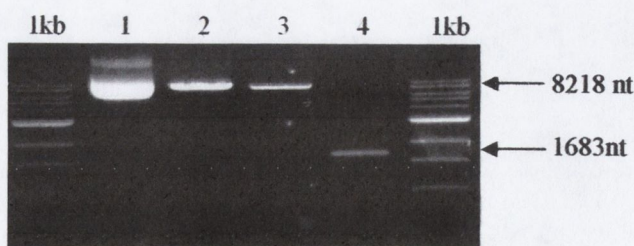


Figure 3.26 LF1-2-3 Δ *Nde I* and *Nde I* fragment from LF1-2.

0.8% agarose gel stained with ethidium bromide, 1kb markers supplied by NEB. Lane 1: undigested LF1-2-3 Δ *Nde I*. Lane 2: *Nde I* digested LF1-2-3 Δ *Nde I*. Lane 3: *Nde I* digested and dephosphorylated LF1-2-3 Δ *Nde I*. Lane 4: 1683 nt *Nde I* fragment excised from LF1-2

3.3.2.8 LF1-2-3

Confirmation analysis of one LF1-2-3 colony by restriction digestion with *Xmn I*. Positive ligation was detected in both colonies where 2 bands of 8821 and 1718 nt were observed, figure 3.27.

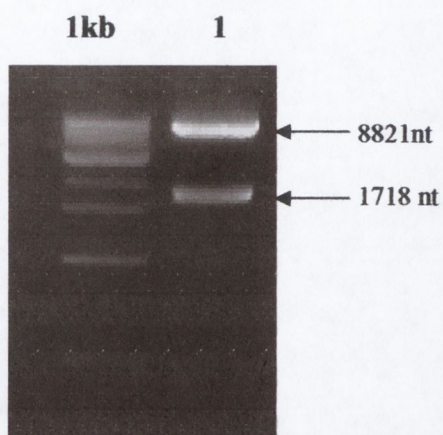


Figure 3.27 LF1-2-3 colony digested with *Xmn I*

0.8% agarose gel stained with ethidium bromide, 1kb markers supplied by NEB. Lanes 1: LF1-2-3 digested with *Xmn I*, positive colonies have 2 bands of 8821 and 1718 nt in length. Lane 1 is positive.

3.3.2.9 LF5-4

Confirmation analysis of three LF5-4 colonies was determined by restriction digestion with *Cla I* and *Eco RV*. Positive ligation was detected in colonies if a 7387 nt band was observed with *Cla I* digests and 2 bands of 3395 and 3992 nt were observed for LF5-4 DNA digested with *Eco RV*, these are illustrated in figure 3.28 below.

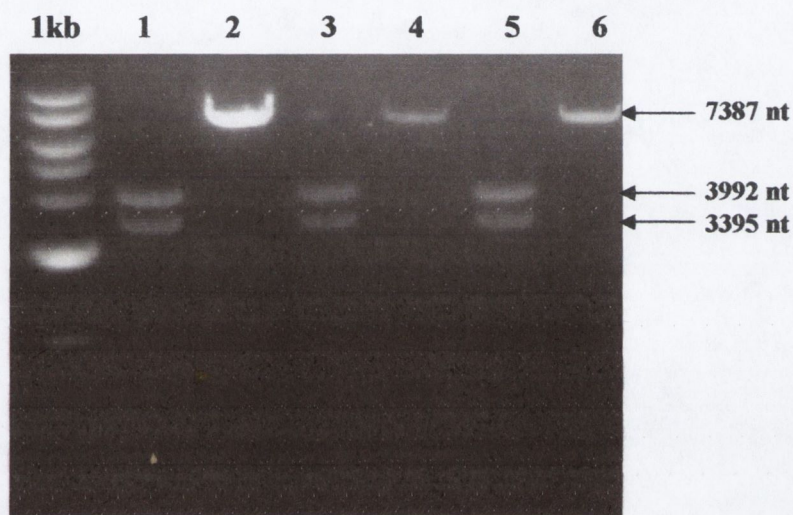


Figure 3.28 Three LF5-4 colonies digested with *Cla I* and *Eco RV*

0.8% agarose gel stained with ethidium bromide, 1kb markers supplied by NEB. Lanes 1, 3, 5: LF5-4 colonies 1-3 respectively digested with *Eco RV*, positive colonies have 2 bands of 3392 and 3395 nt in length. Lanes 2, 4, 6: LF5-4 colonies 1-3 respectively digested with *Cla I*, positive colonies have 1 band, 7387 nt in length.

3.3.2.10B-5'123

On the insertion of Fragment 123 into pB-5' an intermediate (pB-5'123) was generated, seven random colonies were selected and DNA extracted. Confirmation analysis was carried out using *Eco RV*. Successful ligation produced 3 bands upon digestion with *Eco RV* of 5282, 3157 and 1738 nt in length respectively (figure 3.29).

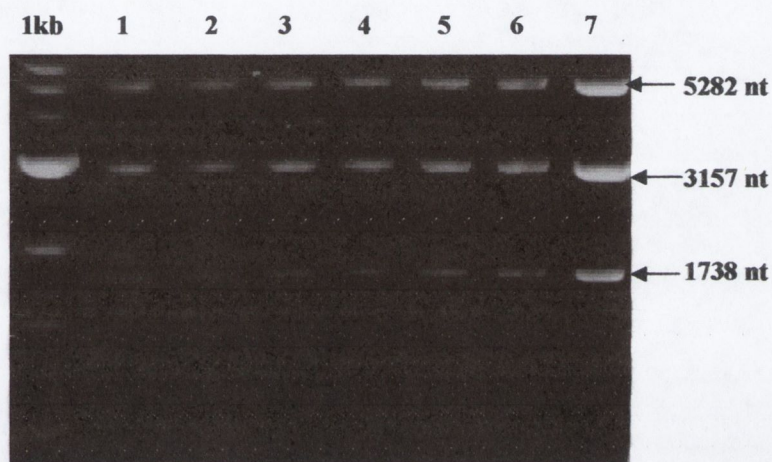


Figure 3.29 Seven pB-5'123 colonies digested with *Eco RV*

0.8% agarose gel stained with ethidium bromide, 1kb markers supplied by NEB. Lanes 1-7: pB-5'123 colonies 1-7 digested with *Eco RV*, positive colonies have 3 bands of 5282, 3157 and 1738 nt in length.

3.3.2.11 pB-5'123*45

The successful ligation of Fragment *45 into the pB-5'123* intermediate, another intermediate (pB-5'123*45) was generated, five random colonies were selected and DNA extracted. Confirmation analysis was carried out using *Eco RV*. Successful ligation produced 3 bands upon digestion with *Eco RV* of 6509, 3239 and 1738 nt in length respectively (figure 3.30).

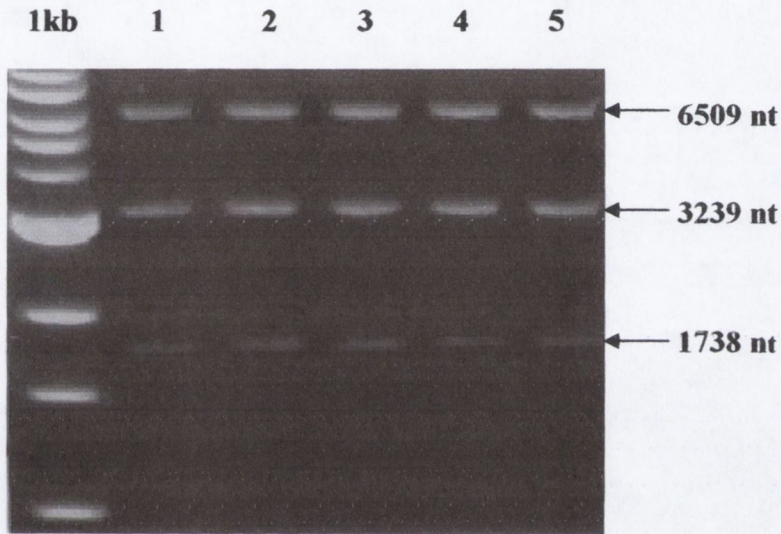


Figure 3.30 Five pB-5'123*45 colonies digested with *Eco RV*

0.8% agarose gel stained with ethidium bromide, 1kb markers supplied by NEB. Lanes 1-5: pB-5'123*45 colonies 1-5 digested with *Eco RV*, positive colonies have 3 bands of 6509, 3239 and 1738 nt in length.

3.3.2.12 RT- Fragment 3 / 4 (prior to *Cla I* digestion)

Fragment 3 / 4 was generated by RT-PCR, the primers designed (table 3.1) successfully amplified a 3384 nt amplicon, the pooled cDNA was run on a 0.8 % agarose gel stained with ethidium bromide. Although two smaller bands approximately 1.5-1.7 kb were visible the correct sized fragment was gel extracted, purified and digested with *Cla I* for ligation into pB-5'123*45. The 3384 nt PCR product can be seen in figure 3.31 below.

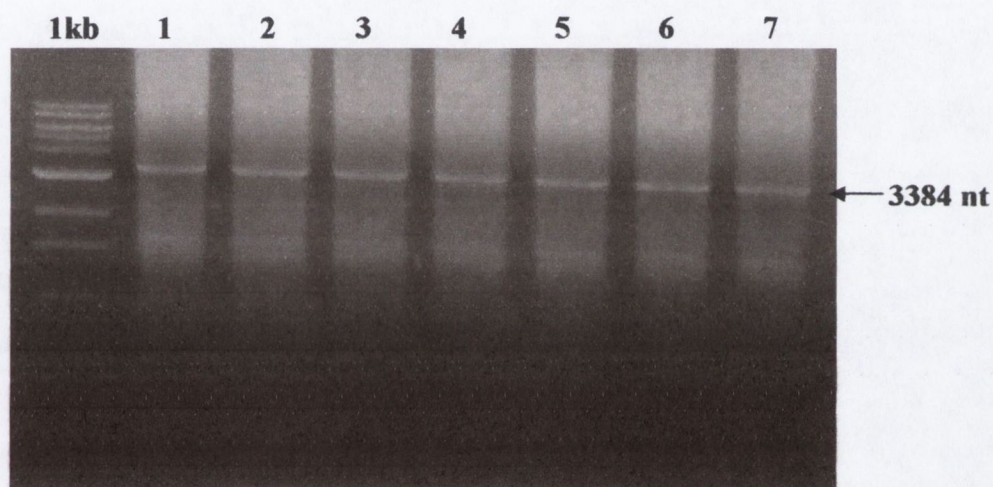


Figure 3.31 Pooled Fragment 3 / 4 PCR amplicons

0.8% agarose gel stained with ethidium bromide, 1kb markers supplied by NEB.

Lanes 1-7: pooled fragment 3 / 4 PCR fragment spanning 3384 nt in length.

3.3.2.13 pB-5'12345

On successfully ligating CHIKV fragment 3 / 4 into pB-5'123*45 in addition to a poly A tail the full-length CHIKV cDNA clone was complete. When digested with *Eco RV* to test orientation of inserts and as a confirmation analysis of ligation, 4 expected bands were seen with sizes ranging from 6510, 3395, 3098 to 790 nt as pictured in figure 3.32a. Full-length cDNA was linearised using the unique *Sac I* enzyme and reverse transcribed into RNA before being electroporated into BHK-21 cells. SFV4 RNA from the pSP6-SFV4 full-length cDNA clone was reverse transcribed as a positive control, both RNA species can be seen in figure 3.32b.

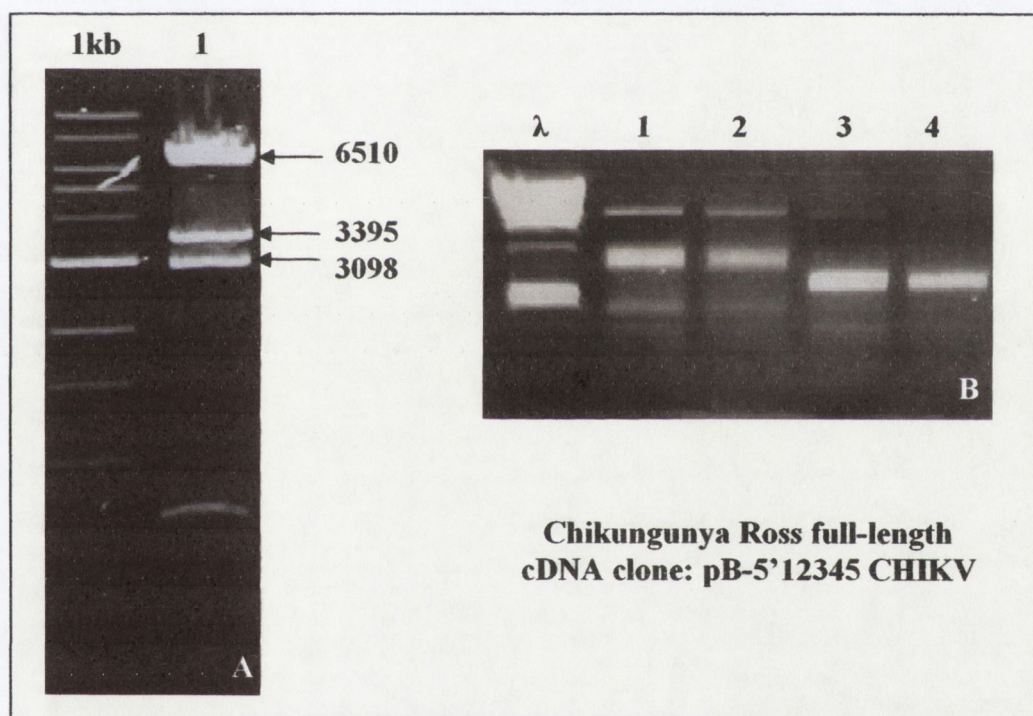


Figure 3.32 pB-5'12345 CHIKV cDNA (*Eco RV*-digested, A) and RNA (B) 0.8% agarose gel stained with ethidium bromide, 1kb and λ Marker supplied by NEB. (A) Lanes 1: pB-5'12345 CHIKV cDNA digested with *Eco RV*, positive confirmation analysis successfully shows 4 bands, ranging from 6510, 3395, 3098 to 1736 nt in size. (B) Lane 1: 5 μ l SFV4 RNA, Lane 2: 10 μ l SFV4 RNA, Lane 3: 5 μ l pB-5'12345 CHIKV RNA, Lane 4: 10 μ l pB-5'12345 CHIKV RNA.

3.4 Discussion

Chikungunya virus (CHIKV) has been responsible for several large epidemics in Africa and Southeast Asia since it was first isolated by Ross (1956) following the Newala epidemic in Tanzania during 1952-1953. A vaccine was developed by Levitt *et al* in 1986 at the U.S. Army Medical Research Institute of Infectious Diseases (USAMRIID). However, the live attenuated CHIKV vaccine was shrouded in controversy as the cell type in which it was developed was changed from the master seed to the production seed, and the vaccine partially reverted, as some of the mutations responsible for attenuation reverted back to the original sequence, thus causing disease rather than preventing it in those vaccinated.

With this in mind, the original Ross strain of CHIKV was sequenced and characterised as part of the research included in this thesis. A full length cDNA clone was constructed using a *de novo* strategy. Several other alphavirus full length clones have been constructed by substituting the virus genome of an existing full-length clone with that of another virus strain. In the case of SP6-CA7 constructed by Tarbatt *et al* (1997), the virus genome of the pSP6-SFV4 full length clone constructed by Liljeström *et al* (1991) was replaced with that of the avirulent SFV-A7. However, in the case of SP6-CA7, the 5' NTR was not substituted with that SFV-A7, and infectious virus produced from what should have been an avirulent, retained a certain degree of virulence. In addition to this, constructing a full length clone *de novo* allows more choice in deciding which promoter to use and what restriction enzymes to include in the multiple cloning site for subsequent manipulations.

The strategy adopted incorporated the use of two commercially available cloning vectors. Initially the genome was amplified over five large fragments using high fidelity proof-reading enzymes to minimise the error rate of mutations during amplification. More recent strategies involve amplifying an entire genome in one fragment using long range PCR, and although preferable this technique was not yet available at the time of this research. By incorporating each of these five fragments in its own cloning vector (L28i) large quantities of CHIKV DNA were generated with a minimal amount of RNA manipulation, reducing the number of spontaneous errors generated within the genome. These fragments were successfully ligated and orientation of insertions confirmed by restriction digestion. They were subsequently excised from one vector and ligated to the next using a series of intermediates until the first 7121 nt of the first open reading frame (ORF) of the CHIKV genome were

incorporated in one vector (LF1-2-3). The remaining 4610 nt of the genome (including the second ORF) was produced in another L28i vector (LF5-4). An existing infectious clone of another alphavirus that shares a high sequence identity with CHIKV termed O'nyong nyong virus (ONNV) was constructed using the pBluescript SK II [+] cloning vector (pB) that utilises the well characterised T7 promoter. The subsequent steps of the strategy in constructing a CHIKV infectious clone were to combine the CHIKV genome from LF123 and LF54 by inserting them into the pB vector. A full length SFV-A7 cDNA clone constructed in our lab by Tarbatt *et al* (1997) was produced by substituting the virulent SFV genome within the pSP6-SFV4 full length cDNA clone constructed by Liljeström *et al* (1991) with that of the avirulent SFV-A7 genome. This was completed relatively effectively; however the 5' NTR of the virulent pSFV-SFV4 clone was not substituted with that of SFV-A7. This resulted in the infectious virus produced from the construct SFV-A7 clone termed CA7, killing approximately 30% of intranasally infected mice while SFV-A7 produced no mortality in infected mice. It was therefore paramount when constructing the full length cDNA CHIKV clone that a strategy was in place to incorporate the CHIKV 5' NTR effectively. The pB cloning vector was specifically chosen with this in mind.

By removing 62 nt of the pB multiple cloning site two restriction enzyme sites present in the CHIKV genome, a restriction site absent in CHIKV (*Kpn I*) and another site present at the 5' terminus of nsP1 of the CHIKV genome (*Bam HI*) were able to be manipulated in order to initially incorporate the CHIKV 5' NTR and subsequently the remainder of the CHIKV genome from LF1-2-3 and LF5-4. The 5' NTR oligonucleotide pair were designed to incorporate both restriction sites mentioned above. By hybridising the oligonucleotide pair a 113 nt fragment was generated. This fragment included a *Kpn I* site upstream of a T7 promoter recognition sequence directly adjacent to the 5' NTR, the 5' NTR and the first 8 nucleotides of the CHIKV nsP1 that the *Bam HI* restriction site occupied. Therefore by digesting the fused oligonucleotide with both these enzymes it was successfully ligated into pB.

Downstream from the *Bam HI* site in pB was an *Spe I* site. The *Spe I* site was also present in L28i, 62 nt downstream from the 3' terminus of the 7121 nt CHIKV fragment in LF1-2-3. The subsequent step was to remove the 7121 nt CHIKV fragment from LF1-2-3 using the *Bam HI* and *Spe I* sites in LF1-2-3 and ligating this in frame with the *Bam HI* site incorporated into the 5' NTR oligonucleotide. This was

successfully completed and the intermediate vector was termed pB-5'123. In order to insert the remaining 4610 nt of the CHIKV genome into pB-5'123 a large deletion was carried out on both pB-5'123 and LF5-4. By excising and discarding the last 2468 of the CHIKV genome incorporated in pB-5'123 using *Cla I* and *Spe I* the last 3831 nt of the CHIKV genome incorporated in LF5-4 could be excised using both enzymes and ligated into *Cla I* – *Spe I* digested pB-5'123. This was completed successfully and generated an intermediate termed pB-5'123*45, where the asterisk represents the region of CHIKV that was removed.

In order to replace this fragment, primers were designed either side of two *Cla I* sites, naturally occurring in CHIKV and encompassing the removed fragment sequence. RT-PCR was again performed using a high fidelity proof-reading enzyme mix and the fragment successfully amplified and DNA-purified. This was then digested with *Cla I*, as was pB-5'123*45 and subsequently successfully ligated into pB-5'123*45 to generate pB-5'12345. This clone included the entire CHIKV genome directly downstream of a T7 promoter, however as the stability of virus mRNA is thought to depend on the presence of a PolyA tail, an oligonucleotide pair incorporating a *Spe I* site at its 5' terminal and a *Sac I* site at its 3' terminal, a run of 18 adenine residues lay between these restriction sites. *Sac I* was chosen as it is a unique site within the entire pB-5'12345 sequence and it occurs only 34 nt downstream of the terminal *Spe I* site at the end of the CHIKV genome.

To produce RNA from the CHIKV full-length cDNA clone it was linearised using the unique *Sac I* site and reverse-transcribed using a T7 polymerase kit that included a Ribo m⁷G Cap analog for capping of the 5' terminus. This was successfully completed and RNA was electroporated into BHK-21 cells in order to produce infectious CHIKV virus. However, despite adequate quantities of CHIKV RNA being produced no infectious virus was produced in electroporated BHK-21 cells, and they showed no signs of c.p.e.

There are two main possible reasons for this. Firstly, as the CHIKV genome was amplified in 6 fragments by RT-PCR, despite the quality of high fidelity proof-reading polymerases used there is always a likelihood of some spontaneous mutations in the amplified genome during PCR. Although the cloning strategy used involved minimal PCR, it is possible that a mutation arose that threw the CHIKV RNA genome sequence out of frame, thus preventing the production of proteins needed for virus propagation. A second possibility stems from a step during the construction of

pB5'123, when in order to ligate the 7121 nt CHIKV fragment into pB-5', an *Spe I* restriction site 62 nt downstream of the CHIKV genome was utilised. It would follow that in the final full-length cDNA clone these 62 nt belonging to the L28i cloning vector would immediately follow the CHIKV 3' NTR and precede the poly(A) tail. Frolov *et al.*, (2001) suggested that the 3' and 5' ends of the Sindbis genome RNAs must interact to initiate replication. Therefore if the same is true for CHIKV, then possibly the addition of 62 nt after the 3' NTR could result in a secondary structure change inhibiting possible interaction with the 5' NTR and preventing RNA replication. In order to deduce what lies behind the lack of production of infectious virus from the CHIKV full-length pB-5'12345 cDNA clone, it should be sequenced and aligned with the CHIKV Ross sequence to check for spontaneous mutations in the genome and to ascertain whether removing the 62 nt from the end of the 3' NTR is feasible.

The full length cDNA CHIKV clone can be used either incorporated within the SFV expression system or developed into its own expression system. For the design of a CHIKV virus-vector vaccine it will need to be fully sequenced and tested both *in vitro* and *in vivo*. On successfully completing this, several possible directions could be followed regarding the production of an efficient and safe CHIKV vaccine. A safe live attenuated virus could be produced from a CHIKV infectious clone. The construction of the full-length CHIKV cDNA clone also allows CHIKV antigens such as the envelope glycoproteins to be easily isolated and inserted into the existing pSP6-SFV4 for expression.

Alternatively, the full-length CHIKV clone could be developed as an expression system enabling the expression of foreign antigens, or reporter genes as has been developed in SFV by Liljeström and Garoff (1994).

Chapter Four

Analysis of the Semliki Forest Virus 5' Untranslated region as a pathogenicity determinant

4.1 Introduction

4.1.1 SFV-induced neuropathogenesis of the murine CNS

SFV elicits different degrees of neurovirulence in mice depending on virus strain, route of administration and the age of the host used. SFV-A7 and SFV-L10 are the prototype avirulent and virulent members of the SFV subgroup. SFV-L10 causes lethal encephalitis 4-5 days post infection (d.p.i) regardless of route of administration and age of mice. It has been shown (Atkins *et al.*, 1985) that virulent strains of SFV such as SFV-L10 induce more extensive damage to neurons in the CNS than avirulent strains such as SFV-A7. The fundamental difference between SFV-L10 and SFV-A7 is the rapidity of the spread of neuronal infection (Balluz *et al.*, 1993). In the case of SFV-L10 this results in a lethal threshold of neuronal damage before the immune system can intervene, whereas SFV-A7 appears to have a partially restricted ability to multiply in neurons, thus allowing the immune system time to intervene and the animal recover (Gates *et al.*, 1985; Fazakerley *et al.*, 1993). Although SFV-A7 is avirulent in adult mice and is asymptomatic, adult survivors show demyelination in the CNS and the virus replicates at least as efficiently as the virulent L10 in cultured cells such as BHK-21 cells (Atkins *et al.*, 1983, 1999)

4.1.2 Virus produced from SFV infectious clones

To date three SFV infectious clones have been constructed. Initially, Liljeström *et al* (1991) constructed a cDNA clone derived from SFV-L10 termed pSP6-SFV4, transcription from which produced infectious virus termed SFV4. Although SFV4 has a slight reduction in virulence when compared to SFV-L10, it kills all mice infected intranasally (i.n.) by 5 d.p.i. although only 60-70% of those infected intraperitoneally (i.pi) die. In 1997, Tarbatt *et al* constructed a cDNA infectious clone of SFV-A7 termed SP6-CA7 by substitution of regions of pSP6-SFV4 with the corresponding regions of SFV-A7. Infectious virus produced from SP6-CA7 termed CA7, was still however partially virulent, killing 20-30% of mice when administered i.n. SP6-CA7 clearly retains a degree of virulence, and is evidently not avirulent as suggested by Tarbatt *et al* (1997). Lastly, in 2000, Tuittila *et al* constructed another SFV cDNA clone using the SFV-A7[74] avirulent virus and substituting the SFV4 genome of pSP6-SFV4 with that of SFV-A7[74] termed rA7[74]. Infectious virus produced from this infectious clone is termed prA7[74] and

showed similar levels of avirulence as SFV-A7[74], although prA7[74] has been shown to kill 10% of mice infected intranasally (Minna Tuittila, personal communication).

4.1.3 Analysis of SFV genomes

In 1997 Tarbatt *et al* carried out a sequence comparison over the entire genome of SFV-A7 and SFV4, finding 227 nt changes in the translated regions of SFV-A7, 48 of which resulted in amino acid changes. The 5' UTR was shown to have two nucleotide changes at positions 35 and 42 although the CA7 infectious virus did not have these changes as it was produced from SP6-CA7 which contained the 5' UTR of SFV4. Tuittila *et al* (2000) carried out sequence comparison over the non-structural protein region between SFV4, rA7[74] and CA7. Comparing these sequences over their entire genomes could prove useful in detecting possible virulence determinants.

4.1.4 Virulence determinants of SFV

Infectious clones have been used successfully to investigate possible virulence determinants within the alphaviruses. Much of the work carried out on SFV and SINV to date has involved two envelope glycoproteins E2 and E1 (Glasgow *et al.*, 1991, 1994; Santagati *et al.*, 1994; Polo and Johnston., 1990). In SFV there are 8 amino acid differences in the E2 glycoprotein between the avirulent SFV-A7 strain and the virulent SFV4 strain. Tarbatt *et al* (1997) substituted a 2104 nt fragment flanked by two *Nde I* restriction enzyme sites in SFV4 with that of SFV-A7. This resulted in a substitution of 5 amino acids in E2 and 6 in E1. Virus produced from this chimaeric genome, termed C8930/11033 was administered intraperitoneally into adult mice, only 20% of mice died, compared to 60% of those infected with parental SFV4. All mice infected with SFV-A7 survived. This suggests that E2 and E1 also play an important role in the neurovirulence of SFV.

The presence of the SFV4 5' UTR in the SP6-CA7 infectious clone could explain the 30-40% death rate among intranasally infected mice. The 5' UTR is thought to be an integral part of virus RNA replication. Previous studies have suggested that the 5' UTR may be important as a virulence determinant. Evans *et al* (1985) showed that a single nucleotide change in the 5' UTR of the Sabin type 3 poliovaccine genome significantly increased neurovirulence in adult mice. Other

investigations involving VEE have also shown that attenuation is partially determined by mutations in the 5' UTR. This appears to be controlled by more than one gene, as only those nt substitutions in the E2 gene combined with those of the 5' UTR resulted in attenuation. There is also evidence to suggest that the 5' UTR is involved in virus replication (Frolov *et al.*, 2001). Thus the rate of synthesis of RNA of each virus might be correlated with rate of survival of host. To further elucidate the possible importance of the 5' UTR as a possible virulence determinant the degree of neuropathology in the brains of mice intranasally infected with different 5' UTR chimaeras was also measured, this is addressed in more detail in Chapter 5 "Pathology".

4.1.5 Construction of SFV 5' UTR chimaeras

In order to investigate whether the 5' UTR plays a role in determining the degree of virulence in infected adult mice, possibly by its involvement in RNA replication, SFV-5'UTR chimaeras were constructed. Measuring the rate of RNA synthesis combined with monitoring the rate of survival and neuropathology caused among mice infected with infectious virus produced from these cDNA clones could provide an insight into the 5' UTR as an SFV virulence determinant. This involved analysing the sequences of the 5' UTRs and designing reciprocal chimaeras that incorporated the 5' UTR nucleotide differences between virulent and avirulent strains of SFV. Studying the survival rates of and the neuropathology caused in infected adult mice intranasally infected with each chimaera and the infectious virus from the three SFV infectious clones was carried out.

4.2 Materials and Methods

4.2.1 Sequence analysis of SFV genomes

cDNA was produced from virus RNA isolated from BHK-21 cells infected with SFV-L10 using an oligo dT₁₈ reverse primer (Promega, USA). 100 µl of SFV-L10 cDNA along with 10 µg of pSP6-CA7 were sent to LARK Technologies, UK for sequencing. LARK Sequenced both genomes using a technique called optimised multiplex PCR (Tettelin *et al*, 1999) whereby multiple PCR primers are used in a single sequencing reaction. Both sequences are submitted to GenBank AY112987 (SFV-L10) and Z48163 (CA7). The entire SFV genome sequences of SFV4, L10, CA7 and prA7[74] were analysed using the multiple alignment web-based software Multalin (F. Corpet, INRA Toulouse, France). Nucleotide differences of the coding regions of the genome resulting in amino acid changes were noted with the position of the amino acid change. The untranslated regions for these four SFV strains were also aligned and investigated as possible virulence determinants.

4.2.2 SFV 5' UTR Sequences

Unlike the rA7[74] infectious clone, pSP6-CA7 contains the 5' UTR of ppSP6-SFV4 as this was not removed at the time of construction. Therefore, the 5' UTR of SFV-A7 was sequenced using a 5' RACE PCR Kit (Roche, Switzerland) in accordance with manufacturer's guidelines. The 5' UTRs of SFV-L10, SFV4, CA7, prA7[74], SFV-A7[74] were also sequenced and aligned using Multalin (F. Corpet, INRA Toulouse, France).

4.2.3 Virus strains and infectious clones

The A7 and L10 strains of SFV was obtained from Dr. C. Bradish, Microbiology Research Establishment (MRE), Porton Down, Wiltshire, UK. The pSP6-SFV4 was a gift from Professor P. Liljestrom, Karolinska Institute, Stockholm, Sweden. The A7[74] infectious clone (rA7[74]) was obtained from Dr. Minna Tuittila, Åbo Akademi, Turku, Finland. The SP6-CA7 was constructed in our laboratory by Catherine Tarbatt. SFV-L10 and A7[74] were obtained from Professor Harry Smith, Dept. of Microbiology, University of Birmingham, UK.

4.2.4 Preparation of virus DNA

BHK cells were infected with SFV-A7, SFV-A7[74] and SFV-L10 and RNA isolated as previously described for CHIK (section 2.10.3.1). In order to produce infectious virus from which to isolate RNA, pSP6-SFV4, rA7[74] and SP6-CA7 first needed to be linearised, reverse transcribed and electroporated into BHK cells.

4.2.4.1 *Spe I* linearisation of SFV infectious clones

For the production of SFV viral RNA, each infectious clone was linearised with the *Spe I* restriction enzyme. This is a unique restriction site in the pSP6-SFV4 infectious clone following the structural protein genes, although an additional *Spe I* restriction site is present in rA7[74] and SP6-CA7 within E2 at position 9032.

For pSP6-SFV4 a total of 5 µg DNA was linearised for 2 h at 37°C in a final reaction volume of 100 µl, containing 10 µl of *Spe I* buffer (NEB; 50 mM NaCl, 10 mM Tris-HCL, 10 mM MgCl₂, 1 mM DTT, pH 7.9), and 5U of *Spe I*. The reaction was then stopped by incubating the samples in a 65°C for 5 min. DNA was purified using a Qiagen Nucleotide purification kit (Qiagen, UK) as described for CHIK in section 2.10.4.3. For SP6-CA7 and rA7[74] partial digests were carried out using 1 µg DNA in a final volume of 20 µl containing 2 µl of *Spe I* buffer and 1U of *Spe I* for each infectious clone incubated at 37°C for 5 different timepoints: 5 min, 15 min, 20 min, 30 min and 1 h. Each linearised infectious clone DNA was pooled, giving a final volume of 100 µl and purified as mentioned above. Plasmid DNA concentration was assessed by mixing a 1 µl aliquot with 1 µl loading buffer and running this on a 0.8% (wt/vol) agarose gel. The concentration of plasmid was estimated from this gel by comparing band intensity with that of 0.25 µg and 0.5 µg Lambda (NEB; *Hind III* and *Eco RI*) DNA molecular weight marker.

4.2.4.2 *In vitro* SP6 RNA transcription

For the production of SFV viral RNA, SP6 RNA polymerase, was used to initiate *in vitro* RNA transcription from the clean *SpeI*-linearised plasmids. Standard reaction mixtures contained 0.5 µg DNA template, 1 x SP6 buffer [40 mM N-2-hydroxyethyl-piperazine-N'-2-ethansulphonic acid-KOH (Hepes-KOH), pH7.4, 6 mM MgOAc, 2 mM spermidine-HCL], 1 mM m⁷G(5')ppp(5')G, 5 mM dithiotreitol, 1 mM each rATP, rCTP, rUTP, 500 µM rGTP, 60 U recombinant RNAsin, and 50 U of SP6

RNA polymerase in 50 µl volume. The reactions were incubated at 37°C for 1 h 50 min and transcripts were analyzed by electrophoresis on a 0.6% (wt/vol) agarose gel.

4.2.4.3 Electroporation

BHK-21 cells were propagated as described in section 2.10.1.1. For each electroporation, one 75 cm² tissue culture flask, containing ~80% confluent BHK-21 cells was used. The cell monolayer was washed and trypsinised as previously described. Each flask was resuspended in 10 ml of fresh BHK medium and centrifuged (1500 rpm, 15 min). Pellets were resuspended in 10 ml PBS, and centrifuged as before. Each *in vitro*-transcribed RNA reaction contained 50 µl of SFV4, SFV-CA7 or SFV-pA7[74] RNA respectively. Cells were resuspended in 700 µl of PBS and was added to 50 µl of each RNA and placed in a 0.4 µm electroporation cuvette. The cuvette was then electroporated at 0.85 kV and 25 µF capacitance, using a BioRad Gene Pulser II. Following 2 pulses, cells were mixed with 20 ml of fresh BHK medium, transferred to a 75 cm² tissue culture flask and incubated for 24-36 h at 37°C in a humidified atmosphere of 5% CO₂.

4.2.4.4 Harvesting SFV infectious virus

Between 24-36 h.p.i the electroporated cell monolayers exhibited cytopathogenic effect (c.p.e), the supernatant was removed and virus was harvested. To harvest virus, the supernatant was removed, centrifuged at 3,000 x g for 10 min to remove cellular debris, and filtered through a 0.2 µm filter (Pall Life Sciences, USA). The resulting virus, was stored at -70°C in 1 ml aliquots. Virus was passaged a further two times and titre was established by plaque assay. Infectious virus RNA was isolated from infected BHK cells monolayers as described previously for CHIK in section 2.10.3.1.

4.2.5 Amplification of SFV 5' UTRs

To amplify the 5' UTR of SFV strains; L10, SFV4, CA7, pA7[74], A7 and A7[74] it was necessary to carry out 5' RACE PCR. An overview of this protocol was described previously in figure 2.1 of Chapter 2 "Sequencing and characterisation of the Ross strain of Chikungunya virus".

4.2.5.1 Primer Design

Primers were designed as outlined previously in section 2.10.3.3. The 5' RACE Abridged anchor primer (AAP) and the Universal Amplification primer (UAP) were supplied in the 5'/3' RACE PCR Kit (Roche, Switzerland). The Genome Specific Primers (GSPs) were reverse nested primers designed from the nsP1 of pSP6-SFV4 genome template, although when this region of each SFV strain was aligned the primers were identical for all SFV strains.

AAP:	5'-GGCCACGCGTCGACTAGTACGGGGGGGGGG-3'
UAP:	5'-CUACUACUAGGCCACGCGTCGACTAGTAC-3'
GSP1: SFV(-) 419	5'-TCCGGGAAGGTGCTGGATAGAG-3'
GSP2: SFV(-) 250	5'-CCAAATTGATCGAAGCAGGAG-3'

cDNA was prepared using a nested primer (GSP1) designed from pSP6-SFV4. Newly synthesised cDNA strand then had a homopolymeric tail added to its 3' end using terminal transferase. The 5' RACE Abridged Anchor Primer was then used to generate second-strand cDNA. This dsDNA then served as the template for a secondary PCR reaction using a nested gene-specific primer (UAP) and inner primer (GSP2). The 5' RACE PCR was carried out in accordance to manufacturer's recommendations, using the same PCR conditions as shown in table 2.4 (section 2.10.3.3.4).

4.2.5.2 DNA Purification

PCR amplicons were run on a 0.8% (wt/vol) agarose gel at 86 mA and extracted using a sterile scalpel (Swann Morton Ltd, UK). The gel fragments were then placed in a sterile 1.7ml microtube (Axigen) and weighed for purification using the Promega Wizard Kit (Promega, USA). A binding buffer (4.5M guanidine isothiocyanate, 0.5M potassium acetate, pH 5.0) was added at 3 volumes of buffer to 1 volume of gel (300 µl of buffer to 100 µg of gel) and the mixture incubated for 10 min at 60°C, with vortexing every 3 mins. The buffer solubilises the agarose gel slice, and provides appropriate conditions for binding of DNA to a silica membrane in a Wizard Column. The mixture was added to a Wizard column and centrifuged (10,000g, 30 sec). The flow-through was discarded and 700 µl of wash buffer (10mM potassium acetate, pH 5.0), 80% ethanol, 16.7 µM EDTA, pH 8.0) added and

centrifuged (10,000g, 30 sec), A further 500 µl of wash buffer was added to remove all traces of agarose and centrifuged (10,000g, 5min). Purified DNA was eluted in 50 µl of pre-heated (60°C) nuclease-free water. 20 µl of each sample was sent to LARK Technologies (UK) with 5 µl of both forward and reverse primers (0.02 µg/ µl) for sequencing.

4.2.5.3 Sequence Alignment

Sequences in both positive and negative orientations were initially processed using ChromasPro software (version 1.22; Technelysium Ltd. Australia). Sequences were then aligned using the online multiple alignment software Multalin (Corpet, F., 1988).

4.2.5.4 Prediction of Secondary structure

The 85 nt 5' UTR sequences of SFV-A7, SFV-L10, and of infectious virus produced from SP6-CA7, rA7[74] and pSP6-SFV4 were processed using MFold version 3.0 (Zuker, M.). Secondary structure was predicted using the default parameters.

4.2.6 Survival of Balb/c mice infected with SFV-A7, SFV-L10 and infectious virus produced from pSP6-SFV4, SP6-CA7 and rA7[74].

Five groups of 10 female Balb/c mice aged 60-80 days (Harlan, UK) were intranasally infected with 40 µl (20 µl per nostril) of 1×10^8 p.f.u / ml SFV-L10, SFV-A7 and infectious virus produced from pSP6-SFV4, SP6-CA7 and rA7[74]. A sixth group was mock-infected with D-PBS (Invitrogen, UK). Deaths were recorded over a 14 day period at which point all survivors were re-infected with SFV-L10 to ensure that initial doses of virus were adequate to induce partial immunity.

4.2.7 Virus titres in Balb/c brains infected with SFV-A7, SFV-L10 and infectious virus produced from pSP6-SFV4, SP6-CA7 and rA7[74].

Two groups of 6 female BALb/c mice aged 60-80 days (Harlan, UK) were intranasally infected with 40 µl (20 µl per nostril) of 1×10^8 p.f.u / ml SFV-L10 and infectious virus produced from pSP6-SFV4. Three mice were sacrificed from each group at 2 d.p.i and 4 d.p.i respectively. Three other groups of 12 Balb/c mice of the same age were intranasally infected with the same titer and volume of SFV-A7 and

infectious virus produced from SP6-CA7 and rA7[74]. Three mice were sacrificed from each group at 2, 4, 6 and 8 d.p.i respectively. Brains were removed and homogenised as described previously in section 2.10.6.2. Titer of virus in the supernatant of brain homogenate was determined by plaque assay.

4.2.8 Construction of SFV 5' UTR chimaeras

In order for 5' UTR chimaeras to be constructed several steps were required before site-mutagenesis could be carried out. Initially on aligning the sequences of all SFV strains it was observed that no unique restriction enzyme sites were present flanking the 5' UTR. A 2104 bp fragment was removed from the SFV infectious clones between nucleotide positions 8910 and 11014 using restriction enzyme *Nde I* (NEB, USA). Removing the 2104 bp also removed two restriction sites; *Eco RV* and *Sph I* at positions 9537 and 9665 respectively, generating a unique *Eco RV* site (278) and *Sph I* (14100) flanking the SFV 5' UTR. These restriction enzymes were then used to remove the 5' UTR from each SFV infectious clone which was ligated into the cloning vector Litmus 38i (L38i; NEB, USA) for site-digested mutagenesis (figures 4.5 and 4.6). For reciprocal 5' UTR exchanges between pSP6-SFV4 and rA7[74] and between SP6-CA7 and rA7[74] the use of L38i was not necessary as direct exchange and ligation of the reciprocal 5' UTR fragments could be performed (figures 4.3 and 4.4).

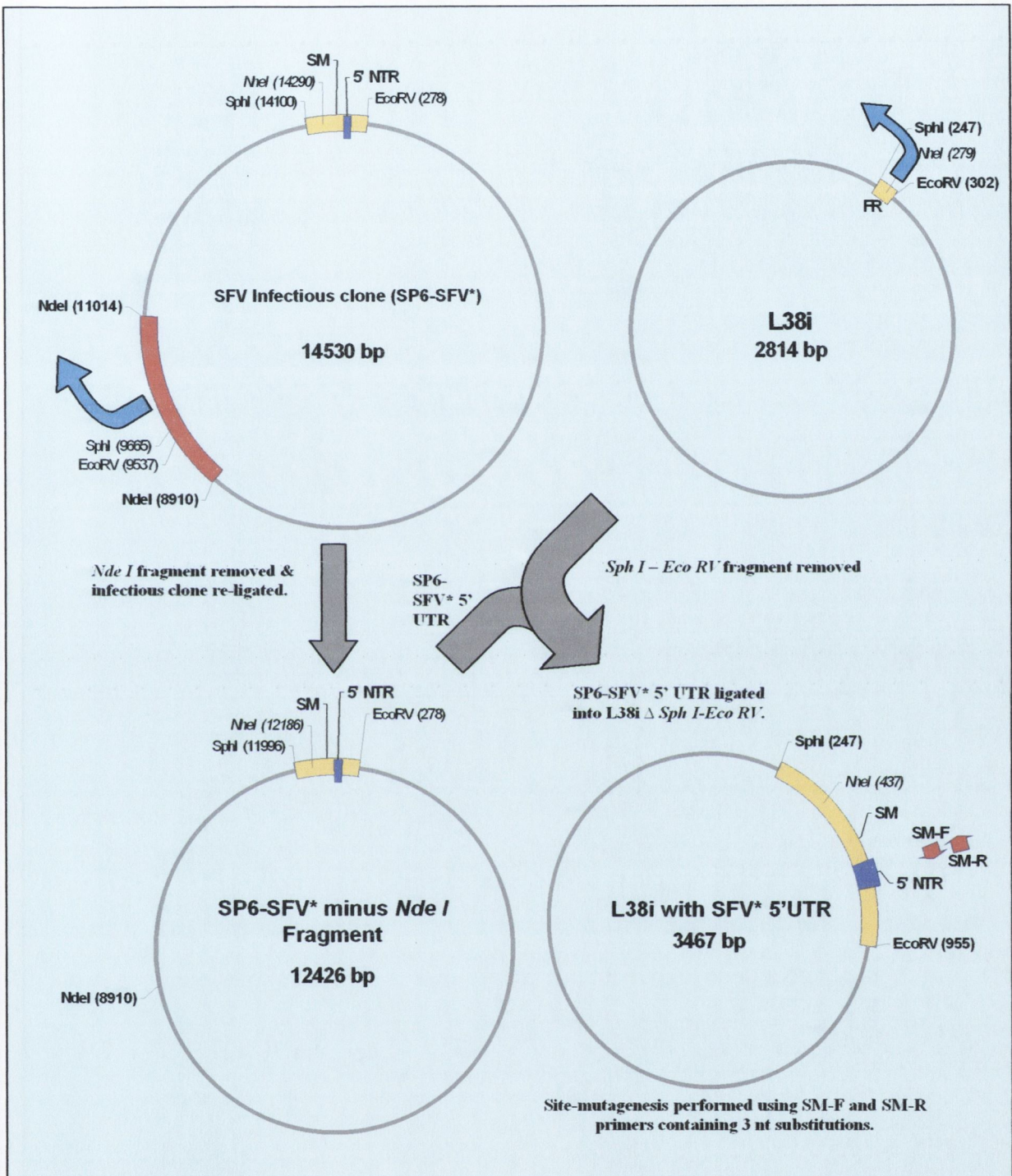


Figure 4.1 Schematic (1 of 2) of strategy used to site-mutagenise SFV infectious clone 5' UTRs to SFV-A7 5' UTR . *SFV Infectious clones (pSP6-SFV4, SP6-CA7 and rA7[74]), SM: Fragment excised for site-directed mutagenesis, FR: Fragment removed (light blue arrows), SM-F and SM-R are the forward and reverse primers (red arrows) containing the 3 nucleotide changes (G, A, T) required to generate SFV-A7 5' UTR sequence.

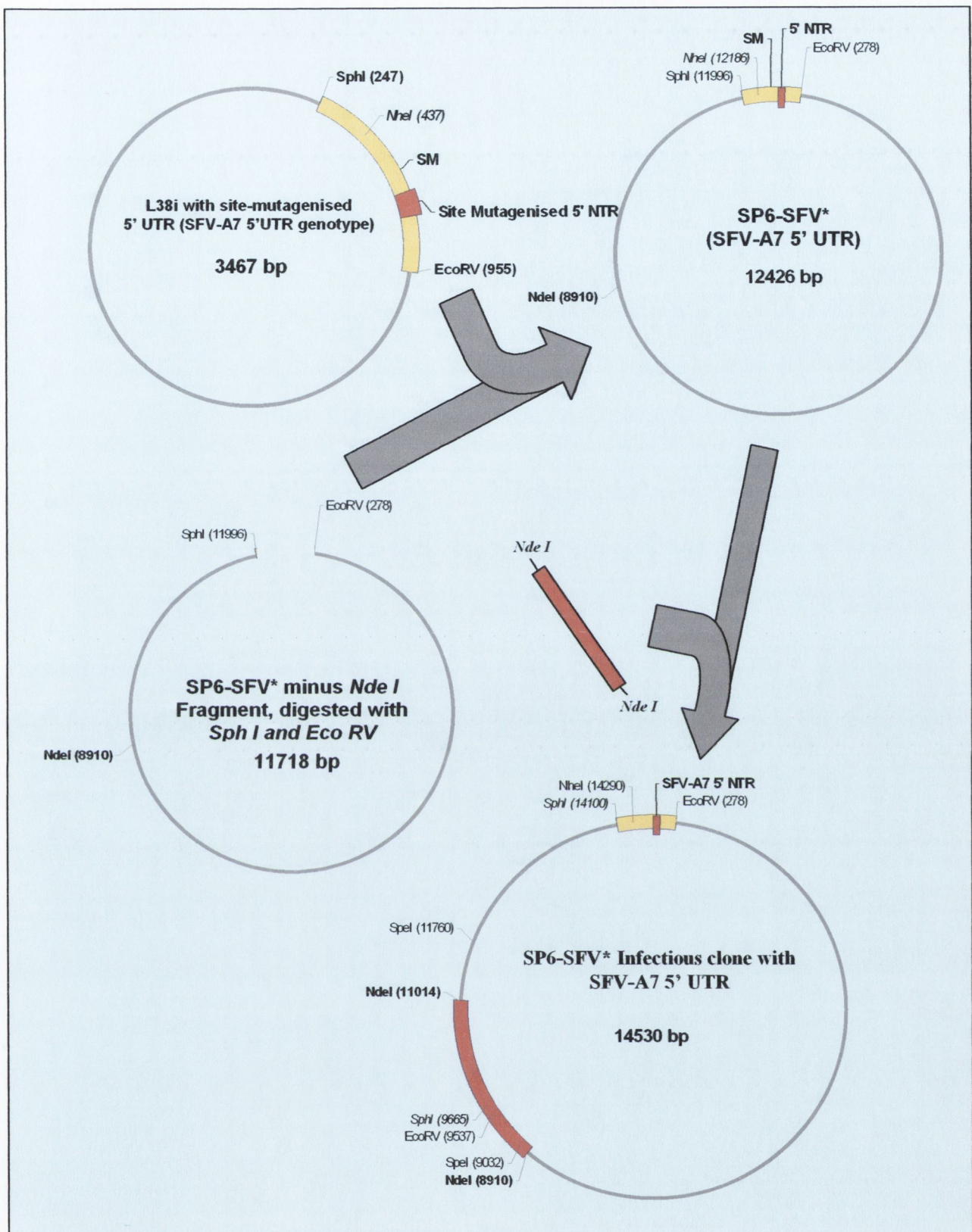


Figure 4.2 Schematic (2 of 2) of strategy used to site-mutagenise SFV infectious clone 5' UTRs to SFV-A7 5' UTR.

4.2.8.1 Preparation of chimaeras I - Restriction Digestion

4.2.8.1.1 Preparation of SFV infectious clones with restriction enzyme *Nde I*

DNA was digested with *Nde I* to remove a 2104 bp fragment between nucleotide positions 8910 and 11014 thereby also removing superfluous *Eco RV* and *Sph I* restriction sites at positions 9537 and 9665 respectively. The following reaction mixtures were digested for 2 h at 37°C: 2 µl (1µg / µl) SFV Infectious clone DNA, 15 µl nuclease-free water, 2 µl 10X *Nde I* NEBuffer (50 mM potassium acetate, 20mM Tris-HCl, 10mM magnesium acetate, 1mM dithiothreitol pH 7.9) and 5U *Nde I* enzyme (NEB, USA). The digested reaction mix (20µl) was run on a 0.8% (wt/vol) agarose gel, and both fragments (2104 and 12426 nt) were excised from the agarose using a sterile surgical blade, placed in a 1.7 ml microtube (Axygen, USA) and weighed. Samples were purified and eluted as described previously in section 2.10.4.1. 2 µl of T4 10X ligase buffer and 1U T4 ligase (Promega, USA) were added to 17 µl of each 12426 nt SFV backbone fragment, the reaction was gently vortexed and incubated overnight at room temperature. The recircularised SFV backbone was transformed in *E. coli* DH5α cells and DNA extracted as described previously in sections 2.4.10.7 and 2.4.10.8. These SFV infectious clones minus a 2104 bp fragment were termed pSP6-SFV4 Δ *Nde I*, SP6-CA7 Δ *Nde I* and rA7[74] Δ *Nde I* respectively. The excised 2104 bp fragment was stored at -20°C until subsequent relegation into the chimaeric clones. An overview of this procedure is illustrated in figure 4.5a.

4.2.8.1.2 Preparation of SP6-SFV Δ *Nde I* infectious clones with *Sph I* and *Eco RV*

The following reaction mixtures were digested for 4 h at 37°C: 3 µl (1µg / µl) of pSP6-SFV4 Δ *Nde I*, SP6-CA7 Δ *Nde I* and rA7[74] Δ *Nde I* DNA, 13 µl nuclease-free water, 2 µl 10X *Sph I* NEBuffer (50 mM NaCl, 10 mM Tris-HCl, 10mM MgCl₂, 1mM dithiothreitol pH 7.9) and 5U *Sph I* and 20U *Eco RV* enzymes (NEB, USA). The digested reaction mix (20µl) was run on a 0.8% (wt/vol) agarose gel, and both fragments (708 and 11718 nt) were excised from the agarose using a sterile surgical blade, placed in a 1.7 ml microtube (Axygen, USA) and weighed. Samples were purified and eluted as described previously in section 2.10.4.1 (figure 4.5).

4.2.8.1.3 Preparation of pSP6-SFV4 / rA7[74] 5' UTR reciprocal chimaeras.

Reciprocal pSP6-SFV4 and rA7[74] 708 nt fragments were exchanged into their respective 11718 nt SP6-SFV backbones. 2 µl of T4 10X ligase buffer and 1U T4 ligase (Promega, USA) were added to a mixture of 1 µl of each purified *Sph I/Eco RV*- digested 11718 nt SFV backbone fragment and 16 µl of the reciprocal 708 nt fragment. The reaction was gently vortexed and incubated overnight at room temperature. Cells were transformed and DNA extracted as described previously. DNA was then digested with *Nhe I* (12186) to confirm insertion of reciprocal 708 nt fragment. On confirmation of insertion, DNA was linearised using *Nde I* (8910), dephosphorylated with Alkaline phosphatase and purified as described previously for Litmus 28 in section 2.10.4.4. Infectious virus was produced as described in section 4.2.1.2 and virus RNA isolated as previously described in section 2.10.3.1.

4.2.8.1.4 Preparation of SP6-CA7 / rA7[74] 5' UTR chimaera

SP6-CA7 / rA7[74] reciprocal chimaeras were produced identically to the pSP6-SFV4 / rA7[74] chimaeras mentioned in section 4.2.8.1.3 above.

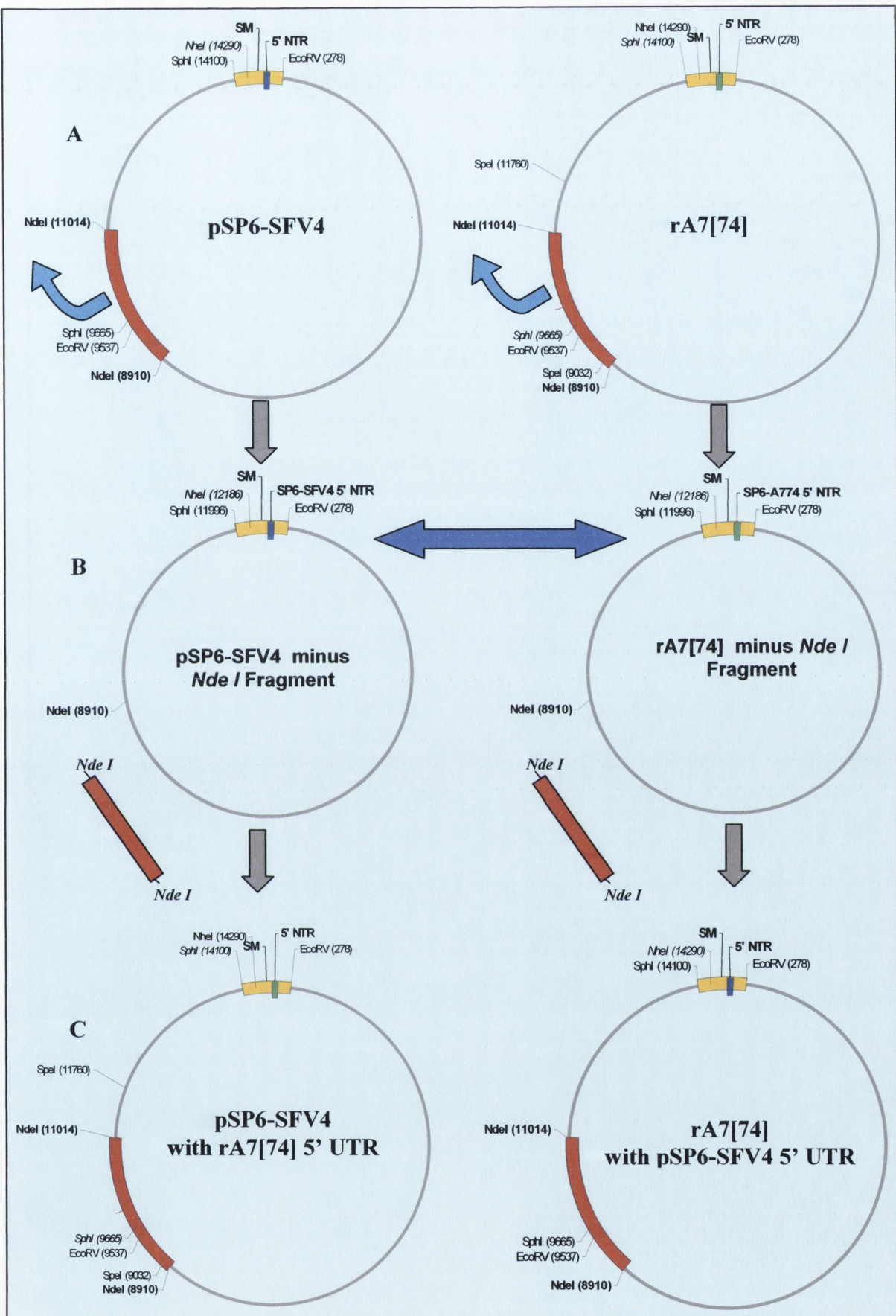


Figure 4.3 Strategy used to create reciprocal pSP6-SFV4 / rA7[74] 5' UTR chimaeras. Light blue arrow represents the excision of *Nde I* fragment (A), dark blue arrow represents reciprocal 5' UTR exchange between pSP6-SFV4 and rA7[74] (B). *Nde I* Fragment represented by red bar is reinserted in last step (C).

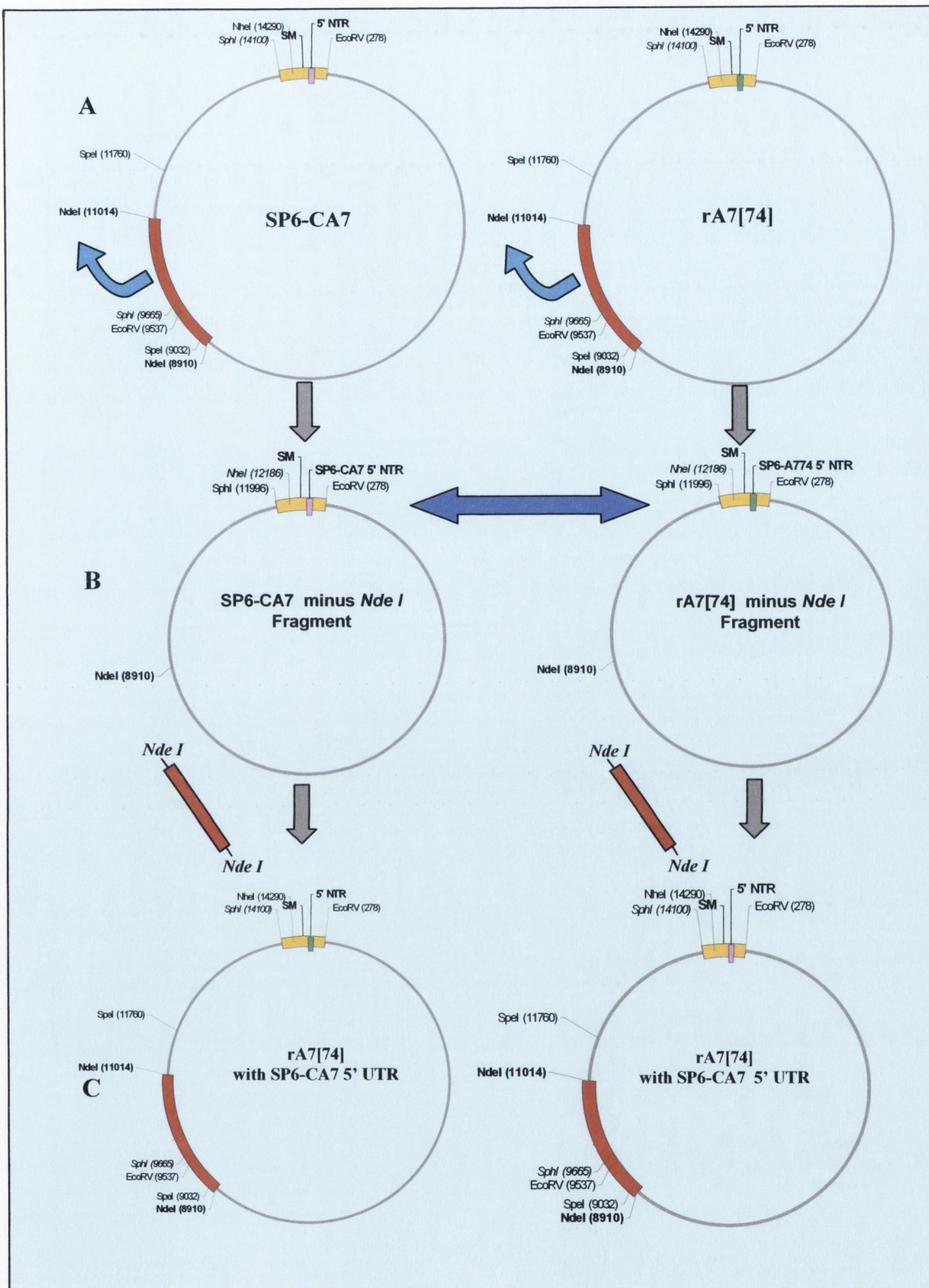


Figure 4.4 Strategy used to create reciprocal SP6-CA7 / rA7[74] 5' UTR chimaeras. Light blue arrow represents the excision of *Nde I* fragment (A), dark blue arrow represents reciprocal 5' UTR exchange between pSP6-SFV4 and rA7[74](B). *Nde I* Fragment represented by red bar is reinserted in last step (C).

4.2.8.2 Preparation of SP6-SFV / SFV-A7 5' UTR chimaeras

4.2.8.2.1 Restriction digestion of L38i with *Sph I* and *Eco RV*

The following reaction mixtures were digested for 4 h at 37°C: 2 µl (1 µg / µl) of L38i DNA, 14 µl nuclease-free water, 2 µl 10X *Sph I* NEBuffer (50 mM NaCl, 10 mM Tris-HCl, 10mM MgCl₂, 1mM dithiothreitol pH 7.9), 5U *Sph I* and 20U *Eco RV* enzymes (NEB, USA). The digested reaction mix (20µl) was run on a 0.8% (wt/vol) agarose gel, the 2757 nt fragment was excised from the agarose using a sterile surgical blade, placed in a 1.7 ml microtube (Axygen, USA) and weighed. The 57 nt *Sph I* / *Eco RV* "dropout" fragment was discarded. The 2757 nt fragment, termed L38i Δ *Sph I* / *Eco RV* was then purified and eluted as described previously in section 2.10.4.1. and stored at -20°C until subsequent ligation of pSP6-SFV4 *Sph I* / *Eco RV* 708 nt fragment for site-directed mutagenesis.

4.2.8.2.2 Site-directed mutagenesis

A substitution of 3 nucleotides A/G (21), T/A(35) and C/T(42) of the SFV4 5' UTR to the SFV-A7 5' UTR genotype was carried out using a QuikChange site-directed mutagenesis kit (Stratagene, USA). The pSP6-SFV4 *Sph I* / *Eco RV* 708 nt fragment was ligated into L38i Δ *Sph I* / *Eco RV* and ligation confirmed using *Nhe I* as described previously for the pSP6-SFV4 / rA7[74] 5' UTR reciprocal chimaeras in section 4.2.2.1.3. The site-directed mutagenesis protocol was followed according to manufacturer's recommendations using the following oligonucleotide primer (SM-F) and its complementary sequence (SM-R). These were designed to incorporate the 3 site-specific mutations (underlined).

SM-F 5' CATACGGCACGCCAAAAGAATTTGTTTCAGCTC 3'
SM-R 5' GAGCTGAAACAAATTCTTTTGGCGTCGCGTATG 3'

Following mutagenesis, 6 random clones were picked for sequence selection, DNA extracted and eluted for sequence confirmation by PCR. On positive confirmation of a successful 3 nt site-directed mutagenesis, one clone was selected that contained the A/T/C → G/A/T nt changes.

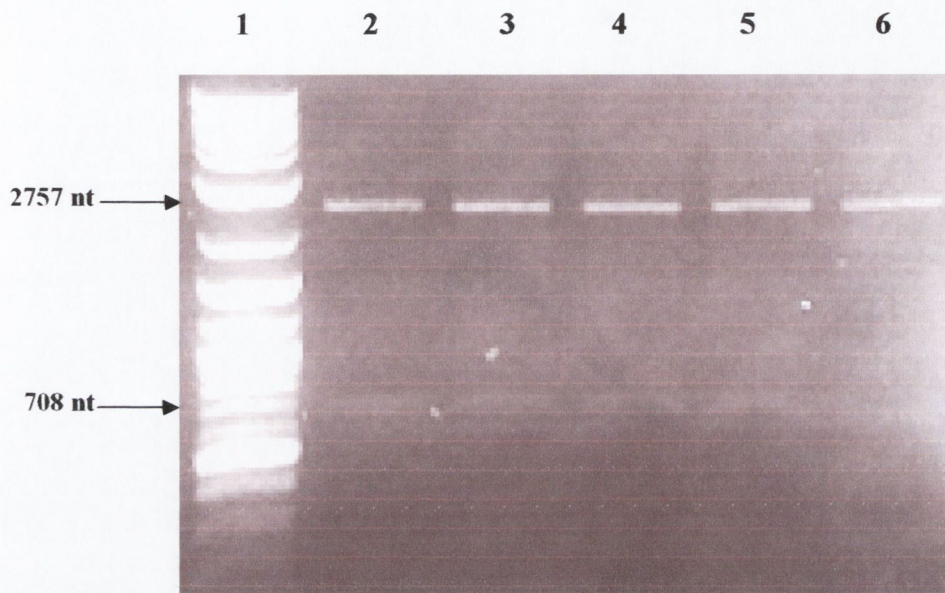


Figure 4.5 Site-mutagenised clones 1-5 digested with *Sph I* and *Eco RV*. 1% agarose gel stained with ethidium bromide. Lane: 1 Kb + 100 bp combined markers, Lanes 2-6: L38i with site-mutagenised 708 nt SFV4 colonies 1-5 digested with *Sph I* and *Eco RV*. L38i backbone is 2757 nt in length with drop out site-mutagenised fragment 708 nt in length.

4.2.8.2.3 PCR

PCR was carried out using oligonucleotides designed from L38i flanking each side of the *Sph I* and *Eco RV* restriction sites, thus amplifying the 708 nt site-mutagenised region within them using the same PCR conditions described in section 2.10.3.3.4. The following forward (L38i-F) and reverse (L38i-R) oligonucleotide primers were used:

L38i-F 5' ATAGGGGCCCGTGCAATTGAAGC 3'

L38i-R 5' CTCACTATAGGCCTTGACTAGAGGGTTCGAC 3'

DNA was then purified and sent for sequencing as described in section 4.2.5.2

4.2.8.2.4 Excision of site-mutated SFV-A7 5' UTR and ligation into SP6-SFV Δ *Nde I* (Δ *Sph I* / *Eco RV*) infectious clones.

DNA extracted from the selected clone that contained the three nucleotide mutations described in section 4.2.8.2.2 was digested with *Sph I* and *Eco RV* to excise the 708 nt site-mutagenised 5' UTR fragment from the L38i cloning vector. This was carried out in the same way as described previously in section 4.2.8.1.2 The 708 nt site mutagenised fragment was then purified as previously described and ligated into each of the SFV Δ *Nde I* (Δ *Sph I* / *Eco RV*) infectious clones. Successful ligation was tested using the restriction enzyme *Nhe I* which for positive ligations gave two bands of 3269 and 9957 nt long, if a ligation was unsuccessful then two bands of 3079 and 8639 were observed.

4.2.8.2.5 Re-ligation of respective *Nde I* fragments.

DNA was linearised with *Nde I* and treated with Antarctic phosphatase in order to reduce recirculisation during the subsequent ligation of each SFV clones respective 2104 nt *Nde I* fragment, these protocols were carried out as described earlier. To test the orientation of the inserted *Nde I* fragment in each SFV clone the restriction enzyme *Eco RV* was used. For a positive orientated ligation two bands of 5271 nt and 9259 nt were observed, in the instance of the fragment inserting in the negative orientation two bands of 4421 and 10109 nt in size were observed.

4.2.8.2.6 PCR confirmation

The sequence of the 5' UTR of each chimaera was ascertained before *in vitro* transcription of the cDNA by PCR. The following primers were designed flanking either side of the 5' UTR.

SFV5'F (nt position) 5'CATTAGGAAGCAGCCCAGTACTAGGTTGAG 3'

SFV5'R (nt position) 5'CATCATTCTCCTGGAAGGCGCAC 3'

PCR conditions used are identical to those used previously. DNA was gel-extracted (figure 4.6), purified and sent to LARK Technologies, UK for sequencing.

4.2.8.2.7 Production of infectious chimaeric virus

Infectious chimaeric virus was produced for each of the six 5' UTR chimaeras listed below in an identical way as infectious virus was produced from pSP6-SFV4, SP6-CA7 and rA7[74] as described in section 4.2.8.

pSP6-SFV4 + SFV-A7 5' UTR termed SFV4 / A7

pSP6-SFV4 + rA7[74] 5' UTR termed SFV4 / rA7[74]

SP6-CA7 + SFV-A7 5' UTR termed CA7 / A7

SP6-CA7 + rA7[74] 5' UTR termed CA7 / rA7[74]

rA7[74] + SFV-A7 5' UTR termed prA7[74] / A7

rA7[74] + pSP6-SFV4 termed prA7[74] / SFV4

4.2.8.2.8 Infectious virus RNA isolation and 5' RACE PCR confirmation of 5' UTRs

Infectious chimaeric RNA was isolated (figure 4.7) and 5' RACE PCR carried out on each sample as described previously for all SFV strains in sections 4.2.5.1

4.2.8.2.9 Plaque assay

All Strains of SFV and infectious virus produced from both chimaeric and non-chimaeric SFV infectious clones were titred by plaque assay as described previously for Chikungunya virus in section 2.10.2.3.

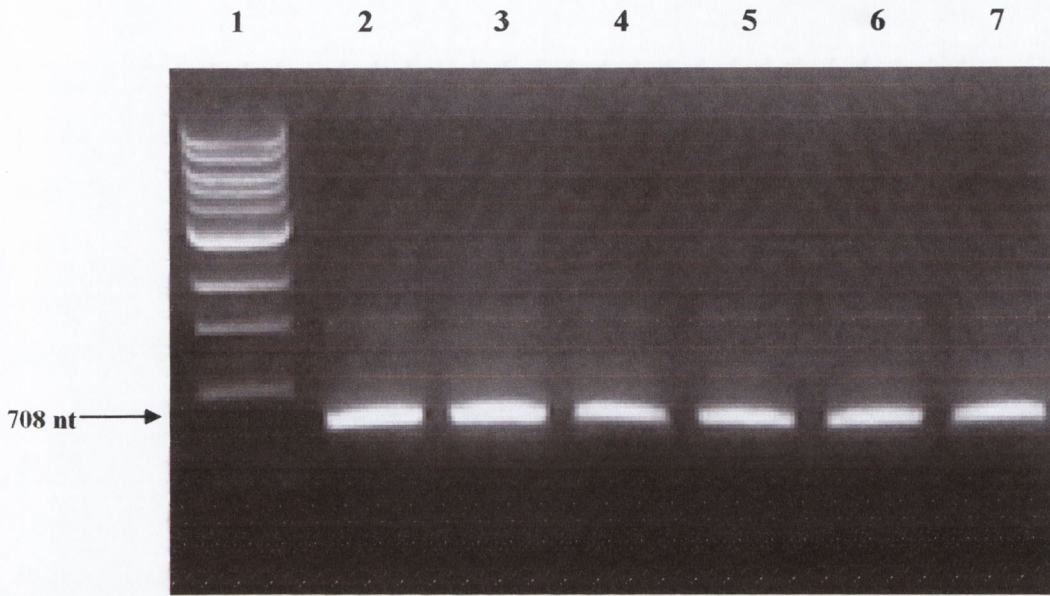


Figure 4.6 SFV 5' UTRs

1% agarose gel stained with ethidium bromide. Lane: 1 Kb marker, Lanes 2-7: 5' RACE PCR-amplified 708 nt SFV DNA. Lane 2: CA7-A7. Lane 3: CA7-rA7[74]. Lane 4: rA7[74]-A7. Lane 5: rA7[74]-pSFV4. Lane 6: pSFV4-A7. Lane 7: pSFV4-rA7[74]. Nomenclature indicates backbone infectious clone with inserted 5' UTR fragment. 708 nt fragments were gel excised, purified and sent for sequencing.

4.2.8.2.10 Intranasal infection of Balb/c mice

Six groups of 10 female Balb/c mice aged 60-80 days (Harlan, UK) were intranasally infected with 40 μ l (20 μ l per nostril) of 1×10^8 p.f.u / ml infectious virus produced from each of the six chimaeric infectious clones. A sixth group was mock-infected with D-PBS (Invitrogen, UK). Deaths were recorded over a 14 day period at which point all survivors were re-infected with SFV-L10 to ensure that initial doses of virus did indeed infect the mice and the concentration of virus administered was adequate to induce partial immunity.

4.2.8.2.11 RNA synthesis of SFV 5' UTR chimaeric virus

The rate of RNA synthesis of virus was measured by infecting subconfluent BHK-21 cell monolayers with viruses at a high M.O.I. (50 p.f.u./cell). Virus was allowed to adsorb in the monolayer for 1 h at 37°C in a humidified atmosphere of 5% CO₂, at which point the inoculum was replaced with BHK medium containing 5 μ g/ml actinomycin D and reincubated for 2 h at 37°C in a humidified atmosphere of 5% CO₂. The inoculum was then removed and fresh BHK medium containing 5 μ g/ml actinomycin D and 1 μ Ci / ml [³H]-*methyl* uridine (Amersham Pharmacia Biotech, Sweden) was added, the cell monolayers were returned to 37°C for a further 2 h. Cell monolayers were then washed twice with PBS and dissolved in 2 ml of 1% (w/v) sodium dodecyl sulphate (SDS) to lyse the cells. On adding 2ml of ice-cold 10% (w/v) trichloroacetic acid (TCA) the mixture was allowed to stand on ice for 15 min. The resulting precipitate was collected on glass fibre discs (Whatmann, USA) using a vacuum manifold (Millipore, USA) and washed twice with 4 ml of ice-cold 5% (w/v) TCA and once with 100% ethanol and air-dried. Filters were then placed in plastic scintillation vials into which 4 ml scintillation fluid (ICN, USA) was added prior to counting using a Tricarb 1500 scintillation counter (3 min count/sample). This procedure was carried out in triplicate for each virus on monolayers at 2, 4, 6, 8 h.p.i. Negative and positive mock-infected controls were used at each time point with the negative control containing no actinomycin D and the positive containing actinomycin D thus allowing the level of background cellular RNA synthesis to be calculated.

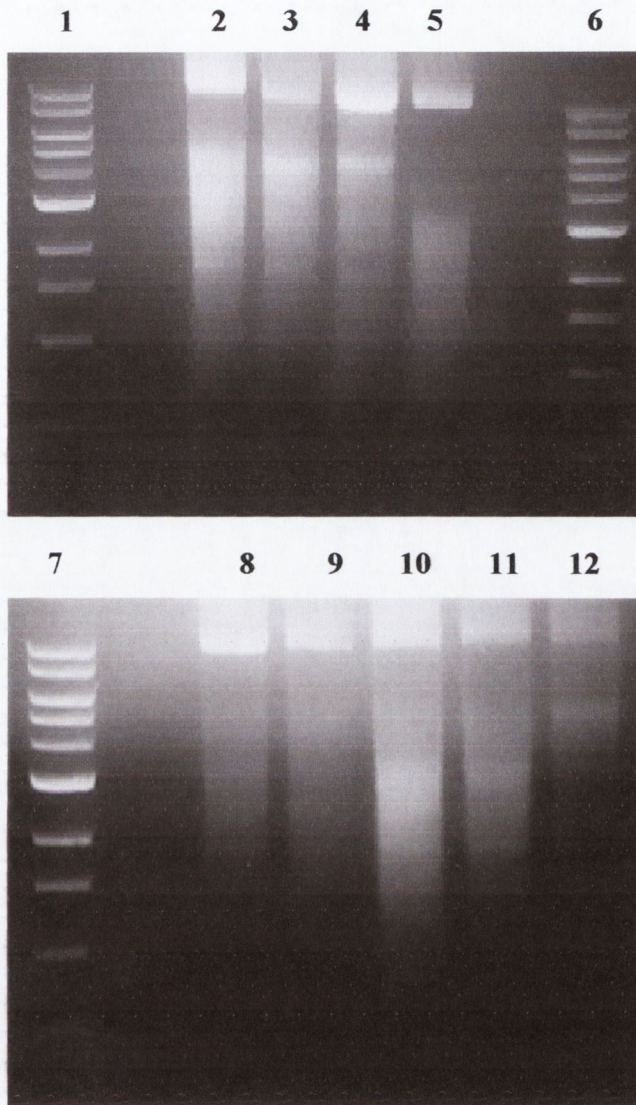


Figure 4.7 In Vitro RNA Transcription. 1% agarose gel stained with ethidium bromide. Lanes 1, 6 and 7: 1 Kb marker, Lanes 2-12: RNA from reverse transcribed infectious clones and chimaeric clones: Lane 2: SP6-CA7. Lane 3: pSP6-SFV4. Lane 4: rA7[74]. Lane 5: SP6-CA7/A7. Lane 8: SP6-CA7/rA7[74]. Lane 9: pSP6-SFV4/A7. Lane 10: pSP6-SFV4/rA7[74]. Lane 11: rA7[74]/A7. Lane 12: rA7[74]/SFV4.

RNA was then electroporated into BHK-21 cells and infectious virus observed by cytopathogenic effect (c.p.e) caused. Virus was filter purified and passaged twice in BHK-21 cells before being purified and titred by plaque assay. Purified titred infectious virus was then used to determine the rate of RNA synthesis *in vitro*, to record the survival rates of in infected mice and to examine the neuropathology caused in the brains of infected adult female Balb/c mice.

4.3 Results

4.3.1 Analysis of SFV strains

4.3.1.1 Amino acid sequence analysis of prototype virulent and avirulent SFV strains

On sequencing the SP6-CA7 genome the sequence was deposited in Genbank (Accession number: Z48163). This was then aligned with the SFV4 (NC003215) and rA774 (M. Tuittila, personal communication) genome sequences. Sequences were analysed on an amino acid (aa) level with the exception of the three untranslated regions (UTRs): the 5' UTR, the junction region and the 3' UTR.

In the nonstructural polyprotein there were six aa differences between the avirulent and virulent strains in nsP1. The differences most relevant to this investigation were those between the avirulent (CA7 and rA774) and virulent (SFV4) strains as these may indicate the regions involved in SFV virulence. In nsP2 there were twelve aa differences between the virulent and avirulent strains one of these being an aa deletion at position 1258 of the virulent genomes. nsP3 showed the most differences between avirulent and virulent SFV genomes with two major deletions in CA7 and rA774. The first deletion was seven aa in length between positions 1742 and 1730, the second was considerably larger spanning forty aa between positions 1812 and 1852. There were also four aa differences between virulent and avirulent nsP3, compared to two in nsP4. There were no nucleotide differences between the highly conserved untranslated junction region in any of the SFV strains analysed.

Differences between virulent and avirulent SFV strains in the structural polyprotein were considerably fewer than in the non-structural polyprotein. There was one aa difference in the capsid protein and two in the E3 glycoprotein. Of the structural proteins E2 showed most differences between virulent and avirulent SFV strains with five aa differences, two of which were adjacent to each other at positions 545 and 546. The last of the structural proteins to be analysed was E1 which contained four differences between SFV4 and CA7 / rA774. These results are shown in tables 4.1 and 4.2.

AMINO ACID POSITION	GENE	SFV4	CA7	prA774
95	nsP1	D	V	V
96	nsP1	S	C	C
237	nsP1	C	S	S
308	nsP1	Y	H	H
387	nsP1	I	V	V
427	nsP1	R	K	K
484	nsP1	V	A	A
534	nsP1	H	R	R
596	nsP2	G	R	R
679	nsP2	V	I	I
764	nsP2	K	L	L
765	nsP2	G	D	D
766	nsP2	T	I	I
767	nsP2	S	Q	Q
768	nsP2	R	A	A
769	nsP2	E	K	K
770	nsP2	N	T	T
771	nsP2	S	V	V
901	nsP2	A	V	V
1052	nsP2	V	E	E
1206	nsP2	S	G	S
1216	nsP2	F	Y	Y
1258	nsP2	-	N	N
1259	nsP2	I	L	L
1347	nsP3	I	I	V
1406	nsP3	A	G	G
1537	nsP3	F	L	L
1585	nsP3	N	D	D
1723	nsP3	G	A	A
1742-1749	nsP3	IADLAAD	-	-
1778	nsP3	A	T	T
1785	nsP3	L	F	F
1812-1852	nsP3	RLGRAGAYIFSSDT GSGHLQQKSVRQNL QCAQLDAVQEEK	-	-
1974	nsP4	D	E	E
2429	nsP4	R	K	K

Table 4.1 Amino acid analysis of SFV Non-structural polyprotein

Amino acids highlighted in yellow indicate matches between the infectious virus produced from the avirulent SFV infectious clones (ic): CA7 and rA7[74] and differences between them and the virulent SFV viruses. Those in blue show matches between infectious virus from one avirulent ic and the infectious virus produced from the virulent pSP6-SFV4. The SFV viruses shared one amino acid change with prA7[74](1206) and one with CA7(1347).

AMINO ACID POSITION	GENE	SFV4	CA7	prA774
62	CAPSID	A	T	T
85	CAPSID	N	K	K
279	E3	A	T	T
291	E3	V	A	A
370	E2	V	I	I
437	E2	K	T	T
495	E2	K	E	E
545	E2	N	S	S
546	E2	M	K	K
700	E2	V	A	A
704	E2	V	A	A
722	E2	V	A	A
880	E1	A	S	S
930	E1	R	K	K
1043	E1	M	T	T
1134	E1	T	K	T
1138	E1	N	D	D
1188	E1	R	K	K

Table 4.2 Amino acid analysis of SFV structural polyprotein

Amino acids highlighted in yellow indicate matches between the infectious virus produced from the avirulent SFV infectious clones (ic): SP6-CA7 and rA7[74] and differences between them and the virulent SFV viruses. Those in blue show matches between infectious virus from one avirulent ic and the infectious virus produced from the virulent pSP6-SFV4. There was only one amino acid change shared between the avirulent rA7[74] and SFV4 at position 1134.

Analysis of the 3' UTR showed that the SFV4 3' UTR is 260 nt in length compared to the CA7 and prA774 3' UTR which is 543 nt in length. There are two major areas of deletion in the virulent 3' UTR, shown in table 4.3 at positions 11183-11439 and 11541-11619. A nucleotide is also absent from the virulent 3' UTR at position 11673. Over the remainder of the 3' UTR there are 6 differences between SFV4 and avirulent SFV strains and an additional nucleotide difference between CA7 and prA7[74] that prA7[74] shares with SFV4 (G/A at position 11726). The CA7 and prA7[74] 3' UTRs only differ from each other by one other nucleotide at position 11358 as shown in table 4.3.

NUCLEOTIDE POSITION	REGION	SFV4	CA7	prA7[74]
11183-11357	3' UTR	-	+	+
11358	3' UTR	-	C	T
11359-11439	3' UTR	-	+	+
11523	3' UTR	G	A	A
11532	3' UTR	G	A	A
11541-11619	3' UTR	-	+	+
11649	3' UTR	G	A	A
11656	3' UTR	C	T	T
11673	3' UTR	-	G	G
11724	3' UTR	T	C	C
11726	3' UTR	A	G	A

Table 4.3 Nucleotide analysis of SFV 3' untranslated region

The nucleotide highlighted in green at position 11358 indicates the sole nucleotide difference between CA7 and rA7[74] that was not present in SFV4

Nucleotides highlighted in yellow indicate matches between the infectious virus produced from the avirulent SFV infectious clones (ic): SP6-CA7 and rA7[74] and differences between them and SFV4. Those in blue show matches between infectious virus from prA7[74] and the infectious virus produced from the virulent pSP6-SFV4. There was only one amino acid change shared between the avirulent rA7[74] and SFV4 at nucleotide position 11726.

4.3.1.2 Sequence of SFV 5' UTR

There were three nucleotides of the 5' UTR at positions 21, 35 and 42 respectively that differed between virulent and avirulent SFV strains (figure 4.9). In SFV-A7 and SFV-A7[74] a cytosine residue was present at position 21 whereas in all infectious virus produced from the three SFV infectious clones an adenine residue was present at position 21. Infectious virus produced from the rA7[74] infectious clone shared an adenine residue with both avirulent SFV strains at position 35, whereas in SFV4 and CA7 this residue was a thymine. Similarly at position 42, prA7[74] shared a common nucleotide with both avirulent SFV strains having a thymine residue where both SFV4 and CA7 had a cytosine residue.

4.3.1.3 Prediction of SFV 5' UTR secondary structure

The secondary structure of the first and largest stem-loop between nucleotides 2 and 29 predicted using MFold version 3.0 is identical for all strains of SFV regardless of the A/G nt difference at position 21. The T/A nt difference at position 35 abolished a stem loop from SFV4 and CA7 that is present in SFV-A7, SFV-A7[74] and in rA7[A4]. The T/C nt difference at position 42 made no difference in the secondary structure of the SFV strains. A small stem loop between positions 45-52 followed by a slightly larger one situated between positions 54 and 71 were present in all strains and infectious virus' 5' UTRs, as illustrated in figure 4.10.

4.3.1.4 Survival of Balb/c mice intranasally infected with SFV

All mice in each group of 10 infected intranasally (in) with SFV-A7 and SFV-A7[74] survived, while CA7 killed 30% of mice infected on 10 d.p.i and rA7[74] killed 10% of those infected on 12 d.p.i. Both virulent strains killed 100% of mice, with death occurring in mice infected with SFV-L10 at 4 d.p.i and those infected with SFV4 at 5 d.p.i. as shown in figure 4.11.

4.3.1.5 Virus titres in brains of Balb/c mice intranasally infected with SFV

At 2 d.p.i peak virus titres in the brain were observed for rA7[74] and SFV-A7[74] with the latter having a ten-fold lower virus titre. SFV4 and SFV-L10 reached titres between 1×10^8 and 10^9 p.f.u / g respectively by 4 d.p.i, a ten-fold higher titre than rA7[74] and CA7, and approximately a thousand-fold higher than SFV-A7. CA7 reached a peak titre of 1×10^7 p.f.u / g at 6 d.p.i. SFV4, SFV-L10, and SFV-A7 reached peak titres at 4 d.p.i, although as mice infected intranasally with SFV-L10 and SFV4 die between 4 and 5 d.p.i it is possible that like CA7 they reach peak titre at 6 d.p.i. (illustrated in figure 4.12).

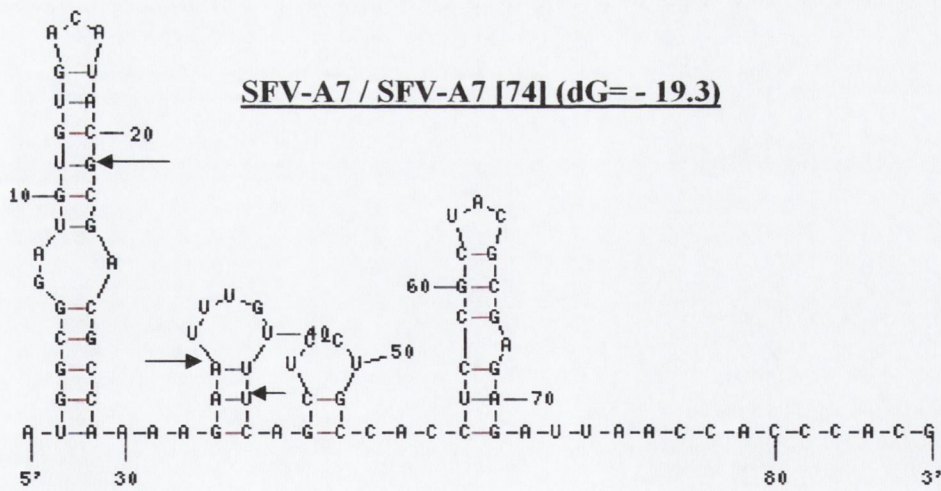
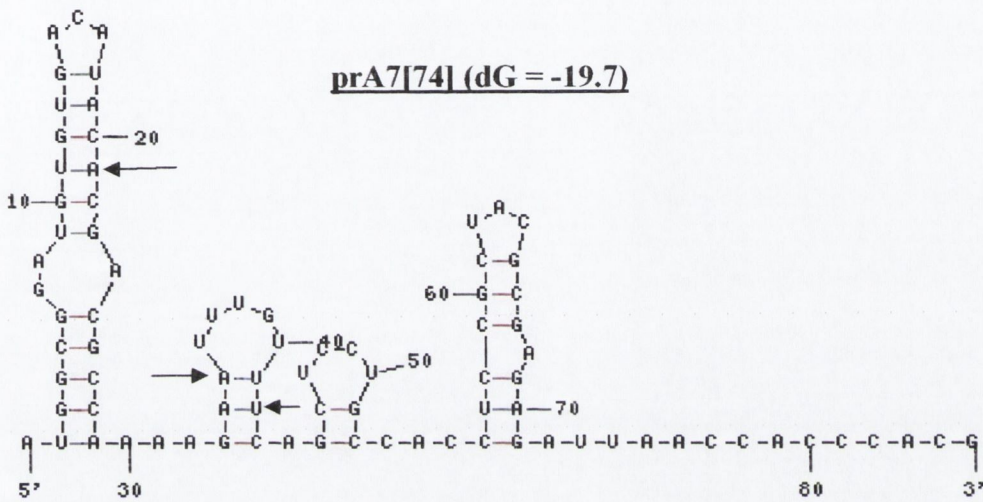
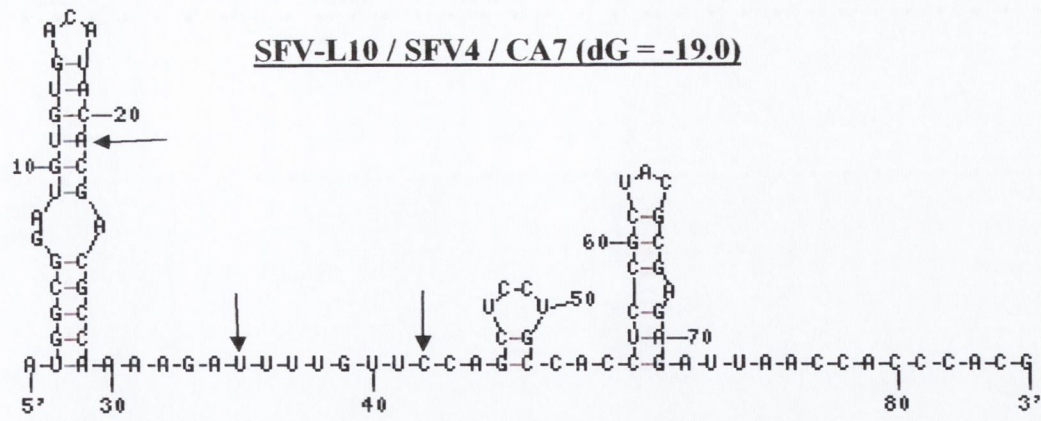


Figure 4.10 Secondary structure of SFV 5' untranslated regions. Stem loops predicted using Mfold version 3.0. dG represents optimal energy necessary for stem loop formation (kcal/mole) at 37°C. Nt differences noted at positions 21, 35 and 42 respectively, with only the nt change at position 35 altering the secondary structure of the second stem loop.

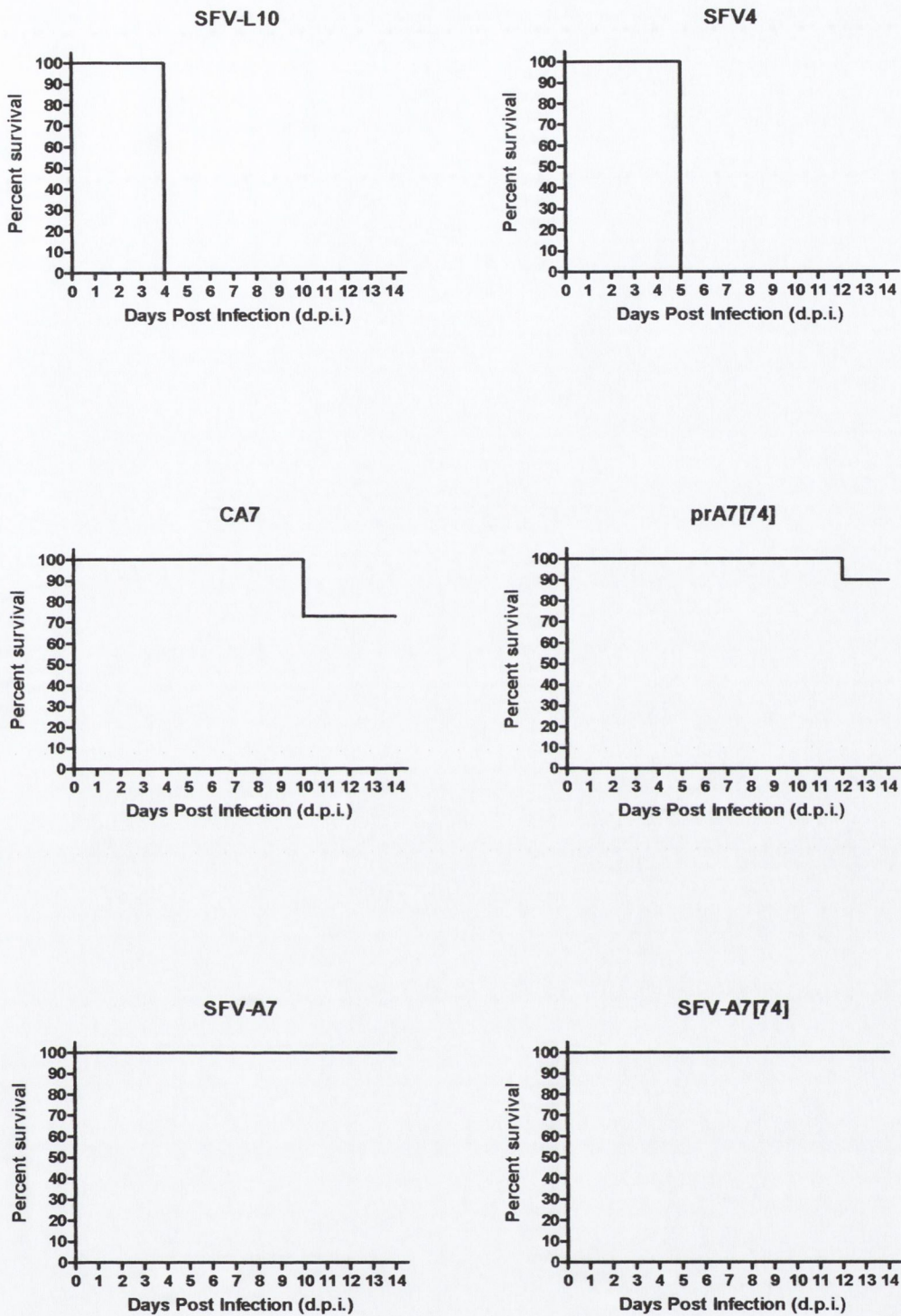


Figure 4.11 Survival of Balb/c mice infected intranasally with SFV

Infectious virus produced from pSP6-CA7 and rA7[74] resulted in 30 and 10% mortalities respectively, at 10 and 12 d.p.i. SFV-L10 shows higher virulence than SFV4 causing 100% mortality at 4 d.p.i compared with SFV4 at 5 d.p.i. 10 Balb/c adult female mice aged between 60-80 days were included in each group for analysis. This experiment was repeated twice to ensure results were not unique to individual mice.

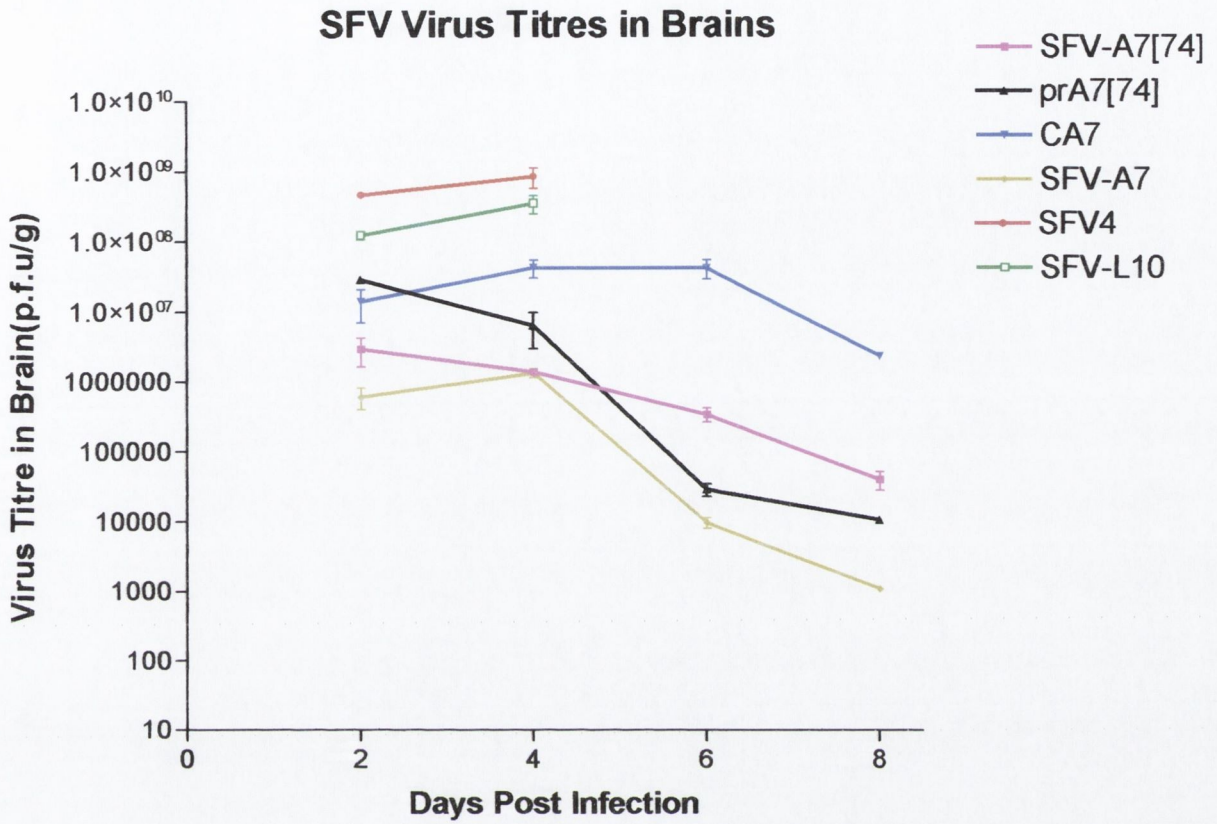


Figure 4.12 SFV titres in brains of intranasally infected Balb/c mice.

Mice (n=12 per virus) were infected intranasally with 1×10^8 pfu/ml of virus.

Infected brains were sampled in triplicate at 2, 4, 6 and 8 d.p.i. Titres of virus within brain homogenate were measured in triplicate by plaque assay with plaque forming units (p.f.u) per gram (g) being assigned as the measurement scale.

4.3.2 Construction and analysis of SFV 5'UTR chimeric virus

4.3.2.1 Sequence of SFV chimera 5' UTRs

The three nucleotides at positions 21, 35 and 42 respectively within the SFV4 5' UTR (A/T/C) were successfully mutated to those of SFV-A7 (G/A/T). The chimeras: pSP6-SFV4 / A7, SP6-CA7 / A7 and rA7[74] / A7 (where the virus on the right of the (/) symbol represents the genotype of the altered or substituted 5' UTR) therefore contained G, A and T at positions 21, 35 and 42 respectively. The rA7[74] 5' UTR containing nucleotides A, A and T at positions 21, 35 and 42 was successfully substituted into pSP6-SFV4 and the reciprocal chimera rA7[74] / SFV4 was also successfully constructed. These results were verified by 5' RACE PCR and subsequent sequencing and can be observed in figure 4.13.

4.3.2.2 Survival of Balb/c mice intranasally infected with SFV 5' UTR chimeric virus

All mice infected with infectious virus from SP6-CA7 / A7 and rA7[74] / A7 survived, whereas no reduction in mortality between SFV4 and the infectious virus from pSP6-SFV4 / A7 was observed. Those mice infected with infectious virus from SP6-CA7 / rA7[74] also all survived, however 10% of mice infected with pSP6-SFV4 / rA7[74] died at 4 d.p.i with the remaining dying at 5 d.p.i, thus 10% died a day earlier than usually observed for SFV4. 10% of mice infected with rA7[74] / SFV4 died at 12 d.p.i. compared to all infected with rA7[74] and rA7[74] / A7 having 100% survival rate (figure 4.14).

4.3.2.3 RNA synthesis of SFV strains and SFV 5' UTR chimeric viruses

Levels of viral RNA synthesis in BHK-21 cells was measured in counts per minute (c.p.m) by a scintillation counter. Cells infected with infectious virus from SP6-CA7 had a c.p.m almost twice as high as SFV-A7 at the peak count of 2 hours post infection (h.p.i) Similarly, virus produced from SP6-CA7/A7 had a peak titre at 2 h.p.i whereas SFV-A7 had a peak titre at 4 h.p.i. Markedly, both SP6-CA7 chimeras had similar growth pattern to CA7 rather than SFV-A7. prA7[74] and rA7[74]/A7 had RNA synthesis levels almost identical to SFV-A7 with a peak titre at 4 d.p.i. The

c.p.m of SFV4-infected cells at 2 h.p.i was almost identical to that of rA7[74]/SFV, whereas pSP6-SFV4/A7 had a similar level of RNA synthesis as SFV-A7. (figure 15). Statistical analyses were carried out on c.p.m for all ten viruses and no statistically significant differences for RNA synthesis between the chimeric viruses and virus produced by the three SFV infectious clones or SFV-A7 was observed.

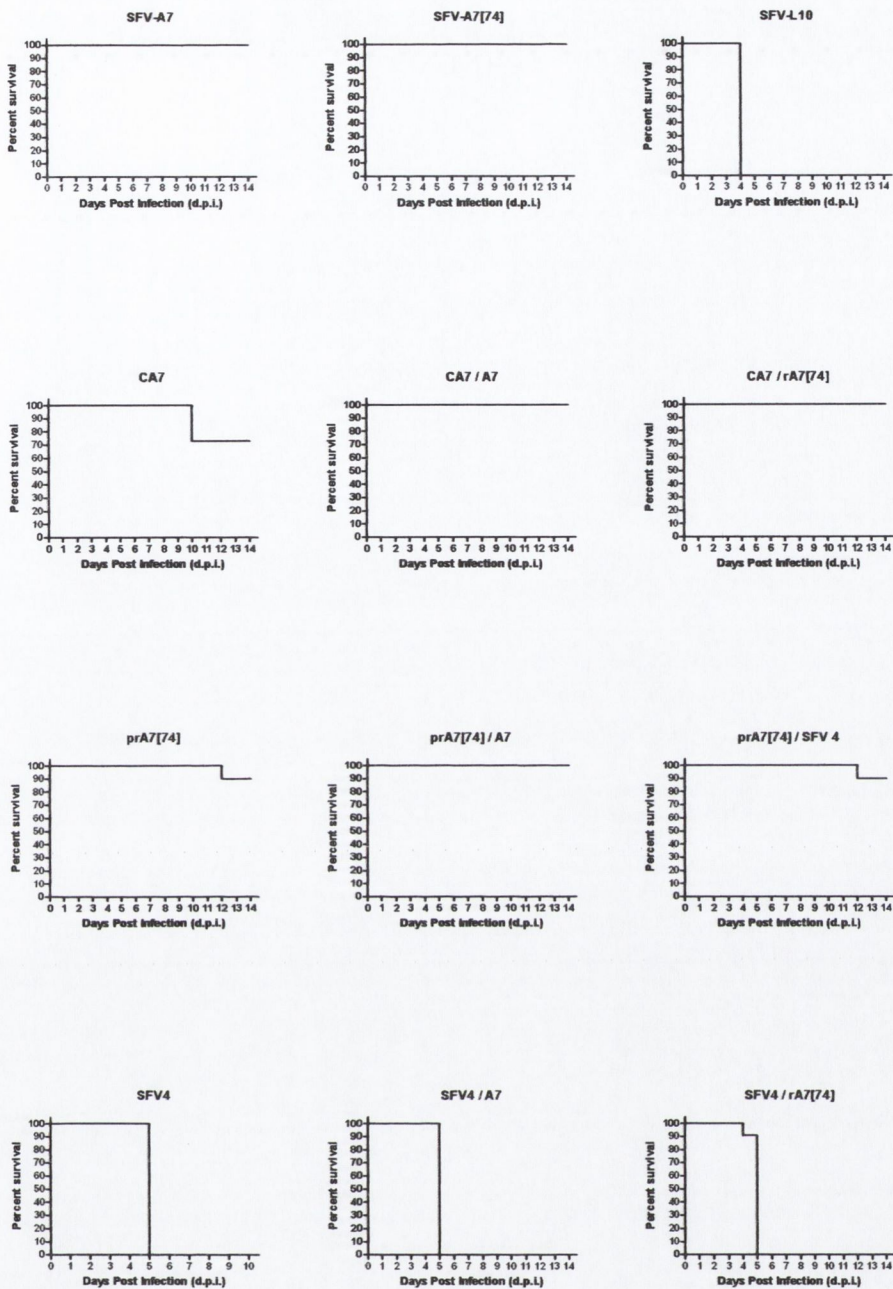


Figure 4.14 Survival Curves of Balb/c mice intranasally infected with SFV-5' UTR chimeric virus

Infectious virus produced from SP6-CA7 / A7 and SP6-CA7 / rA7[74] resulted in 100% survival rate compared to 70% when mice were infected with CA7. Mice infected with prA7[74] / A7 also showed 100% survival rate compared to 90% when infected with prA7[74] however the substitution of the rA7[74] 5' UTR with that of the SFV4 5' UTR did not increase the rate of mortality among infected mice. SFV4 / A7 shows no difference in mortality from SFV4 infection, however the reciprocal rA7[74] 5' UTR substitution caused 10% mortality at 4 .d.p.i, a day earlier than normally seen for SFV4 infection, although was not statistically significant. 10 Balb/c adult female mice aged between 60-80 days were included in each group for analysis.

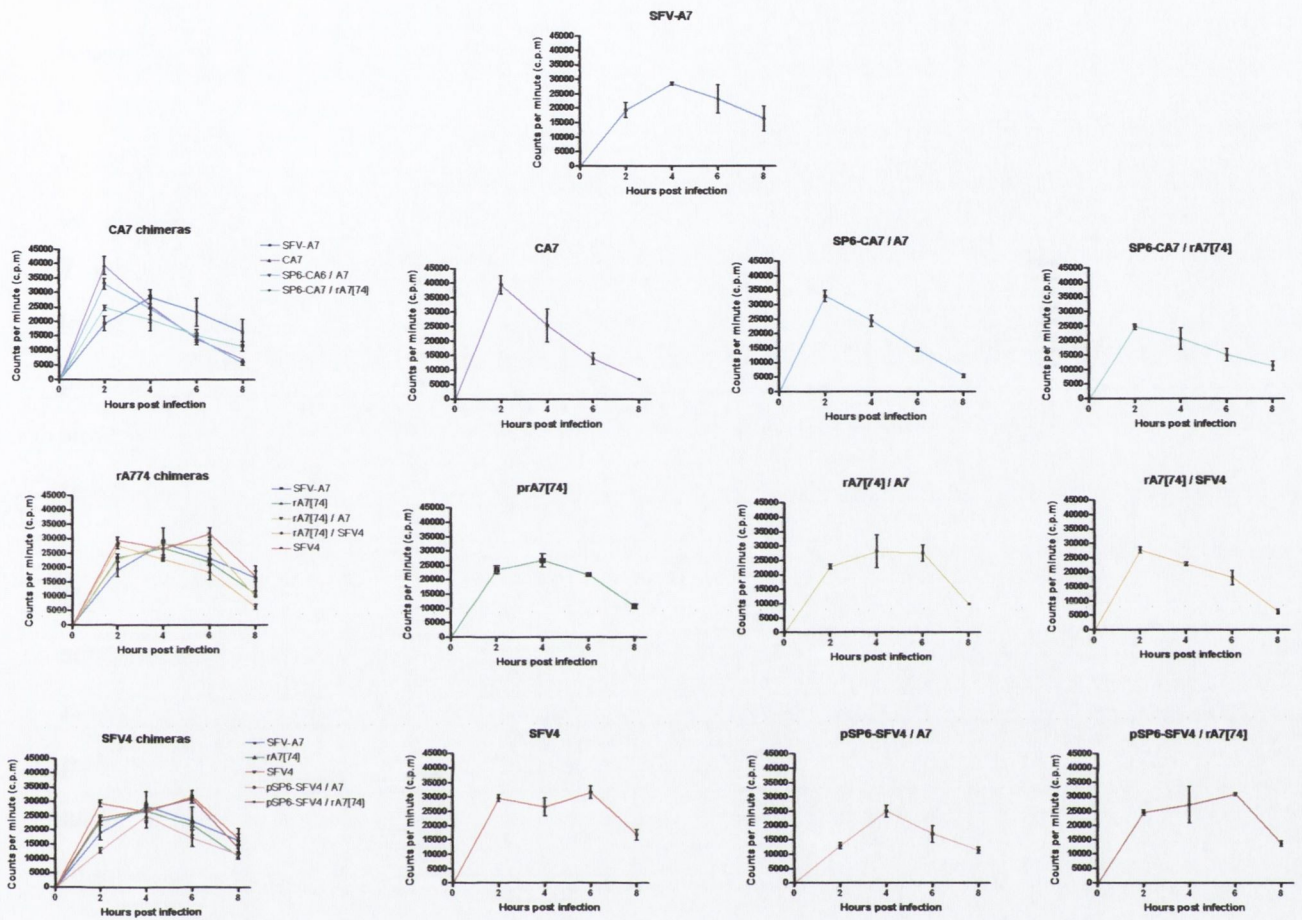


Figure 4.15 RNA synthesis of SFV and SFV 5' UTR chimeric virus (M.O.I. 50) in BHK-21 cells.

4.4 Discussion

On comparing the amino acid sequence of the virulent SFV4 strain to the virus produced from each avirulent infectious clone; CA7 and prA7[74], 50 mutations were found between CA7 and SFV4 and 49 between prA7[74] and SFV4. 32 were located in the non-structural proteins with the remaining 18 in the structural proteins. Other mutations between virulent and avirulent infectious SFV virus included two regions of nsP3 absent in both CA7 and prA7[74] but present in SFV4. The first consisted of 7 amino acids between aa positions 1742 and 1749, the second of 40 amino acids located between positions 1812 and 1852. A 1 aa deletion occurred in SFV4 that was present as an asparagine residue at aa position 1258 in both avirulent viruses. Of most significance in this investigation were the mutations in the non-structural proteins as these may alter the rate of RNA synthesis.

CA7 and prA7[74] shared 8 mutations from SFV4 in nsP1, however in nsP2 CA7 had an additional aa difference to SFV4 compared to prA7[74] which shared a serine residue to SFV4 at position 1206. Conversely, CA7 had an additional isoleucine residue in nsP3 that it alone shared with SFV4 at position 1347, where prA7[74] had a valine residue. nsP4 contained only 2 aa mutations between SFV4 and the avirulent viruses. Overall in the non-structural proteins nsP2 contained the highest number of amino acid mutations between the avirulent viruses and SFV4.

The amino acid mutations located in the nsP1 protein are evenly spaced throughout the protein coding sequence with no mutations located in the extreme N-terminal domain. In addition to this, no amino acid mutations are located at the sites of putative methyltransferase and guanyl transferase motifs, therefore it is probable that these activities are retained by the nsP1 of all three strains of SFV in this investigation. Nonetheless, it could not be ruled out that one or more of the mutations in the nsP1 gene of CA7 and prA7[74] may fall in the RNA recognition site and / or binding site necessary for the initiation of minus-strand synthesis. Hence, conducting an RNA synthesis assay on these viruses was able to confirm if these mutations affect RNA replication.

As mentioned earlier, nsP2 contains the highest number of mutations between SFV4 and the avirulent virus amino acid sequence. CA7 has 15 amino acid differences when compared to SFV4 and an additional amino acid that is deleted in SFV4. prA7[74] has one less mutation than CA7 when aligned to SFV4 as it shares a serine residue with SFV4 at position 1206, it too has a residue at position 1258 that is

absent in SFV4. nsP2 is the most multifunctional protein of the non-structural proteins in alphaviruses and various regions of the gene are required for these functions. The main functions of nsP2 include acting as an autoprotease which processes the viral non-structural polyprotein by cleaving the nsP1/nsP2 and nsP2/nsP3 bonds, it is also postulated that it functions as an RNA helicase capable of RNA duplex unwinding. nsP2 contains ATPase and GTPase activities, therefore may have RNA binding capacities since NTPase activity is stimulated by single-stranded RNA. It has also been shown to be associated with ribosomes and contains nuclear targeting sequences (Peränen *et al.*, 1990) Sawaicki and Sawicki (1993) also suggested that nsP2 plays a significant role in RNA replication as an accumulation of nsP2 proteases leads to a cessation of minus strand synthesis. Having discussed the many postulated functions of nsP2, it appears that most of these mutations do not fall in regions where they may alter the proteinase functions or NTPase activities. However, the prospect that one or more of these functions may be defective cannot be ruled out.

In nsP3 there are 6 mutations between CA7 and SFV4 and 7 between prA7[74] and SFV4 as CA7 shares an isoleucine residue with SFV4 at position 1347 that prA7[74] does not. CA7 and prA7[74] also have two deleted aa regions in nsP3 that are present in SFV4. nsP3 is a phosphoprotein, although the full function of this gene is not fully known. Studies in Sindbis virus showed that mutations in the nsP3 amino terminal domain caused varying defects in subgenomic RNA synthesis and in negative-strand RNA synthesis (Wang *et al.*, 1991; Rikkonen *et al.*, 1994). It was suggested that mutations in the nsP3 affected only early events in replication and possibly prevented the formation of the initial replication complex that synthesises the negative strand template. Amino acid changes found in the amino-terminus of the avirulent nsP3 may therefore be important in affecting early RNA replication events. As the functions of this gene have not been fully determined it is not yet known what the effect of the two deleted regions may be on the avirulent SFV viruses.

The last of the non-structural proteins; nsP4, is an autoprotease that cleaves the alanine-tyrosine bond between nsP3 and nsP4. It has been reported that the amino acid residues 58-75 are highly homologous among alphaviruses indicating that the nsP4 protease is specific for alphaviruses (Takkinen *et al.*, 1990). nsP4 also contains the GDD motif that is conserved in RNA polymerases that remains conserved in both prA7[74] and CA7 nsP4 despite 2 amino acid mutations in the gene, hence the polymerase activity should remain stable in these viruses.

There are 50 possible amino acid mutations between the avirulent strains of SFV and SFV4, these may play a role cumulatively or individual amino acid mutations may exclusively influence virulence in SFV.

A surprising development occurred involving the mortality of Balb/c mice intranasally infected with CA7. The SP6-CA7 infectious clone, constructed by Tarbatt *et al* (1997) by substituting the SFV4 genome of the pSP6-SFV4 infectious clone, constructed by Liljeström *et al* (1991) with that of SFV-A7. However, the author was unable to substitute the 5' NTR of SFV4 with that of SFV-A7. On comparing the mortality rates of Balb/c mice intranasally infected with SFV-A7 and CA7, SFV-A7 killed no mice whereas CA7 caused a mortality rate of between 30 and 40% (Tarbatt, C., unpublished results). An investigation was therefore initiated to study the SFV 5' NTR as a possible virulence determinant in SFV. Previously, two nt changes in the 5'NTR of CA7 when compared to SFV4 had been demonstrated (Tarbatt *et al.*, 1997). However, on sequencing the 5' NTR of SFV-A7, SFV-A7[74], SFV4, prA7[74] and CA7, three mutations were observed at positions 21, 35 and 42 respectively. rA7[74] shared the nt at position 21 with SFV4 and CA7, however shared the both nts at positions 35 and 42 with SFV-A7, which differed in all 3 nts to both CA7 and SFV4. rA7[74] has been shown to occasionally kill 10% of Balb/c mice when administered intranasally (Minna Tuittila, personal communication). SFV4 has been shown to efficiently infect neurons whereas in avirulent SFV strains spread is partially restricted in CNS neurons and infection remains asymptomatic.(Glasgow *et al.*, 1994. It was postulated that because of the 5' NTRs probable involvement in the replication of virus RNA, that this factor may be at least partially responsible for higher rates of mortality in mice. On sequencing and predicting the secondary structure of the SFV 5'NTR it was noted that SFV-A7 and prA7[74] shared 4 stem-loop structures, whereas SFV4 and CA7 lacked the second small stem-loop structure in both the avirulent virus 5' NTRs due to the T/A mutation at position 35.

When mice were infected intranasally with these strains and the titres of virus in the brain determined it was apparent that SFV4 had at a titre over 100 times higher than the SFV-A7 strain and 10 times higher than that of CA7 and prA7[74], indicative of a higher rate of virus replication *in vivo*.

Reciprocal SFV 5' NTR chimeras were constructed to further investigate the relation between the 5' NTR and virus replication. This involved replacing the 5'

NTR of both pSP6-SFV4 and CA7 with those of SFV-A7 and rA7[74]. The 5' NTR of rA7[74] was replaced with that of SFV-A7 and SFV4. Infectious virus produced was infected intranasally in mice to measure mortality and to analyse differences in neuropathology caused by each and the RNA synthesis of each in BHK-21 cells was determined. No statistically significant difference in rate of RNA synthesis in culture was observed between any of the chimeric viruses. It has previously been shown by our group that virulent and avirulent SFV strains have markedly different abilities to infect neurons and cause death but have similar rates of growth in BHK-21 cells. These results do therefore suggest that in BHK-21 cells, the rate of RNA synthesis has not been significantly affected by the presence of 50 amino acid differences over the SFV genomes. Although extremely challenging experimentally, a study of the rate of RNA synthesis of these chimeras in a primary neuron cell culture merits further investigation.

In mice infected with CA7 and prA7[74] containing the SFV-A7 5'NTR no mortalities were detected, in contrast to CA7 with the rA7[74] 5' NTR and prA7[74] with the SFV4 5' NTR which caused the same percentage mortalities as CA7 and prA7[74] alone. Replacing the SFV4 5'NTR with either that of SFV-A7 or rA7[74] did not result in any change in mortality and all mice died by 5 d.p.i. This suggests that although the 5' NTR may be a virulence determinant it is under the control of more than one gene. The neuropathology of infected mice substantiates these findings, with chimeras that have the SFV-A7 5' NTR (with the exception of SFV4) showing a marked reduction in severity of lesions in the olfactory bulbs and brain. In the CA7 chimera that had the rA7[74] 5' NTR, a slight reduction in neuropathology was observed. These results are discussed further in Chapter 5.

This multigenic influence in virulence has previously been investigated by two other groups by combining changes the 5' NTR and the envelope glycoprotein E2. Kinney *et al* (1996) carried out mouse challenge experiments with VEE viruses of the virulent Trinidad donkey (TD) strain and its attenuated vaccine derivative (TC-83). Their results indicated that attenuation was partially determined by mutations within the 5'NTR, with mutations in the E2 envelope glycoprotein also playing a role. In a similar investigation on Sindbis (SV), Kobilier *et al* (1999) showed that substitution of 2 amino acids in E2 of the nonlethal neurovirulent strain of SV (SVN) with Met-190 and Lys-260 of the lethal SVNI strain resulted in the induction of paralysis in 2 and 5-week-old rats. Only substitution of both the 5' NTR and E2 SVNI determinants

produced virus with virulence properties indistinguishable from those of SVNI parent virus.

Although CA7 with the SFV-A7 5' NTR has now been attenuated to be virtually indistinguishable from SFV-A7, investigating the role of E2 and 5' NTR as virulence determinants of SFV would be beneficial. Chimeras have now been constructed in our laboratory that combine reciprocal SFV 5' NTRs with 6 of 8 amino acid mutations in E2 between SFV4 and CA7 and 2 of 4 mutations in E1. These may be very useful in determining the multigenic nature of virulence determinants in SFV. However as there are 50 amino acid differences between the virulent and avirulent strains of SFV other relevant multigenic combinations also warrant further investigation.

Chapter Five

Pathology

5.1 Introduction

The use of animal models to gain insight into the course and outcome of neurotropic viral infections has aided our understanding of viral neuropathogenesis. Sections of CNS tissue removed from infected animals at a series of time points during infection can generate information concerning the type of lesions produced, their topography and the cell populations involved. This information may then be correlated with any clinical symptoms resulting from viral infection.

5.2 Cells of the Central Nervous System

In order to fully comprehend the mechanisms of viral neuropathogenesis it is first important to understand the basic anatomy of central nervous system (CNS). The CNS can be divided into two entities, the brain and the spinal cord. The brain can be further divided into the brain stem which is an extension of the spinal cord, the cerebellum and the two cerebral hemispheres. At the very front of the brain, the olfactory bulbs can be found. (Carpenter, 1991; Brodal, 1992). Both the brain and spinal cord are suspended in cerebrospinal fluid (CSF) described as a fluid cushion for the CNS. CSF acts not only as a drainage route for the waste products of cerebral metabolism but also allows rapid circulation of substances secreted into the CSF to many brain regions (Segal, 2000). The brain is surrounded by the meninges made up of the pia mater and the arachnoid which constitute the leptomeninges and the dura mater (Smith, 1989).

There are two main categories of cells in the CNS; nerve cells known as neurons and support cells termed neuroglia. The support cells outnumber the nerve cells by approximately ten-fold and can be divided into four categories: astrocytes, oligodendrocytes, microglia and ependymal cells. The functions of these cells differ although they all, in part serve as supporting elements for the neurons while segregating groups of neurons from each other. A representation of these cell types is illustrated in figure 5.1

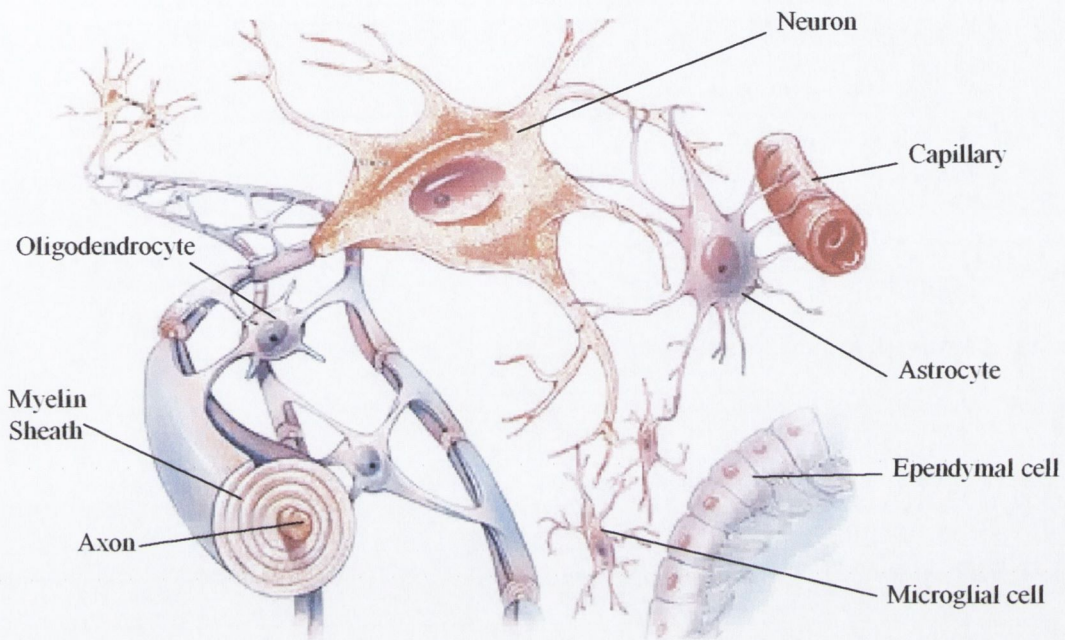


Figure 51 Diagrammatic representation of the cells of the CNS

An overview of the interaction of the neurons with the neuroglia of the CNS, including astrocytes, oligodendrocytes, microglia and ependymal cells. The axon and myelin sheath of a neuron are also indicated as is the interaction of the astrocytic foot processes with surrounding blood capillaries in the brain. (Adapted from http://www.mhhe.com/biosci/ap/holeessentials/student/olc/graphics/hole06chap_s/other/0298.jpg)

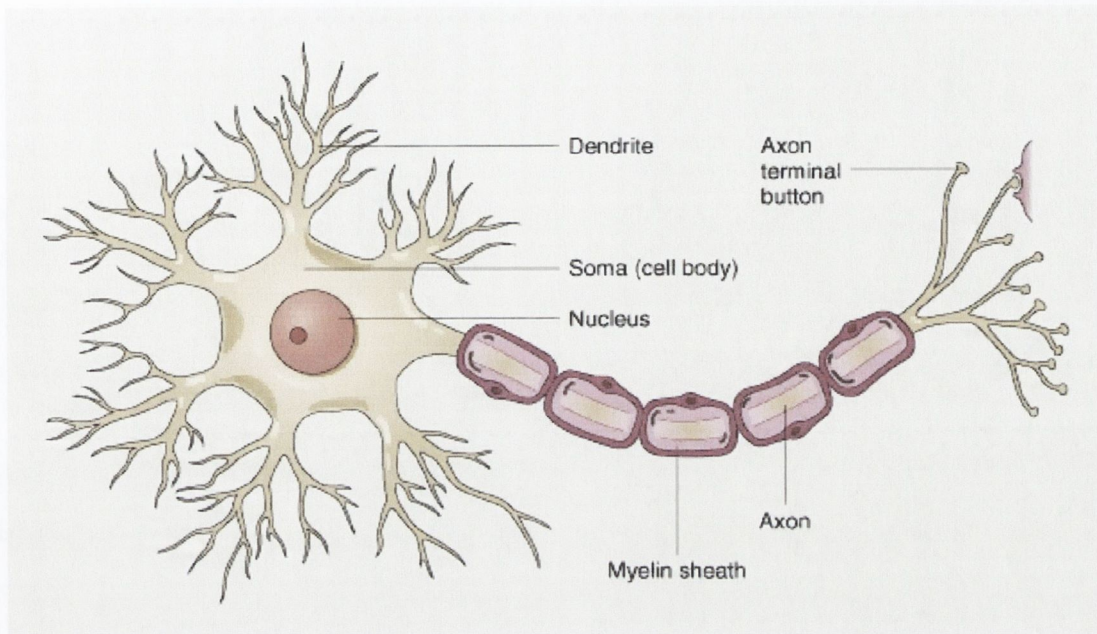
5.2.1 Neurons

Neurons are anatomical and functional units of the central nervous system. Axons clump together in bundles forming nerve fibrils, these in turn also bundle together to form long chains of nerve fibres which make up the nervous system. Individual neurons are composed of three distinct domains: the soma or cell body, the axon and the dendrites (Junqueira *et al.*, 1975; Starr and Taggart, 1989). The neuron is represented in figure 5.2.

The soma is comprised of a nucleus and cytoplasm containing cell organelles such as endoplasmic reticulum (ER), ribosomes and the Golgi apparatus (GA). The nucleus of a neuron is usually centrally located, large and spherical. When the nucleus is examined histologically and stained, chromatin is seen to be dispersed and stains lightly in a web-like pattern compared to the nucleolus, of which there may be several, which stain intensely. Characteristic of the cytoplasm is the large abundance of ribonucleoprotein associated with the rough endoplasmic reticulum (RER) and ribosomes. When viewed by light microscopy, large clumps of RER or Nissl bodies may be seen in some larger neurons, motor neurons in particular (Burns, 1997, Morris, 1987). The GA is prominent in most neurons and is visible as a large loose net surrounding the nucleus. In smaller neurons the GA extends into the base of dendrites (Junqueira *et al.*, 1975). Dendrites are multiple elongated processes extending from the soma to form dendritic trees. These then synapse with other dendrites in order to receive and transmit sensory signals from the environment.

A single tubular axon extends from each neuronal cell body and is responsible for conducting nerve impulses to other cells. Large axons are coated in a fatty insulating sheath called the myelin sheath. This sheath is essential in achieving high speed conduction of nerve impulses. In contrast to dendrites, axons have a constant diameter and do not branch liberally into tree-like structures. Unlike the cytoplasm of the soma, the axonal cytoplasm or axoplasm is poor in organelles. To combat this, new cytoplasm and other constituents are formed in the soma and flow out into the axon (Burt, 1993).

Neurons vary both in size and in their organisation, but they all essentially have the same structure. Neurons found in the olfactory bulbs for example are small and round, whereas those found in the hippocampus are large and pyramidal. Similarly, neurons may be organised into aggregates (nuclei) and laminar formations as is the case for neurons found in the cerebrum and cerebellum.



© 2000 John Wiley & Sons, Inc.

Figure 5.2 Diagrammatic representation of a neuron

The individual neuron is composed of three distinct domains: the Soma, the axon and the dendrites. Within the Soma resides the centrally located, large, spherical nucleus and organelle-containing cytoplasm. Multiple elongated processes extending from the Soma termed dendrites form dendritic branches that synapse with other dendrites to transmit and receive sensory signals. The axon extends from each Soma and is responsible for the conduction of nerve impulses, made faster and more effective by the presence of the surrounding myelin sheath. The terminal buttons of the axon relay and receive sensory signals that pass along the axon. (Adapted from <http://www.usm.maine.edu/psy/broida/101/neuron.JPG>)

5.2.2 Astrocytes

Astrocytes are the largest of the neuroglial cells in the CNS. Their principal role is to act as “scaffolding” for the neurons of the CNS. Other functions include fluid and ionic homeostasis and antigen presentation. Astrocytes, as their name suggests, are star-like in shape and have long processes. Their nucleus is centrally located and spherical, staining lightly under histological examination. Many of their processes have expanded pedicles, known as vascular feet, at their ends as they allow attachment to blood capillaries. Astrocytes also make a variety of contacts with neurons (Burns, 1997, figure 5.1).

There are two types of astrocytes, those found in the white matter termed fibrous astrocytes, and those in the grey matter termed protoplasmic astrocytes (Kimelberg and Norenberg, 1989). Fibrous astrocytes have long, smooth and slender processes that branch infrequently, whereas protoplasmic astrocytes have many branches and their processes are short and broad. Astrocytes in contact with neurons are thought to be important for the exchange and removal of substances, such as the removal or degradation of certain extracellular neurotransmitters from the synaptic spaces, a build up of which are deleterious to neurons. Astrocytic foot processes surrounding blood capillaries in the brain are thought to be involved in forming the blood-brain barrier (BBB; Brodal, 1992).

5.2.3 Oligodendrocytes

Smaller than astrocytes and with shorter, less numerous processes than other neuroglia, oligodendrocytes are located in both the white and grey matter of the CNS. In the white matter oligodendrocytes appear in rows along the myelinated nerve fibres, whereas in grey matter they are mainly localised in close proximity to the neuronal somas and are referred to as satellite cells.

Typically oligodendrocytes have an irregularly shaped, small, dark, lymphocyte-sized nucleus (Burns, 1997) which contains dense clumps of chromatin. The cytoplasm contains numerous cellular organelles, including in particular, free and attached ribosomes, extensive Golgi apparatus and several mitochondria (Burt, 1993).

The function of oligodendrocytes is the production of myelin that surrounds the axons of the CNS. Schwann cells have a similarity to oligodendrocytes in that they also produce myelin, however Schwann cells are involved in myelination of axons in the peripheral nervous system rather than within the CNS. Another

difference between Schwann cells and oligodendrocytes is that the latter myelinate several axonal segments, whereas Schwann cells myelinate single axonal segments. Myelin in the CNS is composed of oligodendrocyte cell membrane that is spirally wrapped around the axons, layers of which are termed lamellae (Brodal, 1992). The more times an oligodendrocyte cell membrane is wound around the axon the thicker the myelin sheath. Myelin is composed of lipids and carbohydrates including myelin-associated protein (MAP), myelin basic protein (MBP) and myelin oligodendrocyte glycoprotein (MOG; Morris, 1987). Detecting oligodendrocytes by immunofluorescence has been achieved by using antibodies against a product of oligodendrocytes termed CNPase.

5.2.4 Ependymal Cells

Ependymal cells are neuroglial cells that line the cerebral ventricles and neural canal. They are closely related to the simple cuboidal epithelial cells of the choroid plexus. Their role is not prominent in most reactions in the brain, however the focal loss of these cells is followed by a compensatory proliferation of subependymal astrocytes. This results in the production of small nodules termed ependymal granulations on the walls of the ventricles giving an appearance referred to as ventricular ependymitis (Morris, 1987, Burns, 1997).

Ependymal cell nuclei stain lightly under histological examination, and the chromatin is evenly dispersed. The cytoplasm has the typical complement of organelles, although has minimal RER. Tight junctions hold the apical and luminal edges of adjacent cells together, although these junctions do not completely surround the ependymal cells, allowing large molecules to move freely between the CSF and the subependymal spaces (Burt, 1993).

Certain viruses, particularly cytomegalovirus (CMV) may produce extensive injury to the ependymal cells, resulting in prominent associated viral inclusions within the cells (Burns, 1997).

5.2.5 Microglia

Microglia have small, elongated, dense cell bodies. Their nuclei contain condensed chromatin and have an elongated shape along the axis of the cell body, thus allowing simple histological identification when compared to other neuroglia cells that possess spherical nuclei. Microglia have a thorny appearance due to their

short processes being covered by numerous small expansions. These cells are not numerous, but can be located in both the white and grey matter of the CNS (Junquiera *et al.*, 1975)

Microglia are in all likelihood derived from circulating monocytes and they function as the major phagocytes in the CNS. When the brain has undergone injury the appearance of microglia changes. The nuclei enlarge and elongate to form rod cells. Microglia containing abundant intracellular lipids are termed gitter cells, and these in turn may aggregate to form microglial nodules.

5.3 Pathology and its Terminology

Similar terminology is used to describe neuropathological processes and outcomes in several different diseases. Inflammation of the brain parenchyma is termed encephalitis, inflammation of the meninges is termed meningitis and inflammation of the spinal cord tissue is termed myelitis. Given that the regions of the CNS are closely joined, more specific terminology such as meningoencephalitis or meningoencephalomyelitis often is applied (Smith, 1989).

Most neurotropic viruses show a tropism for specific cell types leading to lesions characteristic of the infected cell. The types of lesions observed following a viral infection of the CNS are varied and may include necrosis, demyelination, gliosis, and inflammation and spongiform degeneration.

5.3.1 Necrosis

Necrosis refers to the destruction of the neural tissue and frequently is associated with cytotoxic edema. Neuronal necrosis starts with cytoplasmic microvacuolation caused by swelling of both the endoplasmic reticulum and mitochondria. Disappearance of Nissl bodies, condensation of the cell cytoplasm and break up of nuclear material, known as nuclear pyknosis, soon ensues. Basophilic masses appearing on the surface of the neuron correspond to the distortion of small areas of neuronal cytoplasm caused by pressure from swollen astrocytes. The cytoplasm is eventually homogenised and cleared, resulting in the gradual disappearance of neuronal cell bodies (Brodal, 1992).

5.3.2 Demyelination

Demyelination refers to the loss of myelin that surrounds the axons of the CNS. When myelinated fibres are clustered together they appear white in colour and form the white matter of the brain and spinal cord. If only the myelin sheath is damaged nerve function is often restored; this is termed primary demyelination. However, if the underlying axon is damaged, nerve functionality may be permanently lost; this is termed secondary demyelination. Nerve fibres are capable of regrowth and remyelination, however scar tissue (gliosis) often forms and impedes proper growth and recovery (Kimerberg and Norenberg, 1989). Differences in rates of remyelination have been detected in mice of different strains following infection with SFV. For BALB/c mice infected intraperitoneally with SFV-A7, demyelination is maximal at 14 days post infection, at a time where infectious virus has been cleared from the CNS. The lesions are then quickly remyelinated. In contrast, SJL mice similarly infected with the M9 mutant of SFV show demyelinating lesions which may persist up to a year (Donnelly *et al*, 1997, Smyth *et al*, 1990)

5.3.3 Gliosis

Gliosis is the most frequent change in response to CNS damage. Injury to the CNS results in an increase in the size and number of astrocytes and proliferation of microglia. This change is often referred to as reactive astrocytosis, gliosis or glial scars. In addition to possessing increased metabolic activity, reactive astrocytes have more processes and glial filaments than normal astrocytes (Kimelberg and Norenberg, 1989).

5.3.4 Inflammatory Lesions

Inflammatory lesions may be localised or disseminated and consist of perivascular cuffing and infiltrates of various leucocytes primarily macrophages, lymphocytes and neutrophils. The composition of the infiltrates frequently depends on the nature of the infection.

5.3.5 Spongiform Degeneration

Spongiform degeneration refers to vacuolation of neuronal cell populations, astrocyte or oligodendrocyte cell cytoplasm, cell processes or myelin sheaths. It is so called due to the spongy vacuolation visible by light microscopy.

5.4 Routes of Infection into the CNS

5.4.1 The Blood-Brain Barrier (BBB)

The BBB is effectively composed of capillary endothelial cells with extensive tight junctions wrapped with astrocytic foot processes. The astrocytic footplates, the tight junctions of the endothelial cells, and the plasma membranes together form a physical barrier to limit substance diffusion or leakage (Junquiera *et al.*, 1975, Brodal, 1992).

Any loss of the tight junctions between the endothelial cells is responsible for reducing the effectiveness of the BBB. In many cases of viral infection, this is due to the direct infection of the endothelial cells. Several other viruses, however, are capable of crossing the BBB by a mechanism similar to the process of substance diffusion while others are chauffeured across the endothelial cells in infected leucocytes (Johnson, 1982).

5.4.2 Haematogenous Route

The majority of CNS infections result from an infectious agent gaining access to the CNS via the hematogenous route. The precise mechanism by which infectious agents may penetrate the BBB is not fully elucidated for all infectious agents, however, the choroid plexus appears to be a major site of entry. Localisation of infectious agents in the vascular component of the choroid plexus leads to spillage of the infectious agents into the CNS (Smith, 1989).

5.4.3 The Neural route

Although most neurotropic viruses infect the CNS via the hematogenous route, a few utilise the neural route or intra-axonal transport. Typically, transport of rabies virus occurs via sensory and motor nerves at the initial site of infection where the virus travels to the anterior horn cells of the spinal cord. Active cerebral infection is followed by passive centrifugal spread of virus to peripheral nerves (Johnson, 1982; Smith, 1989).

It has been shown in several studies that viruses may also penetrate the CNS via the olfactory nerve endings (Kaluza *et al.*, 1987; Balluz *et al.*, 1993). Our group has used the intranasal route of inoculation to investigate the neuropathogenesis of

Semliki Forest Virus (SFV) and Louping Ill Virus (LIV) infections in mice and lambs (Jerusalmi *et al.*, 2003; Keogh *et al.*, 2002; Sheahan *et al.*, 2002). The intranasal route of inoculation is more stringent than the intramuscular, subcutaneous and intraperitoneal routes and more natural than the intracerebral route.

5.4.4 The Olfactory System

The olfactory system is composed of four main structures: the olfactory epithelium, the olfactory nerve, the olfactory bulbs and the olfactory tracts. It is located in the frontal area of each cerebral hemisphere. An illustration of the location of the human olfactory pathway may be seen in figures 5.3A. The olfactory bulb resides in a corresponding site in mice and other vertebrates and is the first processing centre in the olfactory pathway. It has a typical cortical appearance and is composed of six well defined layers. Several types of nerve cells, the most notable of which are the mitral cells, are present in the grey matter of the olfactory bulbs (Carpenter, 1991; figure 5.3B). The neurons of the olfactory bulb direct their axons via the olfactory tract to the cerebral cortex and various nuclei in the vicinity of the temporal lobe (Brodal, 1992; Burt, 1993).

Viruses rely on bipolar neurons to enter the CNS after intranasal administration. Whereas one end of an olfactory neuron is exposed to the external environment of the nasal cavity, the other end terminates in the CNS. The connections of the olfactory epithelium and olfactory bulb are shown in figures 5.3 A and B.

The olfactory epithelium covers both the posterior and superior regions of the nasal cavity and contains three cell types: olfactory neurons, supporting cells and basal cells. The olfactory neurons are bipolar with dendrites extending to the epithelium and an unmyelinated axon contributing to the olfactory nerve. Supporting or secretory cells are interspersed among the bipolar neurons, with basal cells lying between the neurons and supporting cells. The function of basal cells is to form new bipolar neurons and to separate the epithelium from the underlying connective tissue and cartilage of the cribriform plate (Fitzgerald, 1992). An overview of how viruses travel to the brain through the olfactory mucosa, olfactory bulbs and glomeruli is illustrated in figure 5.3. (Sammin *et al.*, 1999, Sheahan *et al.*, 1981, Atkins *et al.*, 1996)

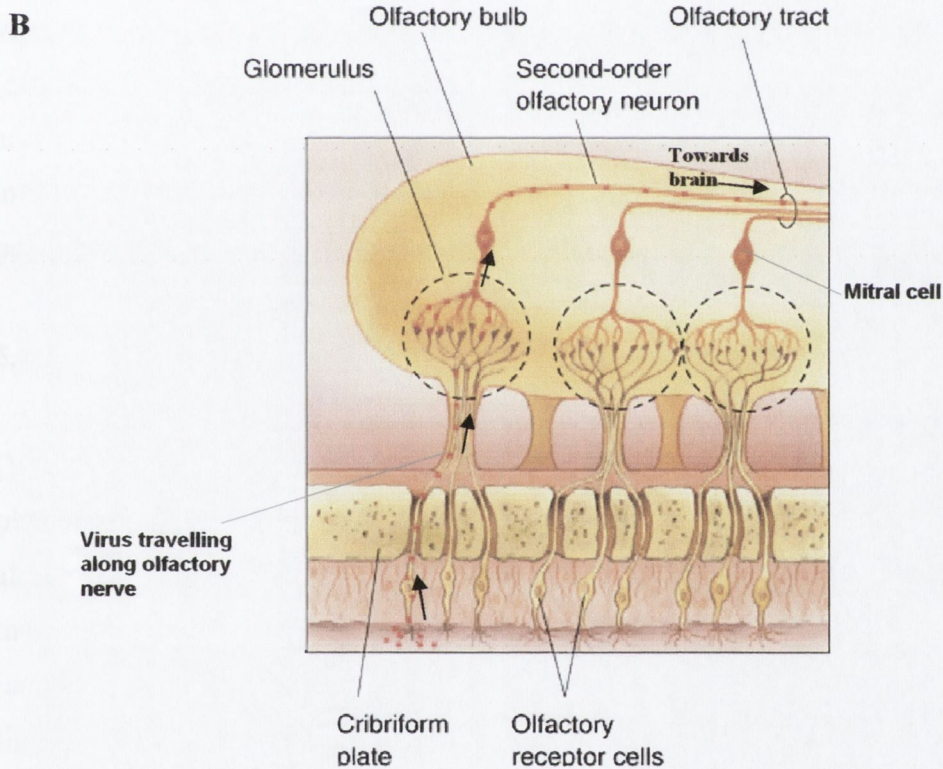
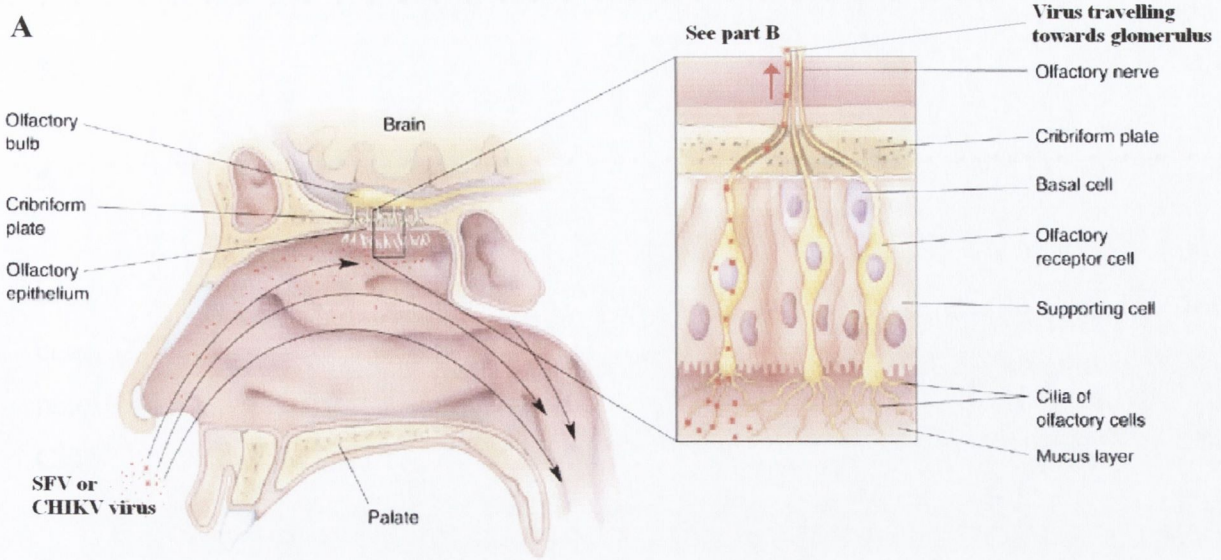


Figure 5.3 Virus infection via the olfactory route

The movement of virus particles from the nasal cavity along branches of the olfactory nerves through the olfactory glomerulus and mitral cells, eventually reaching the brain, is represented by red dots. The direction of travel is illustrated with black arrows.

(Adapted from <http://www.bioon.com/book/biology>)

5.5 Materials and Methods

5.5.1 Intranasal infection of Balb/c mice

Groups of 3 female Balb/c mice per timepoint aged 60-80 days were intranasally infected with 20 μ l per nostril of SFV or CHIKV virus with concentrations of 1×10^8 p.f.u / ml. The health, clinical signs and time of death were recorded over a 7-14 day period. There were two timepoints at 7 dpi and 14 dpi for CHIKV and SFV strains and one timepoint at 7 dpi only for SFV 5' NTR chimaeras.

5.5.2 Brain Perfusion and Fixation

Mice were deeply anaesthetised with halothane and perfused via the left ventricle with phosphate buffered saline (PBS), followed by 10% formol saline (obtained by diluting 100 ml formaldehyde solution (BDH) 1:10 with H₂O and adding 9 g of sodium chloride (Sigma)) for 5 min. Perfused mice were left overnight in formol saline at 4 °C before the brains and olfactory bulbs were removed intact and processed for paraffin embedding, sectioning and staining.

5.5.3 Paraffin embedding and sectioning

Paraffin embedding and sectioning was performed by Ms. Alex Whelan (Veterinary Pathology Laboratory, University College, Dublin). Excised brains and olfactory bulbs were dehydrated in a series of graded alcohol washes; 50% (vol/vol) alcohol for 60 min, 70% (vol/vol) alcohol for 60 min, 90% (vol/vol) alcohol for 60 min, followed by two 40 min washes in absolute alcohol. Samples were then immersed in a 1:1 absolute alcohol: xylene solution for 60 min before being washed 3 times in absolute xylene, for 40 min / wash. This was followed by four individual immersions in paraffin wax; again each for 40 min. Tissue samples were then mounted in paraffin blocks prior to sectioning. Four to six μ m thick paraffin sections were prepared using a microtome, placed on standard microscope slides and fixed with acetone prior to staining.

5.5.4 Histological Staining

Haematoxylin and eosin (H&E) is the most widely used stain for diagnostic histopathology of tissue sections. Haematoxylin is a purple-blue dye that stains DNA, RNA, proteins and other acidic complexes in the cell. As the nucleus of a cell comprises a large quantity of DNA and RNA it appears dark purple following haematoxylin staining. Similarly, the cytoplasm of cells containing significant quantities of ribosomes generates a purple hue termed cytoplasmic basophilia. Eosin is a non-specific dye that predominantly stains basic proteins a pink to red colour, although it does not distinguish between cellular and extracellular proteins (Bancroft and Stevens, 1990). Luxol fast blue is a versatile dye that can combine with many other dyes and is used predominantly for staining myelin. One of the best combinations for use in the study of neuropathology and normal anatomy is Luxol fast blue combined with cresyl violet dye, used for staining neurons (Bancroft and Stevfins, 1990).

5.5.5 Pathology Grading System

Coronal sections of each brain collected from five different levels were examined 'blind' and given an estimated score for the severity and distribution of the pathological changes. Individual parameters were given a score ranging from 0 (no visible lesions) to 5 (severe lesions).

5.6 Results

Consistent with previously reported findings for SFV4 and SFV-A7 by our group (Glasgow *et al.*, 1991, 1994; Tarbatt *et al.*, 1997; Jerusalmi *et al.*, 2003), brain lesions were localised primarily in olfactory pathways. Variation in severity of lesions between individual mice and bilateral symmetry was common. Olfactory bulbs, anterior olfactory nuclei, lateral olfactory tracts, pyriform cortex, anterior commissure, hippocampus, thalamus and cingulate cortex were regular sites of pathological change.

Laminar and focal necrotising lesions at 7 dpi were accompanied by vascular congestion, spongiform degeneration and infiltrates of macrophages and lymphoid cells. Laminar areas of neuronal necrosis were most severe in the olfactory bulbs and in the olfactory and pyriform cortex. Multifocal areas of neuronal necrosis with pyknotic nuclei and hypereosinophilic cytoplasm occurred primarily in the thalamus and hippocampus. Affected areas at 14 dpi were characterised by neuronal depletion and gliosis.

Demyelinating lesions were localised primarily in the olfactory tracts. Areas of demyelination at 7 dpi showed decreased staining with luxol fast blue and infiltrates of lymphocytes and macrophages. Astrocytic proliferation, lipid-laden macrophages and lymphoid perivascular cuffing were prominent in areas of demyelination at 14 dpi. Examples of the above lesions are illustrated in figure 5.1.

5.6.1 Chikungunya Virus – Seven geographically distinct strains

5.6.1.1 CHIKV – Ross

7 d.p.i. – Severe (5+) necrotising lesions in 3 of 3 mice

14 d.p.i. – Severe (5+) necrotising lesions in 1 of 3 mice; less severe (4+) lesions in 2 mice

5.6.1.2 CHIKV – DaKAR

7 d.p.i. – Moderate (3+) lesions in 3 of 3 mice

14 d.p.i. – Moderate (3+) lesions in 2 mice; mild (1+) lesions in 1 mouse

5.6.1.3 CHIKV – 37997

7 d.p.i. – No abnormality detected in 3 of 3 mice

14 d.p.i – Mild (1+) lesions in 1 mouse; no abnormality detected in 2 mice

5.6.1.4 CHIKV – P0731460

7 d.p.i. – Mild (1+) lesions in 1 mouse: no abnormality detected in 2 mice

14 d.p.i – No abnormality detected in 3 of 3 mice

5.6.1.5 CHIKV – 181/25

7 d.p.i. – Mild (1+) lesions in 1 mouse: no abnormality detected in 2 mice

14 d.p.i – No abnormality detected in 3 of 3 mice

5.6.1.6 CHIKV – PH H15483

7 d.p.i. – No abnormality detected in 3 of 3 mice

14 d.p.i – No abnormality detected in 3 of 3 mice

5.6.1.7 CHIKV – SV450

7 d.p.i. – No abnormality detected in 3 of 3 mice

14 d.p.i – No abnormality detected in 3 of 3 mice

5.6.2 Semliki Forest Virus - 5 Strains

5.6.2.1 SFV-A7 & A7[74]

7 d.p.i – Moderate (3+) inflammatory demyelination in 3 of 3 mice

14 d.p.i – Moderate (3+) inflammatory demyelination in 3 of 3 mice

5.6.2.2 SFV4

4 d.p.i – Severe (5+) necrotising lesions in 3 of 3 mice

5.6.2.3 CA7

7 d.p.i – Severe (5+) necrotising lesions in 3 of 3 mice

14 d.p.i – Severe (5+) necrotising lesions in 3 of 3 mice

5.6.2.4 rA7[74]

7 d.p.i – Severe (5+) necrotising lesions in 2 of 2 mice

14 d.p.i – Severe (5+) necrotising lesions in 3 of 3 mice

5.6.3 SFV 5' NTR Chimaeric Viruses

5.6.5.1 CA7 + A7 5' NTR

7 d.p.i – Mild (2+) inflammatory demyelination in 3 of 3 mice

5.6.5.2 CA7 + rA7[A7] 5' NTR

7 d.p.i – Severe (4+) necrotising lesions in 3 of 3 mice

5.6.5.3 rA7[74] + A7 5' NTR

7 d.p.i – Moderate (3+) inflammatory demyelination in 3 of 3 mice

5.6.5.4 rA7[74] + SFV4 5' NTR

7 d.p.i – Severe (5+) necrotising lesions in 3 of 3 mice

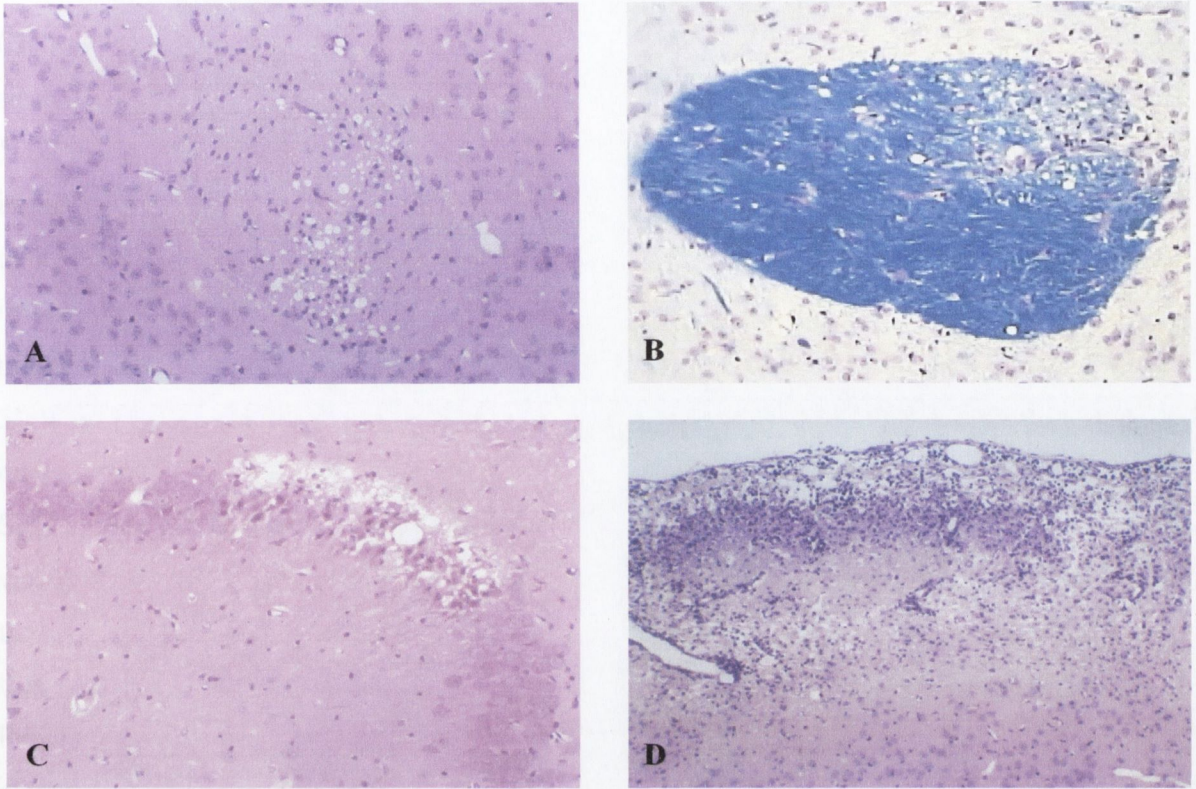


Figure 5.1 Neuropathology in Balb/c mice infected i.n. with CA7, SFV-A7 and CHIKV

(A) Balb/c mouse, CA7, 7 dpi. Spongiform degeneration and demyelination in the anterior commissure. H&E, x 200. (B) Balb/c mouse, SFV-A7, 14 dpi. Focal area of demyelination in the anterior commissure. Luxol Fast Blue, x 200. (C) Balb/c mouse, CA7, 7 dpi. Focal area of spongiform degeneration and neuronal necrosis in the hippocampus. H&E, X200. (D) Balb/c mouse, CHIKV, 14 dpi. Laminar neuronal necrosis and dense infiltrates of lymphocytes and macrophages in the piriform cortex. H&E, x 100.

5.7 Discussion

Pathological examination was carried out to determine whether infections with CHIKV Ross compared to six geographically distinct strains of CHIKV and whether similar pathological changes in the CNS resulted. The neuropathology caused by SFV-5'UTR chimaeras was also investigated to confirm whether SFV4, CA7, and SFV-A7 induced comparable pathological lesions in the CNS, and to determine any involvement of the 5' UTR as a pathogenicity determinant. Histopathology results presented in this investigation demonstrate the changes in the CNS of Balb/c female adult mice infected intranasally with six strains of CHIKV, virulent and avirulent strains of SFV and SFV-5'UTR chimaeras. The intranasal route of inoculation was chosen as it is a more direct natural route for infection of the CNS and results in less variable response than i.p. for SFV-A7 (Sheahan *et al.*, 1996). On comparing the consequences of infection with SFV via the i.n. and subcutaneous routes, Kaluza *et al* (1987) described the spread of virus through neural axons as one of the possible modes of entry into the brain, and indicated that virus in the olfactory bulbs was detected before other areas of the brain. It is this localisation of lesions in the olfactory pathways that greatly facilitates comparative studies between different virus strains.

Identification of lesions in the brain after i.n. infection confirmed that CHIKV has the ability to use the olfactory pathway and spread through neuronal tracts to reach the brain. However, this was only the case for five of the seven strains of CHIKV, with two strains: SV-0451/96 (Thailand) and PH H15483 (Phillipines) showing no induction of lesions. Three strains: 181/25 (Thailand), PO731460 (India) and 37997 (Senegal) caused mild lesions and one strain moderate lesions (DAKAr B16878, C.A.R). Of these viruses, only DAKAr B16878 and Ross were detected in the brains by plaque assay. The brains of mice infected with the Ross strain (Tanzania) exhibited severe necrotising lesions although mice stayed healthy and survived infection. The presence of necrotic neurons suggests CHIKV infection in the brain, however due to the survival of infected animals it is possible that the rate of multiplication of CHIKV in the neurons enables the immune system to intervene before levels of damage caused clinical symptoms or death. The differences in severity of neuropathology caused by these seven CHIKV strains may possibly be explained by their different passage histories possibly affecting their ability to efficiently infect, replicate in, and/or bud from different cell types *in vivo*, in addition to possibly differing in neurovirulence in their natural environments.

A restricted rate of multiplication in neurons was also observed for SFV-A7 and SFV-A7[74] which do not cause death in adult mice and produced moderate inflammatory demyelination. SFV4 however caused severe necrotising lesions and produced a lethal threshold of damage to neurons before the immune system could intervene resulting in 100% mortality by 5 d.p.i. CA7 and rA7[74] also caused severe necrotising lesions in infected adult mice, however only 30 and 10% respectively of mice infected with these viruses died.

Interestingly, mice infected with SFV chimaeras of CA7 and rA7[74] that incorporated the 5' UTR of SFV-A7 showed no mortality and a significant decrease in the severity of lesions caused. It was felt that the lesions induced at 7 d.p.i were sufficient for comparison between viruses, thus mice were not examined at 14 d.p.i. The nucleotide sequence of the CA7 and SFV4 5' UTRs when compared to that of SFV-A7 differed by only three nucleotides. The rA7[74] 5' UTR differed only by one nucleotide at position 21. From the pathology results, the survival rates and sequence analysis, it appears that substituting an adenine residue at position 21 of rA7[74] with the guanine of SFV-A7 results in a 100% survival rate and a reduction in the severity of inflammatory lesions from severe to moderate. In CA7, all three nucleotides at positions 21, 35 and 42 were replaced with those of SFV-A7. Not only was the survival rate of infected mice increased from 70% to 100% but the severity of necrotising lesions was significantly reduced and pathology similar to that seen for SFV-A7 was observed, including mild inflammatory demyelination and perivascular cuffing localised primarily in the olfactory tracts. Substitution of the CA7 5' UTR with that of rA7[74] also resulted in a 100% survival rate in i.n. infected mice, although severe necrotising lesions similar to those caused by rA7[A7] were still observed. No differences in mortality were observed between mice infected with rA7[74] and rA7[74] with the SFV4 5' UTR (two nucleotides at positions 35 and 42 changed to those of SFV4). Similarly, no significant differences in the severity of both laminar and focal lesions in the lateral olfactory tracts, pyriform cortex was observed.

This demonstrates that the 5' UTR has an important role in a virus's ability to replicate efficiently in different cell types in the murine CNS, resulting in differing severities of neurological damage. Subsequently, the ability of an infected animal's immune system to intervene before levels of damage are too severe, results in an increased likelihood of infected animals surviving infection.

Chapter Six

General Discussion

6.1 General Discussion

Chikungunya virus (CHIK) has been attributed to over forty outbreaks since it was first recorded in Tanzania in 1952. The arthritic disease of sudden onset results in severe physical incapacitation in humans. CHIK is predominantly found in Central and Southern Africa and South East Asia, although cases have also been recorded in Australia. The prototype strain was isolated from both mosquitoes and humans by Ross in 1956 following the Tanzania outbreak of 1952-53, and is termed "Ross" (Powers *et al.*, 2000). Early work carried out on CHIK involved investigating the physical properties of the virus and included electron-microscopy, virus formation, protein synthesis analyses, expression of proteins and biological comparisons to other alphaviruses (Igarashi *et al.*, 1970; Chanas *et al.*, 1979a, b; Simizu *et al.*, 1984 Ranadive and Banerjee, 1990). Blackburn *et al* (1995) investigated the antigenic relationship between CHIK and the closely related O'nyong nyong virus suggesting that ONNV was a subspecies of CHIK until Powers *et al* (2000) showed through phylogenetic analyses that they were two independent members of the SF subgroup of alphaviruses. In this investigation, the phylogenetic relationships between strains of CHIK, ONNV and SFV were determined over the non-structural and structural proteins, giving a more accurate representation of the degree of similarity between these viruses than earlier investigations.

In 1986 Levitt *et al* produced a live-attenuated vaccine which later proved to have partially reverted to the unattenuated form. This was due to the cell type in which it was developed being changed from master seed to production seed. Since no good animal model for CHIK virus infection has yet been described, the long-term aim of this investigation was the development of a system to test potential vaccines.

On initiating this investigation, only the sequence of the structural polyprotein of the vaccine strain of CHIK (181/25) submitted by Parker (1994) was available on Genbank. By aligning this sequence to the same region of the Gulu strain of ONNV, a 78% nucleotide identity was observed. The prototype Ross strain of CHIK was therefore originally sequenced using primers designed from the structural polyprotein of 181/25 and the non-structural polyprotein of ONNV Gulu. New primers were designed from each amplified region of CHIK that was sequenced. The 5' and 3' nontranslated regions amplified using 5'-3' RACE PCR. This was the first complete CHIK genome to have

been sequenced and submitted to Genbank, since then two more complete CHIK genomes have been submitted: the S27 strain (Khan *et al.*, 2002) , 37997 (Vanlandingham *et al.*, 2005) and a structural polyprotein sequence of an Indian strain termed Nagpur (Ranadive, 2003). CHIK was subsequently characterised in this investigation, involving an array of studies both *in vitro* and *in vivo*. On comparing CHIK to another virus SFV-A7 that is well characterised in our lab we were able to investigate several facets of this virus. Intranasal infection (i.n.) with CHIK caused not only severe necrotizing lesions in the brains of mice but also focal areas of moderate inflammatory demyelination, accompanied with astrocytic proliferation, neuronal depletion and gliosis. When immunofluorescent studies were carried out it was shown that CHIK infects oligodendrocytes just as efficiently as SFV, possibly a cause of the demyelination observed in the brains.

Subsequent analyses of growth *in vitro* showed that CHIK grew efficiently in BHK-21 cells and efficiently synthesized RNA. To investigate virus growth in cells of the CNS, a primary mixed glial cells culture was established, infected, and cell viability measured. Again, CHIK efficiently infected cells to a similar level as SFV-A7. As alphaviruses are generally thought to be neurotropic viruses, their growth in cell-lines such as BHK-21 or vero cells may not be completely representative of how they function *in vivo*. An experiment to determine the titres of virus in the brains of i.n. infected mice at daily timepoints over 10 days was carried out. Both CHIK and SFV-A7 reached peak titres in the brain at 5 d.p.i. CHIK initially took longer to produce virus particles in the first 48 h.p.i., but grew at a much faster rate than SFV-A7 from that point and had a marginally higher titre at 5 d.p.i. This surge in virus production could possibly be the explanation for the degree of severity of lesions in the brains of CHIK infected mice being significantly more than those caused by SFV-A7.

An *in vivo* experiment was pursued to investigate this further by comparing the *in vivo* virus titres of CHIK six other geographically distinct CHIK strains. The vaccine strain 181/25 and another strain DAKAr B16878 that has been phylogenetically associated with SFV rather than CHIK (Powers *et al.*, 2000) but is thought to be a strain of CHIK were among the 6 strains used. Initially to determine the lethality of these strains groups of mice were infected with each virus, none caused mortality in i.n.

infected mice. Subsequently, brain and blood titres of i.n. CHIK-infected mice were determined. Only two CHIK strains (Ross and DAKAr B16878) produced any virus in the brains of i.n. infected mice, no virus was detected in the blood of any of the mice. The six geographically distinct CHIK strains were supplied by Dr. Ann Powers (CDC, Fort Collins, USA). They have been isolated from mosquitoes following African and Asian outbreaks over the past 45 years. CHIK Ross however has undergone several passages in BHK-21 cells within our laboratory and may have an increased ability to grow *in vivo* in small rodent hosts relative to CHIK strains passaged in mosquito cells. The only other strain of CHIK to be detected in the brain was DAKAr B16878 which although phylogenetically closer to SFV than CHIK, also is the only other one of these strains to have been repeatedly passaged in BHK cells. Other strains were previously grown in *Ae. Pseudoscutellaris* (AP61) mosquito cells, vero cells, rhesus monkey (LLC-MK2) cells and MRC5 human lung cells. CHIK strains also differed in plaque morphology with the 181/25 vaccine strain producing very small plaques when compared to all other CHIK strains. RNA synthesis has no proof-reading activity and can therefore undergo mutations while replicating within the host cell, thereby generating a number of RNA species each differing perhaps by only a single nucleotide change. DAKAr B16878 produced a mixture of small and large plaques suggesting such a mixed population species

The construction of a full length CHIK cDNA clone was achieved through a combination of reverse transcription and long range PCR. Restriction sites within five PCR fragments spanning the CHIK genome and restriction sites present in two commercially available cloning vectors were subsequently used. Throughout this investigation the amount of RT-PCR carried out was kept to a minimum as to avoid the generation of spontaneous point mutations. At each step of the cDNA clone construction, the orientation and size of successfully inserted fragments was verified by restriction digestion using selected enzymes. On generating a full-length clone, it was reverse transcribed using a T7 promoter to generate full length CHIK RNA. At one stage of the construction of the CHIK clone, 62 nucleotides from the litmus 28i cloning vector were introduced downstream of the virus 3' NTR. This was necessary in order for subsequent construction steps to be completed using the *Spe I* restriction site. RNA was then

successfully reverse transcribed from the cDNA clone and electroporated into BHK-21 cells. However, no infectious virus was produced, there are several possible explanations for this.

Kuhn *et al* (1992) tested for rates of SIN RNA synthesis in different cell types using 4 mutants with changes in the 5' NTR and 4 with changes in the 3'NTR. They showed that all the mutants had defects in RNA synthesis and that virus production was host-cell dependent with mouse, chicken and mosquito cells responding differently to each change from the wildtype 3' NTR. Therefore the addition of 62 nt to the extreme 3' end of the 3' NTR may have had a similar effect in CHIK RNA synthesis in electroporated BHK-21 cells. Another explanation for the lack of production of infectious virus could be the possible absence of a poly (A) tail. A poly (A) tail was incorporated into the clone using the *Spe I* and *Sac I* restriction sites.

The most likely reason for the lack production of infectious virus is the generation of spontaneous point mutations due the genome having been amplified by RT-PCR or during fragment-cloning. A high fidelity proof reading polymerase was used to minimize this. The TaqMaster system developed by Eppendorf for amplification of long PCR fragments used a combination of high fidelity proofreading polymerases, however it still has a rate of error in its proof-reading capacity, albeit considerably lower than polymerase combinations produced by other manufacturers. A single nucleotide mutation in the genome could disrupt the read-through of the CHIK open reading frames, or the deletion of a cleavage site. Similarly, nucleotide mutation(s) could result in amino acid changes with the outcome of a particular protein or proteins not forming the correct physical conformation. In order to verify these possible outcomes and to further develop the CHIK full length cDNA clone for future use as a virus-vector vaccine, it should be sequenced using the latest proof reading polymerases. The sequence should then be aligned with the currently sequenced CHIK strains and any observed mutations reverted to the prototype strain.

The range of virulence caused by differing strains of SFV is broad and includes fatal encephalitis, immune-mediated demyelination, fetal abortion and teratogenesis. Virulent strains of SFV produce fatal encephalitis in the murine CNS irrespective of route of infection or age. This is due to a lethal threshold of damage to neurons before the immune system can intervene. Adult mice infected with avirulent strains of SFV are asymptomatic regardless of the route of infection. SFV-A7 and SFV-A7[74] do however induce immune-mediated T-cell dependent demyelination, thought to occur due to a slower rate of multiplication in neurons, affording the immune system time to intervene effectively. Avirulent strains of SFV are not fatal in adult mice, and only in the fetus and in suckling mice is fatal infection produced.

The multiplication of SFV-A7 has shown to be restricted in neurons, both *in vitro* and *in vivo* (Atkins, 1983; Gates *et al.*, 1985; Atkins *et al.*, 1990; Balluz *et al.*, 1993; Fazakerley *et al.*, 1993). Multiplication of SFV-A7 in BHK-21 and glial cells is at least as efficient as SFV4 (Atkins, 1983; Atkins *et al.*, 1990). The possibility exists therefore, that the sequence regions that control neurovirulence for SFV are manifested at the cellular level in the ability of the virus to multiply in neurons and hence cause lethal neuronal damage.

In this investigation, possible neurovirulence and pathogenicity determinants of SFV were examined at a molecular level, initially through sequence comparisons between virulent and non virulent SFV strains and consequently through the production of chimeric viruses and their effects in the adult murine CNS. Previous investigations of pathogenicity determinants of alphaviruses (SFV, SIN, VEE) have predominantly focused on the envelope glycoproteins E1 and E2 (Lustig *et al.*, 1988; Polo *et al.*, 1988; Hahn *et al.*, 1989; Lobigs *et al.*, 1990; Polo and Johnston, 1990; Glasgow *et al.*, 1991; 1994; Kinney *et al.*, 1993; Santigati *et al.*, 1995; Yao *et al.*, 1996). The envelope glycoproteins are intrinsically involved in formation of the spike protein complex and therefore receptor mediated endocytosis, maturation and budding of virus particles. Mutations in E1 and E2 at a molecular level may therefore result in difficulties in virus entry and maturation. Glasgow *et al.* (1991, 1994) showed that attenuating mutations at positions 162 and 168 of the SFV4 E2 glycoprotein affected the maturation and entry patterns of SFV4 in the murine CNS. In a later study, Santigati *et al.* (1995) showed that a

chimera containing 6 of the 8 amino acid mutations in the SFV-A7 E2 protein was attenuated when intraperitoneally (i.p.) into adult Balb/c mice. Tarbatt *et al* (1997) confirmed this on constructing a SFV4 / A7 chimera that contained all the SFV-A7 amino acid substitutions present in E1 and 4 of the 8 mutations found in E2. When adult Balb/c mice were inoculated i.p., only 3 out of 15 mice died compared to 8 out of 13 when infected with a chimera that did not contain the SFV-A7 substitutions. However, when mice were administered both viruses i.n., no significant differences were seen with no mice surviving. It is therefore likely that the pathogenicity determinants of SFV are polygenic.

The 5' NTR appears to also be an important pathogenicity determinant and is directly involved in RNA synthesis. Several studies have investigated the function of the 5' NTR in alphavirus RNA synthesis and its possible role as a virulence determinant (Garoff *et al.*, 1982; Evans *et al.*, 1985; Kawamura *et al.*, 1989; Kuhn *et al.*, 1992; Kinney *et al.*, 1993; Neisters *et al.*, 1990; Frolov *et al.*, 2001; Gorchakov *et al.*, 2004). The 5' NTR is capable of forming stem loop secondary structures thought to be translational enhancers (Garoff *et al.*, 1982). Frolov *et al* (2001) suggested that sequences at the 5' end of the RNA genome (including the 51nt CSE in nsP1) and the complementary sequences at the 3' end of minus-strand RNAs play crucial roles in translation and replication of alphaviruses. In SIN when the first stem-loop structure of the 5' NTR was replaced with the SFV 5'-terminal stem-loop structure, all RNAs produced were incapable of replication. Other studies have concentrated on the 5' NTR of alphaviruses to locate pathogenicity determinants. In VEE, a single point mutation in the 5' NTR was shown to attenuate the virulence of the TC-83 strains (Kinney *et al.*, 1993). In SIN, similarly defined point mutations in the 5' NTR were shown to significantly effect viral replication (Neisters *et al.*, 1990). A more recent study, Kobilier *et al* (1999) showed that a combination of mutations in the 5' NTR and the E2 glycoprotein of SIN that caused no death in rats resulted in a recombinant virus that was fatal to rats. The effect of either 5' NTR or E2 mutations alone did not result in the pathogenic properties in intracranially (i.c.) inoculated rats.

Using an A7 infectious clone termed SP6-CA7, Tarbatt *et al* (1997) noted that although significantly attenuated, the infectious virus produced from this clone termed

CA7 was found to kill a significant percentage of adult mice when administered i.n. The present investigation subsequently determined by sequencing SP6-CA7 that it still retained the 5' NTR of the original pSP6-SFV4 infectious clone from which it was constructed. Three nucleotides in the 5' NTR of CA7 at positions 21, 35 and 42 were identified to be different from the SFV-A7 sequence, possibly responsible for the difference in the mortality rates seen between CA7 and SFV-A7. In support of this hypothesis were the pathology results observed in mice infected with CA7 and SFV-A7 respectively. At 14 d.p.i, it was noted that of the 70% of mice surviving infection with CA7 showed pronounced neuronal necrosis and demyelination. Although SFV-A7 also caused similar levels of demyelination the severity of neuronal necrosis caused by CA7 was significantly higher than that caused by SFV-A7. This result indicated that the virulence domain may lie in the first 42 nucleotides of the SFV 5' NTR.

As mentioned previously, investigations on the 5' NTR of both SIN and VEE showed that mutations in this region were found to influence the degree of neuroinvasiveness, although it was undetermined whether these mutations acted at a translational level or in RNA synthesis. Studies on poliovirus have determined virulence domains in its 5' NTR (Evans *et al.*, 1985; Kawamura *et al.*, 1989). Changes in the 5' NTR were found to attenuate neurovirulence and have been linked to a translational defect which is specific to neural cells (Haller *et al.*, 1996). As mutations in the poliovirus 5' NTR were found to attenuate in a host-specific manner, the same may be true for SFV-A7. A restricted rate of multiplication in neurons and a reduction in RNA synthesis can be observed in SFV-A7 when compared to virulent strains of SFV (Balluz *et al.*, 1993; FAzakerley *et al.*, 1993). It is therefore possible that mutations on the SFV-A7 5' NTR act in host specific manner, perhaps specific to neural cells. In this investigation, SFV-A7 was found in significantly lower titres in the brains of infected mice contrary to the comparable growth rates in BHK-21 cells. Although in this investigation the differences in RNA synthesis between SFV-5' NTR chimeras in BHK-21 cells were not statistically significant, the RNA synthesis may be very different if assayed in primary neural cell cultures.

Another facet of pathogenicity determinants that should be addressed is the possibility of mutations acting synergistically to give rise to a polygenic phenotype. This

occurrence was observed in VEE where mutations in the 5' NTR of the attenuated vaccine derivative (TC-83) were shown to act in synergy with mutations in the E2 protein to produce increased neurovirulence comparable to that of the virulent Trinidad Donkey (TD) strain (Kinney *et al.*, 1993). A similar result was shown in SIN strain AR339 by McKnight *et al.*, (1996) who noted that a single mutation in the 5' NTR acted in synergy with a single mutation in E2 resulting in a reduction in virulence. Other studies investigating mutants with double mutations in the 5' and 3' NTRs of SIN also showed higher degrees of attenuation than those with single mutations (Kuhn *et al.*, 1992).

The CA7 chimeras with the SFV-A7 5' NTR have shown to be avirulent in mice resulting in 100% survival and cause significantly reduced pathology in i.n. infected adult Balb/c mice. However replacing the 5' NTR of SFV4 with that of SFV-A7 showed no significant difference the SFV4 alone in regard to the severity of the neuropathology induced and the mortality rate.

One of the aims of this study was to investigate the involvement of the 5' NTR in neurovirulence, this was achieved. A set of reciprocal chimeras were also designed (although not tested) to incorporate the SFV 5' NTRs, 6 amino acid changes in E1 and 4 of 8 amino acid changes in E2. It is possible that by substituting these regions in SFV4 with those of SFV-A7 that the mutations may act synergistically to reduce mortality and severity of lesions in infected mice. However, it must not be ruled out that regions other than the 5' NTR, E1 and E2 may act as virulence determinants and these too may warrant further investigation.

There were three primary aims of this investigation: the initial aim was to sequence and characterise the prototype strain of Chikungunya virus (CHIK), termed Ross. Secondly to construct a full length cDNA clone of CHIK Ross for the development of a possible vaccine and as a molecular tool for the location of possible virulence determinants within the CHIK genome. The Last aim was to ascertain whether the 5' NTR of SFV was a pathogenicity determinant by creating chimeras between virulent and avirulent strains of SFV. Each of these aims has been achieved.

Chapter Seven

References

7.1 References

1. Adesina, O. A. and H. A. Odelola (1991). "Ecological distribution of Chikungunya haemagglutination inhibition antibodies in human and domestic animals in Nigeria." *Trop Geogr Med* 43(3): 271-5.
2. Ahola, T., J. A. den Boon, et al. (2000). "Helicase and capping enzyme active site mutations in brome mosaic virus protein 1a cause defects in template recruitment, negative-strand RNA synthesis, and viral RNA capping." *J Virol* 74(19): 8803-11.
3. Ahola, T., P. Laakkonen, et al. (1997). "Critical residues of Semliki Forest virus RNA capping enzyme involved in methyltransferase and guanylyltransferase-like activities." *J Virol* 71(1): 392-7.
4. Argos, P. (1988). "A sequence motif in many polymerases." *Nucleic Acids Res* 16(21): 9909-16.
5. Atkins, G. J. (1983). "The avirulent A7 Strain of Semliki Forest virus has reduced cytopathogenicity for neuroblastoma cells compared to the virulent L10 strain." *J Gen Virol* 64 (Pt 6): 1401-4.
6. Atkins, G. J., I. M. Balluz, et al. (1994). "Analysis of the molecular basis of neuropathogenesis of RNA viruses in experimental animals: relevance for human disease?" *Neuropathol Appl Neurobiol* 20(2): 91-102.
7. Atkins, G. J., J. Carter, et al. (1982). "Effect of alphavirus infection on mouse embryos." *Infect Immun* 38(3): 1285-90.
8. Atkins, G. J., E. A. Daly, et al. (1990). "Multiple sclerosis and molecular mimicry." *Neuropathol Appl Neurobiol* 16(2): 179-80.
9. Atkins, G. J. and B. J. Sheahan (1982). "Semliki forest virus neurovirulence mutants have altered cytopathogenicity for central nervous system cells." *Infect Immun* 36(1): 333-41.
10. Atkins, G. J., B. J. Sheahan, et al. (1985). "Semliki Forest virus infection of mice: a model for genetic and molecular analysis of viral pathogenicity." *J Gen Virol* 66 (Pt 3): 395-408.
11. Atkins, G. J., B. J. Sheahan, et al. (1996). "Manipulation of the Semliki Forest virus genome and its potential for vaccine construction." *Mol Biotechnol* 5(1): 33-8.
12. Atkins, G. J., B. J. Sheahan, et al. (1999). "The molecular pathogenesis of Semliki Forest virus: a model virus made useful?" *J Gen Virol* 80 (Pt 9): 2287-97.
13. Atkins, G. J., B. J. Sheahan, et al. (1990). "Pathogenicity of Semliki Forest virus for the rat central nervous system and primary rat neural cell cultures: possible implications for the pathogenesis of multiple sclerosis." *Neuropathol Appl Neurobiol* 16(1): 57-68.

14. Balluz, I. M., G. M. Glasgow, et al. (1993). "Virulent and avirulent strains of Semliki Forest virus show similar cell tropism for the murine central nervous system but differ in the severity and rate of induction of cytolytic damage." *Neuropathol Appl Neurobiol* 19(3): 233-9.
15. Bancroft, J.D. and Stevins A. (1990). *Neuropathological Techniques* pg 346 and 456. Theory and practice of histological techniques, 3rd edition, Raven Press Ltd.
16. Barrett, P. N., B. J. Sheahan, et al. (1980). "Isolation and preliminary characterization of Semliki Forest virus mutants with altered virulence." *J Gen Virol* 49(1): 141-7.
17. Barth, B. U., J. M. Wahlberg, et al. (1995). "The oligomerization reaction of the Semliki Forest virus membrane protein subunits." *J Cell Biol* 128(3): 283-91.
18. Berglund, P., Sjöberg, M., Atkins, G. J., Sheahan, B. J., Liljeström, P. (1993). "Semliki Forest virus expression system: production of conditionally infectious recombinant particles." *Biotechnology (N Y)*. 11(8):916-20.
19. Berglund, P., Quesada-Rolander, M., Puktonen, P., Biberfeld, G., Thorstensson, R., Liljeström, P. (1997). "Outcome of immunization of cynomolgus monkeys with recombinant Semliki Forest virus encoding human immunodeficiency virus type 1 envelope protein and challenge with a high dose of SHIV-4 virus." *AIDS Res Hum Retroviruses*. 20;13(17):1487-95.
20. Berglund, P., Fleeton, M. N., Smerdou, C., Liljeström, P. (1999). "Immunization with recombinant Semliki Forest virus induces protection against influenza challenge in mice." *Vaccine* 5;17(5):497-507.
21. Blackburn, N. K., T. G. Besselaar, et al. (1995). "Antigenic relationship between chikungunya virus strains and o'nyong nyong virus using monoclonal antibodies." *Res Virol* 146(1): 69-73.
22. Bonatti, S., G. Migliaccio, et al. (1989). "Palmitoylation of viral membrane glycoproteins takes place after exit from the endoplasmic reticulum." *J Biol Chem* 264(21): 12590-5.
23. Bradish, C. J., K. Allner, et al. (1971). "The virulence of original and derived strains of Semliki forest virus for mice, guinea-pigs and rabbits." *J Gen Virol* 12(2): 141-60.
24. Burt, A.M. (1993). *Histology and Fine Structure of Nervous tissue*, pg 31-59. Textbook of Neuroanatomy. W.B. Saunders Company
25. Calisher, C. H., O. Meurman, et al. (1985). "Sensitive enzyme immunoassay for detecting immunoglobulin M antibodies to Sindbis virus and further evidence that Pogosta disease is caused by a western equine encephalitis complex virus." *J Clin Microbiol* 22(4): 566-71.

26. Calisher, C. H., T. P. Monath, et al. (1985). "Arbovirus investigations in Argentina, 1977-1980. III. Identification and characterization of viruses isolated, including new subtypes of western and Venezuelan equine encephalitis viruses and four new bunyaviruses (Las Maloyas, Resistencia, Barranqueras, and Antequera)." *Am J Trop Med Hyg* 34(5): 956-65.
27. Carleton, M., H. Lee, et al. (1997). "Role of glycoprotein PE2 in formation and maturation of the Sindbis virus spike." *J Virol* 71(2): 1558-66.
28. Chanas, A. C., Z. Hubalek, et al. (1979). "A comparative study of O'nyong nyong virus with Chikungunya virus and plaque variants." *Arch Virol* 59(3): 231-8.
29. Chanas, A. C., B. K. Johnson, et al. (1979). "Characterization of two Chikungunya virus variants." *Acta Virol* 23(2): 128-36.
30. Chatterjee, S. N., S. K. Chakravarti, et al. (1965). "Virological investigation of cases with neurological complications during the outbreak of haemorrhagic fever in Calcutta." *J Indian Med Assoc* 45(6): 314-6.
31. Chatterjee, S. N. and J. K. Sarkar (1965). "Electron microscopic studies of suckling mouse brain cells infected with Chikungunya virus." *Indian J Exp Biol* 3(4): 227-34.
32. Chaudhuri, R. N., J. B. Chatterjee, et al. (1964). "Calcutta Haemorrhagic Fever." *Bull Calcutta Sch Trop Med* 12: 1-2.
33. Choi, H. K., L. Tong, et al. (1991). "Structure of Sindbis virus core protein reveals a chymotrypsin-like serine proteinase and the organization of the virion." *Nature* 354(6348): 37-43.
34. Clegg, J. C. and S. I. Kennedy (1974). "In vitro synthesis of structural proteins of Semliki Forest virus directed by isolated 26 S RNA from infected cells." *FEBS Lett* 42(3): 327-30.
35. Cross, R. K. (1983). "Identification of a unique guanine-7-methyltransferase in Semliki Forest virus (SFV) infected cell extracts." *Virology* 130(2): 452-63.
36. Cross, R. K. and P. J. Gomas (1981). "Concomitant methylation and synthesis in vitro of Semliki Forest virus (SFV) ss RNAs by a fraction from infected cells." *Virology* 114(2): 542-54.
37. Davis, J. L., H. M. Hodge, et al. (1971). "Growth of chikungunya virus in baby hamster kidney cell (BHK-21-clone 13) suspension cultures." *Appl Microbiol* 21(2): 338-41.
38. Davis, N. L., L. V. Willis, et al. (1989). "In vitro synthesis of infectious venezuelan equine encephalitis virus RNA from a cDNA clone: analysis of a viable deletion mutant." *Virology* 171(1): 189-204.
39. de Curtis, I., K. E. Howell, et al. (1988). "Isolation of a fraction enriched in the trans-Golgi network from baby hamster kidney cells." *Exp Cell Res* 175(2): 248-65.

40. Degroote, F., S. Renault, et al. (1990). "Nucleotide sequence of circular DNA molecules homologous to the 240 bp tandem repeats of the intergenic spacer of *Drosophila melanogaster* ribosomal DNA." *Biol Cell* 69(1): 69-70.
41. Deller, J. J., Jr. and P. K. Russell (1967). "An analysis of fevers of unknown origin in American soldiers in Vietnam." *Ann Intern Med* 66(6): 1129-43.
42. DeTulleo, L. and T. Kirchhausen (1998). "The clathrin endocytic pathway in viral infection." *Embo J* 17(16): 4585-93.
43. Diallo, M., J. Thonnon, et al. (1999). "Vectors of Chikungunya virus in Senegal: current data and transmission cycles." *Am J Trop Med Hyg* 60(2): 281-6.
44. Dick, M., B. U. Barth, et al. (1996). "The E1 protein is mandatory for pore formation by Semliki Forest virus spikes." *Virology* 220(1): 204-7.
45. Dubuisson, J. and C. M. Rice (1993). "Sindbis virus attachment: isolation and characterization of mutants with impaired binding to vertebrate cells." *J Virol* 67(6): 3363-74.
46. Durbin, R., A. Kane, et al. (1991). "A mutant of Sindbis virus with altered plaque morphology and a decreased ratio of 26 S:49 S RNA synthesis in mosquito cells." *Virology* 183(1): 306-12.
47. Evans, D. M., G. Dunn, et al. (1985). "Increased neurovirulence associated with a single nucleotide change in a noncoding region of the Sabin type 3 poliovaccine genome." *Nature* 314(6011): 548-50.
48. Fata, C. L., S. G. Sawicki, et al. (2002). "Alphavirus minus-strand RNA synthesis: identification of a role for Arg183 of the nsP4 polymerase." *J Virol* 76(17): 8632-40.
49. Fata, C. L., S. G. Sawicki, et al. (2002). "Modification of Asn374 of nsP1 suppresses a Sindbis virus nsP4 minus-strand polymerase mutant." *J Virol* 76(17): 8641-9.
50. Fayzulin, R. and I. Frolov (2004). "Changes of the secondary structure of the 5' end of the Sindbis virus genome inhibit virus growth in mosquito cells and lead to accumulation of adaptive mutations." *J Virol* 78(10): 4953-64.
51. Fazakerley, J. K., S. Pathak, et al. (1993). "Replication of the A7(74) strain of Semliki Forest virus is restricted in neurons." *Virology* 195(2): 627-37.
52. Fazakerley, J. K. and H. E. Webb (1987). "Semliki Forest virus-induced, immune-mediated demyelination: adoptive transfer studies and viral persistence in nude mice." *J Gen Virol* 68 (Pt 2): 377-85.
53. Fitzgerald, S. C., M. A. Willis, et al. (1992). "In search of the central respiratory neurons: I. Dissociated cell cultures of respiratory areas from the upper medulla." *J Neurosci Res* 33(4): 579-89.

54. Fleeton, M. N., Sheahan, B. J., Gould, E. A., Atkins, G. J., Liljeström, P. (1999). "Recombinant Semliki Forest virus particles encoding the prME or NS1 proteins of louping ill virus protect mice from lethal challenge." *J Gen Virol.* 80 (Pt 5):1189-98.
55. Fleeton, M. N., Liljeström, P., Sheahan, B. J., Atkins, G. J. (2000). "Recombinant Semliki Forest virus particles expressing louping ill virus antigens induce a better protective response than plasmid-based DNA vaccines or an inactivated whole particle vaccine." *J Gen Virol.* 81(Pt 3):749-58.
56. Forsell, K., M. Suomalainen, et al. (1995). "Structure-function relation of the NH2-terminal domain of the Semliki Forest virus capsid protein." *J Virol* 69(3): 1556-63.
57. Frolov, I., E. Frolova, et al. (1997). "Sindbis virus replicons and Sindbis virus: assembly of chimeras and of particles deficient in virus RNA." *J Virol* 71(4): 2819-29.
58. Frolov, I., R. Hardy, et al. (2001). "Cis-acting RNA elements at the 5' end of Sindbis virus genome RNA regulate minus- and plus-strand RNA synthesis." *Rna* 7(11): 1638-51.
59. Frolov, I., T. A. Hoffman, et al. (1996). "Alphavirus-based expression vectors: strategies and applications." *Proc Natl Acad Sci U S A* 93(21): 11371-7.
60. Fuller, S. D., J. A. Berriman, et al. (1995). "Low pH induces swiveling of the glycoprotein heterodimers in the Semliki Forest virus spike complex." *Cell* 81(5): 715-25.
61. Garoff, H., A. M. Frischauf, et al. (1980). "The capsid protein of Semliki Forest virus has clusters of basic amino acids and prolines in its amino-terminal region." *Proc Natl Acad Sci U S A* 77(11): 6376-80.
62. Garoff, H., A. M. Frischauf, et al. (1980). "Nucleotide sequence of cDNA coding for Semliki Forest virus membrane glycoproteins." *Nature* 288(5788): 236-41.
63. Garoff, H., D. Huylebroeck, et al. (1990). "The signal sequence of the p62 protein of Semliki Forest virus is involved in initiation but not in completing chain translocation." *J Cell Biol* 111(3): 867-76.
64. Garoff, H., C. Kondor-Koch, et al. (1982). "Structure and assembly of alphaviruses." *Curr Top Microbiol Immunol* 99: 1-50.
65. Garoff, H. and K. Simons (1974). "Location of the spike glycoproteins in the Semliki Forest virus membrane." *Proc Natl Acad Sci U S A* 71(10): 3988-92.
66. Garoff, H., K. Simons, et al. (1978). "Assembly of the Semliki Forest virus membrane glycoproteins in the membrane of the endoplasmic reticulum in vitro." *J Mol Biol* 124(4): 587-600.
67. Garoff, H., K. Simons, et al. (1974). "Isolation and characterization of the membrane proteins of Semliki Forest virus." *Virology* 61(2): 493-504.

68. Gates, M. C., B. J. Sheahan, et al. (1984). "The pathogenicity of the M9 mutant of Semliki Forest virus in immune-compromised mice." *J Gen Virol* 65 (Pt 1): 73-80.
69. Gates, M. C., B. J. Sheahan, et al. (1985). "The pathogenicity of the A7, M9 and L10 strains of Semliki Forest virus for weanling mice and primary mouse brain cell cultures." *J Gen Virol* 66 (Pt 11): 2365-73.
70. Geigenmuller-Gnirke, U., H. Nitschko, et al. (1993). "Deletion analysis of the capsid protein of Sindbis virus: identification of the RNA binding region." *J Virol* 67(3): 1620-6.
71. Glasgow, G. M., H. M. Killen, et al. (1994). "A single amino acid change in the E2 spike protein of a virulent strain of Semliki Forest virus attenuates pathogenicity." *J Gen Virol* 75 (Pt 3): 663-8.
72. Glasgow, G. M., M. M. McGee, et al. (1997). "Death mechanisms in cultured cells infected by Semliki Forest virus." *J Gen Virol* 78 (Pt 7): 1559-63.
73. Glasgow, G. M., B. J. Sheahan, et al. (1991). "Two mutations in the envelope glycoprotein E2 of Semliki Forest virus affecting the maturation and entry patterns of the virus alter pathogenicity for mice." *Virology* 185(2): 741-8.
74. Gorchakov, R., R. Hardy, et al. (2004). "Selection of functional 5' cis-acting elements promoting efficient sindbis virus genome replication." *J Virol* 78(1): 61-75.
75. Grakoui, A., R. Levis, et al. (1989). "A cis-acting mutation in the Sindbis virus junction region which affects subgenomic RNA synthesis." *J Virol* 63(12): 5216-27.
76. Griffin DE. Alphavirus pathogenesis and immunity. In: Schlesinger SS, Schlesinger MJ, editors. 1986. *The togaviridae and Flaviviridae*. New York: Plenum Press. p. 209-250
77. Hahn, C. S., Y. S. Hahn, et al. (1987). "Conserved elements in the 3' untranslated region of flavivirus RNAs and potential cyclization sequences." *J Mol Biol* 198(1): 33-41.
78. Hahn, C. S., C. M. Rice, et al. (1989). "Sindbis virus ts103 has a mutation in glycoprotein E2 that leads to defective assembly of virions." *J Virol* 63(8): 3459-65.
79. Hahn, C. S. and J. H. Strauss (1990). "Site-directed mutagenesis of the proposed catalytic amino acids of the Sindbis virus capsid protein autoprotease." *J Virol* 64(6): 3069-73.
80. Hardy, R. W. and C. M. Rice (2005). "Requirements at the 3' end of the sindbis virus genome for efficient synthesis of minus-strand RNA." *J Virol* 79(8): 4630-9.
81. Hardy, W. R., Y. S. Hahn, et al. (1990). "Synthesis and processing of the nonstructural polyproteins of several temperature-sensitive mutants of Sindbis virus." *Virology* 177(1): 199-208.

82. Hardy, W. R. and J. H. Strauss (1988). "Processing the nonstructural polyproteins of Sindbis virus: study of the kinetics in vivo by using monospecific antibodies." *J Virol* 62(3): 998-1007.
83. Hardy, W. R. and J. H. Strauss (1989). "Processing the nonstructural polyproteins of sindbis virus: nonstructural proteinase is in the C-terminal half of nsP2 and functions both in cis and in trans." *J Virol* 63(11): 4653-64.
84. Hearne, A. M., M. A. O'Sullivan, et al. (1987). "Isolation and preliminary characterization of Semliki Forest virus mutants with altered pathogenicity for mouse embryos." *J Gen Virol* 68 (Pt 1): 107-13.
85. Higashi, N., A. Matsumoto, et al. (1967). "Electron microscope study of development of Chikungunya virus in green monkey kidney stable (VERO) cells." *Virology* 33(1): 55-69.
86. Hodgman, T. C. (1988). "A new superfamily of replicative proteins." *Nature* 333(6168): 22-3.
87. Igarashi, A. (1970). "Protein synthesis and formation of Chikungunya virus in infected BHK21 cells." *Biken J* 13(4): 289-302.
88. Igarashi, A. (1970). "Ribonuclease-sensitive infectivity of chikungunya virus from BHK21 cells infected with the virus." *Biken J* 13(1): 39-42.
89. Igarashi, A., T. Fukuoka, et al. (1970). "Structural components of chikungunya virus." *Biken J* 13(2): 93-110.
90. Igarashi, A., P. Nithiuthai, et al. (1970). "Immunological properties of Chikungunya virus and its components." *Biken J* 13(3): 229-31.
91. Ivanov, A. P., O. E. Ivanova, et al. (1992). "Serological investigations of Chikungunya virus in the Republic of Guinea." *Ann Soc Belg Med Trop* 72(1): 73-4.
92. Jerusalmi, A., Morris-Downes, M. M., Sheahan, B. J., Atkins, G. J. (2003). "Effect of intranasal administration of semliki forest virus recombinant particles expressing reporter and cytokine genes on the progression of experimental autoimmune encephalomyelitis." *Mol. Ther* 8(6):886-94.
93. Johnson, R. T. (1982). "Viruses and chronic neurological diseases." *Johns Hopkins Med J* 150(4): 132-40.
94. Junqueira, L.C., Carneiro, J. and Contopoulos, A. (1975). Nerve tissue, pg 138-167. Basic histology. Lange Medical publications.
95. Jupp, P. G., B. M. McIntosh, et al. (1981). "Laboratory vector studies on six mosquito and one tick species with chikungunya virus." *Trans R Soc Trop Med Hyg* 75(1): 15-9.

96. Kaariainen, L., K. Takkinen, et al. (1987). "Replication of the genome of alphaviruses." *J Cell Sci Suppl* 7: 231-50.
97. Kaluza, G., G. Lell, et al. (1987). "Neurogenic spread of Semliki Forest virus in mice." *Arch Virol* 93(1-2): 97-110.
98. Kawamura, N., M. Kohara, et al. (1989). "Determinants in the 5' noncoding region of poliovirus Sabin 1 RNA that influence the attenuation phenotype." *J Virol* 63(3): 1302-9.
99. Keogh, B., G. J. Atkins, et al. (2002). "Avirulent Semliki Forest virus replication and pathology in the central nervous system is enhanced in IL-12-defective and reduced in IL-4-defective mice: a role for Th1 cells in the protective immunity." *J Neuroimmunol* 125(1-2): 15-22.
100. Keranen, S. and L. Ruohonen (1983). "Nonstructural proteins of Semliki Forest virus: synthesis, processing, and stability in infected cells." *J Virol* 47(3): 505-15.
101. Khan, A. H., K. Morita, et al. (2002). "Complete nucleotide sequence of chikungunya virus and evidence for an internal polyadenylation site." *J Gen Virol* 83(Pt 12): 3075-84.
102. Kim, K. H., T. Rumenapf, et al. (2004). "Regulation of Semliki Forest virus RNA replication: a model for the control of alphavirus pathogenesis in invertebrate hosts." *Virology* 323(1): 153-63.
103. Kimelberg, H. K. and M. D. Norenberg (1989). "Astrocytes." *Sci Am* 260(4): 66-72, 74, 76.
104. Kinney, R. M., G. J. Chang, et al. (1993). "Attenuation of Venezuelan equine encephalitis virus strain TC-83 is encoded by the 5'-noncoding region and the E2 envelope glycoprotein." *J Virol* 67(3): 1269-77.
105. Kobilier, D., C. M. Rice, et al. (1999). "A single nucleotide change in the 5' noncoding region of Sindbis virus confers neurovirulence in rats." *J Virol* 73(12): 10440-6.
106. Kuhn, R. J., D. E. Griffin, et al. (1992). "Attenuation of Sindbis virus neurovirulence by using defined mutations in nontranslated regions of the genome RNA." *J Virol* 66(12): 7121-7.
107. Kuhn, R. J., Z. Hong, et al. (1990). "Mutagenesis of the 3' nontranslated region of Sindbis virus RNA." *J Virol* 64(4): 1465-76.
108. Kuhn, R. J., H. G. Niesters, et al. (1991). "Infectious RNA transcripts from Ross River virus cDNA clones and the construction and characterization of defined chimeras with Sindbis virus." *Virology* 182(2): 430-41.

109. Laakkonen, P., T. Ahola, et al. (1996). "The effects of palmitoylation on membrane association of Semliki forest virus RNA capping enzyme." *J Biol Chem* 271(45): 28567-71.
110. LaStarza, M. W., J. A. Lemm, et al. (1994). "Genetic analysis of the nsP3 region of Sindbis virus: evidence for roles in minus-strand and subgenomic RNA synthesis." *J Virol* 68(9): 5781-91.
111. Lemm, J. A. and C. M. Rice (1993). "Assembly of functional Sindbis virus RNA replication complexes: requirement for coexpression of P123 and P34." *J Virol* 67(4): 1905-15.
112. Lemm, J. A. and C. M. Rice (1993). "Roles of nonstructural polyproteins and cleavage products in regulating Sindbis virus RNA replication and transcription." *J Virol* 67(4): 1916-26.
113. Levinson, R. S., J. H. Strauss, et al. (1990). "Complete sequence of the genomic RNA of O'nyong-nyong virus and its use in the construction of alphavirus phylogenetic trees." *Virology* 175(1): 110-23.
114. Levis, R., S. Schlesinger, et al. (1990). "Promoter for Sindbis virus RNA-dependent subgenomic RNA transcription." *J Virol* 64(4): 1726-33.
115. Levitt, N. H., H. H. Ramsburg, et al. (1986). "Development of an attenuated strain of chikungunya virus for use in vaccine production." *Vaccine* 4(3): 157-62.
116. Li, G. and C. M. Rice (1993). "The signal for translational readthrough of a UGA codon in Sindbis virus RNA involves a single cytidine residue immediately downstream of the termination codon." *J Virol* 67(8): 5062-7.
117. Liljestrom, P. and H. Garoff (1991). "Internally located cleavable signal sequences direct the formation of Semliki Forest virus membrane proteins from a polyprotein precursor." *J Virol* 65(1): 147-54.
118. Liljestrom, P. and H. Garoff (1991). "A new generation of animal cell expression vectors based on the Semliki Forest virus replicon." *Biotechnology (N Y)* 9(12): 1356-61.
119. Liljestrom, P., S. Lusa, et al. (1991). "In vitro mutagenesis of a full-length cDNA clone of Semliki Forest virus: the small 6,000-molecular-weight membrane protein modulates virus release." *J Virol* 65(8): 4107-13.
120. Lobigs, M., J. M. Wahlberg, et al. (1990). "Spike protein oligomerization control of Semliki Forest virus fusion." *J Virol* 64(10): 5214-8.
121. Lobigs, M., H. X. Zhao, et al. (1990). "Function of Semliki Forest virus E3 peptide in virus assembly: replacement of E3 with an artificial signal peptide abolishes spike heterodimerization and surface expression of E1." *J Virol* 64(9): 4346-55.

122. Loewy, A., J. Smyth, et al. (1995). "The 6-kilodalton membrane protein of Semliki Forest virus is involved in the budding process." *J Virol* 69(1): 469-75.
123. Lopez, S., J. S. Yao, et al. (1994). "Nucleocapsid-glycoprotein interactions required for assembly of alphaviruses." *J Virol* 68(3): 1316-23.
124. Lundstrom, K. (1997). "Alphaviruses as expression vectors." *Curr Opin Biotechnol* 8(5): 578-82.
125. Lusa, S., H. Garoff, et al. (1991). "Fate of the 6K membrane protein of Semliki Forest virus during virus assembly." *Virology* 185(2): 843-6.
126. Lustig, S., M. Halevy, et al. (1999). "The role of host immunocompetence in neuroinvasion of Sindbis virus." *Arch Virol* 144(6): 1159-71.
127. Lustig S, Jackson AC, Hahn CS, Griffin DE, Strauss EG, Strauss JH. Molecular basis of Sindbis virus neurovirulence in mice. *J Virol*. 1988 Jul;62(7):2329-36.
128. Martin, J. D., W. S. Riggsby, et al. (1979). "The effect of ribonuclease on the replicative forms of Sindbis virus RNA." *Arch Virol* 60(2): 131-46.
129. Mathiot, C. C., G. Grimaud, et al. (1990). "An outbreak of human Semliki Forest virus infections in Central African Republic." *Am J Trop Med Hyg* 42(4): 386-93.
130. Mayne, J. T., C. M. Rice, et al. (1984). "Biochemical studies of the maturation of the small Sindbis virus glycoprotein E3." *Virology* 134(2): 338-57.
131. McInerney, G. M., J. M. Smit, et al. (2004). "Semliki Forest virus produced in the absence of the 6K protein has an altered spike structure as revealed by decreased membrane fusion capacity." *Virology* 325(2): 200-6.
132. McIntosh, B. M., C. B. Worth, et al. (1961). "Isolation of Semliki Forest virus from *Aedes (Aedimorphus) argenteopunctatus* (Theobald) collected in Portuguese East Africa." *Transfusion (Paris)* 55: 192-8.
133. McKnight, K. L., D. A. Simpson, et al. (1996). "Deduced consensus sequence of Sindbis virus strain AR339: mutations contained in laboratory strains which affect cell culture and in vivo phenotypes." *J Virol* 70(3): 1981-9
134. Melancon, P. and H. Garoff (1986). "Reinitiation of translocation in the Semliki Forest virus structural polyprotein: identification of the signal for the E1 glycoprotein." *Embo J* 5(7): 1551-60.
135. Melancon, P. and H. Garoff (1987). "Processing of the Semliki Forest virus structural polyprotein: role of the capsid protease." *J Virol* 61(5): 1301-9.

136. Metsikko, K. and H. Garoff (1990). "Oligomers of the cytoplasmic domain of the p62/E2 membrane protein of Semliki Forest virus bind to the nucleocapsid in vitro." *J Virol* 64(10): 4678-83.
137. Mi, S. and V. Stollar (1991). "Expression of Sindbis virus nsP1 and methyltransferase activity in *Escherichia coli*." *Virology* 184(1): 423-7.
138. Moesby, L., J. Corver, et al. (1995). "Sphingolipids activate membrane fusion of Semliki Forest virus in a stereospecific manner." *Biochemistry* 34(33): 10319-24.
139. Moore, D. L., S. Reddy, et al. (1974). "An epidemic of chikungunya fever at Ibadan, Nigeria, 1969." *Ann Trop Med Parasitol* 68(1): 59-68.
140. Morris-Downes, M. M., Sheahan, B. J., Fleeton, M. N., Liljeström, P., Reid H. W., Atkins, G. J. (2001). "A recombinant Semliki Forest virus particle vaccine encoding the prME and NS1 proteins of louping ill virus is effective in a sheep challenge model." *Vaccine* 19(28-29):3877-84.
141. Morris-Downes, M. M., Phenix, K. V., Smyth, J., Sheahan, B. J., Lileqvist, S., Mooney, D. A., Liljeström, P., Todd, D., Atkins, G. J. (2001). "Semliki Forest virus-based vaccines: persistence, distribution and pathological analysis in two animal systems." *Vaccine* 19(15-16):1978-88.
142. Morrison, J. G. (1979). "Chikungunya fever." *Int J Dermatol* 18(8): 628-9.
143. Niesters, H. G. and J. H. Strauss (1990). "Defined mutations in the 5' nontranslated sequence of Sindbis virus RNA." *J Virol* 64(9): 4162-8.
144. Niesters, H. G. and J. H. Strauss (1990). "Mutagenesis of the conserved 51-nucleotide region of Sindbis virus." *J Virol* 64(4): 1639-47.
145. Oliver, K. R., M. F. Scallan, et al. (1997). "Susceptibility to a neurotropic virus and its changing distribution in the developing brain is a function of CNS maturity." *J Neurovirol* 3(1): 38-48.
146. Ou, D., P. Chong, et al. (1993). "Mapping T-cell epitopes of rubella virus structural proteins E1, E2, and C recognized by T-cell lines and clones derived from infected and immunized populations." *J Med Virol* 40(3): 175-83.
147. Ou, J. H., C. M. Rice, et al. (1982). "Sequence studies of several alphavirus genomic RNAs in the region containing the start of the subgenomic RNA." *Proc Natl Acad Sci U S A* 79(17): 5235-9.
148. Ou, J. H., E. G. Strauss, et al. (1981). "Comparative studies of the 3'-terminal sequences of several alpha virus RNAs." *Virology* 109(2): 281-9.
149. Ou, J. H., E. G. Strauss, et al. (1983). "The 5'-terminal sequences of the genomic RNAs of several alphaviruses." *J Mol Biol* 168(1): 1-15.

150. Ou, J. H., D. W. Trent, et al. (1982). "The 3'-non-coding regions of alphavirus RNAs contain repeating sequences." *J Mol Biol* 156(4): 719-30.
151. Owen, K. E. and R. J. Kuhn (1996). "Identification of a region in the Sindbis virus nucleocapsid protein that is involved in specificity of RNA encapsidation." *J Virol* 70(5): 2757-63.
152. Pardigon, N. and J. H. Strauss (1992). "Cellular proteins bind to the 3' end of Sindbis virus minus-strand RNA." *J Virol* 66(2): 1007-15.
153. Paredes, A. M., D. T. Brown, et al. (1993). "Three-dimensional structure of a membrane-containing virus." *Proc Natl Acad Sci U S A* 90(19): 9095-9.
154. Paredes, A. M., M. N. Simon, et al. (1992). "The mass of the Sindbis virus nucleocapsid suggests it has T = 4 icosahedral symmetry." *Virology* 187(1): 329-32.
155. Peranen, J. (1991). "Localization and phosphorylation of Semliki Forest virus non-structural protein nsP3 expressed in COS cells from a cloned cDNA." *J Gen Virol* 72 (Pt 1): 195-9.
156. Peranen, J., P. Laakkonen, et al. (1995). "The alphavirus replicase protein nsP1 is membrane-associated and has affinity to endocytic organelles." *Virology* 208(2): 610-20.
157. Peranen, J., M. Rikkinen, et al. (1990). "Nuclear localization of Semliki Forest virus-specific nonstructural protein nsP2." *J Virol* 64(5): 1888-96.
158. Peranen, J., K. Takkinen, et al. (1988). "Semliki Forest virus-specific non-structural protein nsP3 is a phosphoprotein." *J Gen Virol* 69 (Pt 9): 2165-78.
159. Phalen, T. and M. Kielian (1991). "Cholesterol is required for infection by Semliki Forest virus." *J Cell Biol* 112(4): 615-23.
160. Polo JM, Davis NL, Rice CM, Huang HV, Johnston RE. Molecular analysis of Sindbis virus pathogenesis in neonatal mice by using virus recombinants constructed in vitro. *J Virol*. 1988 Jun;62(6):2124-33.
161. Polo JM, Johnston RE. Attenuating mutations in glycoproteins E1 and E2 of Sindbis virus produce a highly attenuated strain when combined in vitro. *J Virol*. 1990 Sep;64(9):4438-44.
162. Porter, K. R., R. Tan, et al. (2004). "A serological study of Chikungunya virus transmission in Yogyakarta, Indonesia: evidence for the first outbreak since 1982." *Southeast Asian J Trop Med Public Health* 35(2): 408-15.
163. Powers, A. M., A. C. Brault, et al. (2001). "Evolutionary relationships and systematics of the alphaviruses." *J Virol* 75(21): 10118-31.

164. Powers, A. M., A. C. Brault, et al. (2000). "Re-emergence of Chikungunya and O'nyong-nyong viruses: evidence for distinct geographical lineages and distant evolutionary relationships." *J Gen Virol* 81(Pt 2): 471-9.
165. Precious, S. W., H. E. Webb, et al. (1974). "Isolation and persistence of Chikungunya virus in cultures of mouse brain cells." *J Gen Virol* 23(3): 271-9.
166. Raju, R. and H. V. Huang (1991). "Analysis of Sindbis virus promoter recognition in vivo, using novel vectors with two subgenomic mRNA promoters." *J Virol* 65(5): 2501-10.
167. Ranadive, S. N. and K. Banerjee (1990). "Cloning & expression of chikungunya virus genes coding structural proteins in Escherichia coli." *Indian J Med Res* 91: 386-92.
168. Rice, C. M., R. Levis, et al. (1987). "Production of infectious RNA transcripts from Sindbis virus cDNA clones: mapping of lethal mutations, rescue of a temperature-sensitive marker, and in vitro mutagenesis to generate defined mutants." *J Virol* 61(12): 3809-19.
169. Rikkonen, M., J. Peranen, et al. (1992). "Nuclear and nucleolar targeting signals of Semliki Forest virus nonstructural protein nsP2." *Virology* 189(2): 462-73.
170. Rikkonen, M., J. Peranen, et al. (1994). "ATPase and GTPase activities associated with Semliki Forest virus nonstructural protein nsP2." *J Virol* 68(9): 5804-10.
171. Rikkonen, M., J. Peranen, et al. (1994). "Nuclear targeting of Semliki Forest virus nsP2." *Arch Virol Suppl* 9: 369-77.
172. Robinson, M. C. (1955). "An epidemic of virus disease in Southern Province, Tanganyika Territory, in 1952-53. I. Clinical features." *Trans R Soc Trop Med Hyg* 49(1): 28-32.
173. Ross, R. W. (1956). "The Newala epidemic. III. The virus: isolation, pathogenic properties and relationship to the epidemic." *J Hyg (Lond)* 54(2): 177-91.
174. Salonen, A., L. Vasiljeva, et al. (2003). "Properly folded nonstructural polyprotein directs the semliki forest virus replication complex to the endosomal compartment." *J Virol* 77(3): 1691-702.
175. Sammin, D. J., D. Butler, et al. (1999). "Cell death mechanisms in the olfactory bulb of rats infected intranasally with Semliki forest virus." *Neuropathol Appl Neurobiol* 25(3): 236-43.
176. Santagati, M. G., P. V. Itaranta, et al. (1994). "Multiple repeating motifs are found in the 3'-terminal non-translated region of Semliki Forest virus A7 variant genome." *J Gen Virol* 75 (Pt 6): 1499-504.

177. Sariola, M., J. Saraste, et al. (1995). "Communication of post-Golgi elements with early endocytic pathway: regulation of endoproteolytic cleavage of Semliki Forest virus p62 precursor." *J Cell Sci* 108 (Pt 6): 2465-75.
178. Sarkar, J. K., S. N. Chatterjee, et al. (1965). "Chikungunya virus infection with haemorrhagic manifestations." *Indian J Med Res* 53(10): 921-5.
179. Sarkar, J. K., S. N. Chatterjee, et al. (1965). "The causative agent of Calcutta haemorrhagic fever: chikungunya or dengue." *Bull Calcutta Sch Trop Med* 13(2): 53-4.
180. Sawicki, D. L., L. Kaariainen, et al. (1978). "Mechanism for control of synthesis of Semliki Forest virus 26S and 42s RNA." *J Virol* 25(1): 19-27.
181. Sawicki, D. L. and S. G. Sawicki (1985). "Functional analysis of the A complementation group mutants of Sindbis HR virus." *Virology* 144(1): 20-34.
182. Sawicki, S. G. and D. L. Sawicki (1986). "The effect of loss of regulation of minus-strand RNA synthesis on Sindbis virus replication." *Virology* 151(2): 339-49.
183. Sawicki, S. G. and D. L. Sawicki (1986). "The effect of overproduction of nonstructural proteins on alphavirus plus-strand and minus-strand RNA synthesis." *Virology* 152(2): 507-12.
184. Scheidel, L. M., R. K. Durbin, et al. (1987). "Sindbis virus mutants resistant to mycophenolic acid and ribavirin." *Virology* 158(1): 1-7.
185. Schlesinger, M. J., S. D. London, et al. (1993). "An in-frame insertion into the Sindbis virus 6K gene leads to defective proteolytic processing of the virus glycoproteins, a trans-dominant negative inhibition of normal virus formation, and interference in virus shut off of host-cell protein synthesis." *Virology* 193(1): 424-32.
186. Schlesinger, S. (1993). "Alphaviruses--vectors for the expression of heterologous genes." *Trends Biotechnol* 11(1): 18-22.
187. Sheahan, B. J., P. N. Barrett, et al. (1981). "Demyelination in mice resulting from infection with a mutant of Semliki Forest virus." *Acta Neuropathol (Berl)* 53(2): 129-36.
188. Sheahan, B. J., M. C. Gates, et al. (1983). "Oligodendrocyte infection and demyelination produced in mice by the M9 mutant of Semliki Forest virus." *Acta Neuropathol (Berl)* 60(3-4): 257-65.
189. Sheahan, B. J., M. Moore, et al. (2002). "The pathogenicity of louping ill virus for mice and lambs." *J Comp Pathol* 126(2-3): 137-46.
190. Shirako, Y., E. G. Strauss, et al. (2000). "Suppressor mutations that allow sindbis virus RNA polymerase to function with nonaromatic amino acids at the N-terminus: evidence for interaction between nsP1 and nsP4 in minus-strand RNA synthesis." *Virology* 276(1): 148-60.

191. Shirako, Y. and J. H. Strauss (1994). "Regulation of Sindbis virus RNA replication: uncleaved P123 and nsP4 function in minus-strand RNA synthesis, whereas cleaved products from P123 are required for efficient plus-strand RNA synthesis." *J Virol* 68(3): 1874-85.
192. Simizu, B., K. Yamamoto, et al. (1984). "Structural proteins of Chikungunya virus." *J Virol* 51(1): 254-8.
193. Simons, K. and H. Garoff (1980). "The budding mechanisms of enveloped animal viruses." *J Gen Virol* 50(1): 1-21.
194. Simons, K., A. Helenius, et al. (1973). "Solubilization of the membrane proteins from Semliki Forest virus with Triton X100." *J Mol Biol* 80(1): 119-33.
195. Simpson, D. A., N. L. Davis, et al. (1996). "Complete nucleotide sequence and full-length cDNA clone of S.A.AR86 a South African alphavirus related to Sindbis." *Virology* 222(2): 464-9.
196. Singh, I. and A. Helenius (1992). "Role of ribosomes in Semliki Forest virus nucleocapsid uncoating." *J Virol* 66(12): 7049-58.
197. Sjoberg, M. and H. Garoff (2003). "Interactions between the transmembrane segments of the alphavirus E1 and E2 proteins play a role in virus budding and fusion." *J Virol* 77(6): 3441-50.
198. Skoging, U., M. Vihinen, et al. (1996). "Aromatic interactions define the binding of the alphavirus spike to its nucleocapsid." *Structure* 4(5): 519-29.
199. Smit, J. M., R. Bittman, et al. (1999). "Low-pH-dependent fusion of Sindbis virus with receptor-free cholesterol- and sphingolipid-containing liposomes." *J Virol* 73(10): 8476-84.
200. Smith, L. (1989). Central Nervous System, pg 651-668. Mechanisms of microbial disease. M. Schaechter, G. Nedoff and D Schlessinger (eds.). Williams and Ailkins International Edition.
201. Smyth, J., M. Suomalainen, et al. (1997). "Efficient multiplication of a Semliki Forest virus chimera containing Sindbis virus spikes." *J Virol* 71(1): 818-23.
202. Smyth, J. M., B. J. Sheahan, et al. (1990). "Multiplication of virulent and demyelinating Semliki Forest virus in the mouse central nervous system: consequences in BALB/c and SJL mice." *J Gen Virol* 71 (Pt 11): 2575-83.
203. Soderlund, H., C. H. von Bonsdorff, et al. (1979). "Comparison of the structural properties of Sindbis and Semliki forest virus nucleocapsids." *J Gen Virol* 45(1): 15-26.

204. Starr, C.M., Rozhon, E.J. and Lipton, H.L. (1984). Relationship between host age and persistence of Theiler's virus in the central nervous system of mice. *Infect. Immun.* 43: 432-434
205. Stollar V. Defective interfering alphaviruses. In: Schlesinger RW, editor. 1980. *The Togaviruses*. New York: Academic Press. P. 427-457
206. Strauss, E. G., C. M. Rice, et al. (1983). "Sequence coding for the alphavirus nonstructural proteins is interrupted by an opal termination codon." *Proc Natl Acad Sci U S A* 80(17): 5271-5.
207. Strauss, E. G., C. M. Rice, et al. (1984). "Complete nucleotide sequence of the genomic RNA of Sindbis virus." *Virology* 133(1): 92-110.
208. Strauss, J. H. and E. G. Strauss (1994). "The alphaviruses: gene expression, replication, and evolution." *Microbiol Rev* 58(3): 491-562.
209. Strauss, J. H., E. G. Strauss, et al. (1995). "Budding of alphaviruses." *Trends Microbiol* 3(9): 346-50.
210. Strauss, J. H., K. S. Wang, et al. (1994). "Host-cell receptors for Sindbis virus." *Arch Virol Suppl* 9: 473-84.
211. Subak-Sharpe, I., H. Dyson, et al. (1993). "In vivo depletion of CD8+ T cells prevents lesions of demyelination in Semliki Forest virus infection." *J Virol* 67(12): 7629-33.
212. Takkinen, K. (1986). "Complete nucleotide sequence of the nonstructural protein genes of Semliki Forest virus." *Nucleic Acids Res* 14(14): 5667-82.
213. Takkinen, K., J. Peranen, et al. (1991). "Proteolytic processing of Semliki Forest virus-specific non-structural polyprotein." *J Gen Virol* 72 (Pt 7): 1627-33.
214. Takkinen, K., J. Peranen, et al. (1990). "The Semliki-Forest-virus-specific nonstructural protein nsP4 is an autoprotease." *Eur J Biochem* 189(1): 33-8.
215. Tarbatt, C. J., G. M. Glasgow, et al. (1997). "Sequence analysis of the avirulent, demyelinating A7 strain of Semliki Forest virus." *J Gen Virol* 78 (Pt 7): 1551-7.
216. Thaikruea, L., O. Charearnsook, et al. (1997). "Chikungunya in Thailand: a re-emerging disease?" *Southeast Asian J Trop Med Public Health* 28(2): 359-64.
217. Thein, S., M. La Linn, et al. (1992). "Development of a simple indirect enzyme-linked immunosorbent assay for the detection of immunoglobulin M antibody in serum from patients following an outbreak of chikungunya virus infection in Yangon, Myanmar." *Trans R Soc Trop Med Hyg* 86(4): 438-42.
218. Tuittila, M. T., M. G. Santagati, et al. (2000). "Replicase complex genes of Semliki Forest virus confer lethal neurovirulence." *J Virol* 74(10): 4579-89.

219. Turell, M. J., J. R. Beaman, et al. (1992). "Susceptibility of selected strains of *Aedes aegypti* and *Aedes albopictus* (Diptera: Culicidae) to chikungunya virus." *J Med Entomol* 29(1): 49-53.
220. Turell, M. J. and F. J. Malinoski (1992). "Limited potential for mosquito transmission of a live, attenuated chikungunya virus vaccine." *Am J Trop Med Hyg* 47(1): 98-103.
221. Ulmanen, I., H. Soderlund, et al. (1976). "Semliki Forest virus capsid protein associates with the 60S ribosomal subunit in infected cells." *J Virol* 20(1): 203-10.
222. Ulmanen, I., H. Soderlund, et al. (1979). "Role of protein synthesis in the assembly of Semliki forest virus nucleocapsid." *Virology* 99(2): 265-76.
223. Vasiljeva, L., A. Merits, et al. (2000). "Identification of a novel function of the alphavirus capping apparatus. RNA 5'-triphosphatase activity of Nsp2." *J Biol Chem* 275(23): 17281-7.
224. Vasiljeva, L., A. Merits, et al. (2003). "Regulation of the sequential processing of Semliki Forest virus replicase polyprotein." *J Biol Chem* 278(43): 41636-45.
225. Vihinen, H., T. Ahola, et al. (2001). "Elimination of phosphorylation sites of Semliki Forest virus replicase protein nsP3." *J Biol Chem* 276(8): 5745-52.
226. Vihinen, H. and J. Saarinen (2000). "Phosphorylation site analysis of Semliki forest virus nonstructural protein 3." *J Biol Chem* 275(36): 27775-83.
227. von Bonsdorff, C. H. and S. C. Harrison (1975). "Sindbis virus glycoproteins form a regular icosahedral surface lattice." *J Virol* 16(1): 141-5.
228. Wahlberg, J. M., R. Bron, et al. (1992). "Membrane fusion of Semliki Forest virus involves homotrimers of the fusion protein." *J Virol* 66(12): 7309-18.
229. Wahlberg, J. M. and H. Garoff (1992). "Membrane fusion process of Semliki Forest virus. I: Low pH-induced rearrangement in spike protein quaternary structure precedes virus penetration into cells." *J Cell Biol* 116(2): 339-48.
230. Wang, K. S., R. J. Kuhn, et al. (1992). "High-affinity laminin receptor is a receptor for Sindbis virus in mammalian cells." *J Virol* 66(8): 4992-5001.
231. Wang, X., J. Xie, et al. (1994). "[The effect of Sindbis virus multiplication on gene expression of host cells]." *Wei Sheng Wu Xue Bao* 34(5): 345-54.
232. Wang, Y. F., S. G. Sawicki, et al. (1991). "Sindbis virus nsP1 functions in negative-strand RNA synthesis." *J Virol* 65(2): 985-8.
233. Wang, Y. F., S. G. Sawicki, et al. (1994). "Alphavirus nsP3 functions to form replication complexes transcribing negative-strand RNA." *J Virol* 68(10): 6466-75.

234. Watts, D. M., A. el-Tigani, et al. (1994). "Arthropod-borne viral infections associated with a fever outbreak in the northern province of Sudan." *J Trop Med Hyg* 97(4): 228-30.
235. Weiss, B., H. Nitschko, et al. (1989). "Evidence for specificity in the encapsidation of Sindbis virus RNAs." *J Virol* 63(12): 5310-8.
236. Whitley, R. J. (1990). "Viral encephalitis." *N Engl J Med* 323(4): 242-50.
237. Willems, W. R., G. Kaluza, et al. (1979). "Semliki forest virus: cause of a fatal case of human encephalitis." *Science* 203(4385): 1127-9.
238. Yao, J., E. G. Strauss, et al. (1998). "Molecular genetic study of the interaction of Sindbis virus E2 with Ross River virus E1 for virus budding." *J Virol* 72(2): 1418-23.
239. Yao, J. S., E. G. Strauss, et al. (1996). "Interactions between PE2, E1, and 6K required for assembly of alphaviruses studied with chimeric viruses." *J Virol* 70(11): 7910-20.
240. Zytoon, E. M., H. I. el-Belbasi, et al. (1993). "Mechanism of increased dissemination of chikungunya virus in *Aedes albopictus* mosquitoes concurrently ingesting microfilariae of *Dirofilaria immitis*." *Am J Trop Med Hyg* 49(2): 201-7.
241. Zytoon, E. M., H. I. el-Belbasi, et al. (1993). "Transovarial transmission of chikungunya virus by *Aedes albopictus* mosquitoes ingesting microfilariae of *Dirofilaria immitis* under laboratory conditions." *Microbiol Immunol* 37(5): 419-21.